Proceedings of the Indian Academy of Sciences (Chemical Sciences)

EDITORIAL BOARD

C. N. R. Rao, *Indian Institute of Science, Bangalore (Chairman and Editor of Publications, IASc)*
D. Balasubramanian, *Centre for Cellular and Molecular Biology, Hyderabad*
A. Chakravorty, *Indian Association for the Cultivation of Science, Calcutta*
B. M. Deb, *Indian Institute of Technology, Bombay*
D. V. S. Jain, *Panjab University, Chandigarh*
T. R. Kasturi, *Indian Institute of Science, Bangalore*
V. Krishnan, *Indian Institute of Science, Bangalore*
P. T. Manoharan, *Indian Institute of Technology, Madras*
G. Mehta, *University of Hyderabad, Hyderabad*
S. Rajappa, *CIBA–GEIGY Research Centre, Bombay*
P. Ratnasamy, *National Chemical Laboratory, Pune*
Sukh Dev, *Malti-Chem Research Centre, Baroda*
B. Venkataraman, *Tata Institute of Fundamental Research, Bombay*

Subscriptions

For India, Pakistan, Sri Lanka, Nepal, Bangladesh and Burma, contact:
Editorial Office

For other countries, contact:

M/s J C Baltzer A. G.
Scientific Publishing Company
Wettsteinplatz 10
CH-4058 Basel
Switzerland

Telephone: 61-268925. Telex: 63475

Editorial Office:

Indian Academy of Sciences
P.B. No. 8005
Bangalore 560080
India

Proc. Indian Acad. Sci. (Chem. Sci.), Vol. 93, No. 6, August 1984, pp. 861–904.
© Printed in India.

Nonstoichiometric compounds: A critique of current structural views

J S ANDERSON

Research School of Chemistry, Australian National University, Canberra A.C.T. 2601, Australia

Abstract. The current status of experimental knowledge and theoretical views about nonstoichiometric compounds and heteroionic solid solutions is briefly surveyed, particularly in relation to structural aspects. It is emphasised that there is a little understood transition from the state adequately described by point defect theory, valid for very small deviations from ideal stoichiometry, to the highly organised local structure of crystals with a high formal concentration of defects. The role of short range ordering effects, of microdomains of modified, ordered structure and of defect clusters in different systems is considered. Order-disorder transformations undergone by nonstoichiometric phases at high temperatures present a special problem. The high temperature phases have very high formal defect concentrations, and the site correlation coefficients found experimentally differ but little from those predicted for completely random structures, although the high defect concentrations imply that all the factors promoting short range ordering must be strong.

Theoretical developments are considered. Treatments of pair interaction effects, and calculations of the energetics of defect interaction and the reconstructive formation of defect clusters hold some promise for theoretical development.

Keywords. Nonstoichiometric compounds; superstructure; short range order; microdomains; defect clusters; point defects; extended defects.

1. Introduction

Most of chemistry is concerned with the study of molecular systems, entities which, by definition, are uniquely defined by their immutable chemical composition. Less well understood, and providing a recurrent theme in the chemistry of the solid state, is the fact that there is no absolute, one-to-one correspondence between the composition and the chemical identity of those crystalline solids that have non-molecular, network structures.

Interest in this topic dates from the work of Kurnakow, at the turn of the century, on the phase equilibria in intermetallic systems; but intermetallic chemistry then appeared to lie outside the normal laws of chemistry. The seminal work was that of Chaudron (1921) and of Schenck *et al* (1927). They established that ferrous oxide, the progenitor of the whole series of iron(II) salts, not only had a wide range of composition under equilibrium conditions (from about $FeO_{1\cdot05}$ to $FeO_{1\cdot15}$), but that the stoichiometric composition $FeO_{1\cdot00}$ lay outside the stable range and did not exist. It was the timing of this work that lent it special significance. Structural x-ray crystallography was rapidly developing, and the structures of the simpler inorganic compounds—including the rocksalt (B1 type) structure of ferrous oxide—had been determined. This meant that the purely thermodynamic idea of 'solid solutions', devoid of any structural connotations, must be given a precise meaning in structural, atomistic terms. Concurrently being introduced into physico-chemical thinking were point defects in crystals—unoccupied sites or atoms in (interstitial) positions not proper to the crystal structure.

This notion of crystal imperfections, formulated by Frenkel, Schottky and others to interpret atomic transport processes within crystals, could be extended to cover the way in which the regular, in many cases simple, structure of a crystalline compound could adapt itself, without loss of identity, to changes in the numbers of atoms that must be fitted into sites provided by the crystal structure.

Structure, and how it is related to the thermodynamic, electronic and transport properties of nonstoichiometric compounds, has since been a major field of study. It is now familiar that ideas about this have undergone great changes in recent years, without reaching either finality or any comprehensive interpretation of the phenomena. The literature relevant to this aspect of the physics and chemistry of solids is immense; no single review could attempt to cover it. The object of this review is, rather, to examine current ideas with particular reference to a limited number of chemical systems that exemplify their basis, justification and limitations. This paper deals chiefly with the finite (*i.e.* spatially localised) imperfections in crystals that underlie the formation of truly nonstoichiometric compounds. Treatment of planar defects and other unbounded imperfections is deferred for a subsequent paper.

2. Some general considerations

The essence of crystal theory is *translational symmetry*; the concept of an element of pattern, the unit cell, containing a specified number of atoms of each kind in a completely defined spatial arrangement which, by identical and continuous repetition in three dimensions, builds up the macroscopic crystal. Strictly interpreted, translational symmetry would exclude the existence of any form of disorder in crystals, or any deviation from the ideal composition.

Any physical realistic crystal is an assemblage of a very great number of unit cells; like all real, macroscopic systems it is subject to the overriding principles of *statistical thermodynamics*. Any conceivable perturbation of the perfectly ordered structure, *e.g.* the creation of point defects, has a probability that is not a mathematical zero (above 0° K), but is set by the enthalpic cost of the perturbation and its effect on the entropy of the system. Regarded as a thermodynamically closed system, a crystal embodies a certain equilibrium concentration of defects. Treated as an open system in equilibrium with its environment, the admissible perturbations include the abstraction or addition of component atoms. The composition of the crystal is no longer mandatorily constant. With the publication of the classical paper by Schottky and Wagner (1931) 'On ordered mixed phases', these concepts were introduced into solid state chemistry.

Contemporary with the introduction of the statistical thermodynamic outlook was the accumulation of much evidence that ferrous oxide was by no means unique. The period up to 1940 saw the acquisition of evidence about stoichiometric variability, much of it in the thorough work of W Blitz and his school, in a long series of papers entitled 'Systematic doctrine of affinity'. How crystal defects contributed to nonstoichiometry was diagnosed, in broad terms, beginning with the demonstration, by Jette and Foote (1933), that in ferrous oxide there is a deficit of iron (5 % to 15 % vacant sites), not an in-built excess of oxygen. Oxides, sulphides, carbides, etc., the typical classes of compounds existing only in the condensed state, could be classified, on chemical criteria, as 'Daltonide', of sensibly invariant composition, or 'Berthollide', with significantly variable stoichiometry.

Nonstoichiometric crystals were first interpreted, as regards their structure and their thermodynamics, in terms of the statistical thermodynamics of point defects. This approach was already applied to several systems by Schottky and Wagner in their first papers. However, as structural information has increased, and especially with the development of new experimental techniques, that approach has necessarily been replaced by an emphasis on more far-reaching perturbations of the basic or parent structure: extended defects and new modes of local ordering that retained the coherence of the crystal structure. Without surveying the now vast literature, the present aim is to examine how current concepts are related to the point defect model. The point defect description is a powerful tool within the area of its applicability, and is mathematically more tractable than treatments based on extended defects, but much evidence relating to highly defective solids points to the various forms that extended defects can take. The need is to trace the transition from point defects in highly dilute defect systems to highly structured imperfections in nonstoichiometric crystals, all as a consequence of statistical thermodynamic constraints.

The term 'nonstoichiometric compound' has sometimes been applied loosely, especially in the physical literature. In this review, it is to be defined in strictly operational terms; the criterion is that a crystalline compound, in equilibrium with its environment, behaves as a thermodynamically bivariant system. The chemical potentials of the components are a continuous function of the composition of the solid, over an observable range of composition. For a 'Daltonide' (line phase) there is a discontinuous step, from one equilibrium value of the chemical potential to another, at the unique composition of the compound. In terms of the statistical thermodynamic model, this is an idealization. What constitutes an observable range of composition depends upon the method of observation. As ordinarily used, the term is applied to ranges of composition that are measurable by chemical analysis; methods of counting electrons or positive holes can be orders of magnitude more sensitive. The essence of the problem is to relate the wide-range nonstoichiometric compounds to those that are characterized only in terms of their electronic properties, and that can be quantitatively understood in the terms of point defect theory.

A second operational characteristic, implicit in the definition of a single bivariant phase, is that its translational and space group symmetry remain unchanged across the composition range. Crystal properties may change progressively in magnitude with composition; thus, there is usually a small change in the cell dimensions, following Vegard's law, and the structure factors of some reflections, in x-ray and neutron diffraction, may change significantly. These changes reflect, respectively, the alteration in mean binding energy and the changes in site occupancy; as is discussed below, they may also reflect more profound changes in microstructure. Some properties that are regarded as significant in equilibrium studies, such as the maximum melting point or the composition of congruent vaporization, need not coincide exactly with the ideal composition of the compound, but be detectably displaced from it. The phase breadth is usually unsymmetrical about the ideal composition, the extreme case being found in compounds such as $Fe_{1-x}O$, for which the unit cell composition lies outside the range of stability.

This operational definition of nonstoichiometry does not depend upon any assumptions about the structure of the bivariant phase. The concept of an idealised structure implies that the stoichiometry is uniquely defined by the composition of the repeating unit cell, a reference datum which furnishes a definite number of sites for each

species of atom, in a particular spatial configuration, all sites being occupied by the appropriate kind of atom. The formula of the unit cell—which corresponds exactly to that for a free molecular species—may be complex, with apparently irrational atomic ratios of the constituents, but is none the less unambiguously defined. Thus the niobium oxides $NbO_{2\cdot500}$, $NbO_{2\cdot4906}$, $NbO_{2\cdot4800}$, $NbO_{2\cdot4681}$, $NbO_{2\cdot4545}$ and $NbO_{2\cdot4167}$ do not represent compositions within some range of stoichiometry, but are a succession of discrete, crystallographically defined compounds $Nb_{28}O_{70}$ (Nb_2O_5), $Nb_{53}O_{132}$, $Nb_{25}O_{62}$, $Nb_{47}O_{116}$, $Nb_{22}O_{54}$ and $Nb_{12}O_{29}$. That such closely spaced phases are systematically and structurally related is, however, relevant to the crystal chemistry of nonstoichiometric compounds. Although trivial, these definitions are important because they are occasionally used loosely.

In any nonstoichiometric compound, the number of atoms per *average* unit cell is no longer equivalent to the number of sites. In polar compounds, it is usually, though by no means always, the case that one sublattice (either the cation sublattice or the anion sublattice) remains sensibly invariant, whilst the species tenanting the other sublattice may be either deficient (*i.e.* average cell contents $<$ site number), in which case some sites must be empty, or present in excess (*i.e.* average cell contents $>$ site number), implying that atoms occupy sites not used in the parent structure (interstitial atoms). A simplistic application of point defect ideas directly identified the deficit or surplus of atoms per average unit cell with the concentration of vacancies or interstitials respectively, and thus assumed that the concentration of defects could be equated with the deviation from ideal stoichiometry. It is now clear that that is not a valid generalisation.

Nonstoichiometric compounds are necessarily mixed valence compounds. The electronic structure of polar compounds is best described in terms of the band model, with filled valence band, empty conduction band and an integral ratio of electrons to atoms in any occupied, non-bonding bands (*e.g.* the d^8 band in NiO). A nonstoichiometric compound necessarily has a non-integral electron/atom ratio; impurity levels are created within the band gap, or the population of the non-bonding bands is changed. As Wagner recognised from the outset, nonstoichiometry is thereby directly linked with semiconductor properties, metal-excess compounds being electron conductors, metal-deficient compounds positive hole conductors. More strictly, conduction is likely to be by electron hopping, or polaron migration: large polarons where an equivalent description would be a strict localisation of ions in different valence states, small polarons where the carrier levels lie within a narrow non-bonding band.

A simple model of electrons or positive holes in defect levels cannot hold good for a crystal that departs widely from ideal stoichiometry: the formal concentration of defects becomes too high to neglect interaction effects. One potential consequence of this is that, for some electron/atom ratios the system can lower its energy by forming a superlattice structure, with a multiple of the original unit cell and a correspondingly smaller, filled Brillouin zone. In highly polar compounds, the formation of a superlattice can involve some structural rearrangement, and is considered later.

It is familiar that some classes of compounds between the metals and the nonmetals exhibit fully metallic characteristics, and that there can be a transition between the metallic and the highly polar (whether ionic or covalent) types, as in the monoxides of the transition elements. Where there is overlap of non-bonding and conduction bands, so that electrons occupy states in partially filled bands, the constraints imposed by electronic considerations are less, and are less clear. Any change in the metal/nonmetal

ratio alters the overall electron/atom ratio by augmenting or diminishing the population of states at the Fermi level. The consequences of such changes, and especially the effects of nonstoichiometry on the binding energy of the crystal, depend upon the precise form of the density of states function in the neighbourhood of the Fermi level of the parent structure.

There is a further difference between insulating (wide band gap) compounds and metallic compounds. As already indicated, nonstoichiometry in the former can be validly described in terms of forming ions in a different valence state, compensating a corresponding number of structural defects. Coulomb forces between altervalent ions and structural defects are long range forces, which can furnish the driving force for structural rearrangement; this rearrangement can supervene when the deviation from stoichiometry reaches a level at which the mean spacing between defects, whatever their nature, falls below some critical value. In metallic crystals, the delocalised electrons screen centres of local electron excess or deficit from long range interactions. The tendency for structural reorganization is thereby greatly lessened, but the possibilities for superstructure formation remain, since the mean electron energy can thereby be reduced. It is qualitatively understandable that nonstoichiometric compounds with a wide range of existence should be rather uncommon amongst the more ionic compounds, but should be found with strikingly wide stoichiometric ranges amongst the oxides, nitrides, carbides, etc of the transition metals.

The true nonstoichiometric compounds cannot be discussed without considering the heteroionic solid solutions, in which the cations of a parent structure are replaced by controlled and predetermined amounts of cations of another element, in a different valence state. The outcome of such substitution depends on the valence properties of host and substituent:

Host species	*Substituent*	*Effect*
Variable valency	Fixed valency	Controlled valence of host cations
Fixed valency	Variable valency	Induced valence of substituent cations
Fixed valency	Fixed valency	Controlled structural defects

In the first two cases, there will be some range of chemical potentials within which it is energetically advantageous to alter the electronic structure, rather than to introduce structural defects (vacant sites or interstitials) to compensate for change in the ratio of atoms to valence electrons. Thus lithium-doped nickel oxide exemplifies the first type. The electron/atom ratio required for the averaged rocksalt structure of $Li_xNi_{1-x}O$ is conserved by compensating each Li^+ cation by a Ni^{3+} cation; electrons are withdrawn from the nickel *d* band and the material is a positive hole conductor. Its electronic properties are controlled by the substitution without creating any structural defects, over a wide range of oxygen fugacity. In induced valence, it is energetically advantageous to alter the charge state of the guest cations to that of the host structure, rather than to introduce structural defects. Thus manganese, at low concentrations, is incorporated into Al_2O_3 as Mn^{3+} ions, and into TiO_2 as Mn^{4+} ions.

Directly relevant to the discussion of nonstoichiometry are heteroionic systems of the third type. It was shown at an early stage, by Zintl and Udgard (1939) that substitution of a foreign ion, of different valency, involved the creation of structural defects of the same kind as are involved in the nonstoichiometric materials. The intrinsic defect equilibrium of the host structure is thereby displaced. The important feature of the heteroionic systems is that their defect concentration is very high and is

completely defined by the chemical composition over a wide range of experimental conditions (*e.g.* chemical potentials and temperature), since the imposed defect concentration swamps that arising from the inner equilibrium of the crystals. Moreover, it is frequently possible to extend the stoichiometric unbalance far beyond the range of stability of analogous nonstoichiometric compounds. Work on heteroionic solid solutions has therefore been important in developing ideas about the constitution of nonstoichiometric crystals.

There is, however, an important difference, that affects the response of defect structures to all the interaction effects that tend towards long range order. As is discussed more fully below, Coulomb interactions strongly associate structural defects and electronic defects; they pair up on closely neighbouring sites. In a (homoionic) nonstoichiometric compound, electronic defects are not rigorously localised; cation charge states are interchangeable by electron transfer (polaron migration). As a consequence, structural defects and compensating charges can move together in any ordering processes. In heteroionic solid solutions, the electronic defect is anchored at the site of the substituent cation, and structural defects are thereby pinned and immobilised. Any possibility of establishing some long range order of vacant sites, interstitial atoms, etc is contingent upon transport processes that redistribute the substituent atoms. In some structure types there is a large inherent disparity between the mobility of the anion- and cation-sublattices, so that energetically desirable ordering processes may be completely inhibited. This restriction on long range ordering is one reason why heteroionic solid solutions not uncommonly have a much broader range of stoichiometry than the structurally analogous compounds. Thus, in the pure PrO_{2-x} system, at low temperatures, there is a succession of distinct line phases produced by the superstructure ordering of vacant oxygen sites and of Pr^{3+} and Pr^{4+} cations. A very small concentration of randomly distributed, immobile cations of other lanthanide elements, Ln^{3+}, blocks that ordering and simulates the formation of a nonstoichiometric phase at all temperatures.

3. Point defects

A direct application of the simple statistical thermodynamic model accounts well for the transport, thermodynamic and electronic properties of Daltonide compounds; difficulties arise in applying the same formalism to compounds with a wide stoichiometric range. In the point defect approximation, the creation of a point defect—omission of an atom from a lattice site or insertion of an interstitial atom—affects only a single lattice site. Creation of the point defect polarizes the surrounding crystal structure, resulting in some small displacements of adjacent atoms; the relaxation effects attenuate rapidly with distance from the vacancy or interstitial atom. However, the energetic cost of creating the defect is independent of the way that all other lattice sites are occupied. Whether there is a surplus or a deficit in the number of atoms per average unit cell of the nonstoichiometric crystal can be inferred from experimental data, and simple point defect theory equates that deviation from ideality directly with the concentration of point defects of a known kind.

In that approximation, the theory was at once applied by Wagner, in the 1930s, to several chemical systems, but it was clear that some modification was necessary to allow for interactions between defects at the high concentrations encountered in wide-range

Berthollide compounds. Better approximations, introducing nearest neighbour interactions (Lacher 1937; Anderson 1946; Rees 1954) did, in fact, approximately reproduce the thermodynamic properties of certain chemical systems. However, it is now evident that any satisfactory theory must take account of what is known of defect structure. There is ample evidence that significant deviations from stoichiometry involve localised modifications of the short range order of crystals, and that those perturbations can be more profound than is implied in the concepts of 'vacancy' and 'interstitial'.

The formal concentration of defects in nonstoichiometric compounds is too high for them to be treated as independent point defects. However, systems with statistically randomized defects in very high concentrations are undoubtedly found experimentally. As will be seen from a review of several important examples, order-disorder transformations can generate a complete loss of all long range and medium range site correlations, implying that the enthalpy of ordering is small. That enthalpy of ordering arises from the interactions that determine site preference energies for the mutual location of defects, and the point that is open to dispute is how far those site preference energies still determine the energetic cost and the distribution of defects in the statistically random state. Is any local structure retained? One approach to this question is through the experimental determination of short range order parameters. The evidence is that the distribution of vacant sites or interstitials may differ little from that expected for a completely random structure. The problem is to identify and quantify the constraints that are imposed by the high degree of defectiveness, and to frame a theory for the resulting structure, thermodynamics and transport properties.

Nevertheless, the development of the point defect model has provided a powerful tool for treating many aspects of the physics and chemistry of solids. Point defect vacancies remain as the inescapable primary entities, at least in thought experiments, whether or not they persist as the dominant physical entities in defect structures. Statistical thermodynamics interprets minute deviations from ideal stoichiometry as due to displacements of the inner defect equilibria in any crystal, resulting in a sparse distribution of some kind of structural perturbation. Such defect centres can undoubtedly interact but, in the limiting case of very high dilution, they can be identified with the concept of independent point defects. The experimental and theoretical problem is to understand how that situation evolves into one with more profound microstructural rearrangement, as the concentration of defects is increased. Transport phenomena depend upon the annihilation and creation of defects: individual atoms must jump from properly occupied sites (creating vacancies) to permissibly occupied sites (cancelling a pre-existing vacancy). There is some measure of intrinsic disorder in the most highly ordered structures.

All the processes involved in establishing the inner equilibria of a crystal, and its equilibrium with its environment, can be represented as a set of coupled, quasichemical reactions, which can be handled by mass action law methods. The free energies (and hence the equilibrium constants) for each process can be assigned if the corresponding enthalpy and entropy of reaction can be extracted from experimental data or calculated theoretically. This approach, developed by Kroger and the Philips Laboratory (Kroger 1976) has proved versatile and predictively useful.

All forms of intrinsic disorder could, in principle, be included in the treatment, but without loss of generality we may consider a simple example: a crystal MX, of Schottky type, in equilibrium with its components. The free nonmetal component is taken as the diatomic gas X_2 (as is the usual experimental case, in the high temperature equilibria of

oxides, sulphides, etc.). Treatment of crystals of Frenkel type, or more complex composition would be exactly analogous (*cf* Kroger 1976).

Making no assumptions about the nature of the binding forces (ionic or covalent), the primary process in creating Schottky vacancies can be represented as the displacement of *neutral atoms*, leaving the original electron distribution unchanged. The defect site is effectively electrostatically neutral. Removal of an *ion* from a lattice site would be electrostatically equivalent to placing there a charge of equal and opposite sign; it could be regarded as a second step, the ionization of the defect.

Two distinct kinds of internal equilibria must then be considered.

(a) Point defect equilibria—the primary Schottky step that generates neutral vacancies—symbolized in (1):

$$0 \rightleftharpoons V_M^x + V_X^x \qquad K_S = [V_M^x][V_X^x]. \tag{1}$$

The neutral defects can undergo ionization, which may be represented as putting electrons into the conduction band or positive holes into the valence band at the concentrations n and p respectively:

$$V_M^x \rightleftharpoons V_M' + h^+ \qquad K_a = \mathbf{p}\cdot[V_M']/[V_M^x], \tag{2}$$

$$V_X^x \rightleftharpoons V_X + e^- \qquad K_b = \mathbf{n}\cdot[V_X]/[V_X^x]. \tag{3}$$

If M and X have valence 2 or higher, then further stages of ionization of the defects must be considered. For the present illustrative purpose, attention is restricted to the uni-univalent case. (b) The second intrinsic equilibrium is that of the distribution of electrons between valence band and conduction band states:

$$0 \rightleftharpoons h^+ + e^- \qquad K_i = \mathbf{p}\cdot\mathbf{n}. \tag{4}$$

The magnitude of K_i is determined by the band gap energy, E_i. By combining equations (1) to (4), the intrinsic defect equilibrium can be redefined, in terms of ionised defects, as in (1a):

$$0 \rightleftharpoons V_M' + V_X \qquad K_s' = K_a\cdot K_b\cdot K_S/K_i. \tag{1a}$$

The most important factor determining these equilibrium constants, and hence the defect concentrations, is the corresponding enthalpy of reaction. For equilibrium (1a), E_S (or E_F for Frenkel crystals) can be extracted from experimental data, or can be calculated on certain assumptions about ionicity, polarization and relaxation. Some representative values are listed in table 1. Creation of defects is highly endothermic; for most of the systems for which information is available, E_S is around 2–4 eV per defect pair, and it increases markedly with the tightness of binding of the crystal, *e.g.* in bi-bivalent ionic compounds and in covalent crystals. As a consequence, the intrinsic defect concentrations for nearly all crystals are exceedingly small, even at high temperatures. In table 1, intrinsic defect concentrations are shown for the same relative temperature, $0{\cdot}8 \times T_m$ (T_m = melting temperature, °K). The uncertainties attached to these figures are large, but it appears that, irrespective of composition and structure type, the intrinsic defect concentration at $0{\cdot}8\ T_m$ is of the order 10^{-5}. This conclusion is relevant for the present discussion.

E_i is the width of the band gap (figure 1), and E_a, E_b depend upon the location of the corresponding defect levels within the band gap.

Equilibration of the crystal with its components, at the chemical potential set by the

Table 1. Representative experimental or theoretical enthalpies for intrinsic point defect equilibria; defect concentrations at 0·8 × melting point.

Substance	0·8 *Tm* (°K)	*H's* or *H'f* (eV)	Intrinsic defect concn.	Disorder type
AgBr	605	0·87–1·29	$2{\cdot}5 \times 10^{-3}$	Frenkel cation
CaF_2	1456	2.7–2.8	2×10^{-3}	Frenkel anion
CdS	1740	4.1	3×10^{-5}	Frenkel cation
GeAs	1300	3·8	$7{\cdot}3 \times 10^{-6}$	Schottky
NaCl	922	2·0–2·5	$1{\cdot}5$–$4{\cdot}5 \times 10^{-5}$	Schottky
KCl	895	2·1–2·6	10^{-5}–$7{\cdot}2 \times 10^{-6}$	Schottky
KBr	872	2·5–2·8	5–10×10^{-6}	Schottky
PbS	1190	1·7–2·6	3–6×10^{-5}	Schottky
$PbCl_2$	664	1·5	6×10^{-4}	Schottky
RbI	790	2·1	5×10^{-7}	Schottky
SrF_2	1500	0·6–1·8	1×10^{-2}	Frenkel anion
MgO		4–6	(10^{-5}?)	Schottky
CaO		3–5	(10^{-5}?)	Schottky

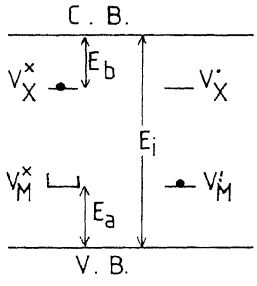

Figure 1. Energy levels of relative neutral and ionised defect levels in a uni-univalent Schottky solid MX.

environment, involves reactions transferring atoms between the gas phase and sites in the crystal, according to either (5a) or (5b):

$$M(g) \rightleftharpoons M_M + V_X^x \qquad K_{TM} = [V_X^x]/\mathbf{p}_M, \tag{5a}$$

$$1/2X_2 \rightleftharpoons X_X + V_M^x \qquad K_{TX} = [V_M^x]/\mathbf{p}_{X_2}{}^{1/2}. \tag{5b}$$

These processes are necessarily equivalent, being linked through the equilibrium

$$MX\ (\text{cryst}) \rightleftharpoons M(g) + 1/2X_2(g) \tag{6}$$

and equation (1). It is convenient here to take the partial pressure of X_2 as the experimentally controlled variable (*e.g.* as in the work on oxide systems). Then $[V_X^x] = K_{TX} \cdot \mathbf{p}^{1/2} X_2$ under all conditions. A final constraint is that, for electroneutrality, there must be balance between all charged species; for the simple case under discussion:

$$\mathbf{n} + V'_M = \mathbf{p} + V_X^{\cdot}. \tag{7}$$

This set of coupled equilibria can be evaluated by recognising regimes in which one or

Table 2. Defect equilibria in a uni-univalent Schottky type crystal MX.

	Range I $n = [V_X^{\cdot}]$	Range IIa $n = p$	Range IIb $[V'_M] = [V_X^{\cdot}]$	Range III $p = [V'_M]$
n	$(K_i K'_s/K_a)^{1/2} R^{-1/2}$	$K_i^{1/2}$	$(K_i K_s'^{1/2}/K_a) R^{-1}$	$(K_i/K_a^{1/2}) R^{-1/2}$
p	$(K_i K_a/K'_s)^{1/2} R^{1/2}$	$K_i^{1/2}$	$(K_a/K_s'^{1/2}) R$	$K_a^{1/2} R^{1/2}$
$[V'_M]$	$(K_a K'_s/K_i)^{1/2} R$	$(K_a/K_i^{1/2}) R$	$K_s'^{1/2}$	$K_a^{1/2} R^{1/2}$
$[V_X^{\cdot}]$	$(K_i K'_s/K_a)^{1/2} R^{-1/2}$	$(K_i^{1/2} K'_s/K_a) R^{-1}$	$K_s'^{1/2}$	$(K'_s/K_a^{1/2}) R^{-1/2}$
$[V_M^X]$	R	R	R	R
$[V_X^X]$	$(K_i K'_s/K_a K_b) R^{-1}$	$(K_i K'_s/K_b K_b) R^{-1}$	$(K_i K'_s/K_a K_b) R^{-1}$	$(K_i K'_s/K_a K_b) R^{-1}$

Variation of defect concentration with non-metal fugacity: function $R = P_{X_2}^{1/2} \cdot K_{TX}$.

other species, on either side of (7), so preponderates as to dominate the situation. The possibilities are:

I $\quad \mathbf{n} = [V_X^{\cdot}]$,

IIa $\quad \mathbf{n} = \mathbf{p} \quad$ if $K_i > K'_S$,

IIb $\quad [V'_M] = [V_X^{\cdot}] \quad$ if $K_i < K'_S$,

III $\quad [V'_M] = \mathbf{p}$.

In each regime, the concentrations of all defect species can then be found to a good enough approximation. Their magnitudes, and in particular how they depend upon the partial pressure of X_2, are shown in table 2; figures 2 and 3 plot log (defect concentration) against the chemical potential of X (*i.e.* $\frac{1}{2}RT \ln \mathbf{p}_{X2}$).

The deviation from stoichiometry is given by (8):

$$\delta = \Sigma[V_M] - \Sigma[V_X]. \tag{8}$$

How that stoichiometric defect varies with the chemical potential of the components is schematically shown in figure 4, for the two cases of figures 2 and 3.

Within the scope of its physical validity, this quasichemical treatment offers a powerful and suggestive way of handling defect equilibria. It brings out the greater

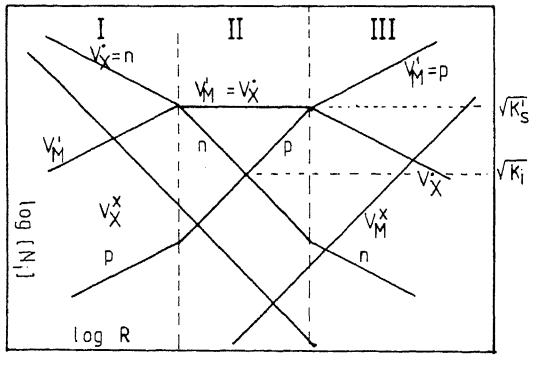

Figure 2. Variation of defect concentrations with R ($= \frac{1}{2}K_{TX} \log P_{X_2}$). Case $K'_s > K_i$.

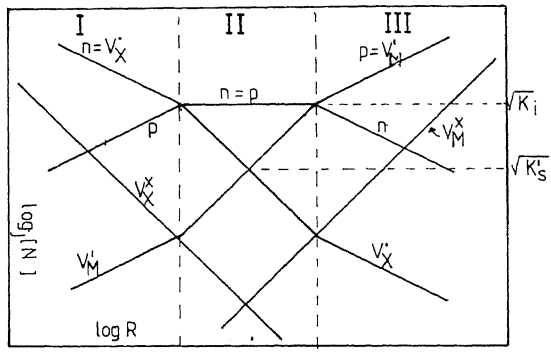

Figure 3. Variation of defect concentrations with R ($= \frac{1}{2}K_{TX} \log P_{X_2}$). Case $K_i > K'_s$.

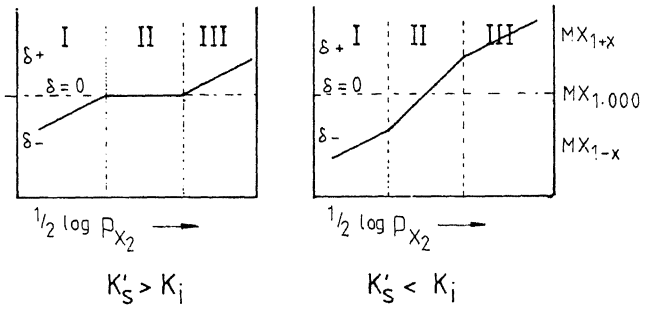

Figure 4. Deviation from stoichiometry as dependent upon P_{X_2}.

complexity of systems involving atoms of higher valence, and is valuable in showing how the internal and external equilibria are affected and displaced by impurities or atoms of a third component, as in the equilibria of heteroionic solid solutions. It gives predictive insight into the way that other defect-dependent properties, *e.g.* diffusion and ionic conductivity, are influenced by stoichiometry and chemical potentials.

Several aspects of the quasichemical model are particularly relevant to the present discussion. The first relates to the relative and absolute magnitudes of the intrinsic equilibrium constants K_i and K'_S or K'_F. In crystals built from ions with $[s^2p^6]$ configuration, E_i is usually large. In compounds of the transition metals, the corresponding excitation process, of lowest energy, is from a non-bonding d^n band, lying in the band gap; E_i is considerably lower. In covalent crystals, the relevant factors are highly dependent on the details of the covalent bonding. Defect creation energies do not appear to vary very widely from one class of compound to another, although the published data show many discrepancies, but do depend significantly on the crystal structure type. For example, the low energetic cost of creating defects in the anion sublattice of all fluorite structures plays an important part in the chemistry of nonstoichiometry.

These correlations are familiar, but serve to emphasise the importance of the band structure of crystalline compounds. In particular, for the case that K'_S (or K'_F) $> K_i$, the stoichiometry necessarily remains practically constant and ideal over a range (often a

wide range) of chemical potential. The limits of this central range may conveniently, if arbitrarily, be taken as defined by the conditions

$$\lim \text{I/II} \qquad \mathbf{n} = [V'_M] = \tfrac{1}{2}[V^{\cdot}_X],$$
$$\lim \text{II/III} \qquad \mathbf{p} = [V^{\cdot}_X] = \tfrac{1}{2}[V'_M],$$

and it can easily be shown that the stoichiometric defect alters only from $-1/\sqrt{2}\delta_0$ to $+1/\sqrt{2}\delta_0$ (where δ_0 is the intrinsic concentration of defects in the stoichiometric crystal, $= K_S'^{1/2}$ across that range; the partial pressure of X_2 must thereby increase by a factor of $(K'_S/K_i)^2$. In every case for which quantitative information is available, δ_0 is very small. It follows that the variability of composition predicted by the point defect model is likely, for typical ionic compounds, to be so small as to be measurable only by techniques that determine the concentrations of current carriers.

No reference has been made to interactions between defects. In so far as these can be represented as introducing equilibria between free defects and associated species, they can be incorporated in the quasichemical formulation. Coulomb attraction between the basic, charged point defects should result in strong association to form uncharged defect pairs:

$$V'_M + V^{\cdot}_X \rightleftharpoons (V_M V_X) \qquad K_{VP} = K^* \cdot [V'_M][V^{\cdot}_X] = K^* \cdot K'_S.$$

The concentration of such associated pairs is therefore independent of the chemical potentials, and can be comparable with, or greater than, the concentration of free point defects. Similarly, like defects can pair up: $V'_M + V_M \rightleftharpoons (V_M)'_2$, stabilized by some delocalisation of the electron wavefunction. The importance of these defect association reactions can be seen from Kröger's thorough analysis of equilibria in the classical exemplar—crystals of the potassium halides.

In a formal and conceptual way, the quasichemical treatment of dilute defect systems is analogous to the theory of electrolytes in solution. For realistic defect concentrations, generalised electrostatic interactions cannot be ignored; the 'ionic atmosphere' effects can be allowed for in a formal sense by a Debye-Hückel treatment, and defect activities should be considered in place of defect concentrations. Such an extension of the point defect approach does not adequately reproduce the thermodynamic and structural characteristics of nonstoichiometric compounds or heteroionic solid solutions.

4. Extended defects

Table 1 indicates the degree of intrinsic disorder that can be expected in typical polar crystals, when reasonable values are assigned to the controlling parameters. When account is taken of the way that defect concentrations depend upon the relevant chemical potentials (table 2), it can be predicted that there can be only very small changes in chemical composition across the whole accessible range of experimental conditions, even though those composition changes are profoundly important for the semiconductor and other electronic properties of the crystals. In contrast with that conclusion, table 3 lists the apparent or net defect concentrations in a few highly nonstoichiometric compounds; as will be seen, the actual number of 'vacancies' and 'interstitials' in these structures is considerably greater than would appear from the apparent defect concentration.

As far as its experimental basis is concerned, the concept of a point defect is largely

Table 3. Apparent net defect concentrations in typical nonstoichiometric compounds and heteroionic solid solutions (*cf.* table 1).

TiC_x	13–50% C sites vacant
TiO_x	0–30% Ti sites, 30%–0% O sites vacant across composition range $TiO_{0.7}$–$TiO_{1.3}$ (above 1000°C)
$Fe_{1-x}O$	5–15% Fe sites vacant (above 600°C)
α-CeO_{2-x}	0–14% O sites vacant (above 600°C)
UO_{2+x}	0–25% interstitial O atoms

dominated by inferences drawn from highly dilute defects in the most highly ionic crystals: colour centres in alkali halides, alkaline earth oxides, CaF_2, etc. For these, a variety of spectroscopic methods (see Fowler 1975) has shown that isolated defects have the expected site symmetry, and that associated defect pairs have the geometry and orientation predicted from point defect arguments. It does not follow that this concept is equally applicable at defect concentrations for which interaction effects become significant, or for crystals in which covalency or collective electron properties are important. For some crystals, the energy of creation of defects can be calculated satisfactorily by the Mott-Littleton and related methods that assume that relaxation about a defect has the site symmetry of the lattice point concerned. In nonstoichiometric crystals where the initial defects interact with the matrix structure, to produce new configurations, it is evident that the relaxation process is highly specific.

This review will first discuss the superlattice ordering of vacant sites or interstitial atoms, as a result of the interactions between them. In the state of lowest energy, sites that are wrongly tenanted, as compared with the parent structure, are then no longer defects, but have become essential elements of the ordering pattern. The more profound interactions between notional point defects and matrix structures create extended defects, which may be either elements of a superlattice or independent defect clusters. These topics will be related, as far as is currently possible, to developments in the theoretical treatment and modelling of nonstoichiometric systems.

5. Nonstoichiometry and superlattice ordering. The layer chalcogenides

Chalcogenides of the 3*d* transition metals (other than Mn) present a series of compounds that exhibit both very wide stoichiometric ranges and closely spaced successions of phases, all based on a common structural pattern. In the intermediate compounds, defects are *eliminated* by long range superstructure ordering, which creates defined structures with compositions intermediate between two structural extremes. They have narrow band gaps or are quasimetallic in character, and the common structural pattern is set by two topologically related structure types: MX_2 with the CdI_2 structure and MX, with the NiAs structure. Both of these are layer structures, based on hexagonal close packing of chalcogen atoms; the chalcogen sublattice appears to persist without significant defects (*i.e.* with only some small statistical point defect concentration) in all the structures. In the MX_2 extreme, metal atoms occupy the octahedral interstices between chalcogen atoms in alternate hexagonal layers, so that the stacking down the unique axis is . . . $XMXXMXXMX$ . . . . The resulting sandwich layers are bound essentially by van der Waals forces, and between them are empty sites of

octahedral coordination. At the other extreme, all these sites are filled, giving the layer sequence . . . *XMXMXMXMX* . . . . Nonstoichiometric behaviour comes from the incomplete occupation of this second set of octahedral sites, a common pattern being the alternation of complete and incomplete sheets of metal atoms. If the fraction of empty sites in the incomplete layers is x, the whole family would be represented by the general formula $M_{2-x}X_2$ ($0 \leqslant x \leqslant 1{\cdot}0$). Not all the chalcogenide systems cover the full composition range; $Cr_2S_3(Cr_{0{\cdot}67}S)$ is the upper limit in the Cr-S system, whereas in the more metallic tellurides the limiting MTe_2 may be approached, *e.g.* in $NiTe_{2-x}$.

In the superstructure phases, the occupied and empty octahedral sites adopt a two-dimensional order in the hexagonal array of potential sites. The full range of possibilities for such structures is (figure 5, scheme A): The potential complexities of such systems are considerable, with superstructure ordering and possible order-disorder transformations at two distinct levels. Such transformations are found experimentally, and most if not all these chalcogenides have a significant, or even an extremely wide range of composition at high temperatures. For many of the systems, the experimental evidence is conflicting; equilibrium and full superstructure ordering are not easily achieved.

Of the systems that have a very wide stoichiometric range, nickel telluride $Ni_{2-x}Te_2$ exists from $NiTe_2$ to $Ni_{1{\cdot}84}Te$. For $x > ca\ 0{\cdot}4$, the diffraction properties are those of the CdI_2-type end member with interstitial nickel: *i.e.*, completely filled and defective layers alternate; for $x < ca\ 0{\cdot}4$, the structure is defective NiAs type, with vacant sites assumed to be present in all metal layers (Coffin *et al* 1974). This holds for material annealed at low temperatures, but no evidence has been found for any ordering in the partially filled layers. Long range order is completely lost at elevated temperatures; the order-disorder transition is diffuse, and the critical temperature (1080°K for $Ni_{1{\cdot}54}Te_2$, about 750°K for $Ni_{1{\cdot}67}Te_2$) is steeply dependent upon the concentration of empty sites in the incomplete layers. In this example, the interactions that produce ordered stacking are clearly stronger than those required to impose two-dimensional order in the layers.

Two-dimensional superstructure ordering in these compounds was first found by Bertaut (1956), for the pyrrhotite phase Fe_7S_8 ('4C pyrrhotite') of the Fe-S systems.

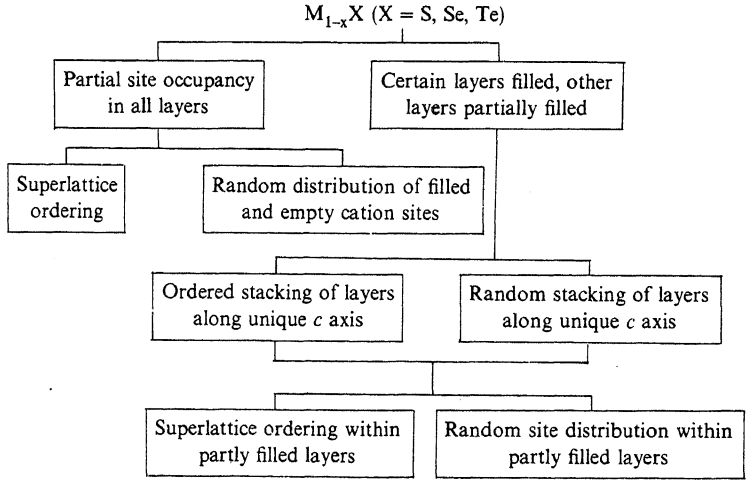
M1−xX (X = S, Se, Te)
Partial site occupancy in all layers
Certain layers filled, other layers partially filled
Superlattice ordering
Random distribution of filled and empty cation sites
Ordered stacking of layers along unique c axis
Random stacking of layers along unique c axis
Superlattice ordering within partly filled layers
Random site distribution within partly filled layers

Figure 5. Scheme A.

This ordered structure is defined by the strict alternation of filled and defective metal layers: . . . $SFe_{1\cdot0}SFe_{0\cdot75}SFe_{1\cdot0}SFe_{0\cdot75}S$ . . ., with empty octahedral positions in the incomplete metal layers arranged as in figure 6(a). Fe_7S_8 (4C pyrrhotite) is the iron-deficient end member of a series of ordered structures $Fe_{1-r}S_r$; $Fe_{1\cdot0}S$ (2C pyrrhotite) the other extreme. In each case the symbol **n**C denotes the number of layers of iron atoms in the repeating stacking sequence. In Fe_9S_{10} (5C) and $Fe_{11}S_{12}$ (6C), the iron-deficient layers (*D* layers) appear to have the same occupancy (one quarter of sites empty) and long range order as in Fe_7S_8, with a higher proportion of filled layers (*F* layers) to *D* layers. A proposed stacking sequence for $Fe_{11}S_{12}$ (Kato *et al* 1975) is: . . . *FFDFDFFFDFDF* . . . *FDFFFDFDFFFDF* . . . . The sequence underlined is an element from the stacking sequence of the 4C superlattice; the implication is that the structure could be regarded as an intergrowth of domains of Fe_7S_8 structure with filled layers, but with out-of-step or antiphase breaks in the stacking. It is evident, however, that the interactions that produce long range ordering are weak; the energy of ordering is small. The careful study of equilibria in the Fe-S system by Nakazawa and Morimoto (1971) shows that disordering sets in at around 100°C and that the ultimate product for all compositions is, IC pyrrhotite with statistically distributed vacant sites in every iron layer. For compositions $Fe_{1\cdot0}S$ to $Fe_{0\cdot95}S$, this complete disordering took place directly; for all compositions between $Fe_{0\cdot95}S$ and $Fe_{0\cdot875}S$, the behaviour was more complex. The superlattice multiplicity became irrational *i.e.* the superlattice was not commensurate with the basic subcell—and changed continuously, with rising temperature. Thus, at the composition of the 6C $Fe_{11}S_{12}$, the superlattice multiplicity for the *c* axis (stacking axis) decreased continuously from 4·5 at 116° to 3 at 200°C, prior to complete disordering at and above 210°C. Kato and Kitamura (1981) and Nakazawa *et al* (1979) find a common basis for ordered structures at particular stoichiometries, and for irrational superlattice multiplicities, in the imposition of a regular, but not necessarily commensurate modulation of the probability of site occupancy. The effect of this is to distribute the vacant sites in a spiral fashion, with a variable pitch. Incommensurability of superlattice structures has been recognized in an increasing number of systems, but understanding of the phenomenon, in nonmetallic structures at least, is limited. Vacancy-vacancy interactions undoubtedly control both the ordering pattern within every *D* layer and the way that *D* layers can be stacked so that the configurational energy is minimized. The incommensurate modulation in some way reflects the operation of these interactions as ordering is impaired at two distinct levels: with rise of temperature, *F* layers increasingly become *D* layers, and long range (but not necessarily short range) order is lost in the *D* layers.

The chromium and titanium chalcogenides are comparably complex. In the system $Cr_{1-r}X$ (X = S, Se, Te), the valence properties of chromium restrict the range of compounds formed ($0 \leqslant r \leqslant 0{\cdot}33$) and the equilibrium state at low temperatures consists of a set of superstructure phases with only narrow ranges of stoichiometry, as shown in table 4. In all of these there is a strict alternation of filled and defective phases . . . *FDFDF* . . ., with good long range order in a succession of two-dimensional superlattice structures of the *D* type layers (figures 6b–e). Cr_7S_8 is the only structure in which the empty sites appear to be randomized. There must undoubtedly be some order-disorder transitions at higher temperatures, but the phase equilibria have not been thoroughly investigated. It is not known whether the structural modulations and incommensurable superstructures found for $Fe_{1-r}S$ constitute a general pattern of progressive disordering in these structures.

Table 4. Ordered phases and stacking sequences in the Cr–S system.

Nominal composition	Observed composition	Layer sequence
CrS*	$Cr_{0.97}S$	... $SCr_{1.0}SCr_{1.0}S$ ...
Cr_7S_8 $Cr_{0.875}S$	$Cr_{0.87}S$–$Cr_{0.88}S$	... $SCr_{1.0}SCr_{0.75}S$ ...
Cr_5S_6 $Cr_{0.833}S$	$Cr_{0.85}S$	... $SCr_{1.0}SCr_{0.67}S$ ...
Cr_3S_4 $Cr_{0.75}S$	$Cr_{0.76}S$–$Cr_{0.79}S$	... $SCr_{1.0}SCr_{0.5}S$ ...
Cr_2S_3 $Cr_{0.667}S$	$Cr_{0.69}S$ (trigonal)	... $SCr_{1.0}SCr_{0.33}S$ ...
Cr_5S_8 $Cr_{0.625}S$	$-Cr_{0.625}S$	... $SCr_{1.0}SCr_{0.25}S$ ...

* Monoclinic distortion of the type structure, with distorted octahedral coordination.

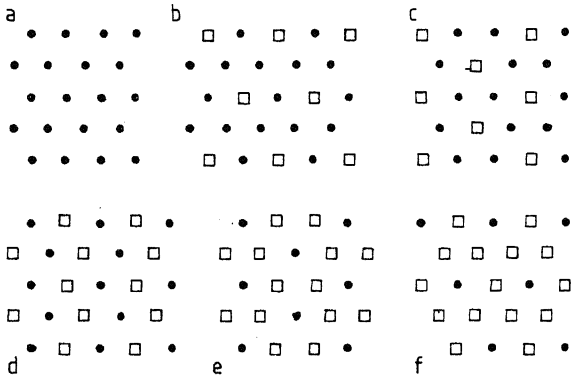

Figure 6. Ordered superstructure arrangements of vacant sites in cation layers of NiAs-type chalcogenides. Fraction of occupied sites: (**a**) 1, (**b**) 3/4, (**c**) 2/3, (**d**) 1/2, (**e**) 1/3, (**f**) 1/4.

Ordering in the Ti-S system is much less perfect, both within the layers and in the stacking of layers. Different workers have reported conflicting results, possibly because of difficulty in establishing true equilibrium and long range order. All the phases intermediate between TiS and TiS_2 have a significant stoichiometric range (table 5) and the reported crystal structures indicate that an irrational fraction of the sites may be occupied in the *D* layers; superlattice ordering is clearly incomplete.

Table 5. Superstructure ordering and stacking sequences in the Ti–S system.

Nominal composition		Reported range	Stacking sequence	Layer sequence
TiS_2	$Ti_{0.5}S$	$Ti_{0.52}S$–$Ti_{0.55}S$	*h*	... $STi_{1.0}STi_{1.0}S$ ...
Ti_5S_8	$Ti_{0.625}S$	$Ti_{0.66}S$–$Ti_{0.67}S$	*cchh*	... $STi_{1.0}STi_{0.2}STi_{1.0}STi_{0.2}S$ ...
Ti_2S_3	$Ti_{0.667}S$	$Ti_{0.67}S$–$Ti_{0.73}S$	*ch*	... $STi_{1.0}STi_{0.4}S$ ...
"$Ti_{2.45}S_4$"	$Ti_{0.61}S$	?	*ch*	... $STi_{1.0}STi_{0.65}S$ ...
Ti_3S_4	$Ti_{0.75}S$	$Ti_{0.77}$–$Ti_{0.78}S$	*chhchch*	... $STi_{1.0}STi_{0.5}STi_{0.95}STi_{0.7}STi_{0.7}$ $STi_{0.95}STi_{0.5}$ ...
Ti_4S_5	$Ti_{0.8}S$	$-Ti_{0.80}S$	*chchh*	... $STi_{0.9}STi_{0.9}STi_{0.6}STi_{1.0}STi_{0.6}S$ ...
		or $Ti_{0.84}S$	?	... $STi_{1.0}STi_{0.65}STi_{0.875}S$ ...
Ti_8S_9	$Ti_{0.89}S$	$Ti_{0.83}S$–$Ti_{0.88}S$	*chh*	... $STi_{0.83}STi_{1.0}STi_{0.83}S$ ...
TiS	$Ti_{1.0}S$	$Ti_{0.94}S$–$Ti_{1.03}S$	*h*	... $STi_{1.0}STi_{1.0}S$ ...

Tilley (1973) showed, by electron microscopy, that materials in the composition range $TiS_{1.25}$ to $TiS_{1.5}$ frequently contained faults of stacking, in the form of the insertion of layers of the wrong kind and composition into the stacking sequence. Such faults can be regarded as accidental nonequilibrium faults. They were rarer in Ti_5S_8, which is better defined stoichiometrically. There is undoubtedly a range in which the composition is genuinely variable and all long range superstructure order is lost, but the extent of this nonstoichiometric phase is not fully agreed. Although there is no well-defined superstructure, there is evidence for the retention of a high degree of short range order. In diffraction experiments, information about this short range order is latent in the diffuse scattering between the Bragg reflections from the basic hexagonal sub-cell. Moret *et al* (1977) systematically examined the diffuse streaking and the diffuse, incommensurate satellite maxima, for compositions between $TiS_{1.5}$ and $TiS_{1.73}$ and found that the observed intensity distribution, and the way it changed with composition, could be reproduced by invoking a model with only two modes of short range ordering, in which interaction between titanium atoms prohibited the occupation of nearest neighbour sites but permitted the occupation of second neighbour or third neighbour sites. In a distribution governed by those rules, microdomains can be identified, with two kinds of local order and extending over a few unit cells of the substructure (figure 7), microdomains A, dominated by third neighbour interactions, have 1/4 of the sites occupied, giving the local composition $TiS_{1.25}$. They can intergrow randomly, and in any proportion, with type B microdomains in which 1/3 of the sites are filled, with the local composition $Ti_{1.33}S_2$. The way sites are occupied in different domains is uncorrelated, so that long range order is completely lost; the boundaries between domains are inherently indeterminate in composition and in their short range order, and will be the location of dynamical exchange of atoms and fluctuations of domain size. A computer simulation of the diffuse scattering, based on the model, was in good accord with the observed diffraction data. A recent theoretical approach to the question of superlattice ordering as a result of pair repulsion effects, considered later, would suggest that atom pairs or vacancy pairs more remote than third neighbours would need consideration for a reliable model of such a system. The model does, however, provide a rational concept of a statistically disordered layer in the hexagonal chalcogenides.

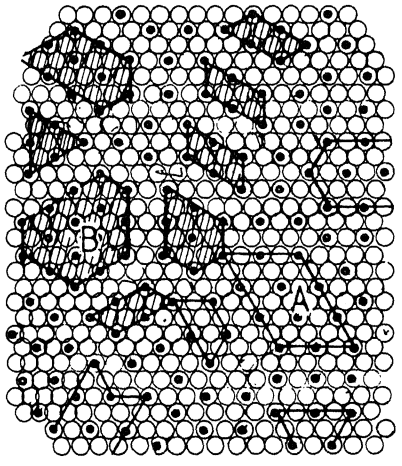

Figure 7. Microdomain model for semi-randomly occupied layers in $TiS_{1.30}$ (after Moret *et al* 1977). Type A microdomains unhatched, type B microdomains hatched.

6. Nonstochiometry and superlattice ordering in rocksalt structures

6.1 *The nature of doped alkali halides*

The simplest possible kind of controlled imperfection is to be found in highly ionic crystals doped with altervalent ions: divalent cations such as Ca^{2+}, Cd^{2+}, Mn^{2+} in alkali halides. Substitution of M^{2+} for A^+ (A = alkali metal atom) must be compensated by creating a cation vacancy. The resulting pair of point defects, $M_A^{\cdot}$ and V_A', can associate through the Coulomb attraction of their effective charges, to neutral dipolar defect pairs $(M_A V_A)^x$. Associated defects of this kind have been extensively studied by relaxation methods and spectroscopic methods, which have confirmed that defect pairs occupy adjacent sites, with the axis of the dipole along ⟨110⟩, as expected; there is also evidence for further association or polymerization of the dipole units.

The concentration of M^{2+} cations that can be doped into alkali halides—*i.e.* the solubility of MX_2 in AX—is steeply dependent on the temperature. When the ionic radii of the cations are closely similar, as in LiF/MgF_2 the solubility at the eutectic temperature may be high, but below about $0{\cdot}8T_m$ it rapidly decreases. For Mn^{2+} and Cd^{2+} in NaCl, Chapman and Lilley (1973) find:

$CdCl_2$ in NaCl	650°K 2×10^{-2} mol%	450°K 3×10^{-5} mol%,
$MnCl_2$ in NaCl	5×10^{-2}	2×10^{-5} mol%.

Cation diffusion in these doped crystals in facile, and is assisted by the possible rotation of the dipoles; aggregation can occur, so that the dopant can be precipitated from solution, to maintain equilibrium, at quite low temperatures. The kinetics of this process have been interpreted in terms of the formation of dimers and trimers of the defect pairs (Cappeletti and De Benedetti 1968; Strutt and Lilley 1972). Stable equilibrium would involve the deposition of the dihalide MX_2 but under any but the slowest cooling rates, the species deposited are metastable phases, which were characterized by Suzuki (1961) as a family $MX_2 \cdot 6AX$, in which the vacant cation sites and divalent cations are arranged in a $2 \times 2 \times 2$ superstructure of the alkali halide parent structure. Sheets of the structure shown in figure 8 alternate with sheets of unchanged rocksalt structure in a f.c.c. arrangement, so that vacant sites and compensating ions occupy second neighbour, not nearest neighbour, sites of the cation sublattice; like defect species occupy fourth neighbour positions.

The reason for easier formation of the metastable Suzuki phase is undoubtedly that it is topologically compatible with the rocksalt structure matrix, with only small dimensional misfit or displacements of atoms. It can therefore be formed by a minimal

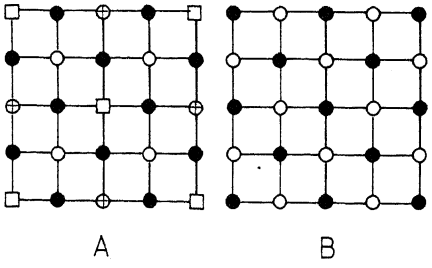

Figure 8. Structure of Suzuki phases: layers of types A and B stacked alternately.

reorganisation of clusters or other units that may pre-exist in the matrix, whereas the structures of the MX_2 compounds are not related to the matrix structure and cannot intergrow coherently. Their deposition would require a nucleation step. The nature of defect clusters in the solid solutions therefore needs further consideration. Brown and Hoodless (1967) argued that the energy of association of a vacancy-impurity dipole pair must depend upon the effective radii of the host and dopant cations. If the dopant is the smaller ion, the distortions and strain energy would be minimized by having the vacancy in the second neighbour site. More recently, Corish and Quigley (1982) have carried out computer simulations by the HADES methods, to calculate the energies of association of different types of cluster. They confirm that the species formed depend upon the relative sizes of host and dopant ions. With smaller dopants, second neighbour dipoles are energetically favoured and there is a small, progressive gain in energy per defect pair as aggregation proceeds, up to a tetramer that would constitute one octant of the Suzuki structure. With larger dopant ions, the next neighbour dipole is more stable, with a considerable gain in energy from forming dimers and trimers which would be ordered in the $\langle 111 \rangle$ plane of the matrix structure. These results confirm the role of dimers and trimers that had been postulated to interpret the transport properties and aggregation kinetics; relevant in the present context is the evidence that they give for some measure of short range structure and order, of a kind that prefigures the formation of superlattice structures. It may be noted that the Suzuki phases are isostructural with $MnMg_6O_8$; it is highly likely that analogous, precursor clusters exist in doped and defective oxide systems.

6.2 *Highly nonstoichiometric carbides and nitrides*

A further stage in the progression from the point defect concept to that of well-defined short range order is found in the most grossly nonstoichiometric of all compounds: the carbides and nitrides of the transition metals (the so-called Hägg or interstitial phases) and the structurally analogous TiO and VO. All are based on close packing of metal atoms, with the nonmetal atoms in octahedral interstices: compounds nominally MX, with the B1, rocksalt structure, and M_2X with hexagonal close packing. They are metallic, with partially filled d band states, so that any interactions due to localised electronic states are minimal, and they are high temperature structures, in that all diffusion-mediated processes are controlled by the large activation energy for non-metal diffusion—4·5 eV per atom in the VC system.

In all these compounds, the available non-metal sites are very incompletely filled and for none of the carbides is the stoichiometric composition attainable; only $TaC_{0.995}$ approaches the limit. In materials quenched from high temperatures, where the only translational symmetry is that of the B1 structure, the phase ranges are very broad; for 'TiC' from $TiC_{0.50}$ to $TiC_{0.87}$, for 'VC', $\sim VC_{0.73}$ to $VC_{0.88}$. Carbides of the lanthanide and actinide elements do reach and exceed the ideal M : C ratio, but not by a simple point defect mechanism. Whilst there is some evidence that carbon can occupy tetrahedral, interstitial sites (*i.e.* simple Frenkel disorder), the excess of carbon is mainly accommodated by substituting a C_2 group (in effect, a C_2^{2-} ion, as in the well-characterised dicarbides such as LaC_2 or CaC_2) on a normal carbon site. In effect, a tetrahedral interstitial carbon atom reacts with an adjacent properly sited carbon atom to form a C_2 unit.

At high temperatures, vacant carbon sites in the rocksalt carbides are statistically

randomized; at lower temperatures, long range ordering of vacant sites can take place. In the VC_x phase, this leads to two superstructures, V_6C_5 and V_7C_8 which undergo first order order-disorder transformations at 1184°C and 1110°C respectively. These superstructure phases themselves have significant composition ranges, and materials intermediate in composition between them show two transformations in DTA experiments (Emmons and Willams 1983). This suggests that they have a high degree of short range order, with microdomains in which the vacant sites are ordered according to either the V_6C_5 pattern or the V_8C_7 pattern. The energy gained by ordering is small, however; for both transitions the latent heat of disordering is about 350 cal per mole of VC_x; a simple application of the Bragg-Williams approximation, assuming complete randomization, would predict an enthalpy of ordering around 435 cal/mole VC_x.

It is by no means likely, however, that short range order is completely lost when long range order disappears at the order-disorder transition. Both the V_6C_5 and the V_8C_7 superstructures are formed by the ordering of vacant sites on to third neighbour positions of the carbon sublattice. This has been attributed essentially to mutual repulsion between vacant sites, due to the elastic strain energy which results from relaxation and atomic displacements. The binding energy within the octahedral shell M_6C surrounding a carbon atom is greater than that of a vacant octahedron M_6V; around the empty site, the metal atoms are displaced outwards by about 0·1 A. The same effects must operate in the random structures, both at high temperatures (where dynamic place-exchange processes compete with short range site preference) and in materials (*e.g.* with $x < 0{\cdot}78$) which undergo no superstructure ordering. Some direct evidence for the persistence of short range order comes from ^{51}V NMR studies of the Knight shift, (Froidevaux and Rossier 1967) which measured the relative numbers of V atoms with 0, 1, 2, 3 adjacent carbon sites vacant in the first shell. The statistics were closer to the pattern of site occupancy in the superstructures than to a random distribution. Similarly, the short range order coefficients α_n for the first, second and third neighbour sites of a vacancy, determined from diffuse neutron scattering, showed the avoidance of first or second neighbour sites (α_1, $\alpha_2 < 0$) and a preference of vacancies for third neighbour positions ($\alpha_3 > 0$).

Superstructure ordering occurs, but less readily, in the other carbides; Nb_6C_5 has been characterized and there is evidence from neutron and electron diffraction for incomplete long range order for several compositions in the ZrC_x systems. The existence of short-range order is however well attested. In all these systems the order-disorder transition temperature is low, relative to the melting point, and the diffusion processes needed to attain order may be too slow for the growth of ordered domains larger than 100–200 Å in size. What remains unknown is the real distribution of vacant sites in the high temperature, disordered equilibrium state: the scale on which the short range ordering forces still impose control over the spacing and spatial disposition of vacancies (For a review see de Novion and Maurice 1977).

One theoretical approach to superstructure ordering is the hypothesis that the pattern of ordering is determined by pair-wise interactions between the species concerned—in the cases just considered, vacancy-vacancy interactions. In principle, the occurrence and the structure of superlattices should be predictable in terms of an Ising model. The underlying assumptions are that the interaction potentials can be correctly formulated and that the pairwise interaction energy will then depend only upon the distance between the two vacancies (or atoms). As a general and much studied problem this is intractable, but Kanamori and others (Kanamori and Kakehashi 1977;

Kanamori 1979) have developed a procedure for searching for the configuration of lowest energy, without calculating the energy of ordering, for any ratio of the components. It has been applied to superstructures based upon the f.c.c. structure. An important question in all discussions of short range ordering is the effective range of interactions; Kanamori's essentially empirical arguments show that it is necessary to take account of interactions out to at least fifth neighbour sites.

In a crystal that contains the atom fraction x of the minority species, the nth neighbour shell provides P_n/xN vacancy pairs per vacancy, when P_n is the total number of nth neighbour vacancy-vacancy pairs in a crystal with N sites. The energy of the system is defined by $E = \Sigma V_n \cdot P_n$, where V_n is the interaction potential for nth neighbours. Without specifying the V_n directly, appeal can be made to experimental facts to establish their sign and relative magnitude, and to predict other superstructure phases. Thus, in the VC_{1-x} system, it can be inferred from the actual occurrence of vacancies in third neighbour positions that V_1, V_2, and V_4 are positive (*i.e.* repulsive), V_3 is negative (attractive). The corresponding numbers of vacancy pairs per vacancy (P_n/xN) in the first five shells can be symbolised S(0,0,3,0,0; 1/8), where the fraction 1/8 of lattice sites is to be occupied by vacancies. The Ising model treatment shows that this configuration would be degenerate in energy with respect to a two-phase mixture of stoichiometric $VC_{1.00}$ and another (unknown) superstructure V_7C_6 with the configuration S(0,0,3,0,3; 1/7) unless the significant range of interactions is extended to the fifth neighbour shell. The existence of V_8C_7 shows that the relevant potential V_5 must be positive and decisive. If the concentration of vacancies is increased above 1/8, vacancies must necessarily be created in fourth or fifth neighbour positions. The maximum concentration that can avoid creating vacancies in the strongly repulsive first and second neighbour positions is 1/6. It can then be shown that for $x = 1/6$ there is a configuration of low energy, symbolised as S(0,0,4,1,2; 1/6), for which there are two geometrical solutions. Both of these superstructures have been observed.

6.3 *Nonstoichiometric B1-type sulphides*

As was discussed earlier, the transition metals from Group V onwards form chalcogenides based upon the NiAs-CdI_2 relationship, with ordered stacking of filled and partially filled hexagonal cation sheets. The d^1 and d^2 transition metals form monosulphides with the basic rocksalt structure, which also exhibit nonstoichiometry due to cation deficiency. Those structures can also be regarded as alternating hexagonal layers of metal atoms and chalcogen atoms, in cubic stacking along the [111] axis of the B1 structure, but they show different characteristics in their propensities for the ordering of defects. Their stoichiometric variability is wide, but the experimental evidence for all systems is very incomplete and somewhat discordant; structural evidence is available only for a few arbitrary compositions within the reported stoichiometric ranges of the $Sc_{1-x}S$ and $Zr_{1-x}S$ systems.

Zirconium monosulphide (or Zr_3S_4) probably exists over a composition range from about $Zr_{0.63}S$ to near stoichiometry (Hahn *et al* 1957). Conard and Franzen (1969) determined a structure for $Zr_{0.77}S$, which may be close to the actual limiting composition, and found that superlattice ordering did not conform to a simple pattern in the distribution of cation vacancies. The monoclinic superstructure cell provides 32 sites for 23 cations, but only one two-fold position is fully occupied; all the other sets of equivalent positions show different degrees of partial occupancy. In any one hexagonal

sheet of cation sites (*i.e.* a (111) sheet of the cubic subcell), site occupancy along every row is modulated. This may be compared with the inferences drawn from revision of the structure of low-TiO, cited below, and leaves unsolved the actual spatial disposition and pair-wise interactions of the sites that are vacant.

For the Sc-S system, rather more information is available. The expected Sc^{3+} compound, Sc_2S_3, is itself a $2\times\sqrt{2}\times 3\sqrt{2}$ superstructure of cation vacancies in a rocksalt matrix structure, with vacant cation sites in second neighbour positions arranged in spirals along the *b* axis (Dismukes and White 1964). Whether this structure disorders at high temperatures is not known. It is not stoichiometrically variable, but loses sulphur at high temperatures to form a second, stoichiometrically variable phase, also derived from the rocksalt type structure, which probably has a wide range of composition. It vaporises congruently above 1700° at a composition around $Sc_{0\cdot80}S$, which is fully disordered at high temperatures. When such material is annealed at 700°, however, vacant sites are ordered into alternate $(111)_{\text{cubic}}$ sheets of cation sites, but not regularly disposed within those cation sheets. This superstructure ordering would conform to behaviour commonly observed in vacancy structures, but recent electron diffraction work (Franzen *et al* 1983) has revealed another effect. Below about 300°C, a second mode of superlattice ordering sets in, which was diagnosed as a secondary ordering of the vacant sites within the defective cation layers, but the resulting superlattice is incommensurate. The vacancies become ordered approximately into every third $(\bar{1}10)_{\text{rhombohedral}}$ plane, but not exactly so; the spacing of the superlattice reflection is $0\cdot346\times d^*(\bar{1}10)$, not $0\cdot333d^*(\bar{1}10)$. This implies that (denoting filled $\bar{1}10$ planes as *F*, defective layers as *D*) the regular layer sequence . . . *FFDFFDFFDF* . . . is occasionally broken by the sequence . . . *FDF* . . . . The anomalies misplace about one *D*-type plane in 13, but are not completely regular.

Incommensurate superlattices of this kind have been found in an increasing number of instances, and particularly in compounds with metallic properties. $Sc_{1-x}S$ is of this kind; the metal atoms in $Sc_{0\cdot80}S$ can be assigned the configuration $3d^{0\cdot4}$, resulting in conductivity by itinerant electrons in the unfilled, narrow 3*d* band. In these circumstances, the incommensurable periodicity could well arise from charge density waves: a static periodic modulation of the electron density coupled with a lattice distortion. The positions of minimum energy, in terms of the collective electron wavefunction, and the potential minima due to the regular periodicity of the S^{2-} anion lattice no longer coincide. The scandium ions are therefore displaced from the ideal lattice sites, optimising the energy of the system by creating occasional displacements of lattice rows (for a discussion of charge density waves in analogous NiAs-type $3d^1$ chalcogenides see Van Bruggen *et al* 1979). If this origin of the irrational superlattice is correct, it is likely that the incommensurability and the transition temperature will be found to depend upon the composition within the $Sc_{1-x}S$ range.

6.4 *Titanium and vanadium monoxides*

Titanium and vanadium monoxides are important for any theories of nonstoichiometry, because of the extreme defectiveness of their nominal rocksalt structures. It was first found by Ehrlich (1939), and fully confirmed by all later work (Banus and Reed 1969) that a large fraction of the sites in both the metal sublattice and the oxygen sublattice is vacant (figures 9 a,b); even in the stoichiometric compounds, about 15% of sites in each sublattice is unoccupied. Although the statistics of site occupancy for both

compounds are very similar, the very different way in which the lattice parameter a_0 depends upon the composition indicates that TiO and VO must accommodate that high formal concentration of vacancies in different ways. The implication is that the defects have some structural organization; if this is the case at lower temperatures, it is improbable that all organized structure is lost under any conditions.

For both systems, the equilibrium diagrams suggest some structural complications, with a transition between high temperature and low temperature forms. High TiO

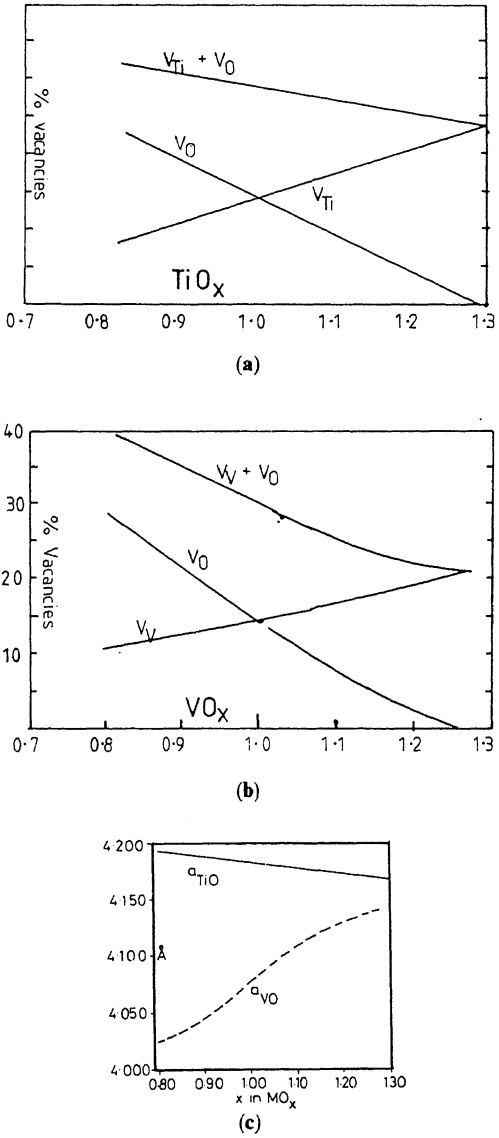

Figure 9. (**a**) Concentration of Ti vacancies and O vacancies in high TiO. (**b**) Concentration of V vacancies and O vacancies in high VO. (**c**) Variation of cell dimension with composition for high TiO and high VO.

appears to have the (averaged) B1 structure, but is stable over a composition range from $TiO_{0.65}$ to $TiO_{1.25}$ at 1500°C. The metal-excess phase limit is markedly shifted at around 1100°C and below 1000°C, low TiO is formed, with a rather narrow composition range. According to Gilles and Wahlbeck (1967), this low TiO coexists with oxygen-rich high TiO, over a restricted range of temperature and composition, but considerable uncertainty remains about the structure of the low temperature oxide between $TiO_{1.0}$ and $TiO_{1.2}$ (Watanabe *et al* 1969; Hilti 1968). Low TiO is monoclinic, with a superstructure based on the B1 subcell found in high TiO; diffuse scattering in the diffraction pattern of the disordered high TiO affords evidence for some short range order in the distribution of vacant sites.

According to Watanabe *et al* (1967) the structure of low TiO has vacancies of both kinds arranged on every third (110) plane of the underlying cubic subcell, giving the stoichiometry $Ti_{5/6}O_{5/6}$; there is some small distortion of the subcell (figure 10). A refinement of this structure (Terauchi *et al* 1978) makes it probable that complete long range order may not be attained, at least for annealing temperatures close to the phase transition; this could possibly be a premonitory phenomenon. There is a significant,

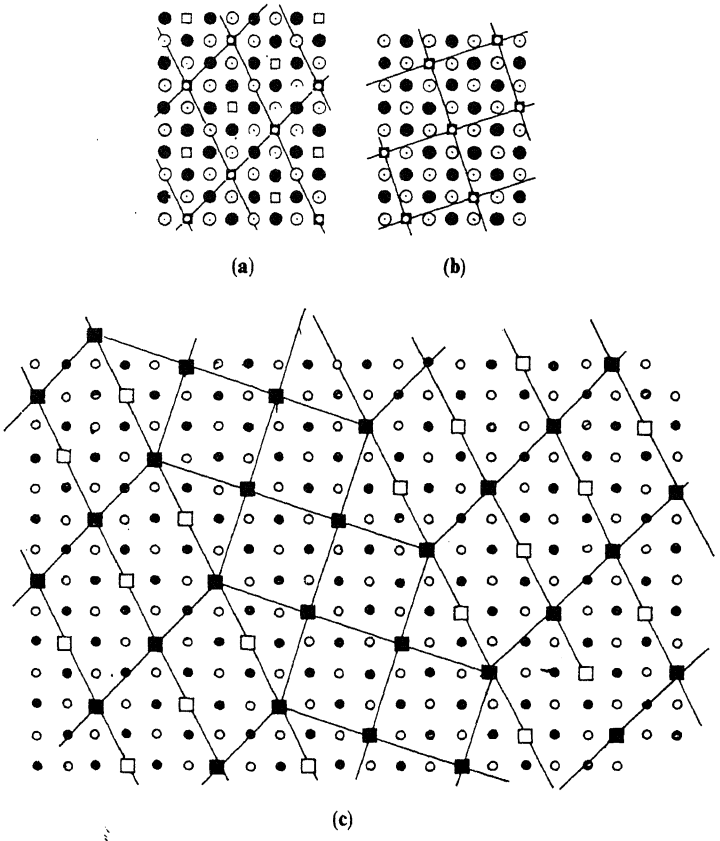

Figure 10. (**a**) Superstructure ordering of vacant Ti sites and O sites in $TiO_{1.00}$ ($Ti_{5/6}O_{5/6}$). Ti cations—filled circles, O atoms—open circles. (**b**) Superlattice arrangement of vacant Ti sites in $TiO_{1.25}$. (**c**) Coherent intergrowth of lamella of $TiO_{1.25}$ in $Ti_{5/6}O_{5/6}$, in formally nonstoichiometric low TiO_{1+x}.

statistically averaged concentration of vacancies (5%) in the (110) cubic planes that Watanabe *et al* regarded as filled. In the partially occupied (110) cubic planes, sites are not completely filled or completely empty, but the fractional occupancy of every site shows a regular wave-like modulation. The general pattern of the superstructure ordering, however, is confirmed.

A second superlattice has been identified at the oxygen-rich limit, $TiO_{1\cdot25}$, and assigned the tetragonal structure shown in (figure 10b) from electron diffraction data. On the assumption (based on the overall site statistics) that the oxygen sublattice is practically fully occupied, one fifth of the titanium sites is vacant in every fifth {310} plane. As with low-TiO, it is likely that a more refined structure determination would modify this model for the superlattice, without changing its essentials. The $(210)_{cub.}$ planes of both superstructures are identical in structure, and the distortions imposed on the underlying f.c.c. array are small. It should therefore be possible for regions with the two superstructures and local compositions to intergrow coherently. Watanabe *et al* (1969) found evidence that well-annealed materials, intermediate in composition between $TiO_{1\cdot00}$ and $TiO_{1\cdot25}$, indeed consist of exceedingly finely intergrown lamellae of the two superlattices; the lamellae may be as little as 20 Å thick. The distribution of vacant Ti sites in such a lamella is shown in figure 10c; it would clearly be possible to postulate more complex modes of superstructure ordering, intermediate between these extremes.

In both superstructures, ordering can be ascribed to pair interactions between vacant sites. Elastic forces arise through small shifts of atomic positions around a vacancy; vacant sites interact with the collective electron system of the crystal. Below about 1000°, the interaction energy is large enough to establish the superlattice; the problem of interest is to determine how far the main features of that ordering pattern are retained in the high TiO structure and evidenced by the diffuse scattering.

Both superstructures have a short c axis ($c_{ss} = a_{cub.}$), which creates strings of vacant sites in second neighbour positions of the titanium (or the oxygen) sublattice—*i.e.* in alternate $(001)_{cubic}$ sheets. Within any one $(001)_{cubic}$ sheet, both superstructures preferentially locate vacancies in third neighbour positions, so disposed as to result in either the $Ti_{5/6}O_{5/6}$ structure (fourth neighbours vacancies in any one $(001)_{cub}$ sheet) or the $Ti_{4/5}O$ structure (fifth neighbours). A unit diffusion jump of $1/2a_{cub}\langle 110\rangle$ would transfer a vacancy from a position belonging to one superstructure to that appropriate to the other. Alternatively described, the oxygen sublattice sites are surrounded by two kinds of polyhedra: complete octahedra of titanium atoms $[OTi_6]$ or incomplete octahedra of the type *trans*-$[OTi_4V_2]$. Similarly, in the low TiO superstructure there are $[TiO_6]$ and $[TiO_4V_2]$ coordination polyhedra. *Correlated* unit shifts of atoms can (a) interchange the positions of complete and incomplete octahedra within any layer or (b) change the orientation of (*e.g.*) $[OTi_4V_2]$ octahedra, thus rotating the local symmetry axes. *Uncorrelated* atom movements would replace $[OTi_6]$ and $[OTi_4V_2]$ octahedra by $[OTi_5V]$ octahedra in any orientation. With increasing randomness, the clustering of vacancies to form polyhedra with three or more empty vertices may occur.

Terauchi and Cohen (1978, 1979) have mapped and analysed the diffuse x-ray scattering from high-$TiO_{1\cdot0}$ at 1050°C, in order to determine the short range order parameters, and have used the experimentally determined order parameters in computer simulation experiments to examine the kind of local structures that they might imply. The outcome is rather inconclusive. The simulation experiments did throw up very small regions that resemble fragments of the superstructure, in larger

numbers than were found in simulations of random vacancy distributions, but the differences were small.

In TiO, all structure elements occupy sites of the underlying f.c.c. lattice: the superstructure comes from the long range order of vacant sites, and in the nonstoichiometric disordered phase at least some vestigial local, short range organization of recent sites is retained. In VO- and also in the monoxides of Mn, Co and Fe, which are all significantly nonstoichiometric rocksalt structures, there is a more drastic perturbation of the parent structure: vacant sites and compensating charges are mutually stabilised by locally modifying the parent structure, forming defect clusters as distinct structure elements.

The VO superstructure is formed only at the oxygen-rich end of the composition range, and unit cell formulae have been assigned for slightly different compositions: $V_{52}O_{64}$ ($VO_{1\cdot23}$) (Andersson and Gjönnes 1970) $V_{244}O_{320}$ ($VO_{1\cdot31}$) (Bell and Lewis 1971) and the most complete determination, $V_{51\cdot6}O_{64}$ ($VO_{1\cdot24}$; but the analytical composition of the sample was $VO_{1\cdot30}$) (Morinaga and Cohen 1979a). At that composition, the oxygen sublattice is essentially filled. Diffraction evidence unambiguously shows that some vanadium atoms occupy tetrahedral sites. Hence the total concentration of vacant octahedral sites is the sum of the stoichiometric deficit plus vacancies created by shifting metal atoms from octahedral to tetrahedral 'interstitial' positions: $M_{oct} \rightarrow M_{I,tetra} + (V)_{oct}$.

Each tetrahedral cation has four vacant octahedral sites as nearest neighbours, forming the structured cluster or complex shown in figure 11a. This cluster is topologically and dimensionally interchangeable with one octant of the parent B1 structure, and in the superlattice four such units are regularly arranged to define a $2\sqrt{2} \times 2\sqrt{2} \times 2$ superstructure (figure 11b). In the ideal $V_{52}O_{64}$, all lattice sites, other than those of the defect clusters are occupied as in the parent B1 structure, but in the vanadium deficient $VO_{1\cdot3}$, some of the octahedral positions appear to be partially occupied. It will be noted that, at least in the $V_{52}O_{64}$ superlattice, all the vacant octahedral sites are in the clusters: there are no free vacancies, whether ordered or disordered.

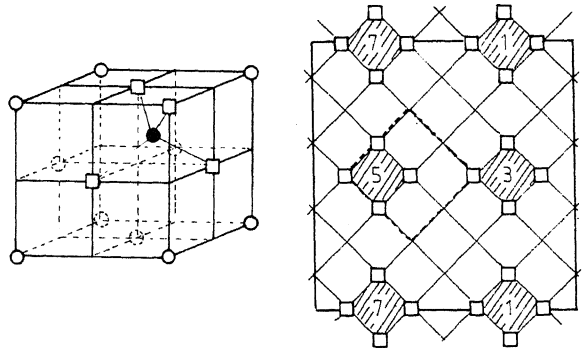

(a) (b)

Figure 11. (**a**) The 4:1 complex of 1 tetrahedral cation and 4 vacant octahedral sites, as one octant of the rock salt sub-cell. (**b**) Ordering of 4:1 defect clusters in rocksalt-type matrix structure, in $VO_{1\cdot30}$. Tetrahedral cations at levels Z = 1/8, 3/8, 5/8, 7/8 of superstructure cell.

The question then is how this highly organized superlattice is related to the disordered, broad range VO_x phase formed at high temperatures, in which there are fewer vanadium vacancies and high concentrations of vacant oxygen sites. Morinaga and Cohen (1979b) have analysed the diffuse x-ray scattering from three preparations in the nonstoichiometric range: $VO_{0.89}$, $VO_{1.17}$ and $VO_{1.28}$, annealed at 1323°K and quenched but hopefully representative of short range order in the VO_x phase. Short range order parameters derived directly from the diffraction data can be used to form a model that fits the observed probability of finding a vacant site or tetrahedral atom with a particular *n*th neighbour environment. It was concluded that tetrahedral vanadium atoms are present, at all compositions, in much the same environment as the cluster of figure 11a, though in variable amounts and randomly distributed. A constraint on model building is that the energy can be minimized, as compared with that of a completely random distribution of vacant sites, by ensuring that there is local charge balance.

As compared with a completely random structure of the composition VO_x, every empty metal site is associated with a virtual (fractional) negative charge; every occupied metal site with a virtual positive charge. Each kind of site will have an energetic preference for first neighbours of the opposite kind. If the B1 structure is regarded as a stack of $(111)_{cubic}$ layers, each layer will be a hexagonal array of sites of the one kind (*e.g.* metal sites), arranged in . . *ABCA* . . . stacking. Next neighbour site preference (local electroneutrality) influences how adjacent sites in consecutive layers should best be occupied; within any one layer, second neighbour and higher interactions determine which hexagonal subsets of sites are preferentially filled, and which have an averaged occupancy. Morinaga and Cohen concluded, on that basis, that the resultant structure should be modulated, with alternating vacancy-rich and vacancy-poor $\{111\}_{cubic}$ planes. The periodicity would approximate to twice that of the B1 parent structure, in accordance with the strong diffuse x-ray scattering. As the composition changed from the oxygen-rich end (where the structure is essentially that of disordered superlattice) to the oxygen-poor end of the phase range, the proportion of virtually filled metal layers would increase, and the modulated partial filling would increasingly affect the oxygen layers. In the metal atom layers, the optimum highest concentration of vacant sites would be for one site in three to be empty; if this were fully ordered, it would be the same as a cation layer from the V_2O_3 corundum structure; if disordered, it could form microdomains of that structure. There is, then, a sense in which the modulation of the disordered VO structure generates elements of V_2O_3 structure at one extreme, and of V_2O structure at the other.

6.4 *Finite extended defects: defect clusters*

What are ordered in the superstructure of the $VO_{1.30}$ phase are not simple defects, but clusters with a characteristic structure, formed by local rearrangement of the matrix structure. It is clusters of this kind that produce nonstoichiometry in the monoxides of the elements that follow vanadium in the first transition series; clusters also dominate the defect chemistry of both substoichiometric and hyperstoichiometric compounds derived from the fluorite type, and it is likely that they play a role in other structural types also.

They prompt a number of questions about how a host structure is locally perturbed to form a defect cluster and how far chemically specific effects determine the form and

steric arrangement of the cluster; about the theoretical justification for regarding the clusters as the significant building blocks of defect structures; and about the role that specific kinds of defect clusters play in crystals that have a widely variable range of stoichiometry. There are several possibilities. The same kind of cluster might be present, right across that range but in variable concentrations; alternatively, the recognized cluster may represent a pattern of local ordering, which can grow and extend to larger or polymeric units as the nominal concentration of interstitial or vacancies is increased. If clusters of the same kind persist in varying concentration, they should be subject to superlattice ordering within a matrix of parent structure. Underlying those problems is the basic question whether, and if so under what conditions, a point defect regime at very small deviations from ideal stoichiometry passes over to an extended defect cluster regime at some higher stoichiometric deficit. On that question, there appears to be very little information extant.

Defect clusters, by definition, are formed by purely local changes in the way lattice sites are occupied; they are necessarily compatible, topologically, with the parent structure. In principle, the requisite local rearrangement to form a defect cluster could be brought about around any lattice site in a crystal, thereby generating a random distribution of defect clusters. They are permutable over all lattice sites and thus contribute to the configurational entropy, but their strict spatial configuration represents some decrease in the entropy of the crystal. It is tempting to regard defect clusters as 'plug in' modules, that might be mixed in with the perfect parent structure in any proportions. This simplistic interpretation of crystals with wide composition ranges may, however, need very critical appraisal.

Much of our thinking about structured defect clusters comes from the study of two classically nonstoichiometric systems; wustite, $Fe_{1-x}O$ and uranium dioxide, UO_{2+x}. Recognition that structured clusters at least partially replaced point defects in $Fe_{1-x}O$ come from Roth's (1960) neutron diffraction study, which showed that a very significant fraction of iron atoms must be assigned to interstitial sites, with tetrahedral coordination. Formation of iron-deficient wustite must therefore involve not only the process (10)

$$(FeO)+\tfrac{1}{2}O_2 \rightarrow 2Fe^{3+}_{oct}+O^{2-}+V_{oct} \tag{10}$$

but also a second step, in which a cation moves from an octahedral site to an interstitial position:

$$Fe_{oct}+V_{int} \rightarrow Fe_{tetr}+V_{oct}. \tag{11}$$

The net reaction would be:

$$2Fe^{2+}_{oct}+\tfrac{1}{2}O_2 \rightarrow Fe^{3+}_{oct}+Fe^{3+}_{tetr}+2V_{oct}+O^{2-}. \tag{12}$$

The tetrahedral iron atom (presumably Fe^{3+}, from ligand field considerations), with a pair of adjacent, empty octahedral sites, would resemble a small element of the spinel structure of Fe_3O_4.

Wustite has a restricted range of existence and is unstable below 560°, but its disproportionation into Fe_3O_4+Fe is slow. Nearly all work on $Fe_{1-x}O$ has been carried out on quenched material, on the assumption that the high temperature structure could be frozen in and retained. That assumption is not necessarily correct. Several workers, particularly Manenc (for a review see Bauer and Pianelli 1980), have found that satellite reflections appear in the diffraction pattern when the quenched

material is annealed at 200–500°C, within its unstable existence range. These satellites indicate some incommensurate ordering process. A homogeneous, probably spinodal decomposition ensues, for compositions with $x < 0{\cdot}09$:

$$Fe_{1-x}O \rightarrow Fe_{1-x-y}O + Fe_{1-x+y}O \tag{13}$$

which builds up a lamellar structure, in which the iron-rich lamellae approach increasingly closely to the ideal composition, as is shown by the progressive change in cell dimensions.

Perfect superstructure order is never reached in a macroscopic crystal: the outcome has a microdomain texture. Koch and Cohen (1969) sought to determine the defect structure from single crystal x-ray diffractometry on $Fe_{0{\cdot}902}O$ and concluded that the defect clusters are more complex than the 4 : 1 cluster that was discussed as an element of the $VO_{1{\cdot}30}$ structure. To account for the observed intensities, particularly of the nearest neighbour and second neighbour diffraction vectors between pairs of vacant sites, and between tetrahedral cations and vacant octahedral sites, they postulated a 13 : 4 cluster (figure 12), with tetrahedral cations in four octants of a f.c.c. cell, in which the central and the 12 surrounding octahedral cation sites were all vacant. The anion lattice thereby remains unchanged. This defect cluster retained the cubic symmetry of the parent structure, but in fact, that symmetry is not readily reconciled with the superlattice periodicity $5/2\,a_0$ found by Manenc for $Fe_{0{\cdot}910}O$, or with the symmetry shown by the electron microscope lattice images (at about 4A resolution) (Iijima 1974). Cubic symmetry in diffraction patterns could, however, be the consequence of degeneracy in microdomains oriented with equal probability in relation to all $\langle 100 \rangle$ cubic axes.

What is important is to relate the defect structures deduced from quenched specimens, at room temperature, to the actual structures under equilibrium conditions. This difficult and general experimental problem has been tackled for very few nonstoichiometric systems; reference has already been made to the somewhat inconclusive high temperature studies of TiO and VO. For several experimental reasons, neutron diffraction may be a more suitable technique than x-ray diffraction for work of this kind. Still awaiting full exploitation are the possibilities presented by high voltage (1 MeV) electron microscopy, for electron diffraction and imaging techniques, using controlled atmosphere high temperature stages. In the case of $Fe_{1-x}O$, short range order parameters have been determined by analysing the diffuse x-ray scattering from a high temperature specimen (Hayakawa *et al* 1974) but more direct evidence comes from using Bragg neutron diffraction to determine the relative concentrations of empty octahedral sites ($[V_O]$) and tetrahedral iron atoms ($[T_I]$) from the structure factors of appropriate reflections. This has been done by Cheetham *et al* (1971) and Gavarri (1978), for wustite held under equilibrium conditions. The ratio V_O/T_I depends upon the particular model postulated for the defect cluster and is more directly informative than the short range order parameters.

Several crystallographically reasonable defect clusters would have rather similar ratios V_O/T_I, and the experimental results (figure 13) do not really discriminate between the possibilities; nor do they establish whether the same clusters are present at all compositions and over the whole temperature range. Cheetham's results would not be inconsistent with the 13 : 4 Koch-Cohen complex and with some dissociation into 4 : 1 clusters, but Gavarri's later work points to clusters with $V_O/T_I \sim 2{\cdot}5$ under all conditions.

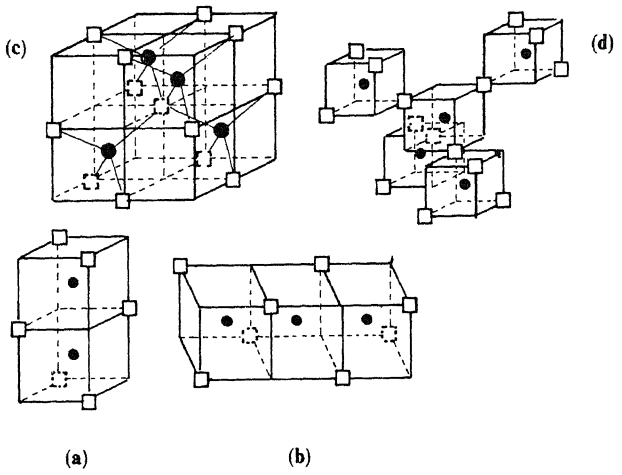

Figure 12. Aggregation of 4:1 clusters to larger defect complexes. (**a**) 6:2 cluster, (**b**) 8:3 cluster, (**c**) 13:4 (Koch-Cohen) cluster, (**d**) 16:5 cluster.

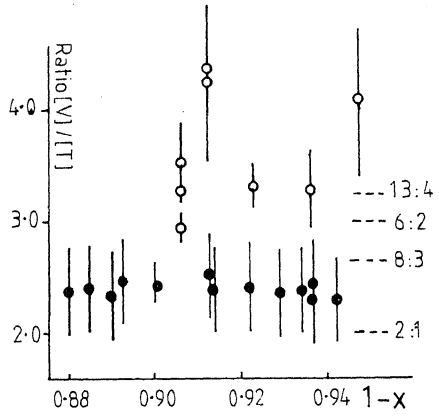

Figure 13. Ratio of concentrations of vacant octahedral sites to tetrahedral, interstitial cations in wustite, from neutron Bragg diffraction. Open circles: results of Cheetham *et al* at 800–1150°C; filled circles: results of Gavarri (1978) at 985° and 1075°C. Ratios expected for certain cluster types shown at right.

Such experimental ambiguities lend extra importance to theoretical treatments of the stability of various cluster models, such as have been carried out by Catlow and his associates (see Catlow 1982), using the HADES and PLUTO computational techniques developed specifically for defect studies. Calculations for $Fe_{1-x}O$ (Catlow and Fender 1975; Catlow *et al* 1977) clearly establish that clusters of the kind considered above are formed with a net gain in energy: transfer of Fe^{3+} cations from octahedral to tetrahedral sites, further aggregation of vacancies and enlargement of the cluster according to the rules of near neighbour and second neighbour site preferences are all exothermic processes. The relative stability of different clusters should be measured by

the gain in energy per net defect, where the net defect, [= (*total number of vacant sites*) − (*number of tetrahedral atoms*)], corresponds to the notional primary process of equation (10).

The basic unit would be the 4:1 cluster (figure 11a) which has a substantially higher binding energy than the simple dipole associate $\{(V''_{oct})(Fe^{\cdot\cdot\cdot}_{tetr})\}$ or Roth's original proposal, $\{(V''_{oct})_2(Fe^{\cdot\cdot\cdot}_{tetr})\}'$. Larger clusters can build up through the linking of the basic 4:1 units, as in figures 12a [6:2], 12b [8:3] and the Koch-Cohen 13:4 cluster figure 12c. The net process for forming any cluster $\{(V_{oct})_m(Fe_{tetr})_n\}$ from the perfect FeO structure could be written:

$$2(m-n)Fe^{2+}_{oct}+\frac{(m-n)}{2}O_2, \rightarrow$$

$$(2m-3n)Fe^{3+}_{oct}+\{(V_{oct})_m(Fe^{3+}_{tetr})_h\}^{-(2m-3n)}+\frac{(m-n)}{2}O^{2-}. \qquad (14)$$

The clusters thus bear a net anionic charge; they incorporate only a minority of the Fe^{3+} cations and must be surrounded by an ionic atmosphere of compensating Fe^{3+} cations in octahedral sites of the matrix structure surrounding each cluster. These compensating ions are significant for the electronic and atomic transport properties, and for the possible ordering of the clusters.

Table 6 compares the binding energy per net defect for some cluster models. These are not the only possibilities; computational problems restrict the calculation of binding energies to the more symmetrical configurations. It is noticeable that the Koch-Cohen 13:4 cluster does not emerge as the most favourable model. In general, the greatest energy gain would appear to come through progressive corner sharing between 4:1 units; larger clusters, such as the 16:5 cluster (figure 12d) could well be important. This cluster is a genuine element from the spinel structure of Fe_3O_4 and could be invoked as a participant or precursor in the disproportionation of wustite. Starting from the perfect B1 structure (as is operationally possible in *e.g.* the $Mn_{1-x}O$ system), oxidation through the stoichiometric range could well involve the successive stages (scheme B):

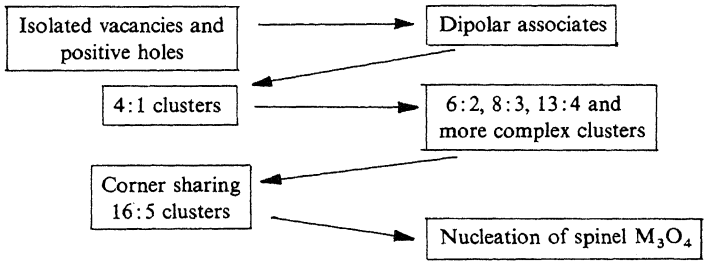
Isolated vacancies and positive holes
Dipolar associates
4:1 clusters
6:2, 8:3, 13:4 and more complex clusters
Corner sharing 16:5 clusters
Nucleation of spinel M_3O_4

Scheme B.

There should be a transition, at some low level of nonstoichiometry, from a point defect regime to a regime dominated by clusters. Only the latter is observable for $Fe_{1-x}O$, but for $Mn_{1-x}O$ Catlow has calculated the relative concentrations of different defect species on the assumption that there is a quasichemical mass action equilibrium

Table 6. Binding energies of defect clusters (eV per net defect).

Associated cluster type	$Mn_{1-x}O$ system	$Fe_{1-x}O$ system
Aggregate of 1 vacancy + 1 M^{3+} cation	0·53	0·63
Aggregate of 1 vacancy + 2 M^{3+} cations	0·71	0·90
4:1 cluster (M^{3+} interstitial)	1·77	1·98
6:2 cluster	2·06	2·42
8:3 cluster	(1·84)*	2·52
13:4 cluster	(0·06)*	2·10
16:5 cluster	(1·94)*	2·38

* M^{2+} cation in interstitial position; After Catlow *et al* (1977).

Table 7. Relative concentration of defect species in $Mn_{1-x}O$ as function of deviation from ideal stoichiometry.

Deviation from stoichiometric composition	Isolated vacancies (%)	Singly ionised vacancies (%)	4:1 clusters (%)	Larger clusters (%)
10^{-5}	100	0	0	0
10^{-4}	95	5	0	0
10^{-3}	58	22	19·5	0·5
10^{-2}	8·3	4·7	77	10
10^{-1}	1	1	76	22

After Catlow *et al* (1977).

between them. The results are shown in table 7. Cluster binding energies are higher for the $Fe_{1-x}O$ system than for the other transition metal oxide systems, so that free point defects and small clusters must be even less significant than in $Mn_{1-x}O$.

What matters for the display of stoichiometric variability is the total free energy of formation of clusters from the perfect parent structure. The large, positive enthalpy of creating the total number of vacant sites and interstitials is partially offset by the exothermic binding energy of the clusters. The critically significant, positive configurational entropy of a random distribution of clusters is reduced by the decrease of entropy involved in local ordering within each cluster. Only the enthalpy of clustering is treated in the stability calculations.

It is evident that these considerations do not fully resolve the problem of the constitution of wustite at high temperatures. This has been critically reexamined by Bauer *et al* (1980), in a careful study of the incommensurate satellite peaks in the diffraction patterns. As Koch and Cohen showed, every Bragg reflection in the reciprocal lattice is at the centre of an array of satellites that, themselves, form a cubic lattice of side $2\delta a$ (where δ is an irrational fraction); the satellites thus correspond to a translational periodicity of $1/\delta \times a_0$ in real space; for each Bragg reflection with the index triplet (h) there are satellites $(h \pm n\delta)$. For the purpose of their Patterson synthesis, Koch and Cohen made the approximation $\delta = 1/3$; although all workers agree that δ is both irrational and variable. From measurements on quenched samples, Bauer *et al* (1980) showed that δ is a linear function of the stoichiometric defect and, moreover, is

slightly dependent upon the temperature at which a given composition was equilibrated before quenching. Electron microscope lattice images, taken using the satellite reflections, represent the Fourier transform of the quasi-periodic structure that generates those satellites; they do not give direct information about atomic positions in real space, but can be taken as correctly representing the relative positions and actual spacing of the entities (*i.e.* the defect clusters) that are responsible for the irrational quasi-periodicity. The important inference drawn from such micrographs was that there is no evidence for microdomains with rational, but different periodicities; rather, and in every sample, there was a similar and uniform distribution, which was not, however, absolutely regular along the ⟨100⟩ and ⟨110⟩ directions. On all the evidence, Bauer *et al* consider that the concept of some single, stable species of cluster, dispersed through the B1 matrix structure, has to be abandoned. In its place they consider a function defining the local probability of finding Fe^{3+} cations in tetrahedral sites, together with octahedral vacancies and consequential displacements of adjacent atoms, as governed by the site preference energies or pair interactions. The irrational superstructure results from an incommensurable modulation of this probability function; the periodicity of the modulation, and the magnitude of the ratio V_0/T_I that characterises the local order at each point, are then averages over the whole crystal. Some constraints can be set. It can be shown that, if there were uniform defect clusters of the type $m:n$, the most compact superlattice for $Fe_{1-x}O$ would have a composition given by

$$x = \delta^3(m-n)/4.$$

Thus, for the Koch-Cohen cluster ($\delta = 0{\cdot}333$), $x = 0{\cdot}083$ ($Fe_{0{\cdot}917}O$). For specimens quenched from 900°C, the observed range of δ was from 0·370 (for $Fe_{0{\cdot}916}O$) to 0·392 (for $Fe_{0{\cdot}892}O$). The corresponding range of $(m-n)$ is from 6·63 to 7·17. If the short range order can be represented as the coexistence of several kinds of cluster $m_i:n_i$, each occurring with the probability p_i, the requirement is that

$$6{\cdot}163 < \sum_i p_i (m_i - n_i) < 7{\cdot}17.$$

To fit this constraint, there must indeed be a variation in the details of the local ordering pattern, from point to point within the crystal, in which clusters of different size could be picked out. It is evident that clusters comparable with the 8 : 3 and 13 : 4 models are likely to be significant structure units, and the model leaves scope for the dynamical situation that must obtain in a high temperature system with a high diffusion rate for the cations. The life of any one cluster will be finite, resulting in a distribution of cluster sizes and geometries. What is left vague, as is the case for some other examples currently considered to be modulated structures, is the origin of the incommensurate modulation of the whole assembly.

7. Nonstoichiometric fluorite derivatives

Closely following Roth's finding, that defects in the rocksalt structure of $Fe_{1-x}O$ are not simple point defects, it became clear that extended, cluster defects replaced point defects in another of the principal type structures. This followed from the structures

found for the anion-excess fluorite compounds, U_4O_9 and the nonstoichiometric $UO_{2\cdot12}$ (Willis 1963, 1964).

Of all the basic type structures, the fluorite structure is the most flexible, for it generates a remarkably varied range of derivative structures, both stoichiometrically variable and fully ordered, in which the *anion/cation* ratio may be either $> 2(AB_{2+x})$ or $< 2(A_{1+y}B_2)$. At an early stage, it was shown by Zintl that in every case studied, the disorder and variable site occupancy was confined to the anion sublattice; although various workers, from time to time, have invoked cation vacancies and disorder in the cation sublattice, such assumptions are not justified. It is a safe hypothesis that the cation sublattice remains sensibly perfect, while the anion sublattice can tolerate a remarkably wide range of anion deficiency or anion excess. This is true both for oxides MO_2 and halides MX_2, formed by metals with variable valence and for heteroinic solid solutions such as CaF_2-YF_3.

This stoichiometric flexibility can be correlated with some inherent characteristics of the fluorite structure. The anion sublattice is mobile, as shown by unipolar anionic conductivity and high self-diffusion rates, even though the activation energies for anion transport processes are not abnormally low. All fluorite structures appear to undergo a transition to a superionic conducting state; the transition is spread over a temperature range, some way below the melting point. By contrast, the cation sublattice has a low mobility; cation diffusion is slow and, in heteroionic crystals, the ordering or disordering of cation distributions can take place only at high relative temperatures. Some important experimental consequences flow from these properties. In homoionic structures, defect interactions can efficiently bring about any superlattice ordering that affects only the anion sublattice; the location of charge compensating electronic defects (altervalent cations) can follow the pattern of local structure by a process of electron transfer (polaron migration). In heteroionic systems, sample preparation is likely to result in a fortuitous and random distribution of cations, which may be frozen in by the immobility of the cation sublattice. Charged defects in the anion sublattice (whether point defects or extended defects) can migrate to and are anchored at the randomly sited altervalent cations. The resulting configuration may well be metastable with respect to some superstructure ground state, but that ground state cannot be reached unless the cations can diffuse and adopt the requisite long range order.

In a formal, point defect sense, all fluorite structures exhibit anion Frenkel disorder. There are strong vacancy-vacancy pair interactions in substoichiometric fluorites, as is evident from the almost invariable pairing of vacant sites into third neighbour positions at the diagonally opposite corners of a cubic coordination group, which can be symbolized $[MX_6V_2]$. The six adjacent cubic coordination groups that share edges with this central unit thereby become $[MX_7V]$ groups. The outcome is the cluster unit shown in figure 14a, with the composition M_7X_{12}; the central cation is then in distorted octahedral coordination.

This unit, can intergrow freely with the parent fluorite structure, and from such intergrowths are derived several modes of superstructure ordering (Rossell and Scott 1977). Linear strings of the clusters, along $\langle 111 \rangle$ of the parent fluorite structure form the structural motif in the M_nO_{2n-2} intermediate oxides of praseodymium; the only motif in Pr_7O_{12} and, intergrown with increasing proportions of pure fluorite structure, in Pr_9O_{16} and the higher oxides. These are low temperature structures, formed through the high mobility of vacant sites in the anion lattice and the facile (electron transfer) ordering of +3 and +4 cations needed to maintain local electroneutrality. In

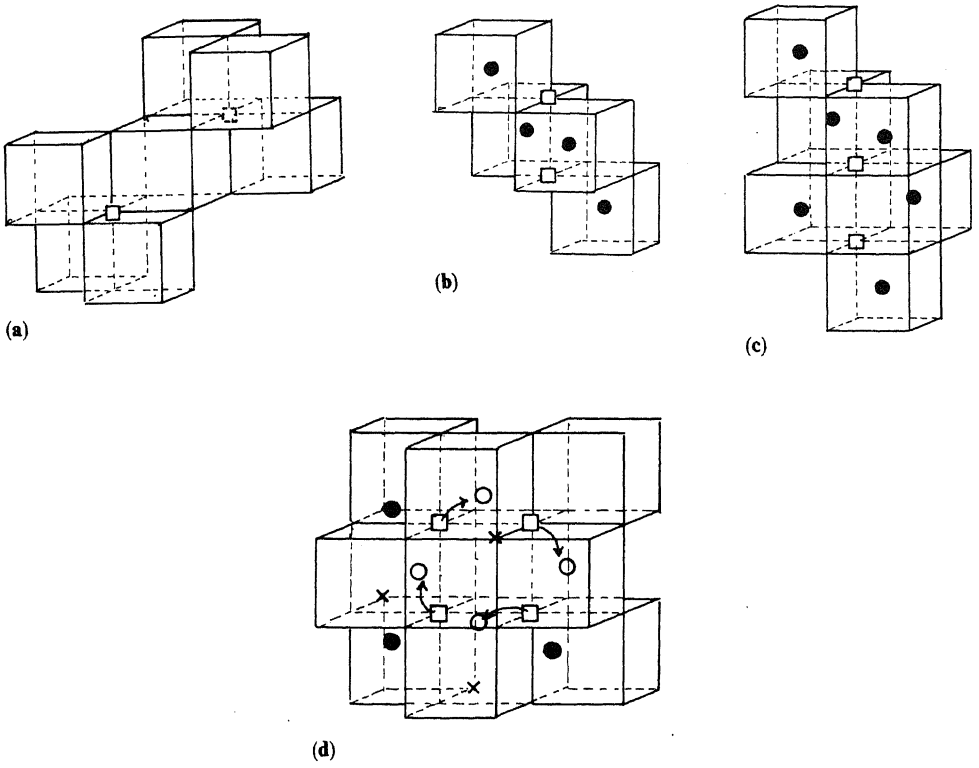

Figure 14. Defect clusters in anion-excess fluorite structures. (**a**) vacancy pair cluster (**b**) 2:2:2 cluster (**c**) 3:4:2 cluster (**d**) 4:4:4 cluster as proposed by Laval and Frit (1983).

heteroatomic systems, the smaller cation usually occupies the octahedral site, but the degree of cation ordering depends upon the relative site preference energies, varying from complete order in UY_6O_{12} to complete randomness in $Zr_3Sc_4O_{12}$. In so far as superlattice ordering depends upon simultaneous ordering of the cations, it is a slow process, conditioned by cation mobility.

Superlattice ordering in other systems can generate zig-zag chains (pyrochlore structures), helical chains (in $Ca_6Hf_{19}O_{44}$) or larger clusters (in $CaHf_4O_9$). Cation ordering is good in the anion deficient systems based upon ZrO_2 and HfO_2 and this is important not only in its technological implications, but also because it sheds light on the defect structure. At high temperatures, all the superstructure phases disorder to a defect fluorite phase MO_{2-x}, which exists over a wide range of composition, as distinct from the narrow existence ranges of the ordered phases. For the praseodymium and cerium oxides, this disordering takes place at a fairly low temperature (*ca* 600°C); the resulting α-phase extends from $MO_{1.71}$ to MO_2. The first supposition might be that the vacancy-pair clusters were randomly dispersed in the defect fluorite phase, but several considerations make that view questionable. The heteroatomic anion-deficient fluorites disorder at much higher temperatures and, for those that have complete cation ordering, the disordering is slow; cation diffusion is rate-controlling. In all these defect fluorite solids, there is a very high formal concentration of anion vacancies, (up to 15% or more of anion sites) and because anion diffusion in fluorites is a vacancy migration

process, the diffusion rate and unipolar ionic conductivity are increased by several orders of magnitude as a result of the extrinsic vacancies in solid solutions, such as $(M, M')O_{2-x}$. As is familiar, this is the basis for the use of CaO- or Y_2O_3-doped zirconia as a solid state, oxygen ion electrolyte. The enhanced mobility does not, however, follow the expectation of a simple vacancy model; if vacancy concentrations alone determined the ionic carrier concentration, the conductivity of MO_{2-x} should be proportional to $x(1-x)$. This is not the case, as shown by extensive work on the technically important $CaO\text{-}ZrO_2$ and $Y_2O_3\text{-}ZrO_2$ systems, and by the work of Nowick *et al* (1979) on $Y_2O_3\text{-}CeO_2$. For the latter, the conductivity rises linearly with concentration up to about 8 mole% Y_2O_3, but falls by four orders of magnitude with further increase to about 20 mole%. It is clear that there are strong interactions. For the partially ordered superlattice phase $Zr_3Er_4O_{12}$, the ionic conductivity is low: the empty fluorite anion positions are not mobile point defects. At 1500°C, when this phase undergoes complete disordering, to $(Zr, Er)O_{1.714}$, the ionic conductivity increases by several orders of magnitude, and this enhanced conductivity is shown at temperatures below 1500° if the fluorite material is retained in the disordered metastable state by cooling.

That there are strong local ordering effects is also evident from the strong diffuse x-ray, neutron and electron scattering, which has been studied by a number of workers. The nature of that short range order is not clear. Rossell has suggested that there are two main alternatives. One is that the distribution of vacant sites is fairly homogeneous throughout the structure, on a short range or medium range scale, but that short range order imposes strong constraints on place exchange processes. Alternatively, the medium range structure may be quite inhomogeneous, with microdomains of the fully ordered superstructures. He has cited evidence for the latter in the Ca-Zr and Ca-Hf oxides, with microdomains of the superstructure phase that can be identified in the systems, a few tens of Angstroms in dimensions. At not too high temperatures, such domains can grow to the extent of nucleation of a new phase, and it is not certain whether the microdomain situation is really a stable state of these systems.

Catlow and Parker (1982) have formulated a theoretical treatment of systems of this kind, which takes account of several significant features of the real systems. As discussed earlier, in connection with $Fe_{1-x}O$, the concept of discrete, localised and immutable defect clusters is unrealistic in heavily defective systems. In the heteroionic fluorites, the immobility of the cation sublattice is a key factor. Consider a crystal containing N anion sites, with a concentration x of dopant cations. Every anion site is surrounded, in its first neighbour shell, by four cations, of which i ($0 \leqslant i \leqslant 4$) are dopant cations; the reasoning could be extended to larger cation shells. For a random distribution of cations, or for any specified distribution, it is possible to calculate n_i, the number of anion sites with i dopant cation neighbours; the binding energy e_i of vacancies in a site of type i can be calculated by the HADES defect simulation programme. An important step is that the distribution of vacancies between the different types of site should conform to a Fermi-Dirac equilibrium; the fraction of the sites n_i occupied by vacancies, x_i is given by

$$x_i = [1 + \exp\{(e_i - e_0)/kT\}]^{-1}$$

where e_0 is a Fermi energy, defined through the condition

$$\Sigma x_i n_i = m \cdot N \cdot x,$$

where m is the number of extrinsic vacancies introduced by each dopant cation (*e.g.* $m = 1/2$ for Y^{3+} in ZrO_2). This distribution describes the overall structure and defines the thermodynamics of the system. By using the same computer simulation techniques to calculate the activation energy for a vacancy jump, the dependence of transport properties (ionic conductivity) upon x can be predicted. The results do show the observed maximum in conductivity, but do not reproduce the properties at higher dopant concentration unless the interaction potentials are adjusted to allow for differences in the sizes of host and dopant cations.

This is essentially a semi-empirical model; its success, in common with all the HADES and PLUTO simulations, is critically dependent upon the interatomic potentials used. It has been employed, with some success, to treat the thermodynamics of the UO_2-CeO_{2-x} system (Catlow and Tasker 1981) and to model the structure of the ZrO_2-CaO system (Butler 1983) which was simulated (a) for the nebulous cluster model and (b) as a microdomain system, with elements of the fluorite-derived structure. It emerged that the two models were almost equal in energy; a microdomain structure was slightly more stable, by 0·09 eV per dopant ion. The conclusion, of interest when compared with Rossell's experimental findings, is that both microdomains of defined structure and the quasi-random defects must coexist, the latter being more important at low dopant concentrations and higher temperatures.

The 'natural' interstitial site in the fluorite structure is the $\frac{1}{2}\ \frac{1}{2}\ \frac{1}{2}$ position; it was accordingly assumed by Zintl and by later workers that interstitial anions would enter that site. The limit of anion-excess nonstoichiometry would thereby be set at the composition M_4O_9 per unit cell, $MX_{2\cdot25}$, with every interstitial site filled. There is considerable experimental evidence that the assumption is valid for sufficiently small concentrations of interstitials. Electron spin resonance and other spectroscopic experiments on CaF_2 doped with lanthanide fluorides—*e.g.* on single crystals of $La_xCa_{1-x}F_{2+x}$ with $x < 0{\cdot}01$—show that the interstitial fluorine has the site symmetry appropriate to the $\frac{1}{2}\ \frac{1}{2}\ \frac{1}{2}$ position; furthermore, no interstitial atoms have been detected at any other positions.

In crystals with a high, formal concentration of interstitials, the situation is completely different, as emerged from neutron diffraction studies by Willis (1963, 1964) of the structures of U_4O_9 and nonstoichiometric UO_{2+x}. In $UO_{2\cdot12}$ (at 800°, and in inner equilibrium) there were no interstitials in the $\frac{1}{2}\ \frac{1}{2}\ \frac{1}{2}$ site. There were vacant anion sites as well as interstitial oxygen atoms, so that the total number of interstitials was greater than the net stoichiometric defect, and the interstitial atoms had two distinct crystallographic environments. In the favoured, but not completely unambiguous model for the resulting defect cluster, one pair of interstitials (O′) is displaced along $\langle 110 \rangle$ on either side of the $\frac{1}{2}\ \frac{1}{2}\ \frac{1}{2}$ position, and a second pair (O″) of atoms is displaced along $\langle 111 \rangle$ from the two anion sites at $\frac{1}{2}\ \frac{1}{2}\ 0$ and $\frac{1}{2}\ \frac{1}{2}\ 1$ creating a pair of vacancies. The cluster of two interstitials of each of two kinds with two vacancies (figure 14b) is termed a 2:2:2 cluster; it is probably not a unique cluster configuration and there may be more extended defects with different ratios of (vacancies): [O′]:[O″]. The experimentally determined partial occupancies of the O′ and O″ sites do not exactly accord with the 2:2:2 model—$UO_{1\cdot87}O'_{0\cdot08\pm0\cdot04}O''_{0\cdot16\pm0\cdot06}$ as compared with the expected $UO_{1\cdot88}O'_{0\cdot12}O''_{0\cdot12}$. The same defect cluster, subject to the same comment, was found for U_4O_9, but now in every unit cell of the basic fluorite structure; the experimental site populations were $UO_{1\cdot74}O'_{0\cdot29\pm0\cdot05}O''_{0\cdot19\pm0\cdot04}$. However, the ordered U_4O_9 structure is still not completely known. The true unit cell is a $4 \times 4 \times 4$ superstructure of the fluorite

subcell which has not so far been successfully solved. Until that is done, the complete geometry of the clusters remains somewhat uncertain, through lack of evidence about the way that statistically partially occupied O′ and O″ sites are related on a scale beyond that of a single subcell. This point is relevant to recent debate about the nature of defect clusters in anion excess fluorites. The introduction of a significant stoichiometric excess of anions undoubtedly imposes a substantial measure of local rearrangement, in which atoms are displaced by around 1 Å from the fluorite cell positions.

Neutron diffraction studies of the CaF_2-YF_3 system by Cheetham *et al* (1970, 1971) showed that exactly analogous defect clusters were formed in heteroionic systems. In these, the association between the interstitial defect clusters and the randomly sited, immobile compensating cations inhibits any superstructure ordering. For 10% YF_3, the observed site occupancies accorded fairly well with the expectation for the 2:2:2 cluster ($Y_{0.1}Ca_{0.9}F_{1.85}F'_{0.14}F''_{0.08}$), but there is evidence for the formations of larger clusters, such as the 3:4:2 cluster (figure 14c) as the excess of anions is increased (as *e.g.* in $Y_{0.25}Ca_{0.75}F_{2.25}$). The accessible composition range of these heteroionic MF_{2+x} structures is very wide, far exceeding the formal net insertion of one interstitial atom per unit cell. Gettman and Greis (1978) found that the pseudofluorite structure extended to $Y_{0.375}Ca_{0.625}F_{2.375}$ at 1000°; some ordering of the cations undoubtedly sets in at 800–1000°C, for the limit of the pseudofluorite phase at 800°C is $Y_{0.285}Ca_{0.715}F_{2.285}$. This still exceeds the expected limitation to $x \leqslant 0.25$. In the process of cation ordering, three discrete superstructure phases were found: $(Y, Ca)F_{2.333}$, $(Y, Ca)F_{2.357}$ and $(Y, Ca)F_{2.425}$, all based upon a fluorite-type subcell. The multiplicities of their superstructures lead to the assignment of the formulae $Ca_{10}Y_5F_{35}$, $Ca_9Y_5F_{33}$ and (not perfectly ordered) $Ca_{7+y}F_{6-y}F_{31-y}$ respectively, which fit an interpretation as successive members of a homologous series M_nF_{2n+5}, with $n = 15, 14, 13$.

Directly relevant to these observations on the heteroionic system is the work of Greis (1977) on the YbF_2-YbF_3 system, in which charge transfer between Yb^{2+} and Yb^{3+} cations permit complete ordering both of defects and compensating charges. In that system, the cubic YbF_{2+x} phase extends to $YbF_{2.19}$, and the fluorite-based structural pattern persists to $YbF_{2.41}$, with four superstructure phases: Yb_3F_7, $Yb_{14}F_{33}$,

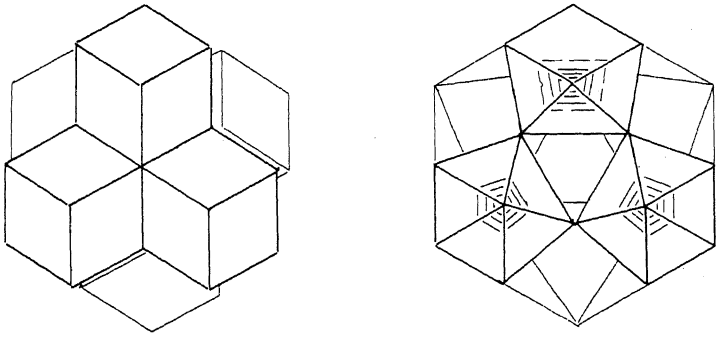

Figure 15. The Greis-Bevan cluster in anion-excess fluorites. (**a**) group of six edge sharing coordination cubes, projected down [111]. (**b**) Conversion of cubes to cubic antiprisms by rotation of inner square face.

$Yb_{27}F_{64}$ and $Yb_{13}F_{32-y}$. These conform to the homologous series referred to above, $Yb_{27}F_{64}$ being a 1:1 intergrowth of the $n = 13$ and $n = 14$ members.

These and related observations have reopened some discussion of the defect clusters in anion excess fluorites. A significant step was a full structure determination of the naturally occurring yttrofluorite mineral tveitite, $Ca_{14}Y_5F_{43}$ ($(Ca, Y)F_{2\cdot26}$), which, as the $n = 19$ member of the homologous series, indicates the common structural pattern of the superstructures (Bevan *et al* 1982). In it, all the cations are very close to the positions of the f.c.c. fluorite structure, but the anions are systematically displaced in a way that generates a new kind of cluster. Figure 15a shows a group of six edge-sharing $[MX_8]$ coordination groups in the fluorite structure, viewed down [111]. If each cube is converted to a cubic antiprism, by rotating the innermost square face, all the internal corners can be shared by incorporating four more anions, to give the unit shown in figure 15b. The core of this cluster is a cuboctahedral cavity that can—permissively rather than mandatorily—accommodate another anion. Anions making up the outer vertices of the cluster are little displaced from ideal fluorite positions, so that the whole can 'plug in' freely into unchanged fluorite structure. An original element of the fluorite structure with the local composition M_6X_{32} is thereby transformed into a cluster M_6X_{37} which underlies the ordered superstructures of the M_nF_{2n+5} series, and which could serve, with minimal strain, as a randomly disposed extended defect in the nonstoichiometric, anion-excess fluorites. It is certainly an important structural motif in a number of well-established crystal structures; it is not yet established that it is an alternative interpretation of all the crystallographic data and should replace the concept of the Willis cluster, in nonstoichiometric fluorites. According to Bendall *et al* (1981) the Greis-Bevan cluster model fits the diffraction data for the nonstoichiometric $SrCl_2 + 10\%\ PrCl_3$ system, and is not incompatible with the earlier work of Cheetham *et al* on $(Ca, Y)F_{2+x}$.

Clusters based on conversion of cubic $[MX_8]$ polyhedra into square antiprisms achieve a closer packing of anions without imposing the unacceptably close interatomic distances between F′ interstitials that are unavoidable in Willis-type clusters. However, Laval and Frit (1983) argue that the Greis-Bevan cluster does not explain the displacement of F″ interstitials along ⟨111⟩, and so fits neither the observed site occupancy nor the spectroscopic evidence (Andeen 1981; Moore and Wright 1981). They propose an alternative cluster model, in which a square antiprism is formed by cooperative rotation of one face of an $[MX_8]$ cube. With small relaxations of anions in the immediately adjacent $[MX_8]$ cubes, a cluster M_9X_{49} could be formed which is virtually unchanged in volume and connectivity from an element M_9X_{44} from the original fluorite structure. It could thus provide up to five interstitial sites or 0·55 interstitials per cation, but less densely packed clusters are probable and Laval and Frit suggest that occupation of three out of the five potential sites would accord well with the site occupancies and the actual interstitial positions found by Cheetham for $(Ca, Y)_{2+x}$. This proposed cluster, with vacancies and anions in positions corresponding to F′ and F″ interstitials (figure 15c) could be regarded as a 4:4:3 cluster and is not completely unrelated to the original concept.

Catlow *et al* (1983) have rejected the Bevan-Greis type of defect cluster, on the basis of their HADES calculations of cluster binding energies, and in the light of a fresh single crystal neutron diffraction study of CaF_2 doped with 5 mole% LaF_3. This was interpreted as unambiguously indicating that the clusters were smaller than is required by the Greis-Bevan (or the Laval-Frit) model. That there would be a net gain in binding

energy by forming Willis type clusters had been shown by earlier calculations on UO_{2+x} (Catlow 1977). The new calculations trace how energy is gained progressively through defect association (table 8).

Table 8. Binding energies for successive stages of aggregation.

Binding energy for $(La_{Ca}^{\cdot}F_i')$ ⟨100⟩ association	0·799 eV
Binding energy for $(La_{Ca}^{\cdot}F_i')$ ⟨111⟩ associate	0·384 eV
Binding energy for $2(La_{Ca}^{\cdot}F_i') \rightarrow 2:2:2$ cluster	0·419 eV
Binding energy for $2:2:2$ cluster $+ F_i' \rightarrow 3:2:2$ cluster	1·283 eV

A rational implication of the data in table 8 is that clustering takes place progressively, as the concentration of interstitials increases, through the continued aggregation of the primary defect species—interstitial anions and the dipolar association of interstitials and compensating cations. However, a necessary consequence of invoking 3 : 2 : 2 clusters is that the clusters bear a net negative charge, and that a corresponding proportion of the altervalent ions must either reside in smaller clusters or be separated from charge compensation. It is by no means clear that the free energy of the system would be optimised by such a distribution. It is more likely that the altervalent cations must be located in or immediately adjacent to the clusters. Hence, larger clusters, such as the Greis-Bevan cluster, must depend upon an appropriate localisation of the altervalent cations, a process that depends upon the diffusion of cations. The structure of defect clusters may not be the same in all systems and at all concentrations and, as Catlow has pointed out, several factors could influence the relative importance of simple clusters and larger, more structured clusters: the relative ionic radii of dopant and host cations, the concentration of dopant and the duration of annealing. If the last is important, it would imply that, for some conditions at least, the simple Willis-type cluster represents a metastable configuration, not the ground state of absolute minimum free energy. It would be valuable to investigate the defect structure of yttrofluorite minerals with a low concentration of lanthanide cations, since only for naturally occurring crystals can it be assumed that annealing and ordering processes have approached completion.

8. Final considerations

No attempt has been made in this review to cover the entire range of nonstoichiometric systems. One whole class of compounds that have been omitted is that based on the stacking of slabs of structure that are demarcated by planar singularities—sheets with changed linkage of coordination polyhedra, as in the crystallographic shear structures, or the brownmillerite layers of the defect perovskites ABO_{3-x}, or sequenced layers of different chemistry, as in the extreme example of the layer ferrites. For the homoatomic systems, such as the CS structure oxides like TiO_{2-x} or WO_{3-x} there must be a transition between a point defect regime at extremely low degrees of reduction and the two-dimensionally infinite extended defect regions of the CS phases but in general these layer structure systems involve problems of long range order, often with remarkably large repeat distances. They do not exhibit reversible transitions between the ordered state and some randomized configuration of variable composition. Disordering would

be a one-dimensional process, it would yield only a very small configurational entropy to offset the expenditure of energy in the disordering reaction. They are *enthalpy-controlled systems*. For kinetic reasons, complete order into discrete phases may not be fully achieved in the preparation of such materials, but the resulting, pseudo-nonstoichiometric products are metastable; the equilibrium state is that of discrete compounds of determinate composition.

In contrast, the systems dealt with here have been *entropy-controlled systems*, and it will be apparent that some fundamental problems are still unresolved, as regards the real space structure of their disordered, stoichiometrically indeterminate high temperature forms, and their relation to the point defect concept.

In some respects the situation is less clear than it appeared to be a decade ago; the accumulating crystallographic evidence and the direct observation of structure in real space by high resolution electron microscopy (but this related almost entirely to enthalpy controlled systems rather than truly nonstoichiometric crystals) appeared to be consistent with the ideas foreshadowed by Wadsley (1962) and Anderson (1962).

The outcome of this reasoning was that the statistically randomized structure actually embodied regions or microdomains with two modes of local ordering: microdomains of a new ordered structure dispersed coherently in a matrix of unchanged parent structure. As has been seen in relation to the Ti-S system, a model of this kind can, by computer simulation, generate a distribution of diffuse scattering (of x-rays, electrons or neutrons) that satisfactorily matches the observed diffraction effects. On the other hand, the converse simulation process, using the short range order parameters deduced from the diffuse scattering to regenerate the configuration that yielded the diffraction data, has not (*cf* the discussion of TiO and VO) supported the microdomain concept. This is not necessarily a definitive objection to it; a given set of order parameters does not correspond to a unique structure, and the simulation process does not necessarily generate the solution that minimises the free energy.

There are, however, some unresolved problems attached to the microdomain concept. The first is the minimum size of a region that is autonomous and characterized by its own local order, as distinct from some arbitrarily selected group of lattice points that has been generated fortuitously in a random distribution. The evidence from the few studies of nonstoichiometric phases under equilibrium conditions is that the short range order parameters differ rather little from those expected for a completely random distribution of defects. In systems (*e.g.* Ti-S, doped ZrO_2) for which a microdomain description is attractive, it appears to be accepted that the probable size of microdomains is in the range 30–100 A. The equilibrium of such systems must be described by the thermodynamics of small systems (Hill 1963), in which the size of the dispersed entities introduces an additional degree of freedom. No satisfactory treatment of nonstoichiometry has as yet been formulated along those lines, and it remains unclear whether a dispersion of microdomains can be the stable, equilibrium state over a wide range of temperature, or whether it must be a precursor stage of nucleation, domain growth and phase segregation.

The ultimate control of structure is thermodynamic, and several semi-empirical lines of theoretical development offer some insight into defect structures. It is firmly established that defect complexes or clusters play a dominant role in some non-stoichiometric systems though, as has been seen, our structural knowledge about those clusters is still incomplete. It is important that theoretical calculations have confirmed that the aggregation of point defects into such clusters, and the observed local

modification of the matrix structure, are usefully exothermic processes. The theory is not yet predictive, however. It treats the stability of a cluster in isolation, whereas this cannot be independent of the existence of other clusters and the configuration around all the sites of the matrix structure. Further, it is practicable to consider only those clusters that are not only structurally plausible in the light of incomplete crystal structure evidence, but are also tractable for the computation. Nevertheless, the advance is significant.

A second main line of theoretical development is the treatment of extended defects, structured clusters and superlattice ordering in terms of the interactions between defects, and between defects and surrounding matrix structure. Kanamori's work, cited above, is significant in that it demonstrates that the pair interactions in any real system operate over a wider range than has hitherto been considered in the statistical thermodynamics of crystals. To make a pair interaction treatment predictive, it would be necessary, however, to have a deeper understanding than we now possess of all the relevant interactions and interaction potentials.

The crucial problem remains the disordered, nonstoichiometric state. In classical point defect theory, a basic postulate is that the enthalpic cost of creating a point defect is independent of the occupancy and configuration about all other lattice sites. This is grossly untrue at the formal defect concentrations involved in disordered non-stoichiometric phases, and it is this feature that invalidates the straightforward application of point defect theory to them. In this context, the work of Catlow and Parker, cited above in relation to anion-deficient doped zirconia, is a promising development.

Even apart from the experimental problems of acquiring microstructural information from nonstoichiometric systems under equilibrium conditions, it is likely that there will be insurmountable limitations to what is accessible. It is, therefore, all the more important that a sound and predictive theoretical basis should be established.

References

Andeen C G 1981 *J. Phys.* **C14** 3557

Anderson J S 1946 *Proc. R. Soc.* (*London*) **A185** 69

Anderson J S 1962 *Nonstoichiometric compounds*, Am. Chem. Soc. *Adv. Chem.* No. 39 p. 1

Banus M and Reed T B 1970 *Chemistry of extended defects in nonmetallic solids* (eds) L Eyring and M O'Keeffe (Amsterdam: North Holland)

Bauer E and Pianelli A 1980 *Mater. Res. Bull.* **15** 177

Bauer E, Pianelli A, Aubry A and Jeannot F 1980 *Mater. Res. Bull.* **15** 323

Bell P S and Lewis M H 1971 *Phys. Status Solidi* 7 431

Bertaut E F 1956 *Acta Crystallogr.* **6** 357

Bendall P S, Catlow C R A and Fender B E F 1981 *J. Phys.* **C14** C4377

Bevan D J M, Strahle J and Greis O 1982 *J. Solid State Chem.* **44** 75

Brown N and Hoodless I M 1967 *J. Phys. Chem. Solids* **28** 2297

Butler J, Catlow C R A and Fender B E F 1983 *Radiat. Eff.* **73** 273 (*Chem. Abs.* **99** 97031)

Cappeletti R and de Benedetti E 1968 *Phys. Rev.* **165** 981

Catlow C R A 1977 *Proc. R. Soc.* (*London*) **A353** 533

Catlow C R A, Chadwick A V and Corish J 1983 *J. Solid State Chem.* **48** 65

Catlow C R A and Fender B E F 1975 *J. Phys.* **C8** 3267

Catlow C R A, Fender B E F and Mixworthy D G 1977 *J. Phys. Colloq.* **C7** 67

Catlow C R A and Mackrodt W C 1982 *Computer simulation of solids* (Berlin: Springer-Verlag) p. 42

Catlow C R A and Parker S C 1982 *Computer simulation of solids* (eds) C R A Catlow and W C Mackrodt (Berlin: Springer-Verlag) p. 222
Catlow C R A and Tasker P W 1981 AERE Report TP 884
Chapman J A and Lilley E 1973 *J. Phys. Colloq.* **C9** 341
Chaudron G 1921 *Ann. Chem.* **16** 221
Cheetham A K, Fender B E F and Cooper M J 1971 *J. Phys.* **C4** 3107
Cheetham A K, Fender B E F and Taylor R I 1971 *J. Phys.* **C4** 2160
Cheetham A K, Fender B E F, Steele D, Taylor R T and Willis B T M 1970 *Solid State Commun.* **8** 171
Coffin P, Jacobson A J and Fender B E F 1974 *J. Phys.* **C7** 2781
Conard B R and Franzen H F 1969 *Extended defects in nonmetallic solids* (eds) L Eyring and M O'Keeffe (Amsterdam: North-Holland) p. 207
Corish J and Quigley J M 1982 *Computer simulation of solids* (eds) C R A Catlow and W C Mackrodt (Berlin: Springer-Verlag) p 265
De Novion C H and Maurice V 1977 *J. Phys. Colloq.* **C7** 211
Dismukes J P and White J G 1964 *Inorg. Chem.* **3** 1220
Emmons G H and Williams W S 1983 *J. Mater. Sci.* **18** 2589
Ehrlich P 1939 *Z. Elektrochem.* **45** 362
Fowler W B 1975 *Treatise on solid state chemistry* (ed.) N B Hannay (New York: Plenum) Vol. 2 p. 133
Franzen H F, Tuenge R T and Eyring L 1983 *J. Solid State Chem.* **49** 206
Froidevaux C and Rossier D 1967 *J. Phys. Chem. Solids* **28** 1197
Gavarri 1978 Thesis, Univ. Paris VI
Gettmann and Greis O 1978 *J. Solid State Chem.* **26** 255
Gilles P W and Wahlbeck P G 1967 *J. Chem. Phys.* **46** 2461, 2465
Greis O 1977 *Z. Anorg. Chem.* **430** 175
Hahn H, Harder B, Mutschke U and Ness P 1957 *Z. Anorg. Chem.* **292** 82
Hayakawa M, Morinaga M and Cohen J B 1974 *Defects and transport in oxides* (ed.) M Seltzer (New York: Plenum) p. 177
Hilti E 1968 *Naturwissenschaften* **55** 130
Hill T L 1963 *Thermodynamics of small systems* (New York: Benjamin)
Iijima S 1974 *Diffraction studies of real atoms and real crystals* (Australian Academy of Science) p. 217
Jette E R and Foote F 1933 *J. Chem. Phys.* **1** 29
Kanamori J 1979 *Modulated structures*, Am. Inst. Phys. Conf. Proc. No. 53 p. 117
Kanamori J and Kakehashi Y 1977 *J. Phys. Colloq.* **C7** 227
Koch F and Cohen J B 1969 *Acta Crystallogr.* **B25** 275
Koto K and Kitamura M 1981 *Acta Crystallogr.* **A37** 307
Koto K, Morimoto N and Gyobu A 1975 *Acta Crystallogr.* **B31** 2759
Kroger F A 1976 *Chemistry of imperfect crystals* (Amsterdam: North Holland) Vol. 2
Laval P L and Frit B 1983 *J. Solid State Chem.* **49** 237
Lacher J R 1937 *Proc. R. Soc. (London)* **A161** 525
Moore D S and Wright J C 1981 *J. Chem. Phys.* **74** 1626
Moret R, Huber M and Comes R 1977 *J. Phys. Colloq.* **C7** 202
Morinaga M and Cohen J B 1979a *Acta Crystallogr.* **A35** 745
Morinaga M and Cohen J B 1979b *Acta Crystallogr.* **A35** 975
Nakazawa H and Morimoto N 1971 *Mater. Res. Bull.* **6** 345
Nakazawa H, Yamamoto A and Morimoto N 1979 *Modulated structures*, Am. Inst. Phys. Conf. Proc. No. 53 p. 358
Nowick A S, Wang Yu, Park D S and Griffith J 1979 *Fast ion conduction in solids* (ed.) P Vashishta (Amsterdam: North Holland)
Rees A L G 1954 *Trans. Faraday Soc.* **50** 335
Rossell H J and Scott H G 1977 *J. Phys. Colloq.* **C7** 28
Roth W L 1960 *Acta Crystallogr.* **13** 140
Schenck R, Dingmann T, Bokmann J, Ebert W, Kesting W, Lepetit G, Muller J and Protje W 1927 *Z. Anorg. Chem.* **166** 113
Schottky W and Wagner C 1931 *Z. Phys. Chem.* **B11** 163
Strutt J E and Lilley E 1972 *Reactivity of solids*, 7th Int. Symp. (eds) J S Anderson, M W Roberts and F S Stone (London: Chapman and Hall) p. 84
Suzuki 1961 *J. Phys. Soc. Jpn.* **16** 67

Terauchi H and Cohen J B 1978 *J. Phys. Chem. Solids* **39** 681
Terauchi H and Cohen J B 1979 *Acta Crystallogr.* **A35** 646
Terauchi H, Cohen J B and Reed T B 1978 *Acta Crystallogr.* **A34** 556
Tilley R J D 1973 *J. Solid State Chem.* **7** 213
Van Bruggen C F, Haas C and Wiegers G A 1979 *J. Solid State Chem.* **27** 9
Wadsley A D 1962 *Nonstoichiometric compounds*, Am. Chem. Soc. Adv. Chem. No. 39 p. 23
Watanabe D, Terasaki O, Jostsons A and Castles J R 1967 *Acta Crystallogr.* **23** 307
Watanabe D, Terasaki O, Jostsons A and Castles J R 1969 *Extended defects in nonmetallic solids* (
L Eyring and M O'Keeffe p. 238
Willis B T M 1963 *Proc. R. Soc.* (*London*) **A274** 134
Willis B T M 1964 *J. Phys.* **25** 431
Zintl E and Udgard 1939 *Z. Anorg. Chem.* **240** 150

Proc. Indian Acad. Sci. (Chem. Sci.), Vol. 93, No. 6, August 1984, pp. 905–916.
© Printed in India.

Radiationless transitions in trivalent lanthanide ions embedded in solids

DEB SHANKAR RAY and MIHIR CHOWDHURY*

Department of Physical Chemistry, Indian Association for the Cultivation of Science, Jadavpur, Calcutta 700 032, India

Abstract. Radiationless transitions in lanthanide ions embedded in glassy and crystalline hosts have been briefly reviewed. The correlations of multiphonon relaxation rates with energy gaps, vibrational frequencies, temperatures and electronic symmetries have been discussed. The essence of various theories, such as Nth order methods, non-adiabatic Hamiltonian method, dynamic coupling model has also been presented.

Keywords. Radiationless transitions; lanthanide spectroscopy.

1. Introduction

In spite of great deal of efforts made in understanding radiationless transitions in photophysics, photochemistry and photobiology, our knowledge of these complex phenomena is rather poor. In recent years considerable progress has been made in this area both from experimental and theoretical points of view and the field has been reviewed from time to time (Reisfeld 1975; Watts 1975; Riseberg and Weber 1976; di Bartalo 1978; MaCarthy and Rhyne 1978; Englman 1979; Lin 1980; Chistian and Taub 1983). The present paper is an attempt to exemplify with a chosen group of molecules the broad generalisations obtained from a vast mass of experimental data, rather than to present an exhaustive survey of the current literature, and to rationalise the key features of the experimental aspects in terms of a theoretical framework. We shall confine ourselves to the nonradiative (NR) relaxation in lanthanide complexes concentrating only on the electronic relaxation in solids which do not involve energy transfer, cross-relaxation (Banerjee *et al* 1981) or similar processes. The reason behind choosing lanthanide ions in glassy and crystalline matrices for this discussion is given below.

(i) Hardly any generalisation emerges for a complicated process like radiationless transition unless a closely similar group of molecules are chosen. The lanthanide ions in various hosts offer themselves as one of the largest well-knit group of closely similar systems (Dieke 1968).

(ii) The large coupling of electronic and nuclear motion in organic molecules makes the NR rates very fast, except for the lowest singlet π, π^* and triplet n, π^* and π, π^* states. Although in a few cases, the luminescence from the lowest singlet n, π^* states (Lippert *et al* 1961; Lippert and Boss 1962; Chowdhury and Goodman 1963; Ghosh and Chowdhury 1981, 1982) and upper excited n, π^* (Ghosh and Chowdhury 1982) and

* To whom all correspondence should be addressed.

π, π^* states (Birks 1973; Murata *et al* 1972; Wild *et al* 1976; Levine *et al* 1974; Hui *et al* 1975; Huber and Mahaney 1975; Griesser and Wild 1980; Choi *et al* 1978) have been reported and although picosecond techniques have recently been developed to follow fast NR processes, accurate data essentially exist only for the lowest state and that too is often complicated by the occurrence of side photochemical reactions or energy transfer processes. In the case of lanthanide complexes, on the other hand, one gets luminescence from a large number of upper states which, because of narrow bandwidth, can be resolved to the finest detail, and because of its slowness, can be measured with high precision. The luminescent excited states of lanthanide ions (Dieke 1968) in various hosts offer a variety of energy gaps, electronic symmetries, site symmetries and lattice frequencies for testing the predictions of the theories of nonradiative rates.

(iii) The Born-Oppenheimer (BO) approximation which form the basis of almost any theoretical approach to the photodynamial problem (Avouris *et al* 1977) demands that the coupling of electronic and nuclear motion must be weak. This weak coupling scheme has proven its greatest validity for lanthanide systems (f^N states); the electronic wavefunctions preserve their atomic character predominantly and nuclear motion acts only as a small perturbation. Although asymmetric vibrations do destroy the symmetry slightly, it is still meaningful to talk of electronic symmetry since the crystal field effect is small. The lanthanide ions thus stand between isolated atoms, where no NR transition occurs excepting trivial collisional processes, and stable molecules where a large number of vibrations and rotations not only cause NR transitions but also mess up things considerably.

(iv) The NR transition is an essential step in the population inversion process in lanthanide ions such as Nd^{+3} in glassy and other media, and thus the NR study of these materials are of great practical importance in connection with lasers and phosphors (McCarthy and Rhyne 1978; Brown 1981; Kaminskii 1981).

2. Multi-phonon relaxation and generalisations

Vibrations are responsible for a modulation of the local crystal field experienced by well-shielded $4f$ electrons and thus cause a transition from one electronic state to another. If the energy separation between the two electronic states corresponds to a single phonon frequency of a vibrational mode, the NR process is very fast. If, however, the energy gap is much larger than the upper limit of the phonon spectrum as is frequently the case, it is apparent that a number of phonons must be involved in the non-radiative decay. Although such multi-phonon NR processes have low probability, they are fast enough to compete with the slow ($\sim 10^{-3}$) radiative transition rates of $f^N - f^N$ transitions. We will first present the main observed generalisations regarding the role of energy gaps, vibrational frequencies and electronic symmetries in controlling the NR rates, and discuss later the various theories proposed.

2.1 *Energy gap law*

It has been demonstrated that for a crystal (Weber 1967a, b, 1968, 1973; Riseberg and Moos 1968; Flaherty and di Bartalo 1973; Nakazawa and Shinoyer 1972) or glassy media (Layne *et al* 1977; Reisfeld *et al* 1975) the most critical factor affecting the multiphonon relaxation rate is the energy gap to the next lower level. The multiphonon decay rates measured for several levels of different Ln^{3+} ions exhibit approximate

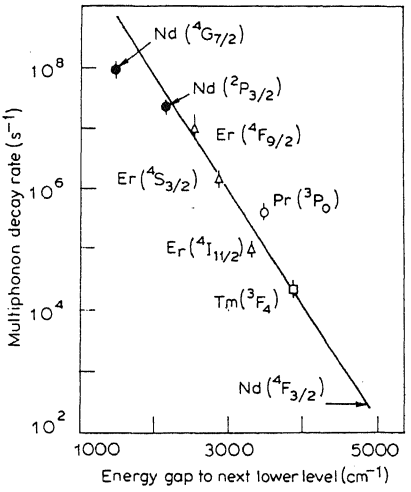

Figure 1. Multiphonon decay rates as a function of energy gap to next lower level for rare earths in silicate glass (from Layne *et al* 1975).

exponential dependence on the energy gap ΔE as $W_{NR} = W_{NR}(0) \exp(-\alpha \Delta E)$, where $W_{NR}(0)$ is the pre-exponential factor and α is a phenomenological constant (whose interpretation we shall find in the next section). Figure 1 illustrates this point (Layne *et al* 1975). The spread of pre-exponential factor with different states, ions and hosts is unexpectedly small. In the case of several glassy hosts different parameters of the exponential energy gap law determined for each glass are valid for a number of transitions and ions. The generality of this exponential gap law is, in fact, so wide that even 'large' isolated organic molecules (Avouris *et al* 1977; Lin 1980) and deep centres in semiconductors conform to the behaviour of ions in crystals, glasses and other condensed media.

2.2 *Effect of vibrational frequencies and temperature*

In organic molecules (Avouris *et al* 1977; Lin 1980) it has been shown through isotopic substitution and dependence of nonradiative rates on temperature that high frequency C–H vibrations play a major role in NR transitions. In the case of lanthanides two types of vibrations offer themselves as candidates *e.g.* metal-ligand vibrations and lattice vibrations. Although the M–L vibrations are strongly coupled with the metal ion electronic states, their frequencies are low, compared to some vibrations within the ligand or lattice, and therefore, they play a relatively minor role. The role of more energetic vibrations of the glassy medium may be illustrated (Reisfeld 1975) with the strong correlation of lifetimes with X–O vibrational frequencies of the lattice (X = B, P, Ge, Te) as shown in table 1. The existence of one dominant high-frequency phonon mode such as lattice cut-off frequency has been assumed by a number of workers (Riseberg and Moos 1967a, b; Fong *et al* 1972). In crystalline hosts the characteristic frequency may at times be substantially less than the maximal one. Thus, for several trivalent rare earth ions in YAG it is nearly 700 cm^{-1} compared to the top lattice frequency of almost 860 cm^{-1}. Apparently, phonon modes with frequencies lower than the cut-off frequency are also capable of participating in the process (Reed and Moos

Table 1. Phonon energies of various oxide glasses and multiphonon relaxation rate (W) from $^1D_2 \rightarrow {}^1G_4$ of Tm^{3+} at 80°K*.

Glass	Bond	Phonon energy (cm^{-1})	W ($\times 10^4$)
Borate	B–O	1340–1480	3·6
Phosphate	P–O	1200–1350	1·9
Germanate	Ge–O	975–800	1·5
Tellurite	Te–O	750–600	3·9 (!)

* From Reisfeld (1975).

1973). Due to the differences in local environments, it is impossible to assign single frequency in glasses and the effective transition rates in glasses are the mean values of various sites. The NR rates, in general, are much faster in glasses than in crystalline hosts. The study of multiphonon decay rates in glasses has led to few practical results; for instance, the realisation that the high-frequency vibration of the glass control the NR rate has led to the design of efficient laser amplifiers (Brown 1981; Kaminskii 1981).

From the study of luminescence characteristics of a large number of hydrated crystals (Heber and Hellwege 1967), it has been established that water of crystallisation enhances the nonradiative transitition rate. The replacement of water molecules by D_2O results in the decrease of radiationless decay rate by a factor of 3–7, exemplifying the role of high frequency O–H vibrations. A similar isotope effect has also been demonstrated in transition metal complexes (Sriram *et al* 1981; Sriram and Hoffman 1982). In this respect the photophysics of RE chelate systems resembles largely that exhibited in hydrocarbon solvents.

The nonradiative decay rates vary with temperature as expected for phonon-induced processes (Weber 1973; Fong and Wassam 1973; Sundberg *et al* 1974; Lauer and Fong 1976; Riseberg and Moos 1967; Reisfeld *et al* 1975). It has been shown by a number of workers that the temperature dependence of NR rates can be fitted into an equation $W = W_0\,(n+1)^N$ where n, the occupation number of phonons is given by Bose-Einstein law (*i.e.* $n = (\exp\frac{\hbar\omega}{KT} - 1)^{-1}$) and N is an integer which can be interpreted theoretically as the order of the process (see later). One such fit for Tm^{3+} in silicate glass is shown in figure 2 where the order of the process and frequency of phonon responsible for the decay matches well with expected values. Occasionally several frequencies are required to fit the temperature variation in glasses. The temperature dependence of homogeneous linewidths of some transitions in Eu^{+3} (Selzer *et al* 1976) and Pr^{+3} (Hegarty *et al* 1979) in different amorphous solids is shown to be quadratic. These anomalous low temperature behaviour in glassy hosts (Selzer *et al* 1976; Hegarty and Yen 1979; Morgan *et al* 1981) is suggestive of a new ion-lattice interaction peculiar to amorphous material.

If there is a metastable fluorescent state just below a state with higher radiative transition rate, frequently the activation energy laws come into the picture at high elevated temperatures (Englman 1979). The temperature dependence of the multiphonon transition has also played an important part in investigating the origin of rare earth fluorescence quenching in connection with the role of $4f^5 5d$ states (Lauer and

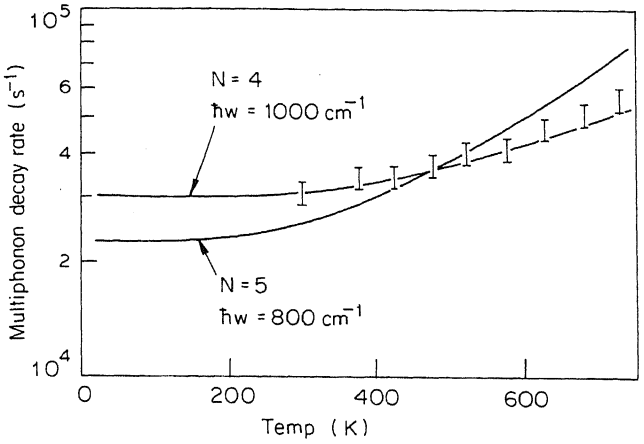

Figure 2. Temperature dependence of $^3F_4$–$^3H_5$ multiphonon emission rate for Tm^{+3} in silicate glass (from Layne *et al* 1975).

Fong 1976; Gaume-Mahn *et al* 1978) and charge-transfer states (Blasse *et al* 1970, 1981; Struck and Fonger 1975, 1976) as intermediary in the nonradiative relaxation processes.

2.3 *The selection rules and electronic factor*

Exceptions to the exponential energy gap law occur (Weber 1967a, b, 1968, 1973; Fong and Wassam 1973) when the selection rule severely restricts the number of terms in the ion-phonon interaction active in inducing transition. Since the transitions of interest are between the electronic states of a given f^N configuration, they involve no change in parity between the initial and final states. Hence, only the even terms in the interaction potential will be important. For an electronic operator of rank r, the triangle rule governing the transition between the J-states is given by $|J - J'| \leqslant r \leqslant |J + J'|$ with $r \leqslant 6$. J-mixing can act to relax this rule. Thus the transition $^5D_0 \rightarrow {}^5D_1$, $^7F_0 \rightarrow {}^7F_1$ (Eu^{+3}, Tb^{+3}), $^3P_0 \rightarrow {}^3P_1$ (Pr^{+3}, Tm^{+3}) are formally forbidden, but may occur by J-mixing or by other mechanisms. Of these $^5D_1 \rightarrow {}^5D_0$ transition in Eu^{+3} is readily amenable to study and the reduced rates have been observed in a number of cases (Weber 1968; Bhowmick and Nugent 1965). The ion-lattice interaction (and hence the nonradiative rate) is also subject to spin selection rule $\Delta S = 0$. The large spin-orbit interaction in lanthanides (Judd and Pooler 1982), however, reduces the importance of this rule compared to the case of organic molecules.

Selective pulsed excitation of crystal field components of $^5D_1$, $^5D_2$ and $^5D_3$ in Eu^{+3} in Eu^{+3}-oxydiacetate has revealed interesting by-passing of levels. It has been demonstrated by Ray *et al* (1981) that $^5D_2$ can decay nonradiatively to $^5D_0$ by two different channels—one directly and another indirectly *via* $^5D_1$. Evidently the CF components of $^5D_2$ behave differently. The differential behaviour of the different crystal field components of $^5D_2$ (A_1, $2E$ in D_3 point group symmetry) has been explained in terms of a new 'soft' selection rule. A number of workers (Richter *et al* 1982; Andrews *et al* 1980; Gardner and Kasha 1969) have shown that in vibrationally deficient systems (*i.e.* where symmetry species for normal vibrational modes of the molecule fail to span all the irreducible representations of the corresponding point group) the electronic factor may become important and forbid a particular NR transition.

3. Theoretical aspects

Owing to the quasicontinuum nature of the vibronic levels in condensed phase, Fermi Golden rule may be used with confidence for finding the probability of the transition from an initial state ψ_i to the final state ψ_f:

$$W_{\text{nr}} = \frac{2\pi}{\hbar} |\langle \psi_i | H' | \psi_f \rangle|^2 \times \text{density of states.}$$

The various theories make different approximations regarding the wavefunctions ψ_i and ψ_f and the perturbation H'. It is convenient to classify the methods adopted into three broad categories: (a) Nth order methods (Kiel 1964; Hagston and Lowther 1973); (b) nonadiabatic hamiltonian methods (Zewail 1978; Lin 1980) and (c) other methods (Fong *et al* 1972; Perlin 1979; Ray *et al* 1981). The Nth order methods use either the Nth order perturbation theory for the first order crystal field term or the first order perturbation theory for the Nth order crystal field term. The second group of methods utilises the nonadiabatic part of the full hamiltonian as the perturbation inducing first order multiphonon NR transition; though developed for crystals, this method is capable of incorporating the basic features of molecular relaxation processes. The theories of category (c) will be discussed later. To give an overview of the main theoretical results we shall briefly outline these methods.

3.1 *Nth order methods*

3.1a. *Nth order time-dependent perturbation method.* This approach has been investigated by Kiel (1964) and applied to the case of Cr^{+3} and Pr^{+3}, following an approach originated by Orbach for spin-lattice relaxation (Orbach 1964). The hamiltonian for the crystal field is expanded in a Taylor series

$$H_{CF} = H_o + \sum_i \left(\frac{\partial V}{\partial Q_i}\right) Q_i + \tfrac{1}{2} \sum_{i,j} \left(\frac{\partial}{\partial Q_i} \frac{\partial V}{\partial Q_j}\right) Q_i Q_j + \ldots,$$

where H_0 is the static crystal field potential and Q_i is the ith normal coordinate. The wavefunctions $|\psi_i\rangle$ and $|\psi_f\rangle$ in the transition matrix element are taken as crude BO states and expressed as a product of the electronic wavefunction $|\phi_i\rangle$ and the product of the individual harmonic oscillator wavefunctions $|n_i\rangle$ characterised by phonon occupation number n_i. The phonon wavefunctions are supposed to be the same in both the electronic states. Thus, we have, in general, $|\psi_k\rangle = |\phi_k\rangle \Pi_i |n_i\rangle$. If the energy gap is equal to N phonons *i.e.* $\Delta E = N\hbar\omega$, then the phonon emission rate W_N in the N th order process is approximately given by the Nth order perturbation theory as

$$W_N = \frac{2\pi}{\hbar} \left| \left(\frac{\hbar}{2M\omega}\right)^{N/2} \sum_{i,j \ldots N = 1,2,\ldots m} (n_i + 1)^{N/2} \times \right.$$

$$\left. \times \frac{\langle \phi_f \left| \frac{\partial V}{\partial Q_i} \right| \phi_{i,f} \rangle \langle \phi_{i,f} \left| \frac{\partial V}{\partial Q_j} \right| \phi_{i,f} \rangle \ldots \langle \phi_{i,f} \left| \frac{\partial v}{\partial Q_N} \right| \phi_i \rangle}{[E_i - E_{i,f} - \hbar\omega]\,[E_i - E_{i,f} - 2\hbar\omega] \ldots [E_i - E_{i,f} - (N-1)\hbar\omega]} \right|^2,$$

where M is the reduced mass, $|\phi_{i,f}\rangle$'s stand for intermediate states. If the simplifying assumptions are made that each matrix element in the last expression may be replaced

by an average and that m phonon modes of the same frequency dominate, we obtain

$$W_N = \frac{2\pi}{\hbar}\left(\frac{\hbar}{2M\omega}\right)^N (n+1)^N\, 2^{2(N-1)}\, m^{2N} \frac{|\langle \phi_i \left|\frac{\partial v}{\partial Q_i}\right| \phi_f \rangle|^{2N}}{|\hbar\omega|^{2(N-1)}}.$$

Here m denotes the number of phonon modes. The expression for W_N yields the following: (i) The temperature dependence is given by the factor $(n+1)^N$ as observed before. (ii) The most energetic phonons will dominate in the rate process since the order $N = \Delta E/\hbar\omega$ will be lowest for those phonons. (iii) For the same glass network (*i.e.* same $\hbar\omega$ and m), the ratio W_N/W_{N-1} is given by

$$W_N/W_{N-1} = 4\left(\frac{\hbar}{2M\omega}\right)(n+1)m^2 \frac{|\langle \phi_i \left|\frac{\partial v}{\partial Q_i}\right| \phi_f \rangle|^2}{(\hbar\omega_i)^2},$$

which for a weak perturbation is nearly equal to a constant $Y (\ll 1)$ *i.e.*

$$W_N/W_{N-1} = Y.$$

This is the central result of the Nth order perturbation method and its utility in the derivation of the energy gap law will be discussed later.

3.1b. *Nth order crystal field method.* Instead of considering Nth order perturbation method in deriving the ratio $W(N)/W(N-1)$, Hagston and Lowther (1973) considered only the Nth order crystal field term (for the first order perturbation) after showing that it was, in fact, the largest term. Taking for intermediate states those exhibiting stark splitting of the initial free ion level and assuming only one phonon-frequency and considering the ratio of the first order perturbation for the Nth order crystal field term to the Nth order perturbation for the first order crystal field term, they arrive at a relation after a number of simplifying assumptions, as follows

$$W(N) = \frac{2\pi}{\hbar}|\langle \phi_i \left|\frac{\partial v}{\partial Q_i}\right| \phi_f \rangle|^2 Y^N,$$

with $Y = W(N)/W(N-1)$.

Y is then assumed to be almost independent of N as in the previous method. We shall now try to see the implications of the simple result obtained by these two methods.

(i) Exponential energy gap and vibrational frequency law: In these two methods the key point to obtain a closed form result is to consider the iterative properties of

$$W(N) = W(N-1)Y,$$

which means that we are considering a series in which the succeeding term is smaller by the characteristic constant number Y. Calculating $W(N)$ from $W(0)$ we obtain,

$$W(N) = W(0)Y^N = W(0)\, e^{N\log\gamma}.$$

If we now replace N by the ratio of the energy gap ΔE and an effective phonon energy $\hbar\omega$ we get

$$W(N) = W(0)\exp(-\alpha\Delta E)$$

with

$$\alpha = (1/\hbar\omega)\log(1/Y)$$

where α and Y are the characteristics of the matrix and the nature of interaction respectively. This basically is the central feature of the theoretical development by Riseberg and Moos (1968) and others (Layne *et al* 1977; di Bartalo 1978; Soules and Duke 1971) for crystals and glasses.

(ii) Temperature dependence: In the two methods temperature dependence occurs through the products of normal mode matrix elements for one-phonon process, as

$$|\langle n_1+1|Q_i|n_i\rangle|^2 \ldots . |\langle n_j+1|Q_j|n_j\rangle|^2$$
$$\text{N factors}$$

where n_i is the average occupation number which is equal to $(\exp\frac{\hbar\omega}{kT}-1)^{-1}$. The last product is proportional to

$$(n_i+1)\ldots(n_j+1),$$

leading to a temperature-dependent factor $(n+1)^N$. The application of the result in identifying the phonon responsible for the NR decay and the order of the process has been discussed earlier.

3.2 *The nonadiabatic hamiltonian method*

In the Nth order method, the wavefunctions for the phonons are described by pure harmonic states which are the same for both the initial and the final electronic states of the ion. With such a model the jumps in phonon quantum number can be made one at a time requiring Nth term in the hamiltonian. But if the vibrational states are allowed to differ in both the electronic states either in geometry or in frequency, changes by more than one quantum number can be obtained in the first order (Frenkel 1931; Avouris *et al* 1977). This is the basic idea for generation of N-phonons in the nonadiabatic hamiltonian approach. The approximations used in this method are common to the treatment of molecular relaxation. In the adiabatic approximation, the total wavefunction of the system is given by the product of electronic wavefunction ϕ_j and vibrational wavefunctions θ_{jv}

$$\psi_{jv}(q, Q) = \phi_j(q, Q)\theta_{jv}(Q).$$

The nonadiabatic part of the full hamiltonian for the crystal, acting as the perturbation including nonradiative transitions is derived from the lattice kinetic energy term as follows;

$$H_{\mathrm{NA}}\psi_{jv} = -\hbar^2\sum_s \frac{\partial\phi_s}{\partial Q_s}\frac{\partial\theta_{jv}}{\partial Q_s}.$$

The moment for transition $iv' \to fv''$ is given by

$$\langle fv''|H^s_{\mathrm{NA}}|iv'\rangle = -\hbar^2\langle\phi_f\left|\frac{\partial}{\partial Q_s}\right|\phi_i\rangle\langle\theta_{fv''}\left|\frac{\partial}{\partial Q_s}\right|\theta_{iv'}\rangle,$$

where the vibrational wavefunctions are approximated by the product of harmonic oscillator wavefunctions

$$\theta_{fv''} = \prod_s \chi_{fv''_s}(Q''_s), \quad \theta_{iv'} = \prod_s \chi_{iv'_s}(Q'_s).$$

The nonrádiative transition rate is then given by

$$W_{nr} = \frac{2\pi}{\hbar} \sum_s |\beta_s|^2 |\langle \chi_{fv'_s} \left| \frac{\partial}{\partial Q_s} \right| \chi_{iv'_s} \rangle|^2 \times \prod_{j \neq s} |\langle \chi_{fv'_j} | \chi_{iv'_j} \rangle|^2 \delta(E_{fv''} - E_{iv'})$$

with

$$\beta_s = -\hbar^2 \langle \phi_f \left| \frac{\partial}{\partial Q_s} \right| \phi_i \rangle ..$$

In this method we encounter the promoting modes s and the accepting modes j characterised by the nonvanishing integrals

$$\langle fv''_s \left| \frac{\partial}{\partial Q_s} \right| iv'_s \rangle \text{ and } \langle \chi_{fv''_j} | \chi_{iv'_j} \rangle.$$

The explicit expressions for the nonradiative rates can be obtained by using the method of Huang and Rhys (1950) or by the Fourier integral representation method of δ-functions (Gelbert *et al* 1970), or the non-integral quantum number approach (Avouris *et al* 1977), leading to the same energy gap law. The theory gives complicated temperature dependence, which can be reduced after suitable approximations to the result we have already obtained by Nth order methods.

3.3 *Other current approaches*

We have discussed the methods emphasising weak coupling limit. For other treatments, a series of papers by Fong and his co-workers (Fong and Wassam 1973; Sundberg *et al* 1974; Lauer and Fong 1976; Fong *et al* 1972) may be referred to. It is basically a quantum-statistical derivation of the weak-coupling-limit rate constant (Fong *et al* 1972) for multiphonon decay within $4f^N$-configuration. The expression was applied to give a numerical fit to experimental data (Fong *et al* 1972; Fong and Wassam 1973). A generalisation of the theory was made to treat f-d relaxation (Sundberg *et al* 1974) and non-resonant energy transfer (Lauer and Fong 1976).

Observation of anomalous low temperature dependence (Selzer *et al* 1976; Hegarty and Yen 1979; Morgan *et al* 1981) of homogeneous linewidths has prompted Lyo and Orbach (1980) to propose a new model which takes into account interaction between the two two-level systems. Multiphonon emission theory of Perlin (1979) is also worth mentioning.

The above models for multiphonon relaxation in rare earth crystals give satisfactory description of a number of experimental observations such as energy gap law, temperature dependence of nonradiative rate, importance of high frequency vibrations etc. However, the main domain of application of the model is where the ion is embedded in a medium whose function is to provide a 'structureless' heat bath. The validity of the rate expression depends on the extent the individual phonon modes and the participating electronic levels are averaged out for a high-order process. However, the consideration of the rare earth crystal with polyatomic ligand suggests that the ligand environment around the metal ion certainly possesses some 'structure' which cannot be neglected. We have already pointed out that Eu^{+3} emission is susceptible to the nature of environment (Blasse *et al* 1981, Richter-Lustig *et al* 1982). The detailed feature of the environment, such as, site symmetry, nature of local and internal ligand modes, the electronic properties (*e.g.* dipole moment, polarisability) of the ligand etc are not amenable to theoretical description in terms of a simple crystal field model. In a number

of cases the radiationless transition between $|J = 1\rangle$ and $|J = 0\rangle$ states becomes suppressed in certain symmetries (Fong *et al* 1972; Weber 1967a, b, c, 1968, 1973) and sometimes it is difficult to correlate the non-radiative rates with energy gap data (Fong *et al* 1972). An understanding of the role of symmetries of the electronic states (Ray *et al* 1981) and the role of states of opposite parity, such as $4f^{n-1}\,5d$ state (Lauer and Fong 1976; Gaumé-Mahn *et al* 1978), also pose problems for the models discussed so far. Keeping in mind the remarkable sensitivity to ligand environment in hypersensitive radiative transitions, it is quite likely that the role of environment should find parallel importance in the nonradiative processes as well. It is in this perspective that a theory of ligand-induced nonradiative transition (Ray and Chowdhury 1981; Strek 1981) has been developed within the framework of 'dynamic coupling' model used earlier in the field of lanthanide spectroscopy to account for hypersensitive transition (Mason *et al* 1975) and optical activity (Sen and Chowdhury 1981; Sen *et al* 1981; Richardson and Faulkner 1982). In this theory the model has been extended from the domain of radiative transition to the realm of nonradiative relaxation and brought into relation with a number of experimental observations. The basic idea is that since in the free lanthanide ion there is no nonradiative decay, the ligand-induced $f^N \rightarrow f^N$ nonradiative process derives transition probability from the polarisability and internal transitions of the ligand. The zero-order wavefunctions are written as the product of wavefunctions of subsystems comprising lanthanide ion with its nearest neighbours and the rest of the ligand. The wavefunctions of the complex are corrected upto first order by taking into account the electrostatic interaction (beyond crystal field) between the two subsystems. The dynamic part of the hamiltonian (nonadiabatic part) brings about the nonradiative transitions from one product state to another. From its consequences the theory may be considered as a synthesis of Nth order methods and nonadiabatic hamiltonian methods, since it incorporates the key features of NR relaxation in solids and in organic molecules. Apart from deriving the usual exponential energy gap and vibration frequency law, the theory clearly brings out the importance of states with opposite parity, electronic symmetries of initial and final states of the rare earth ion, symmetry of the crystal field, internal promoting and accepting modes of the ligand, and finally the dipole moment and the polarisability of the ligand. New nonradiative selection rules including parallalism between radiative and nonradiative rates have been predicted (Ray and Chowdhury 1981; Strek 1981).

4. Concluding remarks

We have outlined the main experimental results in NR processes within the lanthanide Ln^{3+} ions embedded in solids and the various theoretical approaches initiated to explain the results. Although a number of methods of calculation of nonradiative rates between the f^N excited states are in use, the existing data in literature are not extensive enough to provide guidelines to theoreticians working in this field. We hope that with the advent of pulsed mode-locked lasers and time-resolved detection techniques, new experimental data in the short time scale will be available in the near future; the various theoretical predictions and nonradiative selection rules can then be properly examined.

Acknowledgement

We thank our colleagues Dr K Bhattacharyya and D Nath for discussions and collaboration. The photodynamical work was initiated with a SERC (DST) grant.

References

Andrews L J, Lampicki A and McCollum B C 1980 *Chem. Phys. Lett.* **74** 404
Avouris P, Glebert W M and El-Sayed M A 1977 *Chem. Rev.* **77** 793
Banerjee A K, Stewart-Darling F, Flint C D and Schwartz R W 1981 *J. Phys. Chem.* **85** 146
Bhowmick M L and Nugent L J 1965 *J. Chem. Phys.* **43** 1680
Birks J B 1973 *Organic molecular photophysics* (New York: Wiley-Interscience) p. 16
Blasse G, Bril A and de Poorter J A 1970 *J. Chem. Phys.* **53** 4450
Blasse G, Dirksen G J and Zonnevijlle 1981 *Chem. Phys. Lett.* **83** 449
Brown D C 1981 *High peak-power Nd-glass laser Systems* (Berlin: Springer-verlag)
Canters G W 1981 *Chem. Phys. Lett.* **81** 267
Choi K J, Lin H B and Topp R 1978 *Picosecond phenomena* (eds) C V Shank, E P Ippen, S L Shapiro (Berlin: Springer-Verlag)
Chowdhury M and Goodman L 1963 *J. Chem. Phys.* **38** 2979
Christian J W and Taub C J 1983 *Proceedings of sixteenth rare earth research conference, Tallahasse, Parts I, II, III*
di Bartalo B 1978 in *Luminescence in inorganic solids* (ed) B di Bartalo (New York: Plenum Press)
Dieke G H and Sarup R 1958 *J. Chem. Phys.* **29** 741
Dieke G H 1968 *Spectra and energy levels of rare earth ions in crystals* (New York: Wiley)
Englman R 1979 in *Non-radiative decay in ions and molecules in solids* (Amsterdam:North-Holland)
Fisher S 1970 *J. Chem. Phys.* **53** 3195
Flaherty J M and di Bartalo B 1973 *J. Lumin.* **8** 51
Fong F K, Naberhuis S L and Miller 1972 *J. Chem. Phys.* **56** 4020
Fong F K and Wassam W A 1973 *J. Chem. Phys.* **58** 946
Fonger W H and Struck C W 1975 *Phys. Rev.* **B11** 3251
Frenkel J 1931 *Phys. Rev.* **37** 17
Gardner P J and Kasha M 1969 *J. Chem. Phys.* **50** 1543
Gaumé-Mahn F, Gacon J C, Souillat J C, Scriot J and di Bartalo B 1978 in *Rare earths in modern science and technology* (eds) G J McCarthy and J J Rhyne (New York: Plenum Press)
Gelbert W M, Freed K F and Rice S A 1970 *J. Chem. Phys.* **52** 2460
Ghosh S and Chowdhury M 1981 *J. Phys. Chem.* **85** 1280
Ghosh S and Chowdhury M 1982 *Chem. Phys. Lett.* **85** 233
Griesser H J and Wild U P 1980 *Chem. Phys.* **52** 117
Hagston W E and Lowther J E 1973 *Physica* **70** 40
Heber J and Hellwege K H 1967 in *Optical properties of ions in crystals* (eds) H M Crosswhite and H W Moos (New York: Interscience)
Hegarty J and Yen W M 1979 *Phys. Rev. Lett.* **43** 1120
Hoefdraad H E, Stegers F M A and Blasse G 1975 *Chem. Phys. Lett.* **32** 216
Huang K and Rhys A 1950 *Proc. R. Soc. (London)* **A204** 406
Huber J R and Mahaney M 1975 *Chem. Phys. Lett.* **30** 410
Huber J R and Mahaney M 1975 *Chem. Phys.* **9** 371
Hui M H, de Mayo P, San R and Ware W R 1975 *Chem. Phys. Lett.* **31** 257
Judd B R and Pooler D R 1982 *J. Phys.* **C15** 591
Kaminskii A A 1981 *Laser crystal* (Berlin: Springer-Verlag)
Kiel A 1964 in *Quantum electronics* (eds) P Grievet and N Bloembergen (Columbia)
Lauer H V and Fong F K 1976 *J. Chem. Phys.* **65** 3108
Layne C B, Lowdermilk W H and Weber M J 1975 *IEEE J. Quantum Electron.* **11** 798
Layne C B, Lowdermilk W H and Weber M J 1977 *Phys. Rev.* **B16** 10
Levine S, Knight A R and Steer R P 1974 *Chem. Phys. Lett.* **29** 73
Lin S H 1980 *Radiationless transitions* (Amsterdam: North-Holland)

Lippert E, Luder W, Moll F, Nagle W, Boos H, Prigge H and Siebold-Blankenstain J 1961 *Angew Chem.* **73** 695
Lippert E and Boss W 1962 *Z. Phys. Chem.* **31** 321
Lyo K and Orbach R 1980 *Phys. Rev.* **B22** 4223
Mason S F, Peacock R D and Stewart B 1975 *Mol. Phys.* **30** 1829
McCarthy G J and Rhyne J J 1978 *Rare earths in modern science and technology* (New York: Plenum Press)
Miyakawa T and Dexter D L 1970 *Phys. Rev.* **B1** 2961
Morgan J R, Chock E P, Hopewell W D and El-Sayed M A 1981 *J. Phys. Chem.* **85** 747
Murata S, Iwanaga C, Toda T and Kokubun H 1972 *Chem. Phys. Lett.* **13** 101 (and references therein)
Nakazawa E and Shinoyer S 1972 *J. Phys. Soc. Jpn* **28** 1260
Orbach R 1964 *Phys. Rev.* **133** A34
Perlin Y E 1979 *J. Lumin.* **21** 119
Porcher P and Caro P 1978 *J. Chem. Phys.* **68** 4183
Ray D S and Chowdhury M 1981 *Chem. Phys.* **61** 157
Ray D S, Bhattacharyya K, Gupta A K and Chowdhury M 1981 *Chem. Phys. Lett.* **77** 422
Reed E D and Moos H W 1973 *Phys. Rev.* **B8** 980
Reisfeld R 1975 *Structure bonding* **22** 129
Reisfeld R, Boehm L, Eckstein Y and Lieblich N 1975 *J. Lumin* **10** 193
Richardson F S and Faulkner T R 1982 *J. Chem. Phys.* **76** 1595
Richter-Lustig H, Ron A and Speiser K 1982 *Chem. Phys. Lett.* **85** 576
Riseberg L A and Moos H W 1967a *Phys. Rev.* **159** 262
Riseberg L A and Moos H W 1967b *Phys. Rev.* **157** 252
Riseberg L A and Moos H W 1968 *Phys. Rev.* **174** 429
Riseberg L A and Weber M J 1976 in *Progress in optics* (ed.) E Wolf (Amsterdam: North-Holland) vol. 14
Sarai A and Kakitani T 1981 *Chem. Phys. Lett.* **77** 427
Saxe J D, Faulkner T R and Richardson F S 1982 *J. Chem. Phys.* **76** 1607
Selzer P M, Huber D L, Hamilton D S, Yen W M and Weber M J 1976 *Phys. Rev. Lett.* **36** 813
Sen A C and Chowdhury M 1981 *Chem. Phys. Lett.* **79** 165
Sen A C, Chowdhury M and Schwartz R W 1981 *J. Chem. Soc. Faraday. Trans.* **77** 1293
Siebrand W 1971 *J. Chem. Phys.* **55** 5843
Soules T K and Duke C D 1971 *Phys. Rev.* **B3** 262
Sriram R, Hoffman M Z and Serpone N 1981 *J. Am. Chem. Soc.* **103** 997
Sriram R and Hoffman M Z 1982 *Chem. Phys. Lett.* **85** 572
Strek W 1981 Preprint
Struck C W and Fonger W H 1975 *J. Lumin.* **10** 1
Struck C W and Fonger W H 1976 *J. Chem. Phys.* **64** 1784
Sundberg M N, Lauer H V, Chilver C R and Fong F K 1974 *J. Chem. Phys.* **60** 274
Tofield B C and Weber H P 1974 *Phys. Rev.* **B10** 4560
Watts R K 1975 in *Optical properties of solids* (ed.) B di Bartalo (New York: Plenum Press)
Weber M J 1967a *Phys. Rev.* **156** 231
Weber M J 1967b *Phys. Rev.* **157** 262
Weber M J 1967c in *Optical properties of ions in crystals* (eds) H M Crosswhite and H W Moos (New York: John Wiley)
Weber M J 1968 *Phys. Rev.* **171** 283
Weber M J 1973 *Phys. Rev.* **B8** 54
Weber M J, Bass M, Andrigna K, Monchamp R R and Comperchio E 1969 *Appl. Phys. Lett.* **15** 342
Wild U P, Griesser H J, Tuan V D and Oth J F M 1976 *Chem. Phys. Lett.* **41** 450 (and references therein)
Zewail A 1978 in *Luminescence in inorganic solids* (New York: Plenum Press)

Proc. Indian Acad. Sci. (Chem. Sci.), Vol. 93, No. 6, August 1984, pp. 917–926.
© Printed in India.

Use of semiempirical molecular orbital calculations for the evaluation of force fields

A ANNAMALAI, M KANAKAVEL and SURJIT SINGH*

Structural Chemistry Group, Department of Chemistry, Indian Institute of Technology, Madras 600 036, India

Abstract. Various methods, employing molecular orbital calculations of varying approximations, for evaluation of force fields of polyatomic molecules have been reviewed. Applications of CNDO/force method for the force field calculations are specially dealt with in detail because of its ease of operation and being economically more viable in terms of computer time. The calculated C=O stretching force constants for a series of organic molecules are shown to have linear relationship with substituent constants.

Keywords. Force fields; vibrational analysis; molecular orbital calculations; CNDO/force.

1. Introduction

In the past two decades considerable interest has been shown in the calculation of force fields of polyatomic molecules using molecular orbital calculations. The force constant F_{ij} is defined as

$$F_{ij} = (\partial^2 E/\partial q_i \partial q_j)_e \tag{1}$$

where E is the total energy of the molecule and q_i, q_j are symmetry or internal coordinates. The methods for the evaluation of force constants include (Kanakavel 1976) double numerical differentiation (Baron *et al* 1962; Leies 1963; McLean 1964; Goodisman 1963; Paldus and Hrabe 1968), double analytical differentiation (Bratoz 1958; Gerrat and Mills 1968; Bishop and Randic 1966; Bishop and Mancias 1969, 1970; Swanstrom *et al* 1971; Bloemer and Brunner 1972) and analytical differentiation followed by numerical differentiation (Pulay 1969, 1970a, b; Pulay and Meyer 1971, 1972; Pulay 1974). The double numerical differentiation method uses systematic variation of nuclear configuration accompanied by SCF-MO calculations for each configuration. The energy hypersurface built in this fashion is used to evaluate the force constants by numerical differentiation to second order. In double analytical differentiation method, the expression for the SCF energy is differentiated twice to obtain an analytical expression for the force constants in terms of the parameters of the electronic SCF-MO wavefunctions. In the third method developed by Pulay and coworkers (Pulay 1969, 1970a, b; Pulay and Meyer 1971, 1972; Pulay 1974) the energy is differentiated analytically (thus building force hypersurfaces) followed by numerical differentiation to first order. In the series of papers, Pulay and coworkers have shown that their method (also called force method and more recently gradient method) has certain advantages over the other two methods discussed above. The double numerical

* To whom all correspondence should be addressed.

differentiation is not economical because the wavefunctions must be computed for a number of nuclear configurations and might be inaccurate because of the two numerical differentiations. The number of necessary points on the energy surface varies with the strategy used to find the equilibrium configuration but becomes excessive if there are three or more coordinates. In the case of the force method all the force constants $F_{ij}(i = 1 \text{ to } N \text{ and } j \text{ is fixed})$ can be obtained by varying only the coordinates q_j. This advantage is pronounced for molecules with several degrees of freedom. The method makes possible a quick iterative procedure to determine the equilibrium configuration. Semiempirical methods like CNDO/2 have also been used (Pople and Beveridge 1970; Klopmann and O'Leary 1970; Ribegard 1974; Colthup and Orloff 1974) to determine force fields using the energy hypersurface (double numerical differentiation) method. Pulay and Torok (1973) have shown that the semiempirical quantum chemical calculations on molecular geometry and force constants by energy hypersurface method become impractical as the size of the molecule increases and that the application of the force method to semiempirical wavefunctions makes it possible to carry out an economical and simple calculation of molecular geometry and force constants.

2. CNDO/force calculations

Kanakavel *et al* (1976) performed CNDO/force calculations on a series of molecules, H_2CO, F_2CO, CF_4, CHF_3, CH_2F_2 and CH_3F. As discussed by Pulay and Torok (1973) the first derivatives of the total energy with respect to the nuclear coordinates are calculated analytically from the CNDO wavefunctions. The forces acting on each atom in the molecule are computed for an arbitrary geometry. Since the forces are directed towards the equilibrium geometry of the molecule, all atoms are moved in the direction of force over a small distance, say 0·01 Å. The forces are calculated again for the new geometry and the nuclei are allowed to relax towards the equilibrium geometry. The process is repeated until the norm of the forces becomes smaller than the preset threshold value. This method is known as the steepest descent method. When the energy is minimized, the norm of the forces keeps decreasing. It was concluded that when the norm of the forces is less than 0·001 further iterations do not change the energy and geometry to any considerable extent. The experimental and optimized geometries for H_2CO and F_2CO are given in table 1.

The Cartesian forces are calculated for the equilibrium geometry of the molecule.

Table 1. Calculated and experimental molecular geometry parameters (distances in Å and angles in degrees).

	H_2CO			F_2CO	
	Calc.	Exp.*		Calc.	Exp.†
r_{CO}	1·247	1·208	r_{CO}	1·251	1·170
r_{CH}	1·114	1·116	r_{CF}	1·324	1·316
$<$HCH	116·2	116·5	$<$FCF	109·8	107·6

* Tokagi and Oka (1963); † Carpenter (1974).

The molecule is then deformed by an amount $\pm\frac{1}{2}\Delta R_i$ where ΔR_i is the displacement of the ith internal coordinate. The Cartesian forces (f_i) are found for possible configurations representing different modes of vibration. The displacements given for stretching and bending internal coordinates were $\pm 0{\cdot}01$ Å and $\pm 1°$ respectively. For each deformed configuration the symmetry forces (ϕ_i) are calculated by using suitable transformations. The symmetry force constants F_{ij} are obtained as the ratios of $\Delta\phi_i$ and ΔS_j. The GMAT program of Schachtschneider (1964) was used to compute the B matrices. In table 2 the symmetry force constants for H_2CO and F_2CO obtained by CNDO/force method are compared with experimental force fields.

In several cases considered it is found that the stretching force constants obtained by CNDO/force are more than twice the experimental values and the stretch-stretch interaction force constants are slightly different in magnitude in comparison with experimental values. The bending force constants and stretch-bend interaction force constants are found to be comparable with the experimental values. The signs of the interaction constants are in agreement with those predicted by Mills (1963) and Heath and Linnett (1945) based on orbital following arguments. The value of F_{13} in H_2CO is in accordance with HOFF constraint. The stretching force constants, though found to have higher values than the experimental values, have some interesting trends. As can be noticed from table 3, in a series of molecules the CH and CF stretching force constants, in general, are found to have the same trend as the experimental force constants. For example, with increasing number of hydrogens in the series CHF_3, CH_2F_2, CH_3F, CH_4, the calculated force constants for symmetric C–H stretching vibration are found to increase. A roughly similar trend is found in the experimental force constants also. Similarly for ν_{CF} (symmetric stretching) with increasing number of fluorine atoms in the series, CH_3F, CH_2F_2, CHF_3, CF_4 the experimental force constants and those obtained by the CNDO/force method are found to increase. Though the trends in experimental and calculated force constants are found to be similar for corresponding asymmetric stretching vibrations, a similar trend in calculated force constants with increasing

Table 2. Comparison of experimental and calculated symmetry force fields of X_2CO(X=H, F) (mdyn/Å, mdyn and mdyn Å for the stretching, stretching/bending and bending force constants, respectively)[a].

		H_2CO			F_2CO		
Force constants	Assignments	CNDO/Force Calc.	Exp.[b]	*Ab initio*[c]	CNDO/Force Calc.	Exp.[d]	Exp.[d]
F_{11}	CX_2s. str.	11·99	4·963	4·990	25·78	7·601	7·695
F_{12}	CX/CO str.	0·980	0·739	0·676	2·5	1·549	1·491
F_{13}	CX/CX_2 def.	0·101	0·077	0·106	0·330	0·540	0·568
F_{22}	CO str.	30·41	12·903	13·905	31·4	14·818	14·996
F_{23}	CO/CX_2 def.	−0·48	−0·408	−0·414	−0·443	−0·331	−0·488
F_{33}	CX_2 def.	0·614	0·57	0·645	1·134	1·404	1·370
F_{44}	CO wag.	0·469	0·403	0·514	0·65	0·735	0·735
F_{55}	CX_2 a. str.	11·60	4·852	4·909	23·52	5·867	5·718
F_{56}	CX/CX_2 rock.	0·212	0·171	0·157	0·619	0·688	0·635
F_{66}	CX_2 rock.	0·82	0·833	0·946	0·902	1·117	1·146

[a] Kanakavel (1976); [b]Duncan (1973); [c] Pulay (1974); [d] Mallinson *et al* (1975).

Table 3. Comparison of calculated and experimental force constants for stretching vibrations in a series of molecules (in mdyn/A).

Stretching mode	Molecule	Force constant	
		Calc.	Exp.*
ν_{CH} (sym) (A_1)	CH_4	12·700	5·842
	CH_3F	12·205	5·368
	CH_2F_2	11·755	4·873
	CHF_3	11·49	5·340
ν_{CF} (sym) (A_1)	CF_4	27·000	9·250
	CHF_3	25·946	8·669
	CH_2F_2	25·130	7·075
	CH_3F	24·060	5·764
ν_{CH} (asym)	$CH_4(F_2)$	12·08	5·383
	$CH_2F_2(B_2)$	11·421	4·904
	$CH_3F(E)$	11·126	5·433
ν_{CF} (asym)	$CF_4(F_2)$	23·08	6·220
	$CH_2F_2(B_2)$	22·85	5·111
	$CHF_3(E)$	21·265	5·303

* See Kanakavel *et al* (1976).

number of fluorine and hydrogen atoms cannot be found for the series of molecules considered. This is attributed to the fact that ν_{CF} (asymmetric) as well as ν_{C-H} (asymmetric) belong to three different symmetry species. Plots (figure 1) of experimental and calculated force constants of the CH and CF symmetric stretching modes in a series of molecules show different slopes and intercepts. This indicates that there is a definite relationship between experimental and calculated stretching force constants though the indices of the relations may differ for different modes of vibration.

3. Applications

In the conventional least squares method of force fields refinement using vibrational frequencies, the initial force field is set up (Annamalai and Singh 1982a, b, c) by transferring the force constants from structurally related molecules. The final force fields resulting from these calculations are found to depend on the initial force fields. The diagonal force constants may reasonably be transferred among structurally related molecules but such a transfer is rather difficult in the case of off-diagonal force constants since they greatly depend on the nature of molecules and their geometries. The interaction force constants also play an important role in determining the potential energy distributions (PED) of a molecule. It is therefore essential to consider reliable values for these force constants while constructing the initial force field.

As mentioned above simple CNDO/MO calculations predict in general the signs of interaction force constants correctly. The magnitudes of bending, stretch-bend, and bend-bend force constants obtained from these calculations are close to the experimental values whereas those of stretch-stretch interaction constants are about 50% higher than the experimental values. The stretching force constants are exaggerated by a factor

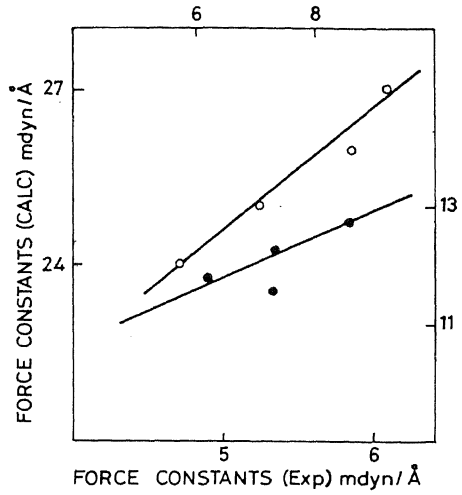

Figure 1. Plots of calculated force constants *vs* experimental force constants for a series of molecules CF_4, CHF_3, CH_2F_2, CH_3F, CH_4. For ν_{C-H} (sym), the X and Y coordinates respectively correspond to lower and RHS values and for ν_{C-F} (sym) O, the upper and LHS values.

of 2–3·5. *Ab initio* calculations prove to yield good results but require a lot of computation time. It is proposed that for large molecules reasonable force fields can be obtained using the following procedure: CNDO/force calculations are performed for the molecule under consideration and the CNDO force field is obtained. The stretch-stretch interaction force constants of the CNDO force field are scaled down using a scale factor. The initial force field is constructed by considering the scaled values of stretch-stretch interaction constants whereas the other interaction and bending force constants are taken from the CNDO force field. The stretching force constants are transferred from structurally related molecules. The initial force field thus constructed is refined further using the vibrational frequencies of normal and isotopic species. Reasonable constraints on the force fields are imposed when the number of force constants to be evaluated is greater than the number of frequencies used. Earlier workers (Kozumutza and Pulay 1975; Torok *et al* 1976) expressed the scale factor for the interaction force constants F_{ij} empirically as the geometric mean of the scale factors for the diagonal force constants F_{ii} and F_{jj}. This requires one to calculate separate scale factors for all F_{ij} force constants. Annamali and Singh (1982) suggested that if the force field has to be further refined using vibrational frequencies, one-common scale factor may be enough to reduce all stretch-stretch interaction constants whereas stretch-bend and bend-bend interaction constants can be transferred from CNDO force field.

We have (Kanakavel 1976; Kanakavel *et al* 1976; Annamalai *et al* 1978; Annamalai 1981; Annamalai and Singh 1982a, b, c 1983a, b; Jothi *et al* 1982; Jothi 1983; Brakaspathy *et al* 1984; Annamali, unpublished results) recently applied the above method for calculation of redundancy-free generalised valence force fields for a series of organic molecules. Studies on carbonyls (Annamalai *et al* 1978; Annamalai 1981; Annamalai and Singh 1982a, b, c, 1983a, b, unpublished) revealed some very interesting results on the effects of substituents on diagonal and off-diagonal force constants.

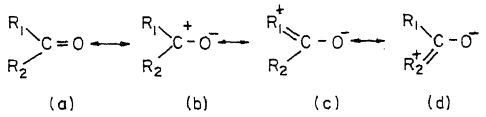

(a) (b) (c) (d)

In the carbonyl compounds, represented by R_1R_2CO, the inductive and resonance effects of the substituents R_1 and R_2 provide a satisfactory basis to understand the influence of the substituents on the electronic structure in and around the carbonyl group. For R_1R_2CO Hartwell *et al* (1948) considered the following contributing structures. The contribution of the structure (b) is controlled by the inductive effects whereas those of (c) and (d) are controlled by the resonance effects of the substituents. The electron attracting groups will decrease the contribution of the structure (b) thus strengthening the carbonyl bond whereas the electron repelling groups will cause the reverse effect. The resonance effects increase the contribution of the structures (c) and (d) leading to a weakening of the carbonyl bond. Accordingly the bond order of CO will change with varying nature of R_1 and R_2. This will lead to a change in the carbonyl stretching force constant $F_{C=O}$. The electron withdrawing or donating character of the substituents has been related to the free energy contributions of the substituents to the free energy of the total molecule (Hine 1962). This has been related to the substituent constants called σ constants as defined by Hammett (1940) and Taft (1956). The σ constants find applications in chemical kinetics (Hine 1962; Hammett 1940; Taft 1956; Taft *et al* 1958) and molecular spectroscopy (Katritzky and Topson 1972) for studying the substituent effects.

Stretching frequencies have often been correlated with σ values and other electrical parameters (Katritzky and Topson 1972). The carbonyl stretching frequencies were correlated with ionization potentials of carbonyl oxygen atoms (Cook 1958, 1961), effective electronegativities of the substituents (Kagarise 1955; Seth-Paul and Duyse 1972), sigma values (Thompson *et al* 1957; Jones *et al* 1957; Nyquist 1967; Liler 1967; Rao *et al* 1958) and carbonyl bond orders resulting from Huckel type calculations (Berthierr *et al* 1952; Forsen 1962). The above calculations showed, however, limited success. It is well known (Mills 1963; Overend and Scherer 1960; Overend *et al* 1961; Evans and Overend 1963) that the frequency of a vibrational mode in a polyatomic molecule is influenced by various factors like: (a) diagonal force constant corresponding to the vibrational mode under consideration, (b) other diagonal force constant as dictated by potential energy distributions, (c) field effects as represented by the interation force constants, (d) mass effects, (e) Fermi resonance interactions in some cases and (f) molecular geometry. Bratoz and Besnainou (1959) have demonstrated that the coupling of carbonyl stretching vibration with other modes is significant. As mentioned earlier, the effects of substituents are directly reflected in the force constants and hence they should be related to σ values and not to the vibrational frequencies.

The inductive and resonance effects of a number of substituents have opposite influences in affecting the carbonyl bond strength and consequently the carbonyl stretching force constant is altered. But it is difficult to guess *a priori* which effect plays the predominant role. However, useful information in this regard can be obtained from any possible relation between force constants and sigma values (σ_1 and σ_R of the substituents). Regarding the frequency correlations, some doubt was expressed by Thompson *et al* (1957) whether logically ν was the quantity to be correlated with σ. It

was suggested alternatively to correlate ν^2 with σ, since it is related to the force constant. The σ values are linearly related to free energies (Hine 1962; Hammett 1940) and hence Katritzky and Topson (1972) suggested that σ might reasonably be related to ν rather than ν^2. Based on these arguments it can be understood that the square root of the force constants are the appropriate quantities and not the force constants which should be correlated with σ values.

In table 4 the values of force constants reported are listed along with the $\Sigma_{R_1,R_2}\sigma_1$ and $\Sigma_{R_1,R_2}\sigma_R$ values. Multiple regression using the relationship

$$F_{C=O}^{1/2} = a_0 + a_1 \sum_{R_1,R_2}\sigma_I + a_2 \sum_{R1,R_2}\sigma_R \qquad (1)$$

was carried out for the force constants obtained. The relationship obtained is satisfactory with a correlation coefficient of 0·98. The coefficients a_0, a_1 and a_2 are found to be 3·578, 0·427 and 0·158 respectively. A constant C is defined as the ratio between a_2 and a_1. The plot of $F_{C=O}^{1/2}$ *vs* $\Sigma(\sigma_I + C\sigma_R)$ is shown in figure 2. The value obtained for the ratio C (0·37) suggests that the inductive term is about three times more significant than the resonance term in determining $F_{C=O}^{1/2}$. The values of $C\Sigma\sigma_R$ are also included in table 4 for reference.

The σ_I and σ_R values for all the substituents considered, except for CH_3 group, are opposite in sign. The coefficients a_1 and a_2 are found to be positive in the correlation obtained above. From these observations, it is concluded that the inductive and resonance contributions have opposite effects on $F_{C=O}$ values for all the substituents except in the case of CH_3 group. The inductive effect enhances the value of $F_{C=O}$ whereas the resonance effect diminishes. Comparison of σ_I with $C\sigma_R$ (*cf* table 4) reveals that, for the substituents F, OH and OCH_3, the actual inductive contribution to the force constant $F_{C=O}$ outweighs the resonance contribution whereas for the substituent NH_2, the reverse is true. This explains why the values of $F_{C=O}$ are higher in acid fluorides and lower in amides than those in corresponding aldehydes. In the case of CH_3 group both the inductive and resonance effects act together in bringing down the

Table 4. Carbonyl stretching force constants (in mdyn/A) obtained, carbonyl stretching frequencies (in cm^{-1}), and substituent constants*.

No.	R_1, R_2	$F_{C=O}$	$F_{C=O}^{1/2}$	$\nu_{C=O}$	$\sum_{R_1,R_2}\sigma_1$	$\sum_{R_1,R_2}\sigma_R$	$C\sum_{R_1,R_2}\sigma_R$
1	H, H	12·812	3·579	1746	0	0	0
2	H, CH_3	12·368	3·517	1743	−0·06	−0·87	−0·03
3	CH_3, CH_3	12·060	3·473	1731	−0·12	−0·14	−0·05
4	H, OH	13·120	3·622	1774	0·28	−0·68	−0·25
5	CH_3, OH	12·692	3·563	1779	0·22	−0·75	−0·28
6	H, OCH_3	13·063	3·615	1754	0·31	−0·63	−0·23
7	CH_3, OCH_3	12·717	3·566	1771	0·25	−0·70	−0·26
8	H, F	14·260	3·776	1837	0·56	−0·59	−0·22
9	CH_3, F	13·545	3·680	1870	0·50	−0·66	−0·24
10	F, F	14·677	3·831	1942	1·12	−1·18	−0·44
11	H, NH_2	12·301	3·507	1710	0·11	−0·78	−0·29
12	CH_3, NH_2	12·023	3·467	1704	0·05	−0·85	−0·31
13	NH_2, NH_2	11·667	3·416	1695	0·22	−1·56	−0·58

* Exner (1972).

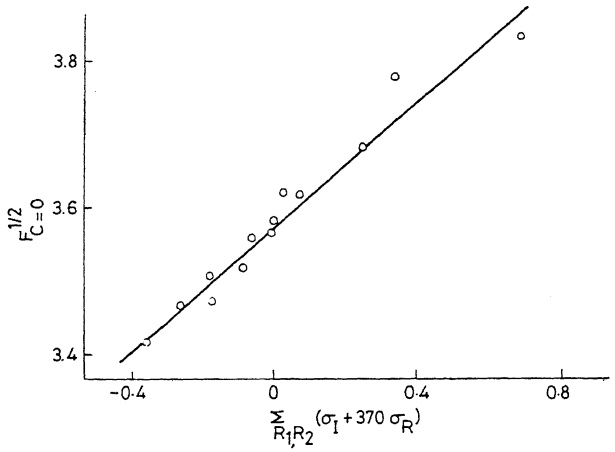

Figure 2. Plots of $F^{1/2}_{C=O}$ against $\Sigma_{R_1,R_2}(\sigma_I + C\sigma_R)$, where σ_I and σ_R are inductive and resonance contributions of the substituent constants.

value of $F_{C=O}$, since both $a_1\sigma_1$ and $a_2\sigma_R$ are negative quantities for CH_3 group. Similar relations were also tried for C–H, C–O, C–N and C–F stretching, C=O bending, R_1CR_2 bending and several interaction force constants.

Other molecules considered in this series included ethylene (Jothi *et al* 1982), amide (Annamalai and Singh 1982b), glyoxol, oxalyl fluoride, biacetyl, acetic anhydride (Kanakavel 1976), fluoroethylenes (Jothi 1983; Kanakavel 1976), allene and fluoroallenes, vinylacetylenes, vinylcynamide and propene (Jothi 1983), diacetamide (Annamalai and Singh 1983a; Kanakavel 1976), nitromethane (Brakaspathy 1984). Murthy and Ranganathan (1982a, 1983) have applied this method to evaluate force fields of carbon suboxide and carbonyl and formyl fluoride. This method has also been applied for the effect of molecular interactions on force fields of donors and acceptors exhibiting alcohol + ketone interactions (Kanakavel 1976) and carbonyl + lithium interactions (Murthy and Ranganathan 1982b).

Torok and Pulay (1978) in their recent calculations compared the results from different semiempirical methods and concluded that CNDO and INDO produce almost identical results. Nelander and Ribbegard (1974) point out that MINDO stretching force constants for linear molecules are close to the experimental values. Kozumutza and Pulay (1975), Kozumutza (1976), Gleghorn and McConkey (1975) and Marmer *et al* (1979) have also used semiempirical MO methods to evaluate force fields with varying degrees of success.

Another method for the evaluation of force fields using MO calculations has been developed by Swanson and coworkers (1978a, b; Rafalko *et al* 1979). It is based on MNDO MO calculations and limited vibrational data. This approach involves molecular orbital constraint of interaction constants and is called MOCIC. Expressed in the language of compliance constants the method has been applied to a series of molecules.

References

Annamalai A, Kanakavel M and Singh S 1978 *Proc. Indian Acad. Sci.* **A87** 337
Annamalai A 1981 Ph.D. thesis, IIT, Madras

Annamalai A and Singh S 1982a *J. Chem. Phys.* 77 860
Annamalai A and Singh S 1982b *Indian J. Chem.* **A21** 949
Annamalai A and Singh S 1982c *J. Mol. Struct. (Theochem)* **87** 169
Annamalai A and Singh S 1983a *Indian J. Pure Appl. Phys.* **21** 82
Annamalai A and Singh S 1983b *Can. J. Chem.* **61** 263
Baron J and Kolos W 1962 *J. Mol. Spectrosc.* **8** 121
Berthier G, Pullman B and Pontis J 1952 *J. Chim. Phys.* **49** 367
Bishop D M and Randic M 1966 *J. Chem. Phys.* **44** 2480
Bishop D M and Mancias A 1969 *J. Chem. Phys.* **51** 4997
Bishop D M and Mancias A 1970 *J. Chem. Phys.* **53** 3515
Bloemer L W and Brunner L B 1972 *J. Mol. Spectrosc.* **43** 452
Brakaspathy R, Jothi A and Singh S 1984 *Bull. Chem. Soc. Jpn* (submitted)
Bratoz S 1958 *Colloq Int. Centre Nat Res. Sci. (Paris)* **82** 257
Bratoz S and Besnainou S 1959 *J. Chim. Phys.* **56** 555
Carpenter J H 1974 *J. Mol. Spectrosc.* **50** 1812
Colthup N B and Orloff M K 1974 *Spectrochim. Acta* **A30** 425
Cook D 1958 *J. Am. Chem. Soc.* **80** 49
Cook D 1961 *Can. J. Chem.* **39** 31
Duncan J L 1973 *Chem. Phys. Lett.* **23** 597
Evans J C and Overend J 1963 *Spectrochim. Acta* **19** 701
Exner O 1972 *Advances in linear free energy relationship* (eds) N B Chapman and J Shorter (London: Plenum) p. 28
Forsen S 1962 *Spectrochim. Acta* **18** 595
Gerrat J and Mills I M 1968 *J. Chem. Phys.* **49** 1718
Gleghorn J T and McConkey F W 1975 *J. Mol. Struct.* **29** 133
Goodisman J 1963 *J. Chem. Phys.* **39** 2397
Hammett L P 1940 *Physical organic chemistry* (New York: McGraw Hill)
Hartwell E J, Richards R E and Thompson H W 1948 *J. Chem. Soc.* 1436
Heath W and Linnett J W 1945 *Trans. Faraday Soc.* **44** 556
Hine J 1962 *Physical organic chemistry* (New York: McGraw Hill) Chap. 4
Jones R W, Forbes W F and Miller W A 1957 *Can. J. Chem.* **35** 504
Jothi A, Shanmugam G, Annamalai A and Singh S 1982 *Pramana* **19** 413
Jothi A 1983 Ph.D thesis, Madras University
Kagarise R E 1955 *J. Am. Chem. Soc.* 77 1377
Kanakavel M, Chandrasekhar J, Subramanian S and Surjit Singh 1976 *Theor. Chim. Acta* **43** 185
Kanakavel M 1976 Ph.D. Thesis, IIT, Madras
Katritzky A R and Topson R D 1972 *Advances in linear free energy relationships* (eds) N B Chapman and J Shorter (London: Plenum)
Klopmann G and O'Leary B 1970 *Topics Curr. Chem.* **15** 447
Kozumutza K and Pulay P 1975 *Theor. Chim. Acta* **37** 67
Kozumutza K 1976 *Acta. Sci. Hung.* **40** 245
Leies G 1963 *J. Chem. Phys.* **39** 1137
Liler M 1967 *Spectrochim. Acta* **A23** 139
Mallinson P D, McKean D C, Holloway D C and Oxfon I A 1975 *Spectrochim. Acta* **A31** 143
Marmer E B, Pouchan C, Dargelos A and Chaillet M 1979 *J. Mol. Struct.* **57** 189
McLean A D 1964 *J. Chem. Phys.* **40** 243
Mills I M 1963a *Spectrochim. Acta* **19** 1585
Mills I M 1963b *IR spectroscopy and molecular structure* (ed) M Davies (Amsterdam: Elsevier) p. 166
Murthy A S N and Ranganathan S 1982a *J. Mol. Struct. (Theochem)* **90** 219
Murthy A S N and Ranganathan S 1982b *Proc. Indian Acad. Sci. (Chem. Sci.)* **91** 535
Murthy A S N and Ranganathan S 1983 *J. Compt. Chem.* **4** 175
Nelander B and Ribbegard G 1974 *J. Mol. Struct.* **20** 325
Nyquist R A 1967 *Spectrochim. Acta* **19** 1595
Overend J and Scherer J R 1960 *J. Chem. Phys.* **32** 1296
Overend J, Nyquist R A, Evans J C and Polts W J 1961 *Spectrochim. Acta* **17** 1205
Paldus J and Hrabe P 1968 *Theor. Chim. Acta* **11** 401
Pople J A and Beveridge D L 1970 *Approximate molecular orbital theory* (New York: McGraw Hill) p. 110

Pulay P 1969 *Mol. Phys.* **17** 197
Pulay P 1970a *Mol. Phys.* **18** 473
Pulay P 1970b *Mol. Phys.* **21** 329
Pulay P and Meyer W 1971 *J. Mol. Spectrosc.* **40** 59
Pulay P and Meyer W 1972a *J. Chem. Phys.* **56** 2109
Pulay P and Meyer W 1972b *J. Chem. Phys.* **57** 3837
Pulay P and Torok F 1973 *Mol. Phys.* **25** 1153
Pulay P 1974 *Theor. Chim. Acta* **32** 253
Rafalko J J, Rzepa H S and Swanson B I 1979 *J. Mol. Struct.* **75** 363
Rao C N R, Goldman G K and Lurie C 1958 *J. Phys. Chem.* **63** 1311
Ribegard G 1974 *J. Mol. Struct.* **20** 325
Schachtschneider J H 1964 Tech. Report, Shell Oil California, pp. 57–65
Seth-Paul W A and Duyse A V 1972 *Spectrochim. Acta* **A30** 211
Swanson B I, Arnold T H, Dewar M J S, Rafalko J J, Rzepe H S and Yamaguchi Y 1978a *J. Am. Chem. Soc.* **100** 771
Swanson B I, Arnold T H and Yamaguchi Y 1978b *J. Mol. Spectrosc.* **78** 125, 139
Swanstrom P, Phomsen K and Yde P B 1971 *Mol. Phys.* **20** 1135
Taft R W 1956 *Steric effects in organic chemistry* (ed.) M S Newman (New York: John Wiley) Chap. 13
Taft R W, Deno N C and Skell P S 1958 *Annu. Rev. Phys. Chem.* **80** 49
Thompson H W, Needham R W and Jameson D 1957 *Spectrochim. Acta* **9** 208
Tokagi K and Oka T 1963 *J. Phys. Soc. Jpn* **18** 1174
Torok F, Hegedus L, Kosa K and Pulay P 1976 *J. Mol. Struct.* **32** 93
Torok F and Pulay P 1978 *J. Mol. Struct.* **46** 43

Proc. Indian Acad. Sci. (Chem. Sci.), Vol. 93, No. 6, August 1984, pp. 927–945.
© Printed in India.

Correlations between topological features and physicochemical properties of molecules

D V S JAIN*, SUKHBIR SINGH and VIJAY GOMBAR†

Department of Chemistry, †Department of Pharmaceutical Sciences, Panjab University, Chandigarh 160014, India

Abstract. The article reviews in brief, the *de novo* group additivity approach and, at length, the different topological approaches to obtain predictive and internally consistent correlations between various properties and structural features of molecules. The stress has mainly been on the molecular connectivity method. A new rational scheme for nomenclature of connectivity indices of different orders and types is introduced. The concept of the perturbation connectivity parameter developed by us recently has been applied to obtain correlations for molar refraction, boiling point, molar volume, heat of atomisation, heat of combustion, heat of vaporisation, magnetic susceptibility and critical constants of alkanes, alcohols and alkylbenzenes. A comparative study of various approaches reveals that the present perturbation topological approach has an edge over other similar methods.

Keywords. Connectivity indices; topological parameters; topology-property correlations; alcohols; alkylbenzenes; physicochemical properties.

1. Introduction

Molecular topology describes the manner of connectedness of atoms in a molecule. This is one of the basic factors responsible for differences in the values of physicochemical properties of isomeric molecules. The problem of establishing quantitative relationships between topology and properties has always been an important research area because such correlations can readily estimate and predict magnitude of properties particularly when experimental determinations are difficult. A great amount of effort has, therefore, been expended in developing procedures for obtaining such correlations. The earliest work in this direction was based upon the *de novo* approach using the additivity model. Towards the middle of the century, however, the problem was looked at from a different angle where molecules are first coded, according to their topology, in terms of numerical indices which are then treated as independent variables in regression analysis. Though the two models have inherent advantages and limitations, the efforts are on to parametrize both the approaches to generate internally consistent correlations possessing predictive powers within the experimental accuracy.

We are primarily interested in the development of the topological parameters. The present article, therefore, reviews, in brief, the work accomplished using the additivity model followed by a treatment, in detail, regarding the basis, terminology and chronological development of various topological parameters with special emphasis on connectivity indices. Recently, the present authors (Gombar *et al* 1983) developed a

* To whom all correspondence should be addressed.

connectivity index, called perturbation connectivity index, which incorporates the effects of atomic environments at topological level. Its correlations with properties like molar refraction, boiling point, molar volume, heat of atomisation, heat of combustion, heat of vaporisation, magnetic susceptibility and critical constants of alkanes, alcohols and akylbenzenes are reported and compared with earlier results.

2. Additivity model

The principle of additivity of atomic contributions was used for correlation studies on molar refraction (Bruhl 1891; Eisenlohr 1910), parachor (Sugden 1924), molar volume (Glasstone 1946) and magnetic susceptibility (Souders *et al* 1949). The predictions were found to be closer to the experimental values when the additivity principle was applied to the bond contributions instead of atomic contributions (von Steiger 1921; Smyth 1925; Fajans and Knorr 1926; Benson and Buss 1958; Pauling 1960; Benson 1976) especially when explicit corrections for bond-bond interactions, influence of nearest neighbouring atoms, steric interactions etc were incorporated (Zahn 1934; Tatevskii 1950, 1951; Allen 1959; Tatevskii and Papulov 1960; Somayajulu and Zwolinski 1966, 1972, 1974). The bond additivity scheme was further refined by taking different groups of atoms as the independent contributing units (Parks and Huffman 1932; Klages 1949; Franklin 1949; Laidler 1956). The contributions of various groups involving hetero atoms, multiple bonds, cyclic fragments etc have been calculated for a variety of physiochemical properties (Platt 1947; Bremner and Thomas 1948; van Krevelen and Chermin 1951; Tatevskii *et al* 1961; Vetere 1976; Benson 1976; Hoshino *et al* 1978; Macknick and Prausnitz 1979; Ogilvie and Abu-Elgheit 1980).

3. Topological approach

3.1 *Molecules as graphs*

In the topological approach a molecule is represented by a hydrogen-supressed graph (HSG) in which each vertex represents a non-hydrogen atom and each edge a bond (Sylvester 1878). A HSG (figure 1) consists of various subgraphs involving different number and arrangement of edges. The number of edges determines the order m and the arrangement decides the type t of the subgraph. Mathematically a HSG is usually represented by a binary adjacency matrix of order $n \times n$ (Sylvester 1878) in which unit and zero elements, respectively, represent bonded and non-bonded situations in a molecule.

3.2 *Development of topology based parameters*

Various indices have been defined in order to numerically encode molecules according to their topology. For n-alkanes the number of vertices (carbon atoms) carries enough topological quantification and significantly correlates with a number of properties (Aranda 1936; Komoshilov 1939; 1940; Colingoert *et al* 1941; Huggins 1941, 1954; Kurtz and Lipkin 1941; Francis 1941; Mibashan 1945; Smithenberg and Mulder 1948; Kurtz and Sankin 1954; Li *et al* 1956). In view of the correlations which could be applicable to branched alkanes as well, Wiener (1947, 1948) proposed that the difference ΔX between any property X of isomeric alkanes could be predicted in terms

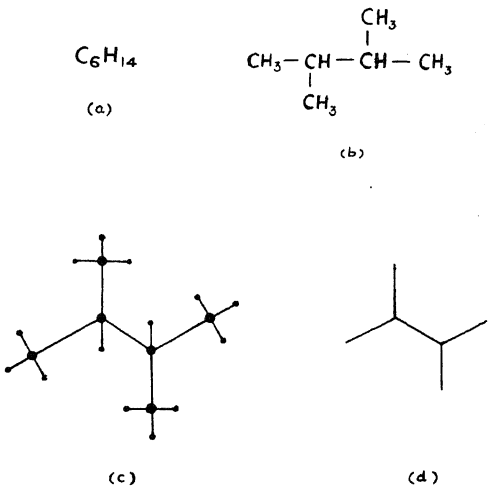

Figure 1. 2,3-dimethylbutane **a.** molecular formula, **b.** structural formula, **c.** molecular graph, **d.** hydrogen-suppressed graph.

of two parameters, *viz* w (path number) and p (polarity number), according to equation (1),

$$\Delta X = \frac{k}{n^2}\Delta w + b\Delta p, \tag{1}$$

where n is the number of vertices in the HSG of the alkanes concerned and k and b are regression coefficients. The polarity number p is the number of pairs of carbon atoms which are separated by three carbon-carbon bonds, and w is calculated according to (2) where d_{ij} is the general element of the distance matrix corresponding to the HSG.

$$w = \sum_{i<j}^{n} d_{ij}, \tag{2}$$

Gordon and Scantlebury (1964) defined a branching index of second order subgraphs B_2 which increases with degree of branching, by (3)

$$B_2 = N_2/(n-1), \tag{3}$$

where N_2 is the number of second order sub-graphs and n is the number of vertices. Using various subgraphs as the contributing units Smolenski (1964) blended the additivity and the topological approaches and observed a good correlation with standard heats of formation in terms of nine types of subgraphs. An integer topological index Z was proposed by Hosoya (1971). Z is related to the number of ways in which k edges are so chosen from the HSG that no two of them are connected. Gutman *et al* (1975) defined a topological index for acyclic polymers and concluded that their thermodynamic stability decreased and reactivity, in general, increased with branching. Randic (1975) distinguished between ten possible types of edges in the HSG of a hydrocarbon by associating each edge between vertices i and j with an index (edge index) equal to $(v_i v_j)^{1/2}$; v_i, being the number of edges converging at vertex i. He defined

a topological index (branching index) to be the sum of all the edge indices existing in a given HSG.

Some topological parameters *viz* information content (IC), complementary information content (CIC), structural information content (SIC) and relative nonstructural information content (RNSIC) have been defined (Basak *et al* 1979, 1982a, b; Basak and Magnuson 1983; Ray *et al* 1981, 1982, 1983; Raychaudhury *et al* 1980; Gombar and Wadhwa 1982) by applying information theory to the total molecular graph. These have, however, been mostly employed in correlation studies on biological properties. The discussion on these parameters is, therefore, not included in this paper. On the same grounds the DARC/PELCO method (Dubois *et al* 1967, 1973, 1976; Mercier and Dubois 1979; Mercier *et al* 1981; Sobel *et al* 1981) is not discussed here.

3.3 *Connectivity indices*

Kier *et al* (1975) defined a unitless topological quantifier called connectivity index χ identical to Randic's branching index for a series of alcohols and esters by treating oxygen atoms equivalent to carbon atoms and double bonds equivalent to single bonds. They obtained useful correlations with many physicochemical and non-specific biological properties (Kier *et al* 1975a, b; Hall *et al* 1975; Murray *et al* 1975, 1976). Since a single parameter cannot completely quantify the topology of a molecule, the approach of connectivity index was extended to higher order terms (Kier *et al* 1976). For more effective quantification of other salient topological features like types of atoms, multiplicity of bonds, cyclic fragments etc, valence connectivity indices, χ^v, of different types were defined (Kier and Hall 1976a, b, 1977; Kier 1980). A connectivity index dependent upon bond length, χ^r, was defined by Gupta and Singh (1978) and its correlations investigated with different biological properties. Jain and Gombar (1979) furthered the concept of path-connectivity indices to binary mixtures of *n*-alkanes. They assumed connectivity index of a binary mixture to be equal to molefraction average of the values of the components. Using first and third order connectivity indices of mixtures they obtained a highly predictive relationship for estimating excess volumes of binary mixtures of *n*-alkanes at different temperatures.

3.3a *Nomenclature of connectivity indices* Some of the higher order subgraphs, as defined by Kier and Hall (1976a), for 1,1,4-trimethylpentane, along with their counts and notations are given in table 1. It can be seen that according to notation given by Kier and Hall (1976a) the sub-graphs with different arrangement of vertices contribute towards same connectivity index. The ambiguity in the definitions is further accentuated when still higher order terms are considered. We have developed a uniform scheme (Gombar-Surjit-Jain (GSJ) scheme) for characterising unique subgraphs. The GSJ notations for connectivity indices corresponding to some of the subgraphs 1,1,4-trimethylpentane are also given in table 1. The superscript on χ equals the number of edges involved and the number of subscripts refers to the number of branchings in the contributing subgraph. The base of a subscript gives the branching position and its power represents the length of the branch. A terminal vertex is always assigned zero position and other vertices are numbered sequentially so that the branched position gets minimum number. Some of the sixth order connectivity indices, thus defined according to the GSJ scheme, are given in table 2. In the term ${}^8\chi_{2^2 2^2}$, read as eight-chi-two-square-two-square, therefore, the contributing subgraph (figure 2) involves 8 edges such that two branchings each of length two are present at position 2.

Table 1. Nomenclature, occurrence count and representative subgraphs in HSG of 1,1,4-trimethylpentane.

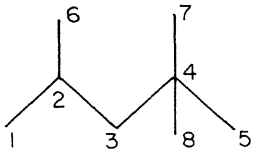

	Representative subgraphs		Resulting connectivity index	
Order	Topology	Occurrence	Kier's-notation	GSJ-notation
2		10	$^{2}\chi$	$^{2}\chi$
3		5	$^{3}\chi_c$	$^{3}\chi_1$
4		1	$^{4}\chi_c$	$^{4}\chi_{11}$
4		4	$^{4}\chi_{pc}$	$^{4}\chi_1$
5		7	$^{5}\chi_{pc}$	$^{5}\chi_1$
5		0	$^{5}\chi_{pc}$	$^{5}\chi_2$
5		1	$^{5}\chi_{pc}$	$^{5}\chi_{11}$

3.3b *Calculation of connectivity indices* For calculation of connectivity index of order m and type t (= P, C, PC or CH) Kier and Hall (1977) extended Randic's (1975) idea of edge indices. Each vertex in a HGS is accociated with a numerical value, called δ-value. The contribution C_j of a subgraph of order m and type t is calculated from (4).

$$C_j = \prod_{i=1}^{m+1} (\delta_i)^{-1/2}. \tag{4}$$

The total of C_j values calculated for all the subgraphs, $^{m}g_t$, of order m and type t gives the required connectivity index, $^{m}\chi_t$, equation (5)

$$^{m}\chi_t = \sum_{j=1}^{^{m}g_t} C_j. \tag{5}$$

The simplest version of connectivity indices is represented by $^{m}\chi_t^s$. In this case heteroatoms are treated equivalent to carbon atoms and double bond equivalent to single bond. The δ-value associated to each vertex in this case is δ^s which is equal to the number of vertices connected to it. In order to treat hetero-

Table 2. Gombar-Surjit-Jain (GSJ) representations of the sixth order connectivity indices and contributing subgraphs.

Subgraph	GSJ notation of connectivity index
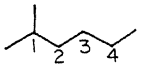	$^{6}\chi_{1}$
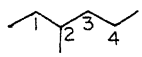	$^{6}\chi_{2}$
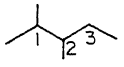	$^{6}\chi_{12}$
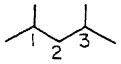	$^{6}\chi_{13}$
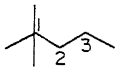	$^{6}\chi_{11}$
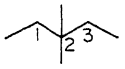	$^{6}\chi_{22}$
	$^{6}\chi_{112}$

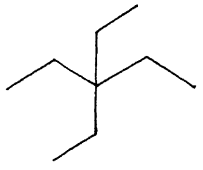

Figure 2. A representative subgraph contributing towards $^{8}\chi_{2^{2}2^{2}}$.

atoms and bond multiplicities specifically which is essential to distinguish molecules $CH_3(CH_2)_2CH_3$, $CH_3(CH_2)_2OH$, $CH_3(CH_2)_2NH_2$, CH_3CH_2CHO, $CH_3CH_2OCH_3$, $CH_3CH{=}CHCH_3$ etc., at topological level, Kier and Hall (1976b) proposed the use of δ^v for δ-values. For the first row heteroatoms δ^v is defined by equation (6) and for higher members in a group by equation (7)*. In (6) and (7) Z_i and Z_i^v, respectively, denote total and valence shell electrons in atoms represented by vertex i and h is the number of hydrogens supressed at vertex i in the HSG.

$$\delta_i^v = Z_i^v - h, \tag{6}$$

$$\delta_i^v = \frac{Z_i^v - h}{Z_i - Z_i^v}, \tag{7}$$

* For halogen atoms a set of empirical δ-values was proposed earlier but in recent compilations (Kier 1980; Kier and Hall 1983) the values derived from general equations (6) and (7) have been quoted for them. For subgraphs involving a fluorine atom the contribution C (cf eq (4)) is empirically assumed to be negative.

Recently Kier and Hall (1983) have proposed a general definition, equation (7a) of valence δ-values

$$\delta_i^v = \frac{Z_i^v - h}{Z_i - Z_i^v - 1}. \tag{7a}$$

The resulting connectivity indices are called valence connectivity indices and are represented by ${}^m\chi_t^v$.

3.3c *Computation of connectivity indices* In the literature an unpublished computer program CFUNC (Hall)* is often cited for computer calculation of connectivity indices upto sixth order. We (Singh *et al* 1984) have developed a program, KNKTVT, in standard FORTRAN which can compute path-connectivity terms upto the highest order possible in a HSG and all the branched-connectivity indices upto seventh order.

The calculation of connectivity indices for a given set of δ-values requires counting of subgraphs of desired order and type. Our program, however, requires only the connection table as the input besides the appropriate δ-values. The program generates a logical matrix of order $n \times n$ whose elements are initiated .TRUE. or .FALSE. depending upon the input connection table. For calculation of a connectivity index of any order and type all the appropriate .TRUE. paths are then picked and their contributions computed.

4. Perturbation connectivity index

The δ^v values do distinguish between heteroatoms and bond multiplicities. However, a look at the δ^v values for methyl propionate (figure 3) reveals that in spite of different atomic environments the two oxygens are assigned equal values. Similar is the case with two terminal methyl carbons as well. We have incorporated the effects of atomic environments by defining perturbation δ-value, δ^P, which is related to δ-value as:

$$\Gamma\delta^P = \delta. \tag{8}$$

Here Γ is a square matrix whose diagonal elements are unity and off-diagonal elements are zero or $-\gamma_{ij}$ depending upon whether element i–j corresponds to non-bonded or bonded situation in a molecule. The perturbation parameter γ_{ij} determines the environmental effect of the nearest atom j bonded to atom i. The elements of the column vector δ can be δ_i^s, δ_i^v or Z_i^v. The selection of δ^s, δ^v or Z^v for δ-values yields, respectively, the connectivity indices ${}^m\chi^P$, ${}^m\chi^{P(v)}$ or ${}^m\chi^{P(e)}$.

To calculate δ_i^P from (8) it is necessary to know the numerical value of γ_{ij}. As there is no *a priori* method for such assignment, the perturbation parameters have to be treated

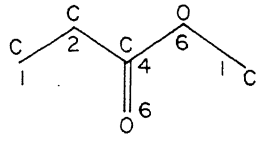

Figure 3. δ^v values assigned to vertices of methyl propionate.

* Program listings can be obtained from: Professor L. G. Hall, Eastern Nazarene College, Massachusetts.

empirically. It can be seen that the Kier's approach (Kier and Hall 1976b) becomes a special case of our general approach when all γ_{ij} are zero. Cammarata (1979) also used a similar approach to quantify molecular topology. However he defined only two parameters M' and A' as:

$$M' = \sum_{i}^{n} \delta_i^P, \tag{9}$$

$$A' = \sum_{i}^{n} (1/\delta_i^P), \tag{10}$$

where δ_i^P were calculated from (7) using $\gamma_{ij} = \gamma_{ji} = \gamma = 0{\cdot}1$ and employing Z_i^v for δ-values.

4.1 *Correlations using perturbation connectivity indices*

A summary of quantitative correlations of a number of physicochemical and biological properties with simple and valence connectivity indices was reported by Kier and Hall (1977). Many more relationships have been obtained since then. The properties correlated so far are collected in table 3. In the following sections we discuss the correlations obtained between the newly defined perturbation connectivity indices ${}^m\chi^{P(e)}$ and some of the physicochemical properties of alkanes, alcohols and alkylbenzenes. The indices ${}^m\chi^{P(e)}$ used in the present correlations have been calculated assuming $\gamma_{ij} = \gamma_{ji} = 0{\cdot}1$ for all vertices i and j. The correlations thus obtained have been compared with those reported in the literature (Kier and Hall 1976a). For all the properties reported here we have obtained the correlations using both valence and perturbation connectivity indices. It was felt necessary first of all to assess the relative merits of the two because the sample set was either different from that reported by Kier and Hall or the systematic procedure was not followed by them for regression analysis.

4.1a *Molar refraction* This is one of the most commonly investigated molecular property for assessing the potential of any newly defined topology quantifier because fairly accurate experimental data on molar refraction R_m are available in the literature for a number of compounds. Kier and Hall (1976a) have investigated at great length the correlations between connectivity indices of various order and types and molar refraction of alcohols (31, 0·153, ${}^1\chi^v$, ${}^3\chi_c^v$, ${}^3\chi_p$, ${}^3\chi_c$)*, ethers (9, 0·291, ${}^1\chi^v$, ${}^3\chi_c$), amines (22, 1·280, ${}^1\chi^v$, ${}^3\chi_p^v$, ${}^3\chi_p$), alkyl halides (17, 0·108, ${}^1\chi$, ${}^1\chi^v$, ${}^3\chi_c$, ${}^3\chi_c^v$, ${}^3\chi_p$), mixed aliphatic compounds (64, 0·364, ${}^1\chi$, ${}^1\chi^v$, ${}^3\chi_c$, ${}^3\chi_c^v$, δ_N^v), alkanes (46, 0·027, ${}^1\chi$, ${}^2\chi$, ${}^3\chi_p$, ${}^4\chi_c$, ${}^4\chi_{pc}$), mono olefinic alkenes (39, 0·147, ${}^0\chi$, ${}^1\chi$, ${}^1\chi^v$, ${}^2\chi$, ${}^3\chi_p^v$, ${}^4\chi_c$) and alkyl substituted benzenes (70, 0·163, ${}^1\chi$, ${}^1\chi^v$, ${}^2\chi$, ${}^2\chi^v$). We have investigated a sample of 55 alkanes and obtained a three-variable correlation, equation (11),

$$R_m = -8{\cdot}171\ {}^0\chi^{P(e)} + 37{\cdot}711\ {}^1\chi^{P(e)} + 8{\cdot}506\ {}^2\chi^{P(e)} + 10{\cdot}429$$
$$n = 55;\ r = 0{\cdot}9999;\ s = 0{\cdot}027;\ F > 9 \times 10^5, \tag{11}$$

which produces statistics comparable to that obtained by Kier and Hall (1976a) using five indices for a relatively smaller sample of 46 alkanes. Equation (11) yields maximum

* The arguments in parantheses are sample size ($n = 31$), standard error ($s = 0{\cdot}153$) and various regression variables.

Table 3. Physicochemial properties correlated with connectivity indices.

Property	Class of Compounds	*n*	*r*	Reference
Aqueous solubility	Alcohols	51	0·978	Hall *et al* (1975)
	Alcohols	48	0·988	Kier and Hall (1976b)
	Alkanes	18	0·958	Hall *et al* (1975)
	Alkyl benzenes	13	0·9890	Kier and Hall (1976a)
	Alcohols	51	0·965	Cammarata (1979)
	Esters	38	0·990	Kier and Hall (1977)
	Ethers	22	0·989	Kier and Hall (1976a)
Boiling point	Alcohols	63	0·970	Hall *et al* (1975)
	Alcohols	48	0·993	Kier and Hall (1976b)
	Alcohols	28	0·9996	Kier and Hall (1976a)
	Alkanes	51	0·9969	Kier and Hall (1976a)
	Amines (primary)	12	0·9991	Kier and Hall (1976a)
	Amines (secondary)	13	0·999	Kier and Hall (1976a)
	Amines (tertiary)	4	0·997	Kier and Hall (1976a)
	Amines (primary)	21	0·999	Kier and Hall (1976b)
	Alkyl halides	24	0·992	Kier and Hall (1976b)
	Ethers	11	0·9882	Kier and Hall (1976a)
	Polyols	9	0·995	Kier and Hall (1976b)
	Carboxylic acids	22	0·996	Gombar (1981)
Cavity surface area	Alkanes and alcohols	69	0·978	Kier *et al* (1975a)
Density	Aliphatic liquid Hydrocarbons	82	0·9889	Kier *et al* (1976)
	Hydrocarbons	13	0·9104	Kier and Hall (1976a)
	Aliphatic alcohols	42	0·9305	Kier *et al* (1976)
	Aliphatic acids	20	0·9831	Kier *et al* (1976)
	Aliphatic ethers	13	0·9104	Kier and Hall (1976a)
Diamagnetic susceptibility	Hydrocarbons	27	0·9999	Kier and Hall (1976a)
	Alcohols	15	0·9993	Kier and Hall (1976a)
Excess volume	Binary mixtures of *n*-alkanes			Jain and Gombar (1979)
Heat of atomisation	Alkanes	44	0·9999	Kier and Hall (1976a)
	Alcohols	19	0·9999	Kier and Hall (1976a)
	Ethers	12	0·9999	Kier and Hall (1976a)
	Monoolefines	37	0·9999	Kier and Hall (1976a)
	Thiols	14	0·9999	Kier and Hall (1976a)
Heat of formation	Alkanes	67	0·9996	Kier and Hall (1976a)
	Alcohols	20	0·9948	Kier and Hall (1976a)
Heat of vaporisation	Alkanes	44	0·9999	Kier and Hall (1976a)
	Alcohols	20	0·9982	Kier and Hall (1976a)
Molar refraction	Alcohols	31	0·9998	Kier and Hall (1976a)
	Alkanes	46	0·999	Kier and Hall (1976a)
	Amines	22	0·9881	Kier and Hall (1976a)
	Alkyl benzenes	70	0·9995	Kier and Hall (1976a)
	Ethers	9	0·9989	Kier and Hall (1976a)
	Halo compounds	17	0·999	Kier and Hall (1976a)
	Mixed	65	0·990	Kier and Hall (1976a)
	Monoolefinic alkenes	39	0·9994	Kier and Hall (1976a)
	Phenyl substituent	25	0·990	Kier and Hall (1976b)
Molar volume	*n*-alkanes at 20°C	14	0·9999	Jain and Gombar (1979)
	n-alkanes at 50°C	13	0·9999	Jain and Gombar (1979)
	n-alkanes at 100°C	15	0·9999	Jain and Gombar (1979)
Molecular polarizability	Mixed	36	0·990	Kier *et al* (1975a)

Table 3. (*Continued*)

Property	Class of Compounds	*n*	*r*	Reference
Octanol-water partition coefficient	Alcohols	49	0·997	Murray *et al* (1975)
	Alcohols	14	0·999	Boyd *et al* (1982)
	Amines	12	0·998	Boyd *et al* (1982)
	Amines	28	0·979	Murray *et al* (1975)
	Carboxylic acids	9	0·996	Murray *et al* (1975)
	Hydrocarbons	45	0·975	Murray *et al* (1975)
	Esters	24	0·999	Murray *et al* (1975)
	Ethers	12	0·976	Murray *et al* (1975)
	Ketones	16	0·993	Murray *et al* (1975)
	Phenols	16	0·988	Boyd *et al* (1982)
	Mixed	66	0·970	Boyd *et al* (1982)
	Mixed	138	0·986	Murray *et al* (1975)
Positronium annihilation cross-section area	Benzene and derivatives	17	0·997	Gombar *et al* (1980)
	Alkanes	47	0·999	Gombar *et al* (1980)
	Compounds containing halogens	31	0·998	Gombar *et al* (1980)
	Compounds containing oxygen	46	0·998	Gombar *et al* (1980)
	Unsaturated compounds	33	0·984	Gombar *et al* (1980)
	Mixed	182	0·996	Gombar *et al* (1980)
Retention indices in squalene	Alcohols		0·994	Kier and Hall (1979)
	Esters		0·991	Kier and Hall (1979)
	Ethers		0·968	Kier and Hall (1979)
	Ketones		0·996	Kier and Hall (1979)
Van der Walls constant-*b*	Mixed	20	0·981	Kier and Hall (1976b)

absolute deviation of 0.1 $cm^3\ mol^{-1}$ and predicts an absolute deviation of more than 0·05 $cm^3\ mol^{-1}$ only for three of the 55 alkanes. It may be noted that the accuracy in the experimental data ranges from 0·007 to 0·05 $cm^3\ mol^{-1}$. For a series of 31 alcohols a 4-variable ($^1\chi^v$, $^3\chi_c^v$, $^3\chi_P$, $^3\chi_c$) equation has been reported (Kier and Hall 1976a) which gives a standard error of 0·153 $cm^3\ mol^{-1}$. Using the zero order perturbation connectivity index, $^0\chi^{P(e)}$, we have found a correlation which produces comparable statistics for a sample of 32 alcohols. It was observed that a 5-variable equation, equation (12), yielded a standard error of 0·02 $cm^3\ mol^{-1}$ which is of the order of the experimental error.

$$R_m = 6{\cdot}032\ {}^0\chi^{P(e)} + 8{\cdot}211\ {}^1\chi^{P(e)} + 3{\cdot}157\ {}^2\chi^{P(e)} + 1{\cdot}115\ {}^4\chi^{P(e)} + 2{\cdot}966\ {}^4\chi_1^{P(e)}$$
$$n = 32;\ r = 0{\cdot}9999;\ s = 0{\cdot}02;\ F > 7 \times 10^5. \tag{12}$$

We also studied a sample of 120 alkyl-substituted benzenes and obtained a 2-variable correlation, equation (13),

$$R_m = 10{\cdot}113\ {}^0\chi^{P(e)} + 1{\cdot}323\ {}^2\chi^{P(e)} - 5{\cdot}994$$
$$n = 120;\ r = 0{\cdot}9999;\ s = 0{\cdot}17;\ F > 3 \times 10^6, \tag{13}$$

which produces statistics comparable to that obtained by Kier and Hall (1976a) using indices $^1\chi$, $^1\chi^v$, $^2\chi$ and $^2\chi^v$ for a smaller sample of 70 alkyl benzenes. It was observed that the stepwise regression procedure picked a 3-variable equation in χ^v, equation (14),

which was better than the 3-variable correlation in $\chi^{P(e)}$.

$$R_m = 2{\cdot}168\ {}^0\chi^v + 5{\cdot}560\ {}^1\chi^v + 0{\cdot}925\ {}^2\chi^v + 6{\cdot}507$$

$$n = 120;\ r = 0{\cdot}9999;\ s = 0{\cdot}11;\ F > 5 \times 10^6. \tag{14}$$

4.1b *Boiling point* The estimation of boiling points t_b has been the subject of several studies (Wiener 1947; Kudchadkar *et al* 1968; Hosoya 1971; Randic 1975; Hall *et al* 1975). For isomeric hexanes and heptanes Kier and Hall (1976b) have compared the quality of correlations obtained between boiling point and various topological indices; Randic's edge index (Randic 1975) was shown to correlate the best. Using simple and valence connectivity indices they have reported correlations for alkanes (51, 2·53, ${}^1\chi$, ${}^4\chi_{pc}$), alcohols (62, 0·86, ${}^1\chi$, ${}^1\chi^v$, ${}^3\chi_p$, ${}^3\chi_p^v$, ${}^3\chi_c$), aliphatic ethers (11, 5·39, ${}^1\chi$, ${}^1\chi^v$), primary amines (12, 1·56, ${}^1\chi$, ${}^1\chi^v$), secondary amines (13, 2·20, ${}^1\chi$, ${}^1\chi^v$), tertiary amines (4, 2·92, ${}^0\chi^v$), aliphatic polyols (9, 3·78, ${}^1\chi$, ${}^1\chi^v$) and alkyl halides (17, 2·57, ${}^1\chi^v$, ${}^3\chi_p$, ${}^3\chi_c^v$). We studied a sample of 235 alkanes, including 96 *n*-alkanes, ranging between 5 and 100 carbon atoms. We obtained a highly significant nonlinear correlation, equation (15).

$$t_b = 916{\cdot}978 - \frac{12406{\cdot}583}{11{\cdot}666 + {}^1\chi} + 4{\cdot}634\ {}^4\chi_1,$$

$$n = 235;\ r = 0{\cdot}9999;\ s = 2{\cdot}789;\ F > 2 \times 10^7. \tag{15}$$

A correlation obtained using ${}^1\chi^{P(e)}$ and ${}^4\chi_1^{P(e)}$, however, was slightly inferior ($s = 4{\cdot}439$°C). For the sub-sample of 96 *n*-alkanes we found that ${}^1\chi$ or ${}^1\chi^{P(e)}$ resulted in equation (16) with identical statistical quality.

$$t_b = 916{\cdot}978 - \frac{4944{\cdot}446}{4{\cdot}806 + {}^1\chi^{P(e)}(\text{or } {}^1\chi)}$$

$$n = 96;\ r = 0{\cdot}9999;\ s = 1{\cdot}185;\ F > 8 \times 10^7. \tag{16}$$

It was observed that the maximum absolute deviation in t_b calculated on the basis of (15) was ~ 10°. It should be noted that the boiling points of the 235 alkanes investigated here range between 9 and 715°C with uncertainties from 0·002 to 20°C (Kovats 1961). Recently Ogilvie and Abu-Elgheit (1981) reported an average error of 2°C in prediction of t_b. The results are firstly based on a sample of 50 alkanes (C_4–C_{20}) and secondly involve as many as 8 substructural parameters.

For a set of 28 monoaliphatic alcohols Kier and Hall (1976a) reported a standard error of 0·86°C using five variables (${}^1\chi$, ${}^1\chi^v$, ${}^3\chi_p$, ${}^3\chi_p^v$, ${}^3\chi_c$). Our investigations on a sample of 62 alcohols led to equation (17), which shows a standard error of 5·62°C.

$$t_b = -345{\cdot}429\ {}^0\chi^{P(e)} + 869{\cdot}933\ {}^1\chi^{P(e)} + 171{\cdot}715\ {}^3\chi^{P(e)} + 194{\cdot}796,$$

$$n = 62;\ r = 0{\cdot}9871;\ s = 5{\cdot}62;\ F = 735, \tag{17}$$

It was observed that the standard error reduced to 2·23 when seven variables (${}^0\chi^v$, ${}^1\chi^v$, ${}^2\chi^v$, ${}^3\chi_p^v$, ${}^3\chi_c^v$, ${}^4\chi_p^v$, ${}^4\chi_{pc}^v$) were included in the regression. It may be noted that Kier and Hall (1976a) studied a selected sample and used connectivity indices from two different sets *viz* simple connectivity indices and valence connectivity indices. As far as we know there is no correlation reported in literature between boiling points and χ indices of alkylbenzenes. For a sample of 47 such compounds we obtained the

following correlations using ${}^{m}\chi^{P(e)}$, equation (18), and ${}^{m}\chi^{v}$, equation (19), indices.

$$t_b = -139{\cdot}449\ {}^{0}\chi^{P(e)} + 362{\cdot}281\ {}^{1}\chi^{P(e)} - \frac{338{\cdot}479}{{}^{1}\chi^{P(e)}} + 143{\cdot}149,$$

$$n = 47;\ r = 0{\cdot}9970;\ s = 5{\cdot}44;\ F = 2345, \tag{18}$$

$$t_b = 31{\cdot}833\ {}^{0}\chi^{v} - 20{\cdot}318\ {}^{2}\chi^{v} - \frac{150{\cdot}277}{{}^{1}\chi^{v}} + 65{\cdot}241,$$

$$n = 47;\ r = 0{\cdot}996;\ s = 5{\cdot}82;\ F = 2049. \tag{19}$$

It was observed that a seven-variable (${}^{1}\chi^{P(e)}$, ${}^{2}\chi^{P(e)}$, ${}^{3}\chi^{P(e)}$, ${}^{4}\chi^{P(e)}$, ${}^{4}\chi_1^{P(e)}$, $1/{}^{0}\chi^{P(e)}$, $1/{}^{1}\chi^{P(e)}$) resulted in a standard error of 1·66°C and a maximum absolute deviation of 3·7°C. For a set of 22 aliphatic saturated monocarboxylic acids (Gombar 1981) a 2-variable correlation, equation (20), in simple connectivity indices has been reported.

$$t_b = 65{\cdot}658 + 37{\cdot}785\ {}^{1}\chi + \frac{5{\cdot}208}{{}^{3}\chi_1},$$

$$n = 22;\ r = 0{\cdot}996;\ s = 3{\cdot}7;\ F = 1320, \tag{20}$$

It produces an average absolute deviation of $< 1{\cdot}5$°C.

4.1c *Density and molar volume* Kier and Hall (1976a) have obtained good correlations for density ρ of alkanes (82, 0·0046, ${}^{3}\chi_p$, $1/{}^{1}\chi$), aliphatic alcohols (40, 0·0030, ${}^{2}\chi$, ${}^{3}\chi_p$, ${}^{5}\chi_p$, ${}^{3}\chi_c^{v}$, $1/{}^{1}\chi$), aliphatic ethers (13, 0·0072, ${}^{3}\chi_p$, ${}^{5}\chi_p$) and aliphatic acids (20, 0·0137, ${}^{3}\chi$, $1/{}^{1}\chi$). However, variation in density of organic compounds is relatively small over a wide range of molecular weights. We have, therefore, chosen to correlate molar volume v_m ($= M/\rho$) with connectivity indices. We have performed regression analysis on molar volumes of 87 alkanes. The correlation obtained, equation (21), predicted v_m with an average absolute deviation below 0·3 % which is of the same order as obtained by Kier and Hall (1976b) from a study on densities of 46 alkanes using a five variable (${}^{3}\chi_p$, ${}^{5}\chi_p$, ${}^{4}\chi_{pc}$, ${}^{5}\chi_{pc}$, $1/{}^{1}\chi$) equation.

$$v_m = 80{\cdot}098\ {}^{1}\chi^{P(e)} + 21{\cdot}252\ {}^{2}\chi^{P(e)} - 45{\cdot}122\ {}^{3}\chi^{P(e)} + 46{\cdot}790,$$

$$n = 87;\ r = 0{\cdot}9999;\ s = 0{\cdot}65;\ F > 9 \times 10^4 \tag{21}$$

Jain and Gombar (1979) obtained correlations between molar volumes of *n*-alkanes at different temperatures and simple connectivity indices. By studying the temperature dependence of the regression coefficients of these correlations they deduced a general relationship to estimate molar volume of *n*-alkanes at any temperature between melting and boiling points. The extrapolation of this general relationship led to limiting values for density and thermal expansion coefficients of polymethylenes.

Investigations on molar volumes of a sample of 54 aliphatic alcohols resulted in a highly significant ($r = 0{\cdot}9993$) correlation with ${}^{0}\chi^{P(e)}$. A three-variable equation equation (22), however, yields a standard error of 0·60 cm^3 mol^{-1}

$$v_m = 40{\cdot}444\ {}^{0}\chi^{P(e)} - 35{\cdot}219\ {}^{3}\chi^{P(e)} + 10{\cdot}562\ {}^{4}\chi^{P(e)} + 5{\cdot}523,$$

$$n = 54;\ r = 0{\cdot}9998;\ s = 0{\cdot}60;\ F > 4 \times 10^4, \tag{22}$$

and predicts molar volumes of only two compounds with a deviation more than 1 $cm^3\ mol^{-1}$.

We also studied molar volumes of 120 alkyl substituted benzenes. A highly significant correlation, equation (23), was obtained which gave an average absolute error of less than 0·3 %. It produced maximum absolute deviation of 4 $cm^3\ mol^{-1}$. A three-variable ($^1\chi^v$, $^2\chi^v$, $^4\chi^v_{pc}$) correlation in valence connectivity indices also resulted in comparable statistics ($s = 1{\cdot}12$).

$$v_m = 32{\cdot}129\ {}^0\chi^{P(e)} + 23{\cdot}445\ {}^2\chi^{P(e)} - 44{\cdot}472\ {}^4\chi^{P(e)} - 27{\cdot}404,$$
$$n = 120;\ r = 0{\cdot}9999;\ s = 1{\cdot}05;\ F > 7 \times 10^5 \qquad (23)$$

4.1d *Enthalpy of atomisation* For hydrocarbons the enthalpy of atomisation ΔH_a is linearly dependent upon the number of carbon atoms (Kier and Hall 1976a). Using n, the number of carbon atoms, along with seven connectivity indices *viz* $^1\chi$, $^4\chi_p$, $^4\chi_{pc}$, $^5\chi_p$, $^5\chi_c$, $^5\chi_{pc}$, and $^6\chi_{pc}$, Kier and Hall (1976a) obtained a correlation which yielded a standard error of 1·55 kJ mol^{-1}. We have observed that a 3-variable correlation, in terms of connectivity indices only, generated by a stepwise procedure is much inferior ($s = 8{\cdot}8$ kJ mol^{-1}) to that obtained with $^m\chi^{P(e)}$, equation (24).

$$\Delta H_a = 2587{\cdot}8\ {}^0\chi^{P(e)} + 124{\cdot}6\ {}^2\chi^{P(e)} - \frac{63{\cdot}2}{{}^0\chi^{P(e)}} + 916{\cdot}6,$$
$$n = 44;\ r = 0{\cdot}9999;\ s = 2{\cdot}82;\ F > 5 \times 10^6. \qquad (24)$$

Studies on heat of atomisation of 21 alcohols also revealed that correlations in $^m\chi^{P(e)}$ are better than those, with the same degrees of freedom, in $^m\chi^v$. It appears that (25) is the best relationship reported so far as it predicts ΔH_a with a standard error of 0·52 kJ mol^{-1} which is of the order of the experimental error.

$$\Delta H_a = 2636{\cdot}5\ {}^0\chi^{P(e)} - 204{\cdot}2\ {}^3\chi^{P(e)} + 244{\cdot}2\ {}^3\chi_1^{P(e)} + 332{\cdot}7\ {}^4\chi^{P(e)} - 0{\cdot}808/{}^1\chi^{P(e)} - 217{\cdot}7,$$
$$n = 21;\ r = 0{\cdot}9999;\ s = 0{\cdot}52;\ F > 1 \times 10^8, \qquad (25)$$

For a sample of 33 alkylbenzenes a 3-variable ($^0\chi^v$, $^1\chi^v$, $^2\chi^v$) equation yielded a standard error of 14·16 kJ mol^{-1} which is once again much inferior to that obtained using corresponding perturbation connectivity indices, equation (26).

$$\Delta H_a = 2375{\cdot}8\ {}^0\chi^{P(e)} + 472\ {}^1\chi^{P(e)} + 254{\cdot}5\ {}^2\chi^{P(e)} - 2769{\cdot}4,$$
$$n = 33;\ r = 0{\cdot}9999;\ s = 2{\cdot}93;\ F > 1{\cdot}75 \times 10^6. \qquad (26)$$

This gives an average absolute deviation of 0·04 %. According to this equation only 3 compounds show absolute deviation of more than 2 kJ mol^{-1} but for 1,2,3,4-tetramethylbenzene which showed rather large deviation of 10·7 kJ mol^{-1}.

4.1e *Diamagnetic susceptibility* We studied the diamagnetic susceptibility χ_M of the same samples of alkanes and alcohols as investigated by Kier and Hall (1976a). The three-variable ($^0\chi$, $^1\chi$, $^2\chi$) equation reported by them is comparable ($s = 0{\cdot}41$) to the one

obtained using corresponding perturbation terms, equation (27)

$$\chi_M = 88{\cdot}430\ {}^0\chi^{P(e)} - 131{\cdot}022\ {}^1\chi^{P(e)} - 22{\cdot}636\ {}^2\chi^{P(e)} - 24{\cdot}607,$$
$$n = 27;\ r = 0{\cdot}9999;\ s = 0{\cdot}40;\ F > 2 \times 10^4. \tag{27}$$

Only four of the 27 alkanes are found to give an absolute deviation of more than 0.5.

Kier and Hall (1976a) have reported a three-variable (${}^0\chi$, ${}^1\chi^v$, ${}^3\chi^v_P$) correlation ($s = 0{\cdot}853$) for χ_M of 15 alcohols. Our stepwise procedure has, however, picked another set of three variables which correlates far better, equation (28).

$$\chi_M = 10{\cdot}012\ {}^0\chi^v + 8{\cdot}603\ {}^1\chi^v + 1{\cdot}951\ {}^4\chi^v_{pc} + 3{\cdot}260$$
$$n = 15;\ r = 0{\cdot}9999;\ s = 0{\cdot}27;\ F > 1{\cdot}00 \times 10^4. \tag{28}$$

The quality of the computer-selected 3-variable equation with ${}^m\chi^{P(e)}$ is found to be midway between ($s = 0{\cdot}42$). For a sample of 12 alkyl benzenes the correlation with ${}^m\chi^{P(e)}$ were better than those in ${}^m\chi^v$. A highly significant correlation, equation (29)

$$\chi_M = 46{\cdot}879\ {}^0\chi^{P(e)} - 45{\cdot}309\ {}^1\chi^{P(e)} - 8{\cdot}126\ {}^4\chi^{P(e)} - 16{\cdot}402$$
$$n = 12;\ r = 0{\cdot}9999;\ s = 0{\cdot}33;\ F > 3{\cdot}00 \times 10^4 \tag{29}$$

resulted in maximum absolute deviation of 0·56.

4.1f *Critical constants* Experimental determination of critical constants T_c, P_c and V_c, is tedious. Their estimation by extrapolation of correlations is, therefore, very useful. A survey of the methods to estimate critical constants of isomeric alkanes has been reported by Spencer and Daubert (1973). Various correlations obtained with connectivity indices are discussed below.

Critical temperature: For a sample of 49 alkanes we obtained equation (30) in terms of simple connectivity indices.

$$T_c = 24{\cdot}433\ {}^0\chi - 11{\cdot}017\ {}^2\chi - \frac{348{\cdot}782}{{}^1\chi} + 531{\cdot}913$$
$$n = 49;\ r = 0{\cdot}9977;\ s = 6{\cdot}03;\ F = 3215. \tag{30}$$

A three-variable correlation in $\chi^{P(e)}$ (${}^0\chi^{P(e)}$, ${}^3\chi^{P(e)}$, $1/{}^1\chi^{P(e)}$) is also found to be comparable ($s = 7{\cdot}83$). Equation (30) predicts T_c within 1–2% which is of the same order as reported by Lydersen (1955) and Nokay (1959). Spencer and Daubert (1973) predicted T_c of alkanes with an error of $< 0{\cdot}5\%$. Average absolute deviations of 0·8% and 0·2% have been reported for two different samples of alkanes (Schmidt and Wenzel 1981). We observed that a 7-variable correlation (${}^0\chi^{P(e)}$, ${}^1\chi^{P(e)}$, ${}^3\chi^{P(e)}$, ${}^3\chi_1^{P(e)}$, ${}^4\chi_1^{P(e)}$, $1/{}^0\chi^{P(e)}$, $1/{}^1\chi^{P(e)}$) resulted in an absolute average error of 0·6% with maximum absolute deviation of 10°K.

For a sample of 13 alcohols we observed that a 3-variable equation in ${}^m\chi^{P(e)}$, equation (31), resulted in an average deviation of less than 1%. The deviation is found to fall below 0·25% when some more terms are included in the regression.

$$T_c = -18{\cdot}443\ {}^2\chi^{P(e)} + 652{\cdot}607\ {}^3\chi^{P(e)} - 737{\cdot}099\ {}^4\chi_1^{P(e)} + 515{\cdot}039,$$
$$n = 13;\ r = 0{\cdot}9964;\ s = 5{\cdot}18;\ F = 414. \tag{31}$$

Schmidt and Wenzel (1981) estimated T_c of 13 alkyl benzenes with an average error of 0·8%. We found that a 2-variable equation in χ^v, equation (32), yields an average error of 1·3%.

$$T_c = 50{\cdot}454\ {}^3\chi_p^v - \frac{181{\cdot}759}{{}^1\chi^v} + 619{\cdot}830$$

$$n = 21;\ r = 0{\cdot}9794;\ s = 8{\cdot}49;\ F = 212. \qquad (32)$$

Critical pressure: Kudchadkar *et al* (1968) estimated P_c of isoalkanes fairly accurately (maximum deviation = $\pm 0{\cdot}14$ atm) using vapour pressure-temperature data. By group contribution methods (Lydersen 1955; Schmidt and Wenzel 1981) errors from 3 to 4% have been reported for alkanes. Equation (33) also gives an average deviation of about 3%.

$$P_c = -7{\cdot}522\ {}^1\chi^{P(e)} + 20{\cdot}872\ {}^3\chi^{P(e)} + 38{\cdot}418\ {}^0\chi^{P(e)} + 20{\cdot}722,$$

$$n = 49;\ r = 0{\cdot}9932;\ s = 0{\cdot}757;\ F = 1092. \qquad (33)$$

This equation is, however, valid only for molecules containing upto 30 carbon atoms.

The P_c of 13 alcohols was found to be correlated with valence connectivity indices, equation (34).

$$P_c = -2{\cdot}554\ {}^0\chi^v + 4{\cdot}164\ {}^4\chi_{pc}^v + \frac{75{\cdot}644}{{}^0\chi^v} + 30{\cdot}942$$

$$n = 13;\ r = 0{\cdot}9976;\ s = 1{\cdot}17;\ F = 615. \qquad (34)$$

This leads to an average error of 2%. A 5-variable ($^0\chi^v$, $^3\chi_c^v$, $^4\chi_{pc}^v$, $1/^0\chi^v$, $1/^1\chi^v$) correlation reduces the error to merely 1% with maximum absolute deviation of 0·75 atm. There are no correlations available for comparison.

Forman and Thodos (1958, 1960) estimated P_c of alkylbenzenes with an average deviation of 3–4%. Schmidt and Wenzel (1981) estimated P_c for 13 alkylbenzenes with an error of 4·4%. Equation (35) predicts the values within 2% error and can be considered the best available so far for prediction of P_c.

$$P_c = 5{\cdot}977\ {}^0\chi^{P(e)} - 3{\cdot}006\ {}^4\chi^{P(e)} + \frac{147{\cdot}098}{{}^0\chi^{P(e)}} - 61{\cdot}816$$

$$n = 21;\ r = 0{\cdot}9912;\ s = 0{\cdot}78;\ F = 318. \qquad (35)$$

This gives a maximum absolute deviation of 1·46 atm.

Critical volume: For a sample of 49 alkanes, whose critical volume, V_c, ranges between 255 cm^3 mol^{-1} and 1200 cm^3 mol^{-1}, we obtained a highly significant correlation with $^m\chi^{P(e)}$, equation (36).

$$V_c = 347{\cdot}458\ {}^1\chi^{P(e)} - 277{\cdot}823\ {}^3\chi^{P(e)} + 141{\cdot}754\ {}^4\chi_1^{P(e)} + 46{\cdot}323$$

$$n = 49;\ r = 0{\cdot}9989;\ s = 10{\cdot}8;\ F = 7026. \qquad (36)$$

This is the best relationship known so far to estimate critical volume of alkanes. The earlier reported relationships yield average deviations of 2·3% (Lydersen 1955), 2% (Reidel 1954) and 1·78% (Vetere 1976) whereas equation (36) gives an average error of 1·4%. Vetere (1976) estimated critical volumes of 10 alcohols within 3% of the experimental values. We found that a 2-variable equation, equation (37), in $^m\chi^{P(e)}$ gives an average error of 1% only; that too for a larger sample.

$$V_c = 273{\cdot}945\ {}^1\chi^{P(e)} - \frac{0{\cdot}368}{{}^3\chi^{P(e)}} + 67{\cdot}370$$

$$n = 13;\ r = 0{\cdot}9997;\ s = 3{\cdot}29;\ F = 8215. \qquad (37)$$

Using a large number of group contributions Vetere (1976) reported an average erro of 0·96 % for a sample of 18 alkylbenzenes. Our studies on 21 alkylbezenes have led t equation (38) which gives comparable quality (average absolute error 1·1 %) in terms o three $^{m}\chi^{P(e)}$ terms only.

$$V_c = 255{\cdot}983\ {}^{1}\chi^{P(e)} - 24{\cdot}649\ {}^{4}\chi_1^{P(e)} - \frac{153{\cdot}108}{{}^{1}\chi^{P(e)}} - 54{\cdot}652,$$

$$n = 21;\ r = 0{\cdot}9980;\ s = 4{\cdot}91;\ F = 1424. \qquad (38$$

4.1g *Second virial coefficient* Even the most carefully determined values of secon virial coefficient B show experimental error of ± 50 cm^3 mol^{-1} for *n*-alkanes (Dymon and Smith 1969). Theoretical prediction of B is, therefore, very useful. Kunz an Kapner (1971) estimated B within 10–15 % of the observed values. We observed significant correlation between B and $^{m}\chi$, equation (39)

$$B = 46{\cdot}322 - 229{\cdot}820\ ({}^{1}\chi)^2$$

$$n = 11;\ r = 0{\cdot}9977;\ s = 41{\cdot}74;\ F = 1942. \qquad (39$$

This equation predicts values with deviation less than 10 %. For 2 of the 11 alkanes th deviation has been found to be more than 50 cm^3 mol^{-1}.

The B values with experimental error of ± 16 cm^3 mol^{-1} are available for 8 alcohol (Dymond and Smith 1969). Polak and Ylu (1972) estimated B values for these alcohol with an average error of 3·2 %. Our study using $^{m}\chi^{P(e)}$ indices led to equation (40) whic gives an average error of 4 %.

$$B = -718{\cdot}847\ {}^{1}\chi^{P(e)} - 2192{\cdot}580\ {}^{3}\chi^{P(e)} - 298{\cdot}738$$

$$n = 8;\ r = 0{\cdot}9914;\ s = 34{\cdot}2;\ F = 143. \qquad (40$$

For a sample of 5 alkylbenzenes we obtained equation (41) which gives a maximu absolute deviation of 5·18 cm^3 mol^{-1}.

$$B = 405{\cdot}171 - 276{\cdot}234[{}^{1}\chi^{P(e)}]^3,$$

$$\bar{n} = 5;\ r = 0{\cdot}9999;\ s = 4{\cdot}9;\ F > 3 \times 10^4. \qquad (41$$

Equation (41), therefore, estimates B values within experimental uncertaintie (± 8 cm^3 mol^{-1}).

5. Present status and future

The internal consistency and predictive capabilities of various correlations mentione above loudly speak for the success of valence and perturbation connectivity indices i the topology-property correlation studies. However, at this stage it is difficult t commit which one of the connectivity indices leads to better correlations for all th physicochemical properties. It seems that perturbation connectivity indices correla marginally better.

In spite of such good correlations which in many cases predict the values of variou properties within experimental accuracy, there is no sound physical basis for them Recently after a careful study on molar volume and enthalpy of vaporisation Edwar (1982) has shown that different χ values give different weights to the contribution o

ubstructures

$$-CH_3, -CH_2-, \geqslant CH \quad \text{or} \quad -\overset{|}{\underset{|}{C}}-.$$

He also pointed out that the information in various higher order χ terms regarding legree of folding (Jain and Gombar 1979) is a function of the mole fraction, Z_g, of gauche conformations. Similar studies on other physicochemical properties should be nteresting to reinforce the observation.

The connectivity indices are derived from the adjacency relationship of nonhydrogen toms. These topology quantifiers, therefore, cannot numerically represent the three-limensional features of molecules. We have recently attempted (Gombar *et al* 1983) to ncorporate the effects of nearest neighbour atoms by defining perturbation connec-ivity indices. In the present study we have arbitrarily assumed $\gamma_{ij} = \gamma_{ji} = 0{\cdot}10$ and in an earlier communication (Gombar *et al* 1984) we have optimized γ ($= \gamma_{ji} = \gamma_{ij}$) against tatistical quality. It should be worth investigating to define γ as a function of bond ength and/or electronic environments. As such all the χ indices do not encode lectronic features of molecules. It is evident from the missing correlations between hese indices and properties like dissociation constant and ionisation potential.

References

Allen T L 1959 *J. Chem. Phys.* **31** 1039

Aranda V G 1936 *An. Quim.* **34** 513

Basak S C, Roy A B and Ghosh J J 1979 in *Proc. Second Int. Conf. on Mathematical Modelling*, Univ. of Missouri, USA, Vol. 2, pp. 851–856

Basak S C, Gieschen D P, Magnuson V R and Harris D K 1982a *IRCS Med. Sci.* **10** 619

Basak S C, Ray S K, Raychaudhury C, Roy A B and Ghosh J J 1982b *IRCS Med. Sci.* **10** 145

Basak S C and Magnuson V R 1983 *Arzneim-Forsch/Drug Res.* **33** 501

Benson S W 1976 *Thermochemical kinetics*, 2nd edn (New York: John Wiley) Ch. 1

Benson S W and Buss J H 1958 *J. Chem. Phys.* **29** 546

Boyd J C, Millership J S and Woolfson A D 1982 *J. Pharm. Pharmacol.* **34** 364

Bremner J G M and Thomas G D 1948 *Trans. Faraday Soc.* **44** 230

Bruhl J W 1891 *Z. Phys. Chem.* 7 140

Cammarata A 1979 *J. Pharmacol. Sci.* **68** 839

Colingoert G, Beaty H A, Juoler R C and Thomos G W 1941 *Ind. Eng. Chem.* **33** 103

Dubois J E, Laurent D and Viellard H 1967 *C. R. Acad. Sci. Paris* **C264** 1019

Dubois J E, Laurent D and Aranda A 1973 *J. Chim. Phys.* **70** 1608

Dubois J E, Laurent D, Bost P, Chambaud S and Mercier C 1976 *Eur. J. Med. Chem.* **11** 225

Dymond J H and Smith E B 1969 *The virial coefficients of gases—A critical comparison* (Oxford: Clarendon Press)

Edward J T 1982 *Can. J. Chem.* **60** 480

Eisenlohr F 1910 *Z. Phys. Chem.* **75** 585

Fajans K and Knorr J 1926 *Chem. Ber.* **59** 249

Forman J C and Thodos G 1958 *A.I.Ch. E. J.* **4** 358

Forman J C and Thodos G 1960 *A.I.Ch. E. J.* **6** 206

Francis A W 1941 *Ind. Eng. Chem.* **33** 554

Franklin J L 1949 *Ind. Eng. Chem.* **41** 1070

Glasstone S 1946 *Textbook of physical chemistry* 2nd edn (Princeton, New Jersey: van Nostrand Reinhold) Ch. 8

Gombar V K, Kapoor V K and Jain D V S 1980 *Indian J. Chem.* **A19** 715

Gombar V, Jain D V S and Singh S 1983 Abstracts of the 35th Indian Pharmaceutical Congress, Paper A-18

Gombar V, Jain D V S and Singh S 1984 Q. S. A. R. (communicated)

Gombar V 1981 *The Pharmacos* **25** 46
Gombar V and Wadhwa L 1982 *Arzneim-Forsch./Drug Res.* **32** 715
Gordon M and Scantlebury G R 1964 *Trans. Faraday Soc.* **60** 604
Gupta S P and Singh P 1978 *Indian J. Chem.* **B16** 709
Gutman I, Ruscic B, Trinajstic N and Wilcox C F Jr 1975 *J. Chem. Phys.* **62** 3399
Hall L H, Kier L B and Murray W J 1975 *J. Pharmacol. Sci.* **64** 1974
Hoshino D, Nagahama K and Hirata M 1978 *J. Chem. Eng. Jpn* **11** 403
Hosoya H 1971 *Bull. Chem. Soc. Jpn* **44** 2332
Huggins M L 1941 *J. Am. Chem. Soc.* **63** 116
Huggins M L 1954 *J. Am. Chem. Soc.* **76** 343
Jain D V S and Gombar V 1979 *J. Chem. Soc. Faraday Trans. I* **75** 1132
Klages F 1949 *Chem. Ber.* **82** 358
Kier L B, Hall L H, Murray W J and Randic M 1975a *J. Pharmacol. Sci.* **64** 1971
Kier L B, Murray W J and Hall L H 1975b *J. Med. Chem.* **18** 1272
Kier L B, Murray W J, Randic M and Hall L H 1976 *J. Pharmacol. Sci.* **65** 1226
Kier L B and Hall L H 1976a *Molecular connectivity in chemistry and drug research* (New York: Academi Press)
Kier L B and Hall L H 1976b *J. Pharmacol. Sci.* **65** 1806
Kier L B and Hall L H 1977 *Eur. J. Med. Chem. Chim. Therapeut.* **12** 307
Kier L B and Hall L H 1979 *J. Pharmacol. Sci.* **68** 120
Kier L B 1980 in *Physical chemical properties of drugs* (eds) S H Yalkowsky, A A Sinkula and S C Valvan (New York: Marcel Decker) Ch. 9
Kier L B and Hall L H 1983 *J. Pharmacol. Sci.* **72** 1170
Komoshilov N F 1939 *Zh. Obshch. Khim.* **9** 701
Komoshilov N F 1940 *Zh. Obshch. Khim.* **10** 945
Kovats E 1961 *Z. Anal. Chem.* **181** 351
Kudchadkar A P, Holcomb W D and Zwolinski B J 1968 *J. Chem. Eng. Data* **13** 182
Kunz R G and Kapner R S 1971 *A.I.Ch. E. J.* **17** 562
Kurtz S S and Lipkin M R 1941 *Ind. Eng. Chem.* **33** 779
Kurtz S S and Sankin A 1954 *Ind. Eng. Chem.* **46** 2186
Laidler K J 1956 *Can. J. Chem.* **34** 626
Li K, Arnett R L, Epstein M B, Ries R B, Bitter L P, Lynch J M and Rossini F D 1956 *J. Phys. Chem.* **60** 140
Lydersen A L 1955 Estimation of critical properties of organic compounds by the method of grou contributions, Coll. Eng. Univ. Wisconsin, Eng. Expt. Sta. Rept.
Macknick A B and Prausnitz J M 1979 *Ind. Eng. Chem. Fundam.* **18** 348
Mercier C and Dubois J E 1979 *Eur. J. Med. Chem.* **14** 415
Mercier C, Sobel Y and Dubois J E 1981 *Eur. J. Med. Chem.* **16** 473
Mibashan A 1945 *Trans. Faraday Soc.* **41** 374
Murray W J, Hall L H and Kier L B 1975 *J. Pharmacol. Sci.* **64** 1978
Murray W J, Kier L B and Hall L H 1976 *J. Med. Chem.* **19** 573
Nokay R 1959 *Chem. Eng.* **66** 147
Ogilvie J F and Abu-Elgheit M A 1981 *Comput. Chem.* **5** 33
Parks G S and Huffman H M 1932 Am. Chem. Soc. Monograph No. 60 (New York: Chem. Catalog. Co
Pauling L 1960 *The nature of the chemical bond* 3rd edn (Ithaca, New York: Cornell Univ. Press) Ch. 3
Platt J R 1947 *J. Chem. Phys.* **15** 419
Polak J and Ylu B C 1972 *Can. J. Chem. Eng.* **50** 553
Randic M 1975 *J. Am. Chem. Soc.* **97** 6609
Ray S K, Basak S C, Raychaudhury C, Roy A B and Ghosh J J 1981 *Indian J. Chem.* **B20** 894
Ray S K, Basak S C, Raychaudhury C, Roy A B and Ghosh J J 1982 *Arzneim-Forsch./Drug Res.* **32** 32
Ray S K, Basak S C, Raychaudhury C, Roy A B and Ghosh J J 1983 *Arzneim-Forsch./Drug Res.* **33** 35
Raychaudhury C, Basak S C, Roy A B and Ghosh J J 1980 *Indian Drugs* **18** 97
Reidel L 1954 *Chem. Eng. Tech.* **26** 83
Schmidt C and Wenzel H 1981 *Can. J. Chem. Eng.* **59** 527
Singh S, Jain D V S and Gombar V 1984 (to be published)
Smithenberg J and Mulder D 1948 *Rec. Trav. Chem.* **67** 813
Smolenski E A 1964 *Russ. J. Phys. Chem.* **38** 700
Smyth C P 1925 *Philos. Mag.* **50** 361, 715

Sobel Y, Mercier C and Dubois J E 1981 *Eur. J. Med. Chem.* **16** 477
Somayajulu G R and Zwolinski B J 1966 *Trans. Faraday Soc.* **62** 2327
Somayajulu G R and Zwolinski B J 1972 *Trans. Faraday Soc.* **68** 1971
Somayajulu G R and Zwolinski B J 1974 *J. Chem. Soc. Trans. Faraday II* **70** 967, 973
Souders M, Mathews C S and Hurd C O 1949 *Ind. Eng. Chem.* **41** 1037
Spencer C F and Daubert T E 1973 *A.I.Ch. E. J.* **19** 482
Sugden J 1924 *J. Chem. Soc.* **125** 32
Sylvester J J 1878 *Am. J. Math.* **1** 64
Tatevskii V M and Papulov 1960 *Russ. J. Phys. Chem.* **34** 115, 231, 335
Tatevskii V M 1950 *Doklady Akad. Nauk SSSR* **75** 819
Tatevskii V M 1951 *Zh. Fiz. Khim.* **25** 241
Tatevskii V M, Banderskii V A and Yarovsi 1961 *Rules and methods for calculating physicochemical properties of paraffinic hydrocarbons* (Oxford: Pergamon Press)
van Krevelen D W and Chermin H A G 1951 *Chem. Eng. Sci.* **1** 66
Vetere A 1976 *A.I.Ch. E. J.* **22** 950
von Steiger A L 1921 *Chem. Ber.* **54** 1381
Wiener H 1947 *J. Am. Chem. Soc.* **69** 2636, 17
Wiener H 1948 *J. Phys. Chem.* **52** 425, 1082
Zahn C T 1934 *J. Chem. Phys.* **2** 671

Proc. Indian Acad. Sci. (Chem. Sci.), Vol. 93, No. 6, August 1984, pp. 947–963.
© Printed in India.

Use of cluster expansion techniques in quantum chemistry. A linear response model for calculating energy differences

SOMNATH GHOSH and DEBASHIS MUKHERJEE*

Department of Physical Chemistry, Indian Association for the Cultivation of Science, Jadavpur, Calcutta 700 032, India

Abstract. In this paper we have reviewed the theoretical framework of the coupled-cluster (CC) based linear response model as a tool for directly calculating energy differences of spectroscopic interest like excitation energy (EE), ionisation potential (IP) or electron affinity (EA). In this model, the ground state of a many-electron system is described as in a coupled cluster theory for closed shells. The electronic ground state is supposed to interact with an external photon field of frequency w, and the poles of the linear response function as a function of w furnish with the elementary excitations of the system. Depending on the general form of the coupling term chosen, appropriate difference energies like EE, IP or EA may be generated. Pertinent derivations of the general working equations are reviewed, and specific details as well as approximations for EE, IP or EA are indicated. It is shown that the theory bears a close resemblance to the equation of motion (EOM) method but is superior to the latter in that the ground state correlation is taken to all orders and may be looked upon as essentially a variant of renormalised TDA. A perturbative analysis elucidating the underlying perturbative structure of the formulation is also given which reveals that the theory has a hybrid structure: the correlation terms are treated akin to an open shell MBPT, while the relaxation terms are treated akin to a Green function theory. A critique of the method *vis-a-vis* other CC-based approaches for difference energies forms the concluding part of our review.

Keywords. Cluster expansion techniques; linear response model; quantum chemistry; excitation energy; ionisation potential; electron affinity.

1. Introduction

One might now say with hindsight that the initial spectacular breakthrough in the theory of molecular electronic structure since the inception of quantum mechanics has mainly been due to the remarkable success of the independent particle model (IPM). With the advent of the sophisticated experimental techniques in the last decade to probe a variety of physicochemical phenomena involving excited or ionised states, it has become increasingly apparent that the IPM could fail at the outset to reproduce even qualitatively a vast body of experimental results. This has spelt a clear message to the theoreticians: there is a need to develop and apply useful correlation theories going beyond IPM and treat the energetics of the excitation and ionisation processes on a comparable and consistent level of accuracy encompassing both the ground and the excited/ionised states. A proper and balanced incorporation of correlation energy appropriate to both the ground and the excited/ionised states thus forms one of the major frontier areas of the present-day quantum chemical research (see *e.g.* Lowdin and Pullman 1983).

While the variational approach like CI or MCSCF still remains as one of the most exploited and widely developed methods for this purpose (Shavitt 1977; Kutzelnigg 1977; Peyerimhoff 1979; Wahl and Das 1977; Jorgensen and Dalgaard 1979), it has also its limitations. With a preselected set of configurations in a truncated Hilbert space the CI wavefunction lacks the 'cluster decomposition property' ensuring the size-consistency (or separability) of the extensive quantities like energy (Primas 1965; Pople *et al* 1976; Bartlett 1981). This size-inconsistency error naturally persists in the calculation of energy differences. Moreover the CI-like approaches are 'indirect methods' for energy difference calculations in the sense that they require two separate calculations for the ground and excited/ionised states. Thus the common correlation terms for the two states which should ideally drop out on taking the energy differences are calculated redundantly. This has stimulated the search for the so-called 'direct methods' which would furnish the relevant energy differences in a one-shot process without separately calculating the energies for the respective states. In formulating these methods for many-electron systems it has transpired that the use of occupation number (or many-body) representation is much more preferable to the less compact Schrödinger representation. As the Hamiltonian H_M in occupation number representation does not explicitly involve the electron number N for the system, this opens up an immediate prospect of calculating with same H_M not only the excitation energies (EE) of a many-electron system having a specific number of electrons but also its ionisation potential (IP) or electron affinity (EA) involving a different number of electrons for the ground and the ionised states. In a direct method, one invokes a suitable 'excitation' or 'ionisation operator' which creates the appropriate excited or ionised states by acting on the ground state and posits suitable forms for these operators. The common correlation terms then automatically drop out on taking the energy differences. The occupation number representation of the relevant equations confers the flexibility of truncation for a given model in the *operator space*, rather than in the *configuration space*, and thus truncation schemes preserving size-consistency may be devised. An additional advantage of the many-body representation utilising the excitation/ionisation operators is that the calculated energy differences become progressively more accurate with increase in the number of electrons in the system.

There exist currently several direct methods for energy difference calculations. They may be divided into two broad categories: (a) perturbative methods like many-body perturbation theories (Bloch and Horowitz 1958; Brandow 1967; Kvasnicka 1977; Lindgren 1974; Johnson and Baranger 1971; Banerjee *et al* 1982a; Hose and Kaldor 1979) and (b) nonperturbative methods like Feynman-Dyson Green function theory (Linderberg and Ohrn 1971; Ohrn and Born 1981; Cizek and Paldus 1974; Csanak *et al* 1979; Oddershedde 1978; Cederbaum and Domcke 1977) and the related superoperator propagator and equation of motion (EOM) techniques (Jorgensen and Simons 1981; Rescigno *et al* 1977) and the open-shell cluster expansion techniques (Mukherjee *et al* 1975; 1977; Mukherjee 1979; Ey 1978; Lindgren 1978; Kvasnicka 1981; Westhaus and Bradford 1975; Reitz and Kutzelnigg 1979; Jeziorzki and Monkhorst 1981; Paldus *et al* 1978). Among these methods, the open-shell perturbation theories are now being increasingly used for IP and EE calculations (Kaldor 1973, 1975a, b; Hubac *et al* 1973; Kvasnicka and Hubac 1974; Yeager *et al* 1978; Lee *et al* 1980; Sheppard and Freed 1981; Yamamoto and Saika 1981; Banerjee *et al* 1982b) and it is now felt that the fully developed computational strategy will soon become competitive with the corresponding variational techniques. The Green function and the associated propa-

gator and EOM approaches have already been developed into a vast computational framework (see *e.g.* Jorgensen and Simons 1981; Ohrn and Born 1981; Resicigno *et al* 1977; Cederbaum and Domcke 1977 for extensive references).

A common shortcoming of the MBPT or the GF methods is their inability to sum up important classes of terms (or diagrams, if framed in a diagrammatic language) to all orders which might dominate in the expressions of the energy differences. Sometimes, for very special classes of terms, suitable infinite summation schemes like geometric approximations (Kelly 1969) or Padé approximations (Guest and Wilson 1979) have been invoked but there is no simple strategy for summing up general classes of diagrams to all orders. The cluster expansion techniques developed in the context of a nonperturbative framework have a decisive advantage in this respect: a cluster amplitude of the wavefunction written in a cluster expansion is a compact way of writing an infinite series of terms of a perturbative series. The cluster expansion based techniques for energy difference calculations utilising the advantages of a direct method are thus expected to obviate the limitations of the other direct methods currently in use. There is now a growing literature on this problem, but the full potentiality of this approach is yet to be explored.

We have been interested in the past decade in developing and applying the open-shell analogue of the closed shell coupled cluster (CC) method which was developed originally for treating the ground state correlation problem (see *e.g.* Kummel *et al* 1978; Bartlett 1981 for extensive references) and was eminently successful. The generalisation of the closed shell CC method to the open shell states is by no means unique or straightforward, and various authors have emphasised on the different aspects of the correlation problem which is peculiar to open shells. The formalisms developed to date can be broadly divided into two categories: (a) those which are specially designed to treat individual open-shell states *per se* and (b) those which are tailored to treat difference energies. In the first category there are the efforts of Mukherjee *et al* (1975) and Jeziorzki and Monkhorst (1981) and in the second there are the works of Mukherjee *et al* (1977); Lindgren (1978); Paldus *et al* (1978); Mukherjee and Mukherjee (1979) and Monkhorst (1977). We shall be mainly concerned in this review with the open-shell coupled cluster techniques for calculating energy differences, and in particular a coupled-cluster based linear response model which is similar in spirit to the EOM method but is a much more highly summed up version and therefore a much more convergent expansion scheme for calculating energy differences directly. The method utilises a coupled-cluster representation of the ground state and, like a direct method as EOM postulates the existence of an excitation/ionisation operator for generating the excited/ionised state from the ground state. Using time-independent many-body techniques, Mukherjee and others (Mukherjee 1979; Mukherjee and Mukherjee 1979) developed the linear response model for calculating the dynamic linear response of a correlated ground state under an external oscillatory perturbation, and sought to extract the excitation spectra of the system from the poles of the dynamic response function. This has since been generalised to incorporate IP/EA calculations (Ghosh *et al* 1981) and also both spin-conserving and spin-forbidden excitations (Ghosh *et al* 1982). Preliminary applications have produced quite encouraging results (Adnan *et al* 1980; Ghosh *et al* 1981; Adnan *et al* 1982). The method has also been rediscovered by nuclear physicists (Emrich 1981), though not in the form in which it was originally developed (Mukherjee 1979; Mukherjee and Mukherjee 1979). An analogous time-dependent formalism was also considered earlier by Monkhorst (1977).

The plan of the review is as follows. In §2 we delineate the pertinent features of t coupled-cluster based linear response theory for difference energy calculations a demonstrate that this naturally leads to a formalism very similar in spirit to renormalised Tamm Dancoff approximation (TDA) of the EOM method. In §3 we discu the choice of the excitation/ionisation operators as well as the cluster ansatz for t ground state and the appropriate truncation schemes. Section 4 gives a perturbati analysis of the relevant equations from the linear response theory showing simultaneous kinship with renormalised GF theory or open-shell MBPT of the Bloc Horowitz type and open-shell MBPT of the Brandow type. Finally, in §5 we include brief critique of this formalism *vis-a-vis* other cluster expansion theories using a simil cluster ansatz.

2. Coupled-cluster based linear response model

2.1 *Basic methodology*

In this subsection we give a resumé of the formal developments of the CC-based line response theory. We shall first discuss the general algebraic structure of the ultima working equations, without explicitly specialising them for either EE or IP/ calculations. Next we reformulate the linear response theory in a way which brings o its theoretical contents as essentially a renormalised variant of TDA.

The CC-based linear response approach invokes two successive cluster expansions a starting uncorrelated ground state function which is chosen as the Hartree-Fock (H determinant ϕ_{HF}. The first cluster expansion incorporates the effect of electro correlation in the ground state and the various cluster operators in this expansi contain n particle-n hole (np-nh) excitations out of ϕ_{HF} in a way entirely analogous the coupled cluster theory for the closed shells (Cizek 1966, 1969). The dynamical line response of the ground state to an external harmonic field is then calculated using t following technique: the system is assumed to interact with an external photon fi where the coupling terms involve creation/destruction of a single photon of a defin frequency. The eigenstate of the composite system comprising the electronic a photon degrees of freedom ceases to contain definite number of photons. The extent electron correlation in the electronic component of the composite system is a changed. The overall change due to the coupling is induced by the second clus expansion operator. The cluster operators in this expansion are composite entit which create/destroy one, two, three photons and simultaneously induce vari np-mh excitation out of ϕ_{HF}. The precise nature of the electronic part of the cluster op ator is dictated by the nature of transition energies under study, *viz* EE, IP or EA. For $n = m$ and for IP/EA $n = m-1/m+1$, as we shall see presently. For linear respo calculations it suffices to restrict the second cluster expansion to linear terms only. T associated response function then involves an expectation-value like quantity tak with respect to the electronic ground state and is proportional to the photon numbe the photon field. The response function may thus be looked upon as a photon s energy and consequently as a linear response function. When the external frequency the photon field matches an excitation frequency corresponding to an element excitation (EE, IP or EA depending on the form of the coupling chosen), the lin response function becomes singular. Thus the energy differences may be calculated

noting the zeros of the inverse of the linear response function. This is the underlying physical picture of the CC-based linear response model.

In the closed-shell CC theory (Cizek 1966, 1969), the exact ground state of a many electron system ψ_{gr} is described in terms of ϕ_{HF} and a cluster expansion operator $\exp(T)$:

$$\psi_{gr} = \exp(T)\phi_{HF}. \tag{1}$$

The associated molecular electronic Hamiltonian H_M may be written in normal order with respect to ϕ_{HF} as the vacuum as

$$H_M = E_{HF} + \sum_A \varepsilon_A N[a_A^+ a_A] + \frac{1}{2!^2} \sum_{\substack{A,B,\\C,D}} \langle A_B|v|C_D\rangle_a N[a_A^+ a_B^+ a_D a_C], \tag{2}$$

where the spin-orbitals for representation have been taken as HF spin orbitals. From now on we shall refer to the spin-orbitals simply as orbitals for brevity.

Let us also invoke a photon field of frequency w, characterised by a Hamiltonian H_{ph}:

$$H_{ph} = wC^+C, \tag{3}$$

where C/C^+ corresponds to a destruction/creation operator of a photon of frequency w. In the absence of any interaction the Schrödinger equation for the composite system may be written as

$$[H_M + H_{ph}]\psi_{gr}\chi_{ph} = E_0\psi_{gr}\chi_{ph}, \tag{4}$$

where χ_{ph} is the photon eigenstate of H_{ph}, and E_0 is the sum of the electronic ground state energy E_{gr} and the photon energy E_{ph}. If now an interaction is switched on between the electronic and photon fields, the unperturbed state $\psi_{gr}\chi_{ph}$ will be changed to a perturbed state ψ' having no definite number of photons. The interaction Hamiltonian H_{int} may be written as (see *e.g.* Mukherjee and Mukherjee 1979)

$$H_{int} = iV_{el}[C - C^+], \tag{5}$$

where V_{el} depends on electronic operators only. The *detailed form* of V_{el} is not important for calculating the energy differences, but its *general form* (*e.g.* whether it conserves the electron number or decreases/increases by one) is dictated by our desire to calculate EE, IP or EA. The interaction will modify the nature of correlations in the electronic system and at the same time will induce photon creation/destruction. In the confines of the linear response theory, we can restrict the cluster operators inducing the change to contain creation/destruction of one photon only. Writing the perturbed state ψ' for the composite system as

$$\psi' = \exp(T)\exp(S)\phi_{HF}\chi_{HF}, \tag{6}$$

where S induces electronic excitations or detachments/attachments with consequent absorption and emission of single photons through C/C^+ operators, S in (6) may be defined as

$$S = iS_{el}[C - C^+] = S^+ + S^-, \tag{7}$$

where S_{el} corresponds to the electronic degrees of freedom S^+ and S^- correspond to the component of S involving C and C^+ respectively. The linear response function for the

electronic ground state depends on the photon frequency w through the w-dependence of the operator S coming from C/C^+ operators. The second order energy shift $\Delta E^{(2)}$ due to the function $S\phi_{\mathrm{HF}}\chi_{\mathrm{ph}}$ involving absorption/emission of one photon may be generally written as

$$\Delta E^{(2)}(w) = n_{\mathrm{ph}} G(V_{\mathrm{el}}, w) + \sum_{m \neq 0} \frac{|\langle \psi_m | V_{\mathrm{el}} | \psi_{\mathrm{gr}} \rangle|^2}{(E_{\mathrm{gr}} - E_M - w)}, \tag{8}$$

where $\psi_{m's}$ are excited/ionised electronic eigen-states reached through the electronic part V_{el} of H_{int}. The first term on the right side of (8) depends on the photon number n_{ph} of the photon field, and it is thus both a photon self-energy and a linear response function. From the general property of a response function in the linear response theory (Karplus and Kolker 1963; Langhoff *et al* 1972), $G(V_{\mathrm{el}}, w)$ has poles for values of w matching an elementary excitation frequency $(E_m - E_{\mathrm{gr}})$. If V_{el} conserves the electron number, $\psi_{m's}$ are then the excited states of the electronic system (of whose ground state is ψ_{gr}), and if V_{el} destroys/creates an electron, the states ψ_m are then various cation/anion eigenstates of the parent electronic system. Thus the poles of $G(V_{\mathrm{el}}, w)$ furnish us with EE, IP or EA depending on the specific choices of V_{el}. At any pole, $S\psi_{\mathrm{gr}}\chi_{\mathrm{ph}}$ is essentially a product of an appropriate excited/ionised state ψ_m and a $(N \pm 1)$-photon state $\chi_{\mathrm{ph}^{\pm}}$. Naturally, the quality of the state ψ_m generated depends upon the choice of S_{el} and S.

We now briefly indicate how one may arrive at the working equations for calculating the energy differences. We start out from (4), and premultiply it with $\exp(-T)$. Noting that H_{ph} does not involve electronic operators, we have, from (4):

$$[\bar{H}_M + H_{\mathrm{ph}}]\phi_{\mathrm{HF}}\chi_{\mathrm{ph}} = E_0 \phi_{\mathrm{HF}}\chi_{\mathrm{ph}}, \tag{9}$$

where the 'dressed' Hamiltonian $\bar{H}_M$ is defined as

$$\bar{H}_M = \exp(-T) H_M \exp(T). \tag{10}$$

Projecting (9) on to the states $\phi_m^* \chi_{\mathrm{ph}}$ where ϕ_m^*'s are the various *np-nh* excited states of ϕ_{HF}, we have

$$\langle \phi_m^* | \bar{H}_M | \phi_{\mathrm{HF}} \rangle = 0, \ \forall_m, \tag{11}$$

which determine the various *np-nh* cluster amplitudes of T, exactly analogous to what one obtains in closed-shell CC theory. In the coupled system in presence of the interaction the corresponding Schrödinger equation reads as

$$[H_M + H_{\mathrm{ph}} + H_{\mathrm{int}}]\psi' = E'\psi'. \tag{12}$$

Premultiplying (12) by $\exp(-T)$, we have

$$[\bar{H}_M + H_{\mathrm{ph}} + \bar{H}_{\mathrm{int}}] \exp(S)\phi_{\mathrm{HF}}\chi_{\mathrm{ph}} = E' \exp(S)\phi_{\mathrm{HF}}\chi_{\mathrm{ph}}, \tag{13}$$

where $\bar{H}_{\mathrm{int}}$ is the transformed interaction $\exp(-T)H_{\mathrm{int}}\exp(T)$, which can be equivalently written as

$$\bar{H}_{\mathrm{int}} = i\bar{V}_{\mathrm{el}}[C - C^+]. \tag{14}$$

Premultiplying (13) by $\exp(-S)$, we have

$$[\bar{\bar{H}}_M + \bar{\bar{H}}_{\mathrm{ph}} + \bar{\bar{H}}_{\mathrm{int}}]\phi_{\mathrm{HF}}\chi_{\mathrm{ph}} = E'\phi_{\mathrm{HF}}\chi_{\mathrm{ph}}, \tag{15}$$

where the double-bar quantities $\bar{\bar{X}}$ are the corresponding transformed operators $\bar{\bar{X}}$

induced by two successive similarity transformations:

$$\bar{\bar{X}} = \exp(-S)\exp(-T)X\exp(T)\exp(S). \tag{16}$$

In the linear response theory, the expansions of all the operators $\bar{\bar{X}}$ are truncated after the terms which are linear in photon creation/destruction operators. Thus we have

$$\bar{\bar{H}}_M \simeq \bar{H}_M + [\bar{H}_M, S], \tag{17}$$

$$\bar{\bar{H}}_{\text{ph}} \simeq H_{\text{ph}} + [H_{\text{ph}}, S], \tag{18}$$

$$\bar{\bar{H}}_{\text{int}} \simeq \bar{H}_{\text{int}}. \tag{19}$$

Projecting (15) on the states $\phi_l^* \chi_{\text{ph}}^{\mp}$ where ϕ_l^* are the states reached through V_{el}, and $\chi_{\text{ph}}^{\mp}$ are photon states with photon numbers $N-1/N+1$, we get

$$\langle \phi_l^* \chi_{\text{ph}}^{\mp} | [\bar{H}_M, S] + [H_{\text{ph}}, S] + \bar{H}_{\text{int}} | \phi_{\text{HF}} \chi_{\text{ph}} \rangle = 0. \tag{20}$$

Utilising the relations

$$C\chi_{\text{ph}} = (n_h)^{1/2} \chi_{\text{ph}}^- \tag{21a}$$

$$C^+ \chi_{\text{ph}} = (n_h + 1)^{\frac{1}{2}} \chi_{\text{ph}}^+ \quad , \tag{21b}$$

we easily find that equation (20) is decoupled with respect to S^- and S^+ in the sense that for χ_{ph}^- only S^+ contributes while for χ_{ph}^+ only S^- contributes. Thus with χ_{ph}^-, we have

$$\langle \phi_l^* | [\bar{H}_M, S_{\text{el}}] | \phi_{\text{HF}} \rangle - w \langle \phi_l^* | S_{\text{el}} | \phi_{\text{HF}} \rangle + \langle \phi_l^* | \bar{V}_{\text{el}} | \phi_{\text{HF}} \rangle = 0. \tag{22}$$

If we now expand S_{el} in terms of various *np-nh* excitations for EE, or $np-(n\pm 1)h$ for IP/EA, then we may generally write

$$S_{\text{el}} = \sum_l S_l \varphi_l^+, \tag{23}$$

where φ_l^+ are the appropriate products of *np-nh* operators and $S_l = S_l(w)$ are the associated cluster amplitudes. We may thus write

$$S_{\text{el}} \phi_{\text{HF}} = \sum_l S_l \phi_l^*. \tag{24}$$

Equation (22) then takes the form

$$\sum_m A_{lm} S_m(w) - w S_l(w) + V_l = 0, \tag{25}$$

where the matrix-elements A_{lm}, and V_l are defined as

$$A_{lm} = \langle \phi_l^* | [\bar{H}_M, \varphi_m^+] | \phi_{\text{HF}} \rangle, \tag{26}$$

$$V_l = \langle \phi_l^* | \bar{V}_{\text{el}} | \phi_{\text{HF}} \rangle. \tag{27}$$

Equation (25) may be written more compactly as

$$\boldsymbol{A}\mathbf{S}(w) - w\mathbf{S}(w) + \mathbf{V} = 0, \tag{28}$$

whence

$$\mathbf{S}(w) = (w \cdot \boldsymbol{I} - \boldsymbol{A})^{-1} \mathbf{V}. \tag{29}$$

The part of the second order energy $\Delta E^{(2)}$ proportional to photon number n_{ph} may be written as

$$\Delta E^{(2)} = \langle \phi_{HF}\chi_{ph}|[\bar{H}_{int}, S]|\phi_{HF}\chi_{ph}\rangle, \tag{30}$$

from which it follows that $G(V_{el}, w)$ is of the form

$$G(V_{el}, w) = \mathbf{Y}(w \cdot I - A)^{-1}\mathbf{V}, \tag{31}$$

from (29). Clearly, $G(V_{el}, w)$ has poles whenever the matrix $(wI - A)^{-1}$ is singular, or equivalently wherever A satisfies an eigenvalue equation of the form

$$A\mathbf{X} = w\mathbf{X}, \tag{32}$$

with w as the elementary excitations (EE, IP or EA).

Equation (32) is the ultimate working equation of the CC-based linear response theory, and it was obtained in this form for EE calculations by Mukherjee and others (Mukherjee and Mukherjee 1979). For an explicit construction of the matrix A, we shall have to specify S_{el}, the nature of truncation of $\bar{H}_M$ as a multicommutator series in T and the truncation in the sum in (24). This we shall illustrate for specific cases in §§3.1 and 3.2.

2.2 *Emergence of a renormalised TDA*

A very useful new insight into the structure of (32) is obtained if we trace back its genesis through (28) to (22). Basically the energy differences are obtained as solutions of the homogeneous part of (22):

$$\langle \phi_i^*|[\bar{H}_M, S_{el}]|\phi_{HF}\rangle = w\langle \phi_i^*|S_{el}|\phi_{HF}\rangle, \tag{33}$$

with w as the relevant difference energies. This equation immediately suggests that there is an underlying commutator form of the EOM-like structure of the working equation in the linear response theory. We may naturally wonder whether we may arrive at (33) starting from a Schrödinger equation for the electronic system only. In the following we show that this is indeed the case.

Assuming that S_{el} converts the ground state ψ_{gr} to the appropriate excited or ionised states, the EOM for energy differences may be written as

$$[H_M, S_{el}]\psi_{gr} = wS_{el}\psi_{gr}. \tag{34}$$

If we now write S_{el} in terms of various *np-mh* excitation operators φ_i^+ only as has been done in (23), then the form of S_{el} corresponds to what one assumes in a generalised TD approach (Dunning and McKoy 1967). If we now use the CC-ansatz for the ground state ψ_{gr}, then premultiplying (34) by $\exp(-T)$ and utilising (10), we have

$$[\bar{H}_M, S_{el}]\phi_{HF} = wS_{el}\phi_{HF}, \tag{35}$$

from which (33) easily follows by projecting on to the excited/ionised states ϕ_i^* reached by the components S_i of S_{el}. The emergence of (35) from EOM indicates that the ground state correlation has been incorporated into $\bar{H}_M$, so that (35) or equivalently (32) is indeed a renormalised version of *np-mh* TDA for EE, IP or EA. Equation (35) has a simple structure if viewed as generated from (34) and it was derived in this alternative fashion by Adnan *et al* (1981) and Ghosh *et al* (1983).

3. Truncation schemes in energy difference calculation

3.1 EE *calculation*

For EE calculations, V_{el} must be an electron number conserving operator and consequently S_{el} would in general be a sum of various *np-nh* excitation operators:

$$S_{el} = \sum_n S_n, \tag{36a}$$

with

$$S_n = \frac{1}{n!^2} \sum_{\substack{P,Q,\ldots \notin \phi_{HF} \\ A,B,\ldots \in \phi_{HF}}} \langle PQ\ldots|S_n|AB\ldots\rangle_a a_P^+ a_Q^+ \ldots a_B a_A. \tag{36b}$$

This form for S_{el} for EE calculations was suggested by Mukherjee and Mukherjee 1979 who also discussed the useful approximations for singlet EE calculations. Following Cizek (1966, 1969), they truncated $\bar{H}_M$ after the quadratic power of T, and approximated T by only the 'pair correlation' cluster operator T_2. The resulting expressions for $\bar{H}_M$ have been extensively discussed by Mukherjee and coworkers who also introduced suitable diagrammatics to arrive at the expressions in a convenient manner. They chose to truncate S_{el} after the two-body term and took the operator S_{el} to be a spin-scalar type for singlet EE calculations. For triplet EE calculations, S_{el} must be chosen as a spin-vector type of operator and the resulting spin-adaptation procedures have been introduced by Ghosh *et al* (1982). Confining S_{el} to atmost two-body terms indicates that the excited states generated receive contributions from $T_2\phi_{HF}$ and $S_2\phi_{HF}$, showing the effect of altered correlations as a result of excitation, as also triply excited configurations simulated by a product operator of the form $T_2 S_1 \phi_{HF}$. The excited states are thus expected to be of high quality.

3.2 IP/EA *calculations*

For IP/EA calculations, V_{el} must be an electron-destroying (creating) operator, and consequently S_{el} a destroying (creating) operator:

$$S_{el}^{IP/EA} = \sum_{n=1,3,\ldots} S_n^{IP/EA}, \tag{37}$$

with

$$S_n^{IP} = \frac{1}{(n-1)!}\frac{1}{n!} \sum_{\substack{P_1P_2\ldots,P_{n-1} \notin \phi_{HF} \\ A_1,A_2\ldots,A_n \in \phi_{HF}}} \langle P_1P_2 \cdot P_{n-1}\phi|S_n^{IP}|A_1A_2\ldots A_n\rangle_a$$

$$[a_{P_1}^+ a_{P_2}^+ \ldots a_{A_2} a_{A_1}] \tag{38a}$$

$$S_n^{EA} = \frac{1}{(n-1)!}\frac{1}{n!} \sum_{\substack{P_1,P_2,\ldots P_n \notin \phi_{HF} \\ A_1,A_2,\ldots A_{n-1} \in \phi_{HF}}} \langle P_1P_2\ldots P_n|S_n^{EA}|A_1A_2\ldots A_{n-1}\phi\rangle_a$$

$$[a_{P_1}^+ a_{P_2}^+ \ldots a_{A_2} a_{A_1}] \tag{38b}$$

with ϕ symbolising a 'no-label' orbital. Ghosh *et al* (1982) gave a useful calculational scheme for IP where n is truncated after three. It is clear that S_{el}^{IP} and S_{el}^{EA} operators are related to each other through (*h-p*) interchange, so that equations for EA can be easily generated from those of IP through *h-p* interchanges. The ionised states for IP under the

approximations of Ghosh *et al* (1982) contain $1h$ and $2h$-$1p$ components generated b $S_1\phi_{HF}$ and $S_3\phi_{HF}$ as also $3h$-$2p$ states from the product excitations of the type $S_1T_2\phi_{HF}$ They are thus again expected to be of high quality as in EE calculations.

4. A perturbative analysis of the CC-based linear response model

In this section, we shall look into the underlying perturbative structure of the line response theory. As may be anticipated from the pre-eminent success of the CC theo for closed shells in summing up classes of Goldstone perturbative diagrams to all orde (Cizek 1966; Kummel *et al* 1978), a similar situation is expected to prevail in t CC-based linear response theory as well. We shall presently find that such is indeed t case. The analysis will also put in proper perspective this approach *vis-a-vis* oth perturbative approaches when looked at from the perturbation theoretic point of vie

Any perturbative development for EE and IP/EA calculations utilising the GF or MB requires specification of the appropriate unperturbed functions. The most comm choice for such functions for EE calculations corresponding to the low-lying excit states are the $1p$-$1h$ determinants, and for IP/EA calculations the $1h$ and/or $1p$ states f GF. Both $1h$ and $1p$ determinants are needed if a one electron GF is used, and IP and EA a obtained in a coupled manner. For MBPT, only the $1h$ or ($1p$) functions are needed f IP(EA) calculations. Naturally for an appropriate comparison the linear respon formalism must be appropriately tailored so that the corresponding starting functio are the same as in GF or MBPT calculations.

For IP(EA) calculations, the CC-based theory starts out with $1h$($1p$) functions, and immediate kinship with MBPT may be discerned here. Again, if one formulates a theory involving only one-hole functions or one-particle functions rather than t complete one electron GF then its poles which give either IP or EA only, *i.e.* IP and calculations may be decoupled by working with restricted kinds of GF s. Specifical one may define hole GF s as

$$G_{AB}(T-T') = i\langle\psi_{gr}|T[a_A(T)a_B^{+}(T')]|\psi_{gr}\rangle \;\forall\; A, B\in\phi_{HF}, \tag{3}$$

and likewise a corresponding particle GF, whose poles provide us with IP or EA. As shall see that the CC-based linear response model has a *hybrid structure* incorporati features of both open shell Rayleigh-Schrödinger MBPT of the Brandow type (Brand 1967) and also of one-hole/one-particle GF. Similarly, we shall indicate that a simil situation holds true for EE calculations as well.

To facilitate our analysis, a diagrammatic analysis of the working equations would useful. We shall show by block diagrams the structure of the working equations (32) f IP/EA and EE. As an example, figures 1(a) and 1(b) depict the equations for calculations. The corresponding equations for EA may be obtained by hole-parti reversal. Similarly, figures 2(a) and 2(b) show the corresponding block-structure for calculations. The matrices corresponding to these block-structures are also indicated the figures. We shall now analyse the perturbative structure of these equations taki IP/EA and EE in turn.

4.1 IP/EA *calculations*

We shall specifically discuss the IP calculations only; for, the EA theory may be eas formulated from the structure for the IP theory by a simple hole-particle reversal. As

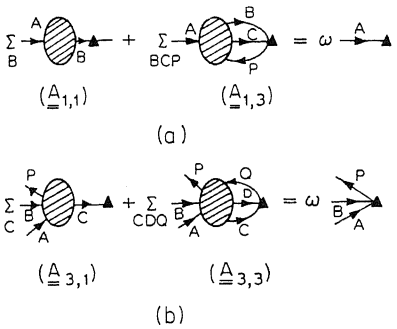

Figure 1. (**a**) and (**b**) depict the diagrammatics of the IP equations for shapes having one and three open lines respectively. The shaded blobs stand for the $\bar{H}_M$-vertices and lines on their left and right connect the ket and bra sides of equation (32). The filled triangles depict the S_{el}-vertices.

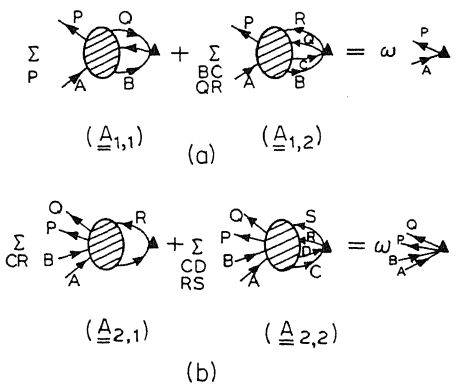

Figure 2. (**a**) and (**b**) depict the diagrammatics of the EE working equations from equation (32).

states are the starting functions for both hole GF and MBPT calculations, we shall have to 'fold' the effect of the S_3 components of figures 1(a) and 1(b) by partitioning technique to have an appropriate simplitude for comparison. Folding the effect of the S_3 manifold from figures 1(b) through figure (1a), we have a pseudo-eigenvalue equation of the form

$$A_{1,1}S_1 + A_{1,3}(w\cdot I - A_{3,3})^{-1}A_{3,1}S_1 = wS_1, \tag{40}$$

with a corresponding block-structure as shown in figure 3. This looks like a Dyson equation for the hole GF because of the appearance of a w-dependent term $(w\cdot I - A_{3,3})^{-1}$. (Alternatively, (40) may be viewed as Bloch Horowitz pseudo-eigenvalue equation (Bloch and Horowitz 1958) as far as a low order perturbative analysis is concerned).

We now invoke the now well-established perturbative analysis of the closed-shell CC theory. The crux of such an analysis is that a T-diagram having a specific shape (characterised by the number of incoming and outgoing hole-particle lines) is a sum over all the Goldstone-diagrams of the same-shape. Using the concept of the generalised time ordering (GTO) (Brandow 1967, 1970), one may show (Kummel *et al* 1978), that the sets of diagrams related by GTO (*i.e.* having movable 'legs' which can be variously placed with respect to each other) may be compactly represented by a factorable diagram where a global energy denominator between the vertices is replaced in the diagram by products of local energy denominators corresponding to each 'leg'. Figure 4 shows one such factorisation for a T_2 diagram in a closed-shell CC theory. Recalling that the matrices $A_{1,1}$, $A_{1,3}$ and $A_{3,1}$ all involve the transformed Hamiltonian $\bar{H}_M$ involving a multicommutator expansion in powers of T, the associated diagrams will also involve such factorised diagrams. Specifically as the T operators can only connect an H_M vertex only from the right, a diagrammatic representation of any $\bar{H}_M$ operator having a specific shape will be represented by a sum of factorised Goldstone diagrams having the same topological structure of the $\bar{H}_M$ diagram whose factorised components will look as *downward going trees only*. As an example, the free structure of a two-body $\bar{H}_M$ vertex is depicted in figure 5.

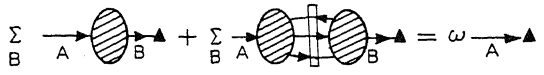

Figure 3. The 'folded' form of equation (40) for IP calculations. The rectangular box cutting the lines joining the two blobs in the figure depicts the matrix-inverse $(w \cdot I - A_{3,3})^{-1}$.

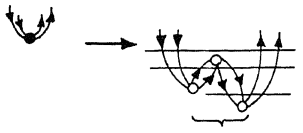

Figure 4. Generation of Goldstone diagrams admitting of GTO from the Goldstone expansion of a T_2-vertex. The lines are drawn vertically to effect an easier comparison with perturbation theory. The horizontal bar cutting the lines stands for an appropriate Goldstone energy denominator. The two-V-vertices covered by the brace are the two 'legs' admitting of GTO.

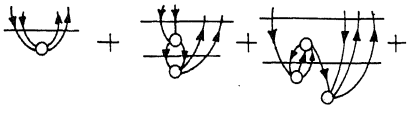

Figure 5. The generation of downward growing trees of increasing complexity from the Goldstone expansion of the T_2 vertex of figure 4.

For a perturbative analysis, we expand the series for T in each of the A matrices in terms of factorised Goldstone diagrams, and also expand out $(w \cdot I - A_{3,3})^{-1}$ in terms of $(w \cdot I - \Delta E^0)^{-1}$ involving orbital energies only and the rest ΔV $(= A_{3,3} - \Delta E^0)$ involving the two-body vertex V of Hamiltonian (equation (2)) and also the multicommutator terms involving T. Using the T_2-approximation scheme discussed in §2, the diagrams that are generated upto third order are shown in figure 6. Let us note that the matrix $A_{1,1}$ in (40) generates only the correlation terms (figures 6(a) to 6(d)) where the entry point of the hole line is below its exit point, while the w-dependent term in (40) generates the relaxation terms only. The important point to notice here is that *the correlation terms do not have any w-dependence at all*, because they are all generated by the composite H_M-T vertices which have only Rayleigh-Schrödinger energy denominators stemming from the Goldstone expansion. This part thus has the underlying perturbative structure resembling a Brandow open-shell MBPT (Brandow 1967). The energy denominators are local whenever there are components in a diagram admitting of a GTO. Moreover the denominators do not involve the labels of the lines emanating on the top of the diagram if they are not connected to the T vertices, just as is expected of a nonhermitian (unsymmetric) open shell theory as Brandow's. *The relaxations terms* (figures 6(d) to 6(g)) on the other hand, *are w-dependent* as they come out of the folding. These terms are thus analogous to the w-dependent self-energy terms of a hole GF or a Bloch-Horowitz theory. We have used single bars between successive vertices where they stand for Goldstone and double bars when they indicate w-dependent GF or Bloch-Horowitz denominators. The hybrid structure of the linear response theory is thus immediately apparent.

The above analysis raises an interesting formal problem. Viewed from a GF or Bloch-Horowitz theory, the w-independence of the correlation terms implies that the w-dependence has been expanded out, much in the same spirit as is done, for example, in Brandow's conversion of the Bloch-Horowitz series to the Rayleigh-Schrödinger series. The successive correction terms arising out of such an expansion must, therefore, have

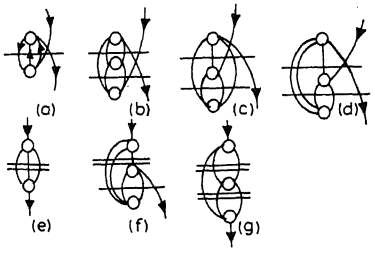

Figure 6. All the diagrams for IP upto third order generated by the expansion of (40) as powers of V. The double bars indicate Bloch-Horowitz type of w dependent denominators. Note that the denominator of the bottom part of figure 6(f) is Goldstone type because it originates as a Goldstone tree from a T_2-vertex.

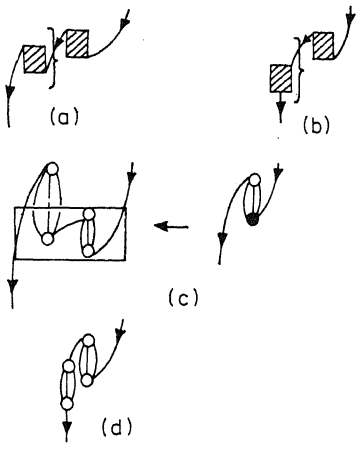

Figure 7. (**a**) and (**b**) are the 'correction terms' which should appear in (40) stemming from the conversion of the w-dependent terms of the correlation to w-independent form. (**c**) and (**d**) show two specific diagrams that are generated from the terms considered in the text. The part of the diagram (**c**) in the box is the part originating from the nonlinear CC equation for T_2. The parent diagram is shown on the right in (**c**).

to be explicitly incorporated in a potentially exact theory and we show that such terms are indeed present in the linear response theory. These terms will look like insertions on basic w-independent correlation diagrams.

Upto the fourth order of perturbation theory we have to look for two kinds of insertions as shown in figures 7(a) and (b). Clearly, an appropriate two-body part of $\bar{H}_M$ calculated from the complete nonlinear CC theory for closed shell will automatically incorporate the component figure 7(a), as is shown explicitly in figure 7(c). The other component is not explicitly present. But one may show that if the w-term in $A_{1,3}\ (w\cdot \mathbf{1}-\Delta E^0)^{-1}\ A_{3,1}$ is expanded also as

$$w_\alpha \simeq \varepsilon_\alpha + \Delta f_\alpha, \tag{41}$$

corresponding to a root w_α lying closest to the unperturbed orbital energy ε_α, then the first correction generates figure 7(b). This is depicted in figure 7(d). Thus both terms are present, either explicitly or implicitly, in the linear response theory.

In the T_2-approximation, the theory is correct upto second order of perturbation theory and contains important classes of third order diagrams. The remaining third order diagrams are not all generated in this approximation, although most of them tend to cancel each other due to mutual 'antigraph' relation (Cederbaum and Domcke 1977). The pilot calculations (Ghosh *et al* 1981; Ghosh *et al* to be published) indicate that the performance of the CC-based linear response model is better than the hole GF method-indicating that the missing terms are indeed unimportant, and also that the infinite summations involving Goldstone downward trees are much more important in predicting difference energies like IP.

We conclude this subsection by indicating another peculiar formal feature of the linear response theory. Suppose we include the T_1-operators as well in our closed-shell CC calculations (this probably is energetically unimportant, but useful for bringing out the aspect of the problem we want to discuss presently). A typical diagram in the correlation term coming from T_1 may be depicted as in figure 8(a), which will contribute a third order perturbation diagram on Goldstone expansion as shown in figure 8(b). A straightforward exhaustive analysis reveals that the conjugate 'mirror image' diagram, as shown in figure 8(c) is totally absent in the theory so long as S_{el} is confined to S_1 and S_3 only. By expanding the operator space to include S_5 operators as well, as shown in figure 8(d), one may recover the conjugate diagram, as shown in figure 8(c). Thus there is an inherent asymmetry in the generation of terms upto a given order of perturbation theory in the linear response model. This stems largely from the feature that the GTO in the Goldstone expansion of T acts only downward in a CC theory.

4.2 *EE calculations*

A perturbative analysis involving upto the third order diagrams is extremely unwieldy because it will generate a plethora of diagrams. However, the basic features of the theory may be visualised if the effect of the S_2 block in figure 2(b) is folded in figure 2(a). A Goldstone expansion of the resulting matrices $A_{1,1}$, $A_{1,2}$ and $A_{2,1}$ will then yield the perturbative expansion of EE. The resultant diagrams upto second order are shown in figure 9. These are the only diagrams upto second order. For relevant comparison, either a Bloch-Horowitz theory involving $1p$-$1h$ starting functions or a p-h GF has to be invoked. For the latter, the de-excitation manifold has to be folded in. The third order and higher order diagrams obtained by factorised Goldstone expansion involving GTO are again more important than an order by order expansion, as is evidenced by the numerical performance of the method (Adnan *et al* 1980, 1982). The hybrid nature of the theory in treating the correlation and relaxation terms are again apparent, and the corresponding correction terms may also be discerned at higher orders (Ghosh *et al* to be published).

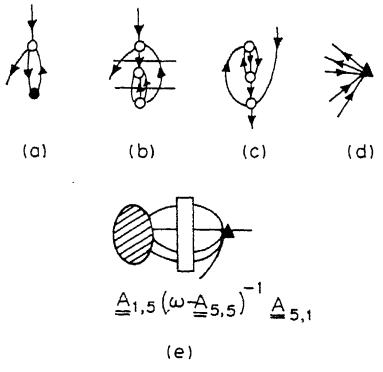

Figure 8. (**a**) A typical T_1 diagram contributing to (40) for IP. A third order diagram obtained from it is shown in (**b**). The conjugate diagram to (**b**) is shown in (**c**). (**d**) shows an S_5 vertex. (**e**) shows the block structure of the diagrams obtained by folding the effect of S_5 generating (**e**).

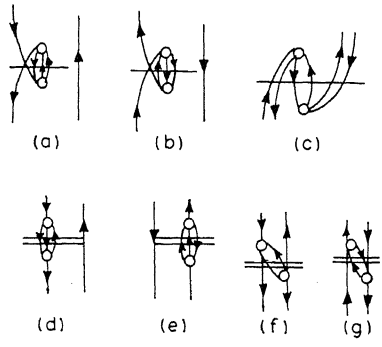

Figure 9. All the perturbation diagrams at the second order obtained from (32) for EE. (**a**) to (**c**) are the correlation terms and (**d**) to (**g**) are the relaxation terms.

5. Relationship with other CC-based theories for difference energy

In this section, we shall briefly indicate the relation of the formalism reviewed above with other CC-based approaches for treating difference energies. Elaboration of the technical difference is avoided for the sake of brevity and only the basic structural comparisons are outlined.

Monkhorst (1977) has developed a time-dependent version of the CC-theory for calculating dynamical response of a system under an external perturbation having a harmonic time variation. The evolution of the system is followed by invoking the adiabatic hypothesis. As is often acknowledged, a time-dependent evolution treated in the framework of perturbation theory involves the so-called 'secular' or divergent terms, and this needs an explicit and careful consideration of the 'phase' of the perturbed function (Langhoff *et al* 1972). Monkhorst thus had to introduce suitable phases in his perturbed wavefunction to get rid of these secular terms, which makes the development somewhat roundabout because one also needs the *ad hoc* introduction of damping factors corresponding to the adiabatic hypothesis. Monkhorst's approach and the time-independent approach discussed in this paper are like Fourier-transforms of each other as far as the basic structure is concerned—the advantages of a time-independent version being that the secular terms are naturally absent and that the relation of the theory with the renormalised TDA approach is much more transparent. Moreover, in a time-dependent approach, the identification of the excited/ionised functions as $S_{el}\exp(T)\phi_{HF}$ is not easy to visualise. The time-dependent version of the IP/EA calculations has not been developed so far to our knowledge.

Recently, Emrich (1981) has derived an EOM version for EE calculation in nuclear physics essentially along the lines of the derivation described in (34)–(35). Unfortunately Emrich missed the earlier expositions of the linear response theory (Mukherjee 1979; Mukherjee and Mukherjee 1979; Adnan *et al* 1982) and did not notice the equivalence of the linear response theory with a renormalised TDA.

Paldus *et al* (1978) developed a variational theory for difference energy calculations by starting from excited/ionised functions of the form $S_{el}\exp(T)\phi_{HF}$ similar to what is done in a linear response theory. Consequently they start from expectation value like quantities

$$\Delta E = \frac{\langle\psi_{gr}|S_{el}^{+}H_M S_{el}|\psi_{gr}\rangle}{\langle\psi_{gr}|S_{el}^{+}S_{el}|\psi_{gr}\rangle} - \frac{\langle\psi_{gr}|H_M|\psi_{gr}\rangle}{\langle\psi_{gr}|\psi_{gr}\rangle} \tag{42}$$

and show that the second term cancels with a component of the first term leading to

$$\Delta E = \frac{\langle\phi_{HF}|\exp(T^{+})S_{el}^{+}H_M S_{el}\exp(T)|\phi_{HF}\rangle_L}{\langle\phi_{HF}|\exp(T^{+})S_{el}^{+}S_{el}\exp(T)|\phi_{HF}\rangle_L}, \tag{43}$$

where the suffix L indicates that all the connected diagram expression for ΔE have to be taken. ΔE is thus a ratio of two polynomials involving T/T^{+} unlike a simple polynomial as in a CC-based linear response theory. Variation of ΔE with respect to the cluster amplitudes of S_{el} in (43) leads to a Hermitian generalised eigenvalue problem of the Roothaan type. The linear response theory is related to Paldus approach but is nonvariational and differs from the latter in the following two important aspects that (a) the $\bar{H}_M$ in linear response theory is a terminating series while the linked quantities in (43) are nonterminating, and (b) linear response working equations are nonhermitian eigenvalue equations, while Paldus' method involves a generalised eigenvalue equation.

We believe that the linear response theory provides a viable and potentially compact method for direct calculation of energy differences like EE, IP and EA. The pilot calculations on prototypal model systems have produced quite encouraging results. The real potentiality of the approach will be revealed in more realistic applications of the theory in the *ab initio* framework, and such studies are currently being undertaken in our laboratory.

Acknowledgements

The authors wish to thank Dr P K Mukherjee, Dr S Adnan and Dr S Bhattacharya who have taken part in the various stages of the development of the work presented here and also Dr M Prasad for numerous discussions. Partial financial support from INSA is also gratefully acknowledged.

References

Adnan S, Bhattacharya S and Mukherjee D 1980 *Mol. Phys.* **39** 519
Adnan S, Bhattacharya S and Mukherjee D 1982 *Chem. Phys. Lett.* **85** 204
Banerjee A, Mukherjee D and Simons J 1982a *J. Chem. Phys.* **76** 1972, 1979
Banerjee A, Mukherjee D and Simons J 1982b *J. Chem. Phys.* **76** 1995
Bartlett R 1981 *Annu. Rev. Phys. Chem.* **32** 359
Bloch C and Horowitz J 1958 *Nucl. Phys.* **8** 91
Brandow B 1967 *Rev. Mod. Phys.* **39** 771
Brandow B 1970 *Ann. Phys.* **57** 214
Cederbaum L S and Domcke W 1977 *Adv. Chem. Phys.* **36** 206
Cizek J 1966 *J. Chem. Phys.* **45** 4256
Cizek J 1969 *Adv. Chem. Phys.* **14** 35
Cizek J and Paldus J 1974 *J. Chem. Phys.* **60** 149
Csanak G, Taylor H S and Yaris R 1971 *Adv. At. Mol. Phys.* **7** 288
Dunning T H and McKoy V 1967 *J. Chem. Phys.* **47** 1735
Emrich K 1981 *Nucl. Phys.* **A351** 379, 397
Ey W 1978 *Nucl. Phys.* **296** 189
Guest H P and Wilson S (ed.) 1979 *Proceedings of the Daresbury Study Weekend* (UK: SRC)
Ghosh S, Mukherjee D and Bhattacharya S 1981 *Mol. Phys.* **43** 173
Ghosh S, Mukherjee D and Bhattacharya S 1982 *Chem. Phys.* **72** 161
Hose G and Kaldor U 1979 *J. Phys.* **B12** 3827
Hubac I, Holubec A and Kvasnicka V 1973 *Chem. Phys. Lett.* **23** 381
Jeziorski B and Monkhorst H J 1981 *Phys. Rev.* **A24** 1668
Johnson M B and Baranger M 1971 *Ann. Phys.* **62** 172
Jorgensen P and Dalgaard E 1979 *Chem. Phys. Lett.* **65** 559
Jorgensen P and Simons J 1981 *Second quantisation-based methods in quantum chemistry* (New York: Academic Press)
Karplus M and Kolker H J 1963 *J. Chem. Phys.* **39** 1493, 2997
Kelly H P 1969 *Adv. Chem. Phys.* **14** 129
Kaldor U 1973 *Phys. Rev. Lett.* **31** 1338
Kaldor U 1975a *J. Chem. Phys.* **62** 4634
Kaldor U 1975b *J. Chem. Phys.* **63** 2199
Kummel H, Luhrman K and Zabolitzsky J G 1978 *Phys. Rep.* **36** 1
Kutzelnigg W and Hubac I 1974 *J. Chem. Phys.* **60** 4483
Kvasnicka V 1977 *Adv. Chem. Phys.* **36** 345
Kvasnicka V 1981 *Chem. Phys. Lett.* **79** 89
Langhoff P W, Epskin S T and Karplus M 1972 *Rev. Mod. Phys.* **44** 602
Lee Y S, Sun H, Sheppard M and Freed K F 1980 *J. Chem. Phys.* **73** 1472

Linderberg I and Ohrn Y 1971 *Propagators in quantum chemistry* (New York: Academic Press)
Lindgren I 1974 *J. Phys.* **B7** 2441
Lindgren I 1978 *Int. J. Quant. Chem.* **S12** 33
Lowdin P O and Pullman B 1983 in *New horizons of quantum chemistry* (Dordrecht: Reidel)
Monkhorst H J 1977 *Int. J. Quant. Chem.* **S11** 421
Mukherjee D, Moitra R K and Mukhopadhyay A 1975 *Mol. Phys.* **30** 1861
Mukherjee D, Moitra R K and Mukhopadhyay A 1977 *Mol. Phys.* **33** 955
Mukherjee D 1979 *Pramana* **12** 203
Mukherjee D and Mukherjee P K 1979 *Chem. Phys.* **39** 325
Nakatsuji H 1978 *Chem. Phys. Lett.* **59** 362
Nakatsuji H 1979 *Chem. Phys. Lett.* **67** 329
Oddershedde J 1978 *Adv. Quant. Chem.* **11** 275
Offerman R, Kummel H and Ey W 1976 *Nucl. Phys.* **A273** 349
Ohrn Y and Born G 1981 *Adv. Quant. Chem.* **31** 1
Peyerimhoff S and Buenker R 1979 in *Excited states in quantum chemistry* (eds.) C Nicolaides and D Beck (Dordrecht: Reidel Publishing Co.)
Paldus J, Cizek J, Saute M and Laforgue L 1978 *Phys. Rev.* **A17** 805
Pople J A, Binkley J S, Seger R 1976 *Int. J. Quant. Chem.* **S10** 1
Primas H 1965 in *Modern theoretical chemistry* (ed.) O Sinanoglu, Vol. 2 (New York: Academic Press)
Reitz H and Kutzelnigg W 1979 *Chem. Phys. Lett.* **66** 111
Rescigno T N, Yeager D L, McCurdy C W and McKoy V 1977 *Modern Theor. Chem.* **3** 349
Roos B 1972 *Chem. Phys. Lett.* **15** 153
Saute M, Laforgue L, Paldus J and Cizek J 1979 *Int. J. Quant. Chem.* **15** 463
Shavitt I, 1977 *Modern Theor. Chem.* **3** 189
Sheppard M and Freed K F 1981 *Int. J. Quant. Chem.* **15** 21
Siegbahn P and Schaeffer H M 1975 *J. Chem. Phys.* **62** 3488
Wahl A C and Das G 1977 *Mod. Theor. Chem.* **3** 51
Westhaus P and Bradford E G 1975 *J. Chem. Phys.* **63** 5416
Yamamoto S and Saika A 1981 *Chem. Phys. Lett.* **78** 316
Yeager D L, Sun H, Freed K F and Herman M 1978 *Chem. Phys. Lett.* **57** 490
Yeager D L, Sun H, Freed K F and Herman M 1980 *J. Chem. Phys.* **72** 4158

Proc. Indian Acad. Sci. (Chem. Sci.), Vol. 93, No. 6, August 1984, pp. 965–976.
© Printed in India.

Search for a density-based alternative quantum mechanics of many-electron systems

B M DEB

Department of Chemistry and Group of Theoretical Studies, Indian Institute of Technology, Bombay 400 076, India

Abstract. There are three reasons for seeking an alternative density-based quantum mechanics of many-electron systems, incorporating both interpretive and basic quantum mechanical aspects: (i) failure of popular *ad hoc* chemical concepts under *ab initio* scrutiny; (ii) failure of *ab initio* calculations to provide simple concepts; and (iii) highly attractive concepts and pictures generated by the electron density in three-dimensional space. At present the three interlinked pillars for such a density mechanics (in contrast to wave mechanics) are: (a) density functional theory; (b) quantum fluid dynamics; and (c) property densities in three-dimensional space. This article describes several studies dealing with these aspects. Although a density mechanics may well be an impossible ideal to realize, the search for it is indeed rejuvenating the whole of quantum chemistry.

Keywords. Density mechanics; electron density; densityfunctional theory; quantum hydrodynamics.

1. Introduction

The central theme in quantum chemistry is the prediction and interpretation of physicochemical phenomena. In order to understand the behaviour of the chemical world, the chemist would prefer to employ simple, attractive concepts and pictures, enabling him to visualize and discourse in a classical language, as far as possible. Through successive generations, this desire on the part of the chemist has resulted in his using a number of popular *ad hoc* ideas which have passed into the folklore of chemistry. Many of these popular ideas provide an interesting contrast between myth and reality in that they collapse when subjected to careful scrutiny through highly accurate *ab initio* calculations; several such examples are discussed in § 2. However, the *ab initio* calculations themselves have been unable to provide simple but rigorous concepts and pictures for use by all chemists. This is because it is very difficult to visualize, tabulate or interpret the many-electron wavefunction. As opposed to these dilemmas, recent years have seen the emergence of a number of highly attractive, visually delightful new insights into chemical binding, molecular geometry, molecular reactivity, etc based on the electron density (ground and excited) and associated quantities in the three-dimensional (3D) space. These insights were not accessible directly through the wavefunction. A few such examples are described in § 3.

In view of the above considerations, it appears natural to think of an 'alternative' quantum mechanics of many-electron systems, which would be based on the electron density and associated quantities rather than the wavefunction, so that the generation of simple chemical concepts and pictures with solid theoretical foundations becomes possible.

There are two *interlinked* aspects of such a density-based alternative quantum

mechanics: (i) *interpretive aspect, i.e.* given the electron density $\rho(\mathbf{r})$ in 3D space, what information of physical, chemical and biological significance can be extracted from it? (ii) *Basic, quantum mechanical aspect*, dealing with the fundamental properties of the single-particle density. Both these aspects will be briefly discussed in this article.

The scientific literature on electron density studies has been growing at a fast pace over the past ten years. In three previous articles (Bamzai and Deb 1981a; Ghosh and Deb 1982a; Deb 1984) and a book (Deb 1981a), the reader would find comprehensive discussions on various facets of the electron density. In this short article, especially in §§ 3 and 4, we constrain ourselves to describing mainly some of the new concepts and formalisms developed at our laboratory.

2. Failure of popular *ad hoc* ideas under *ab initio* scrutiny

Out of many such examples, we present only four in this section, without going into details.

2.1 *Hund's rule of maximum multiplicity*

Consider a two-electron atom. "The conventional mythical explanation of why the triplet (parallel) [state] lies lower [compared to singlet] is that, because electrons with parallel spins tend to keep apart . . . their repulsion is less than in a singlet (paired) [state]. This is not so. Detailed calculation on some cases has shown that the repulsion between the electrons is greater in triplet states than in singlets, and that the lowering of the energy is due to the modification of the electron-nucleus attraction. Thus, in a triplet atom the electron distribution contracts, and is stabilized by the improved nuclear attraction: the electron repulsion rises because the electrons are closer together, but this increase does not defeat the improvement in the nuclear attraction" (quoted from Atkins 1974).

2.2 *Electron exchange and chemical binding*

Consider the electronic Hamiltonian for the H_2 molecule

$$H(1,2) = h(1) + h(2) + g(1,2). \tag{1}$$

According to the Heitler–London method, the ground-state energy of the H_2 molecule is

$$E = (Q + K)/(1 + \Delta), \tag{2}$$

where $Q = \langle ab|H|ab\rangle \equiv$ 'coulomb integral', $K = \langle ab|H|ba\rangle \equiv$ 'exchange integrated', $\Delta = \langle ab|ba\rangle = S_{ab}^2$ and $S_{ab} \equiv$ overlap between the hydrogenic orbitals a and b. Since K is negative, it was concluded for many years that 'exchange forces' are responsible for chemical binding. But, if the atomic orbitals are assumed to be orthogonal, K becomes positive. Since the orbitals are not orthogonal,

$$K = \langle ab|g|ba\rangle + 2S_{ab}\langle a|h|b\rangle. \tag{3}$$

true exchange integral (positive) — one-electron integral (negative)

Clearly, binding occurs not because of exchange (the first integral in (3)) but due to

electron-nuclear attraction which makes the second integral in (3) negative (McWeeny and Sutcliffe 1976).

2.3 *Orbital hybridization and molecular geometry*

A long perpetuated myth seems to be that since in H_2O, NH_3 and CH_4 the HAH angle is either tetrahedral or close to it, the hybridization of the central atom must be sp^3 or close to it. The best way to estimate the extent of hybridization is to calculate accurately the *ab initio* delocalized molecular orbitals (MOS) of the system and then unitarily transforming them into localized orbitals. From this it turns out that the bond hybrids and the lone-pair hybrids on the central atom in H_2O and NH_3 are not sp^3. In case of H_2O, the localized bond orbitals do have considerable s character, but the angle between them is only slightly greater than 90° (bent or banana bond). The angle between localized lone-pair orbitals is 124° (*i.e.*, more sp^2 than sp^3). For NH_3, similar conclusions are valid and one again finds bent bonds (see Edmiston and Ruedenberg 1966).

In an interesting work, Jarvie *et al* (1973) examined the effects of hybridization in CH_4 by performing calculations in which the s-type basis functions (and four associated electrons) of the C atom were completely deleted and replaced by an appropriate effective nuclear charge. The preferred shape of the molecule was still tetrahedral. Therefore, the authors concluded that $2s \rightarrow 2p$ promotion and/or hybridization is not responsible for the tetrahedral shape of CH_4. It appears that if there is a direct one-to-one correspondence between hybridization and molecular geometry, it is not yet known.

2.4 *Ring current in aromatic hydrocarbons*

Due to the pioneering works of K S Krishnan, L Pauling, F London and others, in the nineteen thirties, the anisotropic magnetic susceptibility of aromatic hydrocarbons had been attributed to the ability of the cyclic π-electron system to sustain a superconducting ring current. This also explains why proton magnetic reasonance in benzene occurs at unexpectedly low field strengths. The concept of ring current was well entrenched in chemistry until the situation was upset by a strongly worded paper by Musher (1965). According to a proof of London, ring current is not possible for the σ electrons of, *e.g.* benzene. "This argument is fallacious—and London's proof is incorrect—as it can be shown that the susceptibility due to a 'ring current' exactly equals the sum of the susceptibilities of electrons localized in segments of a ring . . . We have demonstrated that there is no reason to single out the π-electron system of aromatic hydrocarbons for special treatment of their magnetic properties in terms of 'ring currents' . . . Any suggestion that 'aromaticity' . . . be defined in terms of the ability of . . . [the] molecule to sustain a ring current must be considered unreasonable" (quoted from Musher 1965). The controversy raised by Musher's work persists to this day.

So far, the most accurate calculations on the magnetic susceptibility of benzene have been performed by Lazzeretti *et al* (1982) who interpreted their results in a way that endorses the final departure from any ring current ideas. Nevertheless, it is quite likely that this concept may be partially rehabilitated on the basis of quantum fluid dynamics (see § 4).

The above four examples are just a few among a manifold of *ad hoc* concepts, much

used but without solid theoretical foundations, which have mesmerized generations of chemists by their qualitative elegance. As exemplified in the following section, perhaps the only way to recover or regenerate such concepts is through the electron density.

3. New concepts arising from the electron density

3.1 *The nature of chemical binding*

Perhaps the most detailed study of chemical binding in molecules has been through the examination of electron densities, difference densities, and the like, in various molecules (Bader 1981). For a diatomic molecule, the difference density is obtained by subtracting superimposed atomic densities at a particular internuclear distance (R) from the molecular density at the same R. The contours of the difference density vividly describe the extent of charge reorganization due to the interaction resulting in the formation of a chemical bond. For the H_2 molecule, when $R \simeq 8$ a.u., electron correlation causes a simultaneous generation of atomic dipoles at the two hydrogens, pointing towards each other. In other words, the centroid of each hydrogen's electron density shifts towards the other hydrogen. This is the origin of London dispersion forces. It is not the interaction of these atomic dipoles which produce the leading term ($-C_6R^{-6}$) in the dispersion series, but rather the attraction of each distorted electron density for its own nucleus that gives the R^{-7} attractive force. Note that in the familiar physical explanation of the origin of London forces, a time-dependent picture of oscillating dipoles was inconsistently grafted onto a time-independent perturbation treatment.

At the equilibrium value of R, electron density flows into the binding region between the two protons as well as behind them. Thus, the attractive part of the diatomic potential energy curve arises due to electron-nuclear attraction while the repulsive part arises due to nuclear-nuclear repulsion and electron-nuclear attraction. These and many other points have been discussed at length by Bader (1981).

3.2 *First-order static Jahn-Teller effect in VCl_4*

The electronic ground state of tetrahedral VCl_4 is doubly degenerate, ^2E. This interacts with the A_1 and E vibrational modes of the molecule, where A_1 corresponds to the totally symmetric stretching mode and E corresponds to a nontotally symmetric bending mode leading to Jahn-Teller (JT) distortion. Let us take VCl_4^+ with a nondegenerate ground state as the reference molecule and let us assume that the doubly degenerate nonbonding e MOS responsible for the JT distortion in VCl_4 are composed mainly of either d_{z^2} or $d_{x^2-y^2}$ AO on the vanadium atom. By using Hellmann-Feynman theorem and schematic representations of these charge distributions, it is possible to obtain (Coulson and Deb 1969; Deb 1973), without making a computation, detailed insights into the nature of the JT distortion in the molecule, which were not obtainable before. Calculation of distortion energies then led to the conclusion that the ground state of VCl_4 is a 50:50 mixture of elongated and flattened tetrahedra. This agreed nicely with experimental findings. Earlier elaborate treatments of the problem, on the basis of degenerate perturbation theory, had yielded quite conflicting results. But, a direct use of the electron density, instead of the wavefunction, greatly simplified the problem, made it visually transparent and the solution was highly satisfying.

3.3 HOMO *postulate and a force model for molecular shapes*

It was popularly believed that MO theory is incapable of making sitting-at-the-desk predictions about the shapes of molecules, without doing detailed computations. That this belief is not justified was proved by developments in qualitative MO theory in which the valence MOS of a molecule using an *sp* basis were constructed, arranged in a proper energy sequence, their electron densities examined and molecular shape predictions made in ground and excited states, all done without making any computation (Deb 1974, 1975; Deb *et al* 1974, 1976). The basis for this approach was the Hellmann-Feynman force interpretation (Coulson and Deb 1971), using electron density, of Walsh's rules of molecular geometry, as well as the HOMO postulate (Deb 1974, 1975). The HOMO postulate says that molecular shapes are mainly determined by the electron-nuclear attractive forces generated by the electron density in the highest occupied MO; if the HOMO is insensitive to shapes, then the next lower MO is to be examined and so on. This model has been remarkably successful in predicting and correlating a large amount of structural information about AH_2, AH_3, AH_4, AH_5, AB_2, AB_3, AB_4, AB_5, ABC, H_2AB, HAB_2, B_2AC, $HAAH$ and $BAAB$ molecules, where A, B and C are nonhydrogenic atoms. Among the interesting successes of this model is the prediction of a bond angle of about 140° (the actual value is 136°) for the ground triplet ($^3B_1$) of carbene molecule (CH_2) and predicting the shapes of larger molecules from those of their fragments. For small and medium-size molecules, this is probably the most versatile and successful qualitative model, utilizing the considerable power and elegance of MO theory. For large molecules, application of qualitative MO theory becomes increasingly difficult. For a detailed discussion of this and another interesting density-based approach to molecular shapes (and reactivity), see Nakatsuji and Koga (1981).

The HOMO postulate model seems to be the only one that made geometry predictions for unknown or nonexistent molecules. In order to test these predictions, and to compare with six other current models of molecular geometry, the following molecules were synthesized quantum chemically and their structures determined by a careful application of CNDO/2 and INDO methods: HCLi, HBBe, $HBLi^-$, HCB, HNBe, HNB^+, HBB^-, $NaHLi^+$, LiB_2^+, $MgBe_2$, LiB_2^-, MgB_2, LiH_3^+ (unstable), H_3O^-, CH_5^-, HBO_2^{2+} (unstable) and HBF_2^{2+} (unstable). The HOMO postulate is the most successful with these molecules, having only one exception ($NaHLi^+$) while the Mulliken-Walsh model stands next with three exceptions, *viz* $NaHLi^+$, HNB^+, HBF_2^+ (Deb and Mahajan 1982; Mahajan and Deb 1982a, b).

3.4 *The spatial partitioning of a molecular system: Definition of an atom in a molecule or solid*

One of the major problems in chemistry has been to obtain a model-independent precise definition of an atom in a molecule or solid; in other words, how do we partition a molecule into atomic fragments. This is also linked with the unsolved problem of transferability of group or fragment properties from molecule to molecule. Using ideas from catastrophe theory, graph theory and exploiting certain quantum mechanical properties of the electron density, Bader *et al* (1980, 1981) have provided a very precise model-independent definition of the boundaries of the fragments of a molecular system. Starting from the point of minimum density between a pair of adjacent nuclei, a line in the partitioning surface follows the path of steepest descent through the electron

density $\rho(\mathbf{r})$. The definition is made quantitative by requiring that $\rho(\mathbf{r})$ be partitioned by those closed surfaces through which the flux of $\nabla\rho(\mathbf{r})$ is everywhere zero. In other words, if $S(\mathbf{r})$ is such a surface, then

$$\nabla\rho(\mathbf{r})\cdot\mathbf{n}(\mathbf{r}) = 0 \tag{4}$$

for all $\mathbf{r}$ belonging to $S(\mathbf{r})$, where $\mathbf{n}(\mathbf{r})$ is a unit vector normal to $S(\mathbf{r})$ at $\mathbf{r}$. The only surfaces which satisfy this condition are those which contain stationary points in the electron density, *i.e.* points at which $\nabla\rho(\mathbf{r})$ vanishes.

A partitioning surface is thus a collection of all gradient paths which both originate (generally at infinity) and terminate (generally at a saddle point) at stationary points in the electron density (see also Bader 1981).

The above four examples are just a few of many interesting studies where the use of electron density directly leads to outstanding physical insights into the problems concerned. Although, in principle, all these informations were contained in the wavefunction, it was extremely difficult to extract them (for more examples, see Bamzai and Deb 1981a; Deb 1981a and Deb 1984). Even though this "change in emphasis from wavefunction to [electron density] . . . for interpretive purposes is rather like leaving the main road to sniff at some wayside flowers . . . who knows? – this might yet turn out to be the most exciting development in quantum chemistry" (quoted from Bamzai and Deb 1981a), *viz* the tantalizing possibility of a density-based quantum mechanics of atoms, molecules and solids.

4. Some interlinked basic quantum mechanical properties of the electron density

The following is a scheme for a density-based quantum mechanics of many-electron systems (arrows signify interlinking):

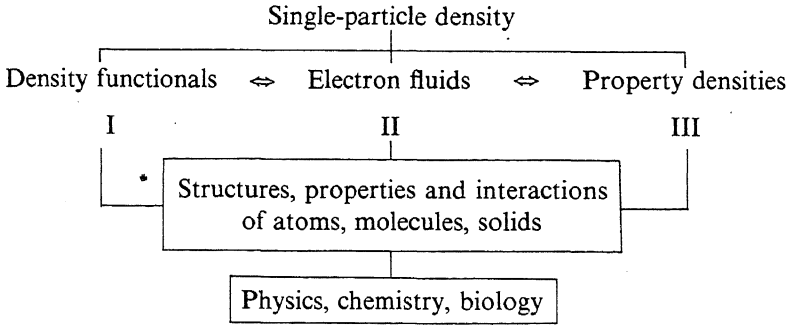

For detailed discussions on density functional theory (I), hydrodynamical (nonlinear) transcription of the wave equation (II) and property densitites (III), see Bamzai and Deb (1981a), Ghosh and Deb (1982a) and Deb (1984). It is clear that the above interlinked framework would, in principle, result in unified approaches for developing very useful qualitative and quantitative models in 3D space for all branches of science. To reemphasize, the main objectives of this broad viewpoint are: (i) simplicity and enhanced visuality; (ii) 'classical' interpretations in 3D space; (iii) rigorous but transparent physics; and (iv) a drastic reduction in computational labour, exemplified later in this section through (a) direct density calculation by solving one equation, instead of N

equations ($N \equiv$ number of electrons), and (b) dynamic polarizability calculation by solving two perturbative equations instead of $2N$ equations.

We now consider briefly certain key elements of the above framework.

4.1 *An electrostatic stress tensor*

Let E_ν and F_ν be the νth components of internal electric fields due to the nuclear and electronic charge distributions, ρ_N and ρ respectively. Let $S_{\mu\nu}$ be an electrostatic stress tensor (cartesian) in the 3D space of a many-electron system, satisfying the force density equation

$$S_{\mu\nu,\mu} = \rho_N(E_\nu + F_\nu) + \rho(E_\nu + F_\nu). \tag{5}$$

Then, one of the solutions of (5) is

$$S_{\mu\nu} = N_{\mu\nu} + L_{\mu\nu} + P_{\mu\nu} = \frac{1}{4\pi}(G_\mu G_\nu - \tfrac{1}{2}\delta_{\mu\nu}\mathbf{G}\cdot\mathbf{G}), \tag{6}$$

where

$$N_{\mu\nu} = \frac{1}{4\pi}(E_\mu E_\nu - \tfrac{1}{2}\delta_{\mu\nu}\mathbf{E}\cdot\mathbf{E}), \tag{7}$$

$$L_{\mu\nu} = \frac{1}{4\pi}(E_\mu F_\nu + E_\nu F_\mu - \delta_{\mu\nu}\mathbf{E}\cdot\mathbf{F}), \tag{8}$$

$$P_{\mu\nu} = \frac{1}{4\pi}(F_\mu F_\nu - \tfrac{1}{2}\delta_{\mu\nu}\mathbf{F}\cdot\mathbf{F}), \tag{9}$$

$$\mathbf{G} = -\nabla V_{\text{mol}}, \tag{10}$$

V_{mol} being the molecular electrostatic potential (see Politzer and Daiker 1981). Thus, the electrostatic stress tensor and its three components have the same form as Maxwell's stress tensor for classical electromagnetic fields. The stress concept contains the Hellmann-Feynman viewpoint as a special case (Deb and Bamzai 1978, 1979).

The electrostatic stress tensor has been applied to obtain a local view of chemical binding in the H_2^+ and H_2 molecules (Deb and Bamzai 1979; Bamzai and Deb 1981b). For the H_2 molecule, S_{zz} (z along the internuclear axis) for a point in the antibinding region passes through a minimum near the equilibrium internuclear distance. In this viewpoint, chemical binding occurs due to the variation of electrostatic pressure from point to point in such a manner as to cause the vanishing of the total electrostatic force density or the difference force density or both at certain points on the internuclear axis.

4.2 *A comprehensive stress tensor within density functional theory*

The above electrostatic stress tensor is but a part of a comprehensive stress tensor which can be derived by using density functional theroy (DFT) and thereby the link between DFT and quantum fluid dynamics (QFD) begins to develop. Let $\mathbf{F}(\mathbf{r})$ be the net local force density and $\boldsymbol{U}$ a comprehensive stress tensor. Then, it can be shown (Deb and Ghosh 1979)

$$\mathbf{F}(\mathbf{r}) = \nabla\cdot\boldsymbol{U} = 0, \tag{11}$$

$$\boldsymbol{U} = \boldsymbol{T} + \boldsymbol{I}_{\text{xc}} + \boldsymbol{S}, \tag{12}$$

where $\boldsymbol{T} \equiv$ Bohm stress tensor (contribution from kinetic energy), $\boldsymbol{I}_{\text{xc}} \equiv$ Exchange-correlation stress tensor and $\boldsymbol{S} \equiv$ Electrostatic stress tensor. All the above stress tensors can be expressed through DFT.

Equation (11) has a fluid dynamical interpretation. It is a special case of Navier-Stokes equation

$$\rho \frac{d\mathbf{v}}{dt} = \nabla \cdot U. \tag{13}$$

For static stationary states ($\mathbf{v} = 0$) (13) as well as the continuity equation

$$\frac{\partial \rho}{\partial t} + \nabla \cdot (\rho \mathbf{v}) = 0 \tag{14}$$

are trivially satisfied. The real velocity field $\mathbf{v}$ vanishes in this case whereas the imaginary velocity field $\mathbf{u}_i = -\frac{1}{2}\nabla \ln \rho_i$, where $\rho = \Sigma_i \rho_i$, gives rise to viscosity coefficients.

In this viewpoint, the picture of the many-electron system is that of a nonuniform continuous fluid subjected to classical (coulomb) and quantum (kinetic + *xc*) forces. The system is stable due to the balance of these forces. Illustrative calculations were reported for the H_2^+ molecule (Deb and Ghosh 1979). Subsequently, the concept of a stress tensor has been used by Bader (1980) as well as Bader and Nguyen-Dang (1981) to derive the mechanics of an atom in a molecule, and by Parr *et al* to derive a microscopic thermodynamics (see Parr 1983).

4.3 *QFD of many-electron systems in 3D space in presence of external electric and magnetic fields*

Since a QFD equation of motion in 3D space in terms of $\rho(\mathbf{r}, t)$ could not be obtained by earlier workers, we employed an orbital partitioning of $\rho(\mathbf{r}, t)$ to achieve this objective, *via* natural orbitals (NOS). The starting point is the Adams-Hirschfelder equation

$$\hat{F}\phi_k = i\hbar\, \partial\phi_k/\partial t, \tag{15}$$

where $\hat{F}$ is the NO Hamiltonian and the time-dependent NO ϕ_k is written as

$$\phi_k = \rho_k^{1/2} \exp[iS_k/\hbar]. \tag{16}$$

For each NO, this yields a continuity equation and a Navier-Stokes equation. In the latter, the net force density arises from the Lorentz force of the electric and magnetic fields, the body force and the tensorial force. The last has contributions from a viscous and a turbulence stress tensor. The picture of the N-electron fluid is as follows (Ghosh and Deb 1982b):

(i) It consists of individual fluid components (NO) with density ρ_k and current density $\mathbf{J}_k$, in 3D space.
(ii) The motion of each component is governed by the Bohm force, the Coulomb force, the *xc* force and the Lorentz force.
(iii) In the absence of a magnetic field, each component velocity is irrotational; but, the net velocity field is rotational.
(iv) The irrotational character of each fluid component is destroyed by molecular rotation (a Coriolis force comes in).
(v) Electron spin introduces another term in $\mathbf{J}_k$.
(vi) The motion of the entire electron fluid or each fluid component can be followed *via* quantum streamlines, obtained by integrating the velocity field.

(vii) Physical observables for the fluid are:

Charge density, $\rho = \sum_k \eta_k \rho_k$

Current density, $\mathbf{J} = \sum_k \eta_k \mathbf{J}_k$,

where η_k is an NO occupation number. The net velocity cannot be obtained by such summation and is not an observable. Note that the concept of ring current (§ 2.4) can be soundly reformulated by means of the current density.

4.4 *A time-dependent DFT and its QFD analogue: A close subtle link between DFT and QFD*

Consider a time-dependent (TD) external potential consisting of a harmonic electric perturbation. In this case, by utilizing a variational principle for quasiperiodic solutions to the TD wave equation, it is possible to prove Hohenberg-Kohn theorem for a nondegenerate quasiperiodic ground state of the many-electron system (Deb and Ghosh 1982). This results in another type of orbital partitioning of $\rho(\mathbf{r}, t)$ in terms of DFT orbitals. The entire analysis of § 4.3 can be carried over to this case.

The TD analogue of Kohn-Sham one-particle equation is obtained through the following sequence of steps:

(i) Define a Lagrangian density for the N-electron fluid by writing the TD energy density as a sum of macroscopic kinetic energy density of the fluid, an intrinsic energy density (the Hohenberg-Kohn functional) and a correction term (neglected for small perturbations).
(ii) Using this Lagrangian density, minimize the corresponding action integral with respect to variations in the densities and velocities of the fluid components, using the equation of continuity as a constraint.

For details see Deb and Ghosh (1982). A more general TDDFT has recently been suggested by Runge and Gross (1984).

In a recent work, Ghosh and Deb (1984) have extended the link between DFT and QFD to the relativistic domain.

4.5 *A differential equation for the direct calculation of electron density*

The key equation in DFT is

$$\delta E[\rho]/\delta\rho - \mu = 0, \tag{17}$$

where μ is the chemical potential, and the unknown energy functional

$$E[\rho] = T[\rho] + V[\rho] + E_{xc}[\rho], \tag{18}$$

T being the kinetic energy. The crux of the problem in DFT is to develop a good kinetic energy-density functional with proper local behaviour (Chattaraj and Deb 1984). Such a functional was obtained by Deb and Ghosh (1983) as

$$t[\rho] = -\frac{1}{4}\nabla^2\rho + \frac{1}{8}\frac{\nabla\rho\cdot\nabla\rho}{\rho} + C_k f(\mathbf{r})\rho^{5/3}, \tag{19}$$

where C_k is the Thomas-Fermi constant and $f(\mathbf{r})$ is an unknown function. The

Table 1. Atomic kinetic energies (a.u.).

Atom	Equation (21)	Hartree-Fock value
He	2·860	2·862
Ne	128·133	128·546
Ar	526·575	526·812
Kr	2749·439	2752·026
Xe	7228·187	7231·961

N-representability criteria were satisfied by taking $\rho(\mathbf{r}) = |\phi(\mathbf{r})|^2$. Equation (17) then leads to the new nonlinear DFT equation (Deb and Ghosh 1983)

$$[-\tfrac{1}{2}\nabla^2 + V_{\text{eff}}]\phi = \mu\phi. \tag{20}$$

Equation (20) was solved numerically for Ne, Ar, Kr and Xe, by using model potentials. This gave $\rho(\mathbf{r})$ and E, in good agreement with Hartree-Fock results.

Another expression for the kinetic energy density functional is (Haq *et al* 1984)

$$t[\rho] = C_k \rho^{5/3} - \frac{1}{40}\frac{\mathbf{r}\cdot\nabla\rho}{r^2}. \tag{21}$$

Using Hartree-Fock atomic densities (Clementi and Roetti 1974), (21) gives the following values of the kinetic energy. The agreement is better than any other similar prescription in the literature.

4.6 *Frequency-dependent multipole polarizabilities*

Using the formalisms in §§ 4.4 and 4.5, one can derive two perturbative equations for the 2^L-pole polarizability ($L = 1, 2, \ldots$), instead of the usual $2N$ equations (Ghosh and Deb 1983a). The equations can be solved variationally (much faster, Ghosh and Deb 1982c, 1983b) or numerically (more accurate, Ghosh and Deb 1983a). The results are new and cannot be compared with any other results at present. However, the static polarizability values, obtained by using the Hartree-Fock density as unperturbed function, agree with coupled-Hartree-Fock and experimental values better than many-body perturbation-theoretic and other density-functional values. For details, see Ghosh and Deb (1983a).

4.7 *Z-dependence of ground-state energies of neutral atoms*

This is a vintage problem in atomic physics. Recently, Chattaraj *et al* (1984) have suggested that the Hartree-Fock energy of neutral atoms may be simulated as

$$-E(Z) = Z^{7/3}(C_7 + C_6 Z^{-1/3} + C_5 Z^{-2/3} + C_4 Z^{-1} + C_3 Z^{-4/3}), \tag{22}$$

where the C's are universal constants and Z is the nuclear charge. C_7 is the Thomas-Fermi value, C_6 is the Scott (1952) value and C_5 the Schwinger (1980, 1981) value. In (22) all the C's are *derived*, and *not adjusted*, parameters and their *physical significance is completely clear*. The following table gives the energy values. Again, the agreement is better than that obtained previously, the He atom being the worst case.

Table 2. Comparison of $E(Z)$ values with Hartree-Fock energies (a.u.).

Z	$-E(Z)$	$-E_{HF}$
2	2·766	2·862
10	128·4	128·5
34	2398·7	2399·8
80	18405·0	18409·0

5. Conclusion

The present article has only pointed out certain constructional elements necessary to develop a quantum mechanics of atoms, molecules and solids based on the single-particle density. There is a very long way to go for developing a complete alternative to the usual wavefunction-based quantum mechanics, in the sense that density has not yet penetrated significantly into many areas dominated by the wavefunction, *e.g.* atomic/molecular collisions and symmetry. Until then, and until a first-principles direct accurate calculation of electron density becomes possible, density mechanics will remain complementary to wave mechanics. There is also a feeling that the density objectives of transparent simplicity, enhanced visuality and mathematical rigour are too idealistic to be ever achieved. Whatever be the final outcome of this search for an alternative density-based quantum mechanics, there is no doubt that the coming years promise great excitement.

Acknowledgement

It is a pleasure to thank Drs Geeta Mahajan, Anjuli Bamzai, Swapan Ghosh, Shamsul Haq, Amitabha Mukherjee, Mukunda Das, Mr Pratim Chattaraj and Mr Girija Pattanaik for their collaboration in the electron density studies from this laboratory. A research grant from the Department of Atomic Energy is gratefully acknowledged.

References

Atkins P W 1974 *Quanta: A handbook of concepts* (Oxford: Clarendon) p. 100
Bader R F W 1980 *J. Chem. Phys.* **73** 2871
Bader R F W 1981 in *The force concept in chemistry* (ed) B M Deb (New York: Van Nostrand-Reinhold) p. 39
Bader R F W, Tal Y, Anderson S G and Nguyen-Dang T T 1980 *Isr. J. Chem.* **19** 8
Bader R F W and Nguyen-Dang T T 1981 *Adv. Quantum Chem.* **14** 63
Bader R F W, Nguyen-Dang T T and Tal Y 1981 *Rep. Prog. Phys.* **44** 893
Bamzai A S and Deb B M 1981a *Rev. Mod. Phys.* **53** 95, 593
Bamzai A S and Deb B M 1981b *Int. J. Quantum Chem.* **20** 1315
Chattaraj P K and Deb B M 1984 *J. Sci. Ind. Res.* (in press)
Chattaraj P K, Mukherjee A, Das M P and Deb B M 1984 (to be published)
Clementi E and Roetti C 1974 *At. Data Nucl. Data Tables* **14** 177
Coulson C A and Deb B M 1969 *Mol. Phys.* **16** 545
Coulson C A and Deb B M 1971 *Int. J. Quantum Chem.* **5** 411
Deb B M 1973 *Rev. Mod. Phys.* **45** 22

Deb B M 1974 *J. Am. Chem. Soc.* **96** 2030
Deb B M 1975 *J. Chem. Educ.* **52** 314
Deb B M (ed) 1981a *The force concept in chemistry* (New York: Van Nostrand-Reinhold)
Deb B M 1981b *Curr. Sci.* **50** 973
Deb B M 1984 in *Local density approximations in quantum chemistry and solid state physics* (eds) J Avery and J P Dahl (New York: Plenum) p. 75
Deb B M, Sen P N and Bose S K 1974 *J. Am. Chem. Soc.* **96** 2044
Deb B M, Bose S K and Sen P N 1976 *Indian J. Pure Appl. Phys.* **14** 444
Deb B M and Bamzai A S 1978 *Mol. Phys.* **35** 1349
Deb B M and Bamzai A S 1979 *Mol. Phys.* **38** 2069
Deb B M and Ghosh S K 1979 *J. Phys.* **B12** 3857
Deb B M and Mahajan G D 1982 *Indian J. Pure Appl. Phys.* **20** 360
Deb B M and Ghosh S K 1982 *J. Chem. Phys.* **77** 342
Deb B M and Ghosh S K 1983 *Int. J. Quantum Chem.* **23** 1
Edmiston C and Ruedenberg K 1966 in *Quantum theory of atoms, molecules and the solid state* (ed.) P O Löwdin (New York: Academic Press) p. 263
Ghosh S K and Deb B M 1982a *Phys. Rep.* **92** 1
Ghosh S K and Deb B M 1982b *Int. J. Quantum Chem.* **22** 871
Ghosh S K and Deb B M 1982c *Chem. Phys.* **71** 295
Ghosh S K and Deb B M 1983a *J. Mol. Struct. Theochem.* **103** 163
Ghosh S K and Deb B M 1983b *Theor. Chim. Acta* **62** 209
Ghosh S K and Deb B M 1984 *J. Phys.* A (in press)
Haq S, Chattaraj P K and Deb B M 1984 (to be published)
Jarvie J, Wilson W, Doolittle J and Edmiston C 1973 *J. Chem. Phys.* **59** 3020
Lazzeretti P, Rassi E and Zanasi R 1982 *J. Chem. Phys.* **77** 3129
Mahajan G D and Deb B M 1982a *Indian J. Pure Appl. Phys.* **20** 453
Mahajan G D and Deb B M 1982b *Indian J. Pure Appl. Phys.* **20** 527
McWeeny R and Sutcliffe B T 1976 *Methods of molecular quantum mechanics* (New York: Academic Press) p. 151
Musher J I 1965 *J. Chem. Phys.* **43** 4081
Nakatsuji H and Koga T 1981 in *The force concept in chemistry* (ed.) B M Deb (New York: Van Nostrand-Reinhold) p. 137
Parr R G 1983 *Ann. Rev. Phys. Chem.* **34** 631
Politzer P and Daiker K C 1981 in *The force concept in chemistry* (ed.) B M Deb (New York: Van Nostrand-Reinhold) p. 294
Runge E and Gross E K U 1984 *Phys. Rev. Lett.* **52** 997
Schwinger J 1980 *Phys. Rev.* **A22** 1827
Schwinger J 1981 *Phys. Rev.* **A24** 2353
Scott J M C 1952 *Philos. Mag.* **43** 859

Proc. Indian Acad. Sci. (Chem. Sci.), Vol. 93, No. 6, August 1984, pp. 977–1001.
© Printed in India.

Exchange interactions in some low-dimensional metal dithiolene complexes

P KUPPUSAMY, B L RAMAKRISHNA and P T MANOHARAN*
Department of Chemistry, Indian Institute of Technology, Madras 600036, India

Abstract. Low-dimensional systems are formed by planar metal dithiolene complexes which stack as columnar structures in the solid state. Stronger interactions among units within a chain leads to highly anisotropic magnetic properties. The magnetic effects are a manifestation of exchange interaction, J and can be studied through detailed EPR techniques in conjunction with magnetic susceptibility and x-ray crystal structure. A brief review of such studies carried out mostly in our laboratory is presented along with the relevant background materials.

Keywords. Metal dithiolenes; low-dimensional systems; exchange interactions; electron paramagnetic resonance; magnetic susceptibility; x-ray crystal structure.

1. Introduction

In the past few years, there has been considerable interest in the chemical and physical properties of low-dimensional materials as is borne out by the numerous conferences that have been held and monographs that have been written (Keller 1975, 1977; Interrante 1974; Hatfield 1979; Miller 1982). Interest in low dimensional (LD) systems, for a long time was focussed less on the physics peculiar to it than on the possibility that their study would provide a better understanding of the various cooperative phenomena in solids. However, LD systems are very interesting in their own right, as the dimensionality of the systems proves to be very important for their critical behaviour and also because these systems display phenomena which are not to be found in higher dimensions (Steiner *et al* 1976).

The discovery of a number of LD metallic, magnetic and some superconducting systems in the past decade has led to the blossoming of an entirely new inter-disciplinary area covering organic, polymer and inorganic chemistry and solid state physics. The fillip for the detailed investigation of the physics and chemistry of these systems was initially provided by an interesting proposal by Little (1964) of the possibility of room temperature superconductivity *via* the exciton electron mechanism. Although the prediction of the above hypothesis is far from experimental realization it has led to the discovery of a wide variety of interesting phenomena in substances with high anisotropy, such as LD metallic state, metal-insulator transition, spin-Peierls transition, highly anisotropic magnetic properties, etc.

Both organic and inorganic examples of LD materials have been investigated. The organic ones, usually based on tetrathiafulvalene, tetramethyl *p*-phenylenediamine, N-methylphenazinium, 7,7,8,8-tetracyanoquinodimethane and their derivatives have been extensively studied (Melby *et al* 1962; Shchegolev 1972; Soos and Klein 1975) and

* To whom all correspondence should be addressed.

we shall not touch up on them in this paper. Low-dimensional systems are also formed by planar transition metal complexes which stack as columnar structure in the solid state (Miller and Epstein 1976). Though there are not as many examples as in the organic systems, there have been many families of complexes discovered, *e.g.* based on partially oxidised metalloporphyrins (Petersen *et al* 1977), metal dithiolene complexes (Underhill and Ahmad 1981), mixed valent platinum cyanide salts (Krogmann and Hausen 1968), etc. Apart from the interesting conducting properties, there are many LD magnetic insulators whose study as magnetic model systems has led to a greater understanding of the theory of cooperative phenomena in solids (De Jongh and Miedema 1974; Hone and Richards 1974).

In this paper we shall exclusively deal with the compounds based on metal dithiolene complexes, discussing some in greater detail and mentioning other examples just in passing, the choice being prejudiced by the authors' research interests.

2. Metal dithiolenes

Metal dithiolenes (figure 1) are a well-studied class of metal organic compounds (McCleverty 1968) since their discovery in 1962 (Gray *et al* 1962; Schrauzer and Mayweg 1962; Davidson *et al* 1963). They are well known for their overall planar geometry irrespective of the metal or its oxidation state. In addition they exhibit a number of characteristics which make them particularly attractive candidates as π-acceptor units in the formation of donor-acceptor compounds. These include the ability to undergo reversible electron transfer reactions to yield stable species, the large delocalization of the highest occupied molecular orbital of π-symmetry, the existence of species with sufficiently high electron affinity to remove an electron from a wide variety of organic donors, in general good solubility and stability in organic solvents. Even, perhaps more importantly, these complexes possess a considerable degree of structural (both molecular and electronic) flexibility available *via* the changes in the central metal atom, M, ligand substituent, X and the counter ion, R^+, which can be varied in a systematic way to study the effect of molecular features on the solid state structure and properties.

The variety of metal dithiolenes may be appreciated through the illustration of many examples in table 1, where the many unique physical and chemical phenomena

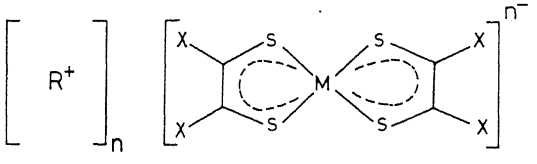

M = a variety of transition metal ions such as Fe, Co, Ni Cu, Au, Pd, Pt, Rh, etc.

X = various ligand substituents such as H, CH_3, C_6H_5, CF_3, CN, etc.

R^+= inorganic or organic cations

n = 0, 1 or 2

Figure 1. Molecular structure of *bis*(ethylene 1,2-dithiolato) metal complexes.

exhibited by these compounds are mentioned. The chemical structures of the compounds abbreviated in table 1 are presented in figure 2.

A classification of the donor-acceptor compounds formed by the metal dithiolene compounds based on an earlier classification of organic charge-transfer systems (Soos and Klein 1976) is presented in figure 3. The factors taken into account for this classification are mainly crystal structure and magnetic behaviour. An example for each subdivision is provided in the figure.

We are primarily interested in our laboratory in cooperative magnetic phenomena investigated by magnetic susceptibility and electron paramagnetic resonance (EPR) measurements. We would like to establish correlation between the structural and magnetic parameters and probe charge-transfer interaction *via* the spin Hamiltonian parameters wherever possible.

3. Introduction to exchange interaction

Exchange coupling is entirely orbital in nature though formally equivalent, *via* the Pauli principle, to the cosine coupling between the spin magnets of various atoms (Van Vleck 1932). The exchange Hamiltonian, generally known as the Heisenberg-Dirac-Van Vleck (HDVV) Hamiltonian can thus be quite generally written as

$$\mathscr{H}_{ex} = -2\sum_{ij} J_{ij}\,\hat{S}_i\cdot\hat{S}_j, \tag{1}$$

or in terms of spin components

$$\mathscr{H}_{ex} = -2\sum_{ij} J_{ij}(\alpha\, S_i^x\cdot S_j^x + \beta\, S_i^y\cdot S_j^y + \gamma\, S_i^z\cdot S_j^z). \tag{2}$$

The values of α, β, and γ in (2) define the nature of exchange coupling. When $\alpha = \beta = \gamma = 1$, the isotropic Heisenberg exchange results. When $\alpha = \beta = 0$ and $\gamma = 1$ the exchange coupling is said to be Ising and this represents the extreme situation of anisotropy. On the other hand the XY (or planar Heisenberg) model of exchange coupling is obtained for $\alpha = \beta = 1$ and $\gamma = 0$. The totally anisotropic case results when $\alpha \neq \beta \neq \gamma$. For linear chain interactions j can be taken to be $i+1$. A positive value of J corresponds to ferromagnetic coupling with the unpaired electrons coupled parallel to each other while a negative value for J corresponds to antiferro-magnetic coupling with an antiparallel coupling of the spins.

Experimental and theoretical studies have shown that in many materials the magnetic part of the Hamiltonian can be quite accurately represented as a bilinear interaction in a set of spins S_i and the Hamiltonian is successfully employed in the interpretation of magnetic properties of several compounds in the solid state (Moriya 1963)

$$\mathscr{H}_{ij} = -2J_{ij}\,\hat{S}_i\cdot\hat{S}_j + \vec{D}_{ij}\cdot[\hat{S}_i\times\hat{S}_j] + \hat{S}_i\cdot\overleftrightarrow{\Gamma}_{ij}\cdot\hat{S}_j. \tag{3}$$

The isotropic exchange, J_{ij} tends to align the spins parallel or antiparallel depending on the sign of J and dominates the static properties such as susceptibility, specific heat, etc whenever $\Delta g/g \leqslant 0{\cdot}1$. D_{ij} is an antisymmetric vector ($D_{ij} = -D_{ji}$) and tends to align the spins perpendicular to each other, thus opposing J. The magnitude of D_{ij} to first order is $\approx (\Delta g/g)\,J$, where Δg describes the orbital contribution to the g tensor. In order to

Table 1. Some unique examples of metal dithiolene compounds with interesting features.

Compound	Interesting features	Comments	References
$NH_4Ni(mnt)_2 \cdot H_2O$	High conductivity with dominant charge transport along the anion stack.	Possesses quasi 1D structure and shows a broad phase transition in the range 150–200 K involving charge density wave formation and lattice dimerization.	Isett *et al* (1980)
Li $M(mnt)_2 \cdot 2H_2O$ M = Ni, Pd and Pt	High conductivity with a metal semiconductor transition at 220 K.	Conduction pathway involves the whole anion and not just the metal orbitals—susceptibility studies support weak electron-electron repulsion.	Cooper *et al* (1983)
$(NBu_4)_{0.29}$ $Ni(dmit)_2$	Highly conducting mixed valent system.	The first example of a conducting metal complex where two dimensionality is a key factor.	Valade *et al* (1983)
TTF^+ M $(thiete)_2^-$ M = Cu, Au	Spin-Peierls instability	The first 1D antiferromagnetic system to exhibit the theoretically predicted spin-Peierls instability, a lattice dimerization that is apparently driven by the spin-phonon interaction of the 1D spin system.	Jacobs *et al* (1976)
Pyrene-$Ni(thiete)_2$ Perylene-$Ni(thiete)_2$	Neutral donor-acceptor compounds.	Semiconducting behaviour.	Schmidt *et al* (1969)
$(TTT)_{1.2}$ $Ni(edt)_2$	Thermally activated conductivity.	A quasi 1D periodically distorted conductor with great similarity to $K_2Pt(CN)_4Br_{0.3} \cdot 3H_2O$ and offers an interesting opportunity to study Peierls instability in a commensurate crystal field.	Interrante *et al* (1978)
$(Tropylium)^+$ $Ni(thiete)_2^-$	1:1 ionic salt with magnetism coming only from the anion stack.	Forms segregated stacks with alternating tropylium cations and anions.	Wing and Schlupp (1970)
$(Tropylium)^+$ $Ni(mnt)_2^-$	1:1 ionic salt with magnetism coming only from the anion stack.	Forms segregated uniform stacks of anions and cations with antiferromagnetic coupling along the anion stack.	Manoharan *et al* (1981)
$NMP^+Ni(mnt)_2$	1:1 ionic salt with magnetism coming only from the anion stack.	Stacks as dimers in the crystal with strong intra-dimer interaction and shows thermally activated triplet exciton EPR.	Kuppusamy *et al* (1984a)
$TMPD^+Ni(mnt)_2^-$	Charge transfer ion-radical salt with magnetism coming from both the cation and anion stacks.	Uniform segregated stack structure with short contacts between the D^+ and A^- units which allow charge transfer and weak interchain interaction.	Ramakrishna *et al* (1983); Ramakrishna and Manoharan (1983a)
$(Perylene)_2^+$ $M(mnt)_2^-$ M = Cu, Ni, Pd, Pt, Au	Reasonably good conducting charge transfer salt.	The electron transport for conduction is mainly in the perylene stack.	Alcacer *et al* (1980)
$(TMPD^+)_2Ni(mnt)_2^{2-}$	Mixed stack where the $TMPD^+$ ions are coupled into dimers.	Frenkel type triplet excitons are observed whose motion has been studied by the temperature dependence of fine structure.	Hove *et al* (1972)

$(NMP^+)_2Cu(mnt)_2^{2-}$	Mixed stack of the type *DAD-DAD*.	Weak exchange interaction in this LD system has been studied by EPR linewidth.	Kuppusamy and Manoharan (1983); Kuppusamy *et al* (1984b)
$(NBu_4^+)_2Cu(mnt)_2^{2-}$	LD system with very weak exchange interaction between the $Cu(mnt)_2^{2-}$ units.	The value of the exchange parameter is of the order of the copper hyperfine interaction and hence the unique possibility of measuring J directly from the EPR line position.	Plumlee *et al* (1975)
$(NEt_4^+)\ M(mnt)_2^-$ M = Ni, Pd and Pt	Stack as dimers and the very strong intradimer interaction yields almost diamagnetic substances at low temperatures.	Though conductivity is very low, there is still a high anisotropy ($\sigma_{\parallel}/\sigma_{\perp} \simeq 10^6$) along the stack axis and perpendicular to it.	Weiher *et al* (1964); Kobayashi and Sasaki (1977); Ramakrishna and Manoharan (1984)
$(MB^+)_2Cu(mnt)_2^{2-}$	First example of nonplanar metal chelate unit.	Triplet-triplet interaction observed in EPR spectra.	Snaathorst *et al* (1981)
$(NMe_4^+)_2Cu(mnt)_2^{2-}$	Another example of nonplanar metal chelate unit.	Shows interesting temperature dependent EPR linewidths.	Kuppusamy and Manoharan (1984a)

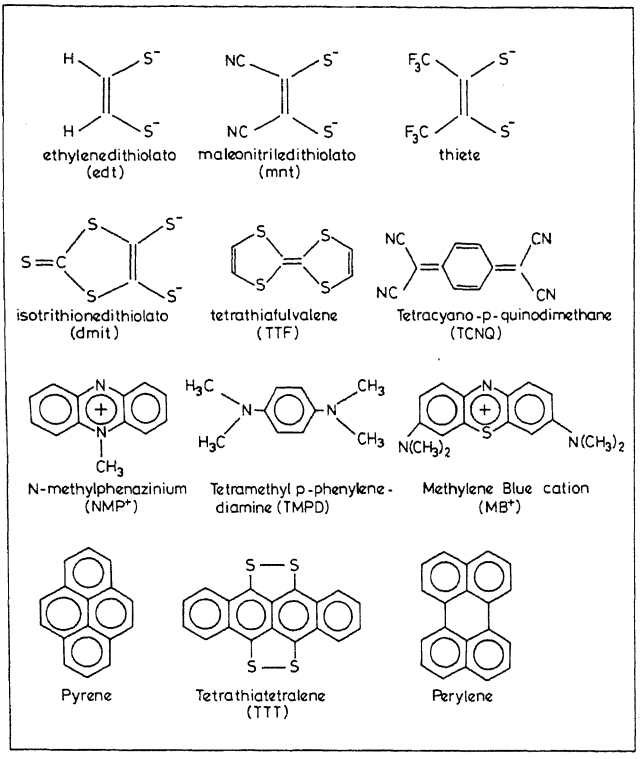

Figure 2. Chemical structures of compounds abbreviated in table 1.

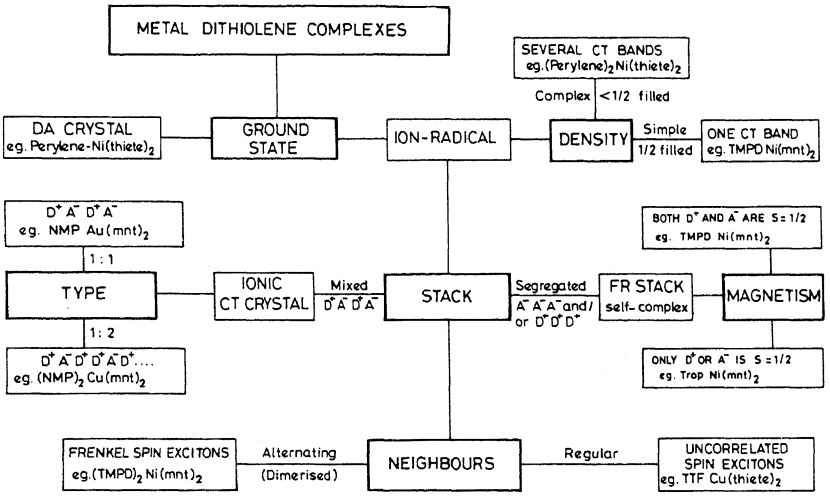

Figure 3. Schematic classification of metal dithiolenes based on structure and magnetism.

have a non-zero antisymmetric coupling between the two ions, it is necessary that the g-tensors of the two ions be different, and that there should not exist an inversion centre at the mid-point of the line joining the two ions.

Γ_{ij}, the anisotropic exchange tensor also tends to align the spins parallel or

antiparallel but defines a direction along which the coaligned spins have maximum energy—much like the classical dipole-dipole interaction. The anisotropic term arises from spin-orbit coupling and its magnitude is of the order $\approx (\Delta g/g)^2 J$. The bulk magnetic properties are often quantitatively given by J since the anisotropic exchange Γ is considerably smaller, *e.g.* it is of the order of $10^{-2}J$ for Cu(II) ions. Anisotropic exchange interaction corresponds to an effective dipolar coupling, with the principal axis determined by the g tensor of the complex and hence is also called pseudo dipolar coupling.

Exchange interaction has basically two types of effects—static and dynamic. The static effect is caused by the removal of degeneracies and the magnitude of splittings which is a measure of the strength of the interaction and can be determined by measuring the properties such as susceptibility, specific heat, etc which varies with temperature assuming a Boltzmann distribution. For a discussion of dynamic effects of exchange it is convenient to regard J as a spin-flipping frequency. One can in principle measure J from dynamic properties such as linewidth, provided the theory is good enough to relate these two quantities.

Although J is most often determined by static methods, EPR is a more sensitive tool particularly for a very small J or for small interchain interactions which are masked in the gross susceptibility.

Often one needs to study the EPR linewidth as a function of angle, Zeeman frequency and temperature to separate out the various contributions such as hyperfine, dipolar and anisotropic exchange and also to obtain separately the secular and nonsecular contributions. Furthermore, this requires a prior knowledge of precise g- and hyperfine anisotropic values in the absence of dipolar and exchange fields.

3.1 *Consequences of exchange in* LD *compounds*

Recent experimental and theoretical studies as reviewed by de Jongh and Miedema (1974) and Hone and Richards (1974) have been focussed on LD systems (Keller 1975) with strong exchange $J \approx 10$ to $100\,\mathrm{cm}^{-1}$. In general, EPR in systems with strong exchange leads to an 'exchange-narrowed' line whose shape, angular dependence, field dependence, etc yields information about the dimensionality of the exchange coupled network and about the local magnetic interactions. In the case of LD systems there are two qualitative differences expected. They are: (i) the lineshape should be non-Lorentzian and (ii) the angular and temperature dependences are quite different from what is predicted for three-dimensional (3D) systems.

Deviations from Lorentzian behaviour of EPR lines were first observed in $N(CH_3)_4MnCl_3$ (TMMC) by Dietz *et al* (1971). In 3D systems only short-time behaviour ($t_1 < \hbar/J$) of the spin correlation is important and so the linewidth can be adequately given by the relation

$$\Delta B_{pp} = (\pi/2)^{\frac{1}{2}} \langle \Delta\omega^2 \rangle / \omega_e, \tag{4}$$

where $\langle \Delta\omega^2 \rangle$ is the mean square deviation from the Larmor value and ω_e is the exchange frequency.

In LD systems long time spin correlations are important (figure 4) even when kT exceeds J by an order of magnitude. The disturbance which was initially confined to say i, will spread evenly throughout the system and hence the spin correlation function $\psi(\tau)$

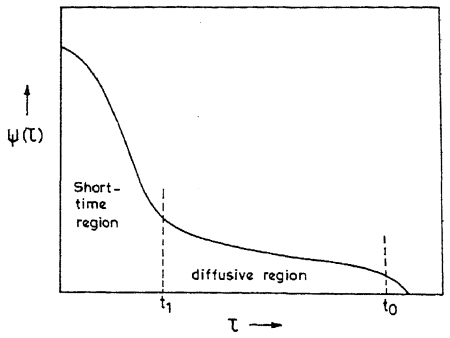

Figure 4. Schematic representation of the decay of the autocorrelation function $\psi(\tau)$. The short time region upto $t_1 \simeq \hbar J^{-1}$ is Gaussian while the diffusive region extends to t_0. For times $\tau > t_0$ the 1D $\tau^{-1/2}$ diffusion is cut off by interchain coupling.

or $\langle S_i(\tau)S_j \rangle$ is governed by diffusion processes (Hughes *et al* 1975) and can be written as

$$\psi(\tau) \alpha \langle S_i(\tau) S_i \rangle \alpha \tau^{-d/2}, \tag{5}$$

where d is the dimensionality of the system. The characteristic decay time, τ_c defined as

$$\tau_c = \int_0^\infty \psi(\tau)\, d\tau \tag{6}$$

converges when $d = 3$ since the $\tau^{-3/2}$ dependence of $\psi(\tau)$ is sufficiently rapid to make the integral converge and hence the long time diffusive tail does not seriously alter the exchange narrowing formula. For $d = 1$, however, $\tau^{-1/2}$ dependence of $\psi(\tau)$ leads to a lineshape which is the Fourier transform of $\exp[-At^{3/2}]$ which is somewhat midway between Gaussian and Lorentzian lineshapes as shown in figure 5. This non-Lorentzian lineshape has been verified in TMMC (Dietz *et al* 1971) and in α-Cu^{II} (N-methylsalicylaldiminato)$_2$ (Bartowski and Morosin 1972).

3.2 *Interchain exchange and its effects on the 1D lineshape*

In reality there are numerous transition metal salts and organic ion-radical complexes which are seemingly 1D systems but show nearly Lorentzian lineshapes characteristics of 3D systems. The reason is that it apparently takes only a small interchain coupling constant, J' to change the observed lineshape from the $\exp[-At^{3/2}]$ to Lorentzian. When $J' \ll J$, the short time behaviour of any spin correlation function is largely determined by the nearest neighbour intrachain exchange, J. Weak interchain contributions are important at long time, where they effectively cut off the slow diffusive decay $t^{-1/2}$ of 1D systems. Beyond the cut-off (t_0 in figure 4) the decay becomes exponential. The cut-off time t_0 is related to J' by

$$t_0^{-1} \propto |J'|^{4/3}/|J|^{1/3}. \tag{7}$$

Hennessy *et al* (1973) have predicted that J'/J greater than 10^{-3} is required to suppress the diffusive behaviour of spins along the chain and to get nearly Lorentzian shapes.

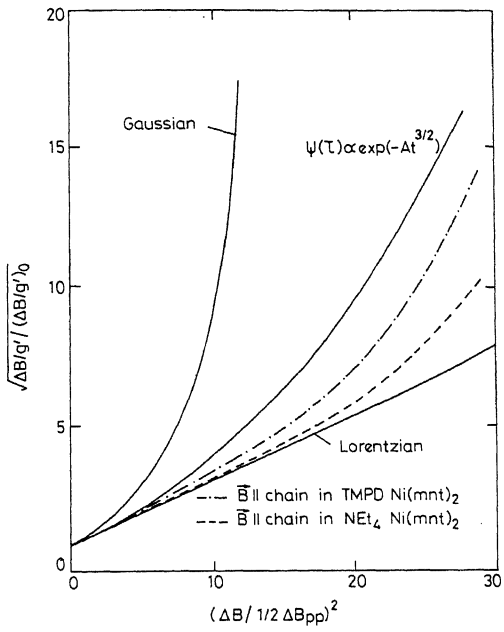

Figure 5. Theoretical and observed lineshapes of derivative lines.

3.3 *Spin correlation functions*

Exchange-narrowed magnetic resonance linewidth has been shown to be related to Fourier components of spin time-correlation functions—two-spin correlations in the case of hyperfine and four-spin correlations in the case of dipolar broadening. The normalized two-spin correlation function

$$C_{ij}(t) = \left[\frac{3}{S(S+1)}\right] \langle S_i^z(t)\, S_i^z(0)\rangle \tag{8}$$

has been investigated primarily for the case $i = j$, with $C(t) = C_{ii}(t)$. The two-spin autocorrelation function $C(t)$ has been computed by Windsor (1967), for classical spins by Blume and Hubbard (1970) at high temperature and by Carboni and Richards (1969) for finite linear chains. A Gaussian form for $C(t)$ was suggested by Anderson and Weiss (1953).

The dipolar interaction, on the other hand, leads to four-spin correlation functions given by

$$C_{ijkl}(t) = \left[\frac{3}{2S(S+1)}\right]^2 \langle S_i^+(t) S_j^+(t) S_k^-(0)\, S_1^-(0)\rangle. \tag{9}$$

Even after restricting to only diagonal correlation, a further approximation of strong decoupling is usually made which gives,

$$\langle S_i^+(t)\, S_j^+(t)\, S_k^-(0)\, S_l^-(0)\rangle \simeq \langle S_i^+(t)\, S_i^-(0)\rangle^2 \propto C^2(t). \tag{10}$$

The above expression is exact for vanishing interchain exchange. The general theories

of magnetic resonance relate the width (Γ) of the exchange narrowed line to the amplitude of local (dipolar and hyperfine) fields and for $kT \gg J_{ij}$ to Fourier components of spin correlation functions.

$$\Gamma_{\text{total}} = \Gamma_{\text{hyperfine}} + \Gamma_{\text{dipolar}}$$
$$= a^{(0)} g(0) + a^{(1)} g(\omega_0) + M_2{}^{(0)} f(0) + M_2^{(1)} f(\omega_0) + M_2^{(2)} f(2\omega_0), \qquad (11)$$

where $g(\omega)$ and $f(\omega)$ are given by

$$g(\omega) = \tfrac{1}{2} \int_{-\infty}^{+\infty} \exp(i\omega t)\, C(t)\, dt, \qquad (12)$$

$$f(\omega) = \tfrac{1}{2} \int_{-\infty}^{+\infty} \exp(i\omega t)\, C^2(t)\, dt, \qquad (13)$$

$a^{(0)}$ and $a^{(1)}$ are respectively the secular and nonsecular hyperfine second moments while $M_2^{(0)}$, $M_2^{(1)}$ and $M_2^{(2)}$ are respectively secular ($\Delta m_s = 0$) and nonsecular ($\Delta m_s = \pm 1$ and $\Delta m_s = \pm 2$) dipolar second moments. The second moment calculations for the dipolar and hyperfine fields are straightforward (Soos *et al* 1973).

Since the spin correlations arising from $\mathscr{H}_{ex}$ are isotropic, angualr and/or frequency-dependent EPR line-width provides equations in which the only unknowns are the Fourier components of various spin correlation functions. Hence it is possible to sort out the individual components. The Fourier components thus obtained can be fit to a one parameter form of $C(t)$—either Gaussian form of $C(t)$ proposed by Anderson and Weiss (1953) or Blume-Hubbard's (1970) high temperature approximation model, to get the exchange parameter for the system.

In highly LD systems the secular contributions to the second moments are likely to be enhanced, *i.e.*

$$M_2^{\text{low d}} = M_2^{\text{total}} + \eta\, M_2^{(0)}. \qquad (14)$$

The parameter η ranges from 0 to ∞. For $\eta = 0$, we have the usual 3D case for $J \gg g\beta B_0$, where secular and non-secular terms contribute equally. The limit $\eta \to \infty$ leads formally to an angular dependence dominated by $M_2^{(0)}$. In practice, η values of order unity are consistent with Lorentzian lines and slightly enhanced secular components. For simplicity it is generally assumed that the same enhancement holds for both hyperfine and dipolar contributions.

4. Exchange interactions in metal dithiolene systems

As mentioned in §1, by virtue of their highly planar geometry, metal dithiolenes stack as columnar structures in the solid state. Stronger interaction among units within a chain than between chains leads to anisotropic properties. We are mainly interested in the magnetic properties of the system as understood through preliminary susceptibility and detailed EPR studies. These magnetic effects are a manifestation of exchange interaction, J and our aim is to get a handle on the sign, magnitude and dimensionality of exchange in these systems. We have experimental realizations covering the whole range of J regimes:

(i) $J \gg \mathscr{H}_{\text{Zeeman}} \gg \mathscr{H}_{\text{broadening}}$,

(ii) $J \geqslant \mathscr{H}_{\text{Zeeman}} \gg \mathscr{H}_{\text{broadening}}$,

and (iii) $\mathscr{H}_{\text{Zeeman}} > J > \mathscr{H}_{\text{broadening}}$,

and as well as $J > kT$, $kT > J$ and $kT \gg J$. These systems are studied basically through x-ray crystal structure, magnetic susceptibility, EPR linewidth and lineshape to get an understanding about the dynamic effects of the exchange interactions. In our effort to characterise new examples of LD systems, we have synthesised and studied a few Ni(III) and Cu(II) dithiolenes and a brief review of the interesting results is outlined in the following sections.

4.1 *Crystal structure*

In general, irrespective of the particular form of dithiolene ligands or the counter cations, the MS_4 core is strictly planar and possesses D_{2h} symmetry. Typical values of M–S bond lengths are given in table 2. The $M(\text{mnt})_2^-$ systems have a shorter M–S bond compared to $M(\text{mnt})_2^{2-}$ systems. The cyanide (–C≡N) bond length is very sensitive to the changes in the metal oxidation state or in general to the total electron density in the anion unit. Any partial charge transfer to the metal system, hence, should be reflected in the C≡N bond length and so can be taken as an indication of charge transfer. An examination of C≡N bond length given in table 2 shows that in TMPD Ni $(\text{mnt})_2$ the C≡N distance is large compared to other Ni(III) compounds but is closer to Ni(II) compounds. This along with the fact that there are several short contact distances between the C≡N group of $Ni(\text{mnt})_2^-$ and the TMPD unit indicates that there has been some electron transfer from TMPD^+ to $Ni(\text{mnt})_2^-$. Further evidence is obtained from the fact that the TMPD^+ unit of this compound has very pronounced quinonoid structure and the bond distances are much closer to TMPD^{2+} rather than TMPD^+, indicating that it has acquired more than a single positive charge. Thus we have a strong structural evidence of charge transfer from TMPD^+ unit to $Ni(\text{mnt})_2^-$ unit.

An important feature in the structure of these mnt chelates is that they all stack in columns along a specific crystallographic axis. Based on the nature of the units that make up the stack and as well as how these units are stacked, one can get either a mixed stack (in cases where both the units are planar) or a segregated stack (self-stack). Typical examples are given in table 3. Both of these types can have their units (say D, donor and A, acceptor) uniformly spaced or alternatingly spaced. Charge transfer may occur either by direct lateral overlap in the case of mixed stacks ($D^+A^-D^+A^-\ldots$) or by edge-wise contacts between $D^+D^+D^+\ldots$ chains and $A^-A^-A^-\ldots$ chains in the case of segregated stacks.

Alternation of interplanar spacings in segregated structure of $M(\text{mnt})_2^-$ systems invariably leads to dimerization of the anions. The dimerization occurs involving the metal ions bridging to one of the sulphur atoms of the other anion of the same dimer as shown in figure 6. The Ni . . . S (bridging, out-of-plane) distances range from 3·45 Å to 4 Å compared to the Ni–S (in plane) distances ~ 2·15 Å. In such cases the stacking is referred to as 'diadic'. However, interdimer interactions along the stack cannot be totally ruled out, particularly when the metal atom alternation distances are not very large. The extreme case of an 'isolated' dimer stack (zero-dimensional, then) can also be envisaged crystallographically, but in reality small interdimer interactions as well as

Table 2. A comparison of bond lengths in Å found in some selected $M(mnt)_2^{n-}$ systems.

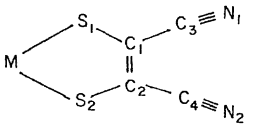

Compound	M–S_1	S_1–C_1	C_1=C_2	C_1–C_3	C_3≡N_1	Reference
$(NEt_4)^+Ni(mnt)_2^-$	2·144 (2)	1·719 (9)	1·359 (12)	1·437 (13)	1·125 (13)	Kobayashi and Sasaki (1977)
$(TMPD)^+Ni(mnt)_2^-$	2·152 (4)	1·708(15)	1·315 (18)	1·431 (18)	1·155 (12)	Ramakrishna and Manoharan (1983a)
$(TMPD)_2Ni(mnt)_2^{2-}$	2·173 (2)	1·731 (5)	1·379 (6)	1·414 (7)	1·148 (6)	Hove *et al* (1972)
$(NMP)^+Ni(mnt)_2^-$	2·138 (3)	1·710 (8)	1·361 (9)	1·445 (9)	1·136 (8)	Kuppusamy *et al* (1984a)
$(NMP)^+Au(mnt)_2^-$	2·317 (4)	1·75 (2)	1·33 (2)	1·445 (2)	1·15 (2)	Kuppusamy *et al* (1984c)

Table 3. Nature of packing arrangements found in metal dithiolene complexes.

Compound	Nature of stack	M–M distance(s) along stack axis (Å)	Exchange $-2J$, cm^{-1}	Reference (for structure)
(NEt_4) Ni $(mnt)_2$	alternating	4·14, 4·31	490[a]	Kobayashi and Sasaki (1977)
(PPh_3Me) Ni $(mnt)_2$	alternating	4·40, 4·45	620[a]	Fritchie (1966)
(Trop) Ni $(mnt)_2$	segregated, uniform	7·458	8·8	Manoharan *et al* (1981)
(TMPD) Ni $(mnt)_2$	segregated, uniform	7·334	120	Ramakrishna and Manoharan (1983a)
$(NPhMe_3)$ Ni $(mnt)_2$	alternating	3·83, 4·41	—	Mahadevan *et al* (1983)
(NMP) Ni $(mnt)_2$	segregated, alternating	4·16, 7·87	241	Kuppusamy *et al* (1984a)
(NMP) Ni $(bdt)_2$[b]	mixed	10·148	< 1	Mahadevan *et al* (1984a)
(NEt_4)Ni $(bdt)_2$[b]	uniform	7·576	< 1	Kuppusamy and Manoharan (1984b)
(NBu_4)Ni $(sdt)_2$[c]	uniform	8·874	< 1	Mahadevan *et al* (1984b)
$(Cudmp_2)$Ni $(mnt)_2$[d]	uniform	13·25	< 1	Venkatalakshmi *et al* (1984)
$(NMP)_2$Cu $(mnt)_2$	mixed	11·417	0·13	Kuppusamy *et al* (1984b)
$(MB)_2$Cu $(mnt)_2$	segregated, alternating	7·115, 10·743	5·2	Snaathorst *et al* (1981)
$(NMe_4)_2$ Cu $(mnt)_2$	uniform	13·23	< 1	Mahadevan and Seshasayee (1984)
(NMP) Au $(mnt)_2$	mixed	7·739	—	Kuppusamy *et al* (1984c)
(NBu_4) Au $(tdt)_2$[e]	uniform	9·336	—	Mazid *et al* (1981)

[a] Weiher *et al* (1964); [b] bdt: benzene-1,2-dithiolato; [c] sdt: stilbene-1,2-dithiolato; [d] dmp: 2,9-dimethyl-1,10-phenanthroline; [e] tdt: toluen-3,4-dithiolato.

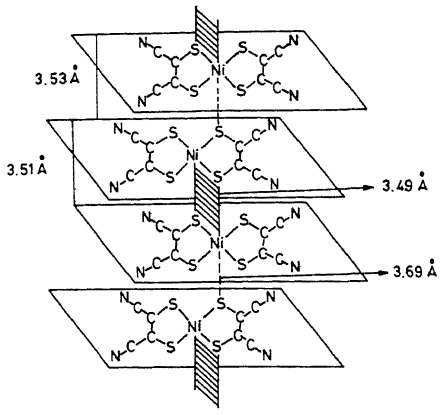

Figure 6. The anion stack of $NEt_4Ni(mnt)_2$ showing the alternation in the Ni–S overlaps.

interstack interactions make it a higher dimensional one. Nevertheless, crystallographic work can help one to guess the dimensionality of the interactions. For exact conclusions one has to naturally resort to magnetic studies.

4.2 *Magnetic susceptibility*

In the last two decades there has been considerable progress in the description of LD magnetic systems. We focus particular attention on the magnetic susceptibility and low-lying excited states of antiferromagnetic 1D Heisenberg ($S = 1/2$) chains. The case of uniform exchange between spins along the chain has been studied mainly by Bonner and Fisher (1964), and Bulaevskii (1962), while the case of nonuniform or alternating exchange along the chain has been considered by Bulaevskii (1969) and Duffy and Barr (1968). The spin coupling Hamiltonian for these cases of 1D systems is

$$\mathscr{H} = \sum_{i=1}^{N/2} (J_1 S_{2i} \cdot S_{2i-1} + J_2 S_{2i} \cdot S_{2i+1}). \tag{15}$$

Defining $\alpha = J_2/J_1$, we get the uniform chain for $\alpha = 1$, alternating chain for $\alpha < 1$ and the limiting case of isolated dimers for $\alpha = 0$. An important difference in the feature of susceptibility (χ) *vs* T of the above cases is that the susceptibility for the uniform infinite chains is nonvanishing at absolute zero and that the two nonuniform chains at either extremes of α are essentially similar at low temperatures with χ vanishing exponentially.

The variation of magnetic susceptibility with temperature has been shown for two such extreme cases, namely $\alpha = 1$ and $\alpha = 0$ in figures 7 and 8.

Magnetic susceptibility measurements on $Trop^+ Ni(mnt)_2^-$ (Manoharan *et al* 1981) down to 4·2 K showed a broad maximum, characteristic of 1D systems, at 8 K indicating a sizable antiferromagnetic interaction (figure 7). The data could be fit into the Bonner-Fisher (1964) expression for uniform chains with $J = -4{\cdot}4\ cm^{-1}$. It should also be noted from the inset of figure 7 that below T_{max} the susceptibility does not at all follow the behaviour of 1D chain and this has been explained as due to ferromagnetic interactions between the chains below T_{max}.

A slightly complex dependence of χ on T has been observed for $TMPD^+ Ni(mnt)_2^-$ (Ramakrishna and Manoharan 1983a), where both the anion and the cation are

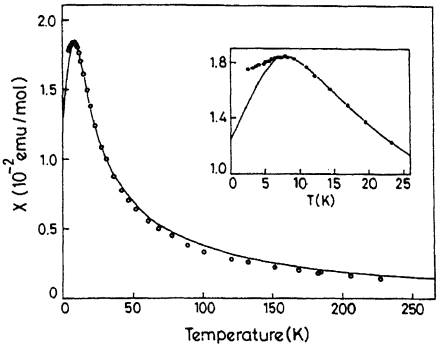

Figure 7. Variation of χ_M with temperature for Trop$^+$ Ni (mnt)$_2^-$ (uniform chain). Solid line represents the theoretical susceptibility calculated by the linear chain Heisenberg model. The inset shows the fit near the T_{max} region.

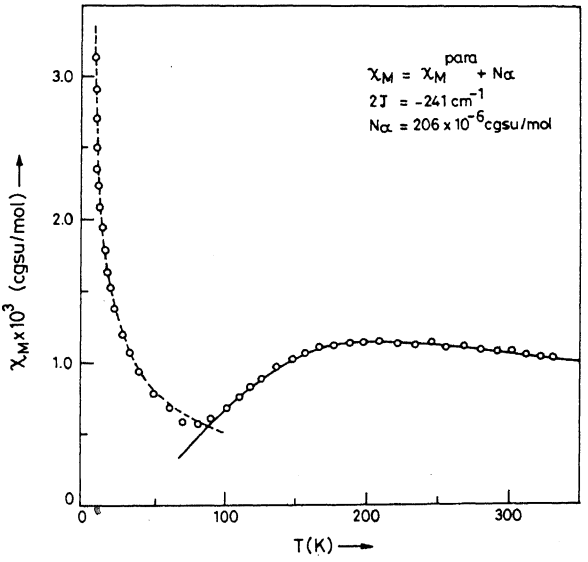

Figure 8. Variation of χ_M with temperature for (NMP$^+$)Ni(mnt)$_2^-$ (dimeric chain). The solid line above $T = 90$ K represents the theoretical susceptibility calculated from equation (17) while that below $T = 70$ K represents the susceptibility calculated by using the ECP model (equation (18)).

paramagnetic having one unpaired electron each. The susceptibility studies down to 4·2 K showed the presence of two temperature regions—a Curie-type behaviour below 100 K and an almost temperature-independent susceptibility above 100 K (figure 9). The low temperature regime susceptibility has been analysed on the basis of the random exchange Heisenberg anitferromagnetic linear chain (REHAC) model (Bulaevskii 1969; Soos and Bondeson 1980). The occurrence of chemical or packing defect is quite general in LD systems and can have drastic consequences on the magnetic and transport properties. Finite chain effects in magnetic systems produce divergent susceptibilities

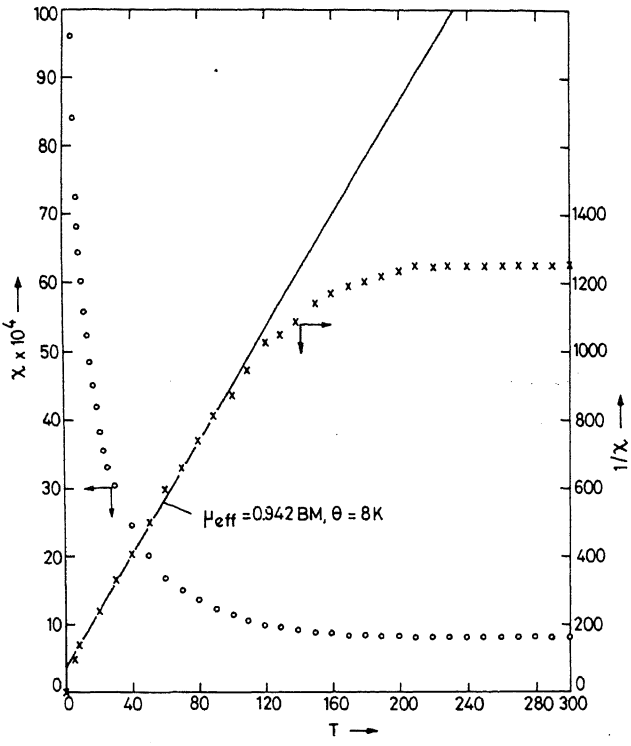

Figure 9. Temperature variation of susceptibility of TMPD$^+$Ni(mnt)$_2^-$. The χ^{-1} *vs* T plot shows clearly the two-temperature regimes $T < 100$ K, where a Curie-Weiss behaviour is seen and $T > 100$ K where χ is almost temperature independent.

associated with odd length segments. In such cases the susceptibility deviates from Curie behaviour and shows a power law behaviour, instead:

$$\chi(T) = AT^{-\gamma} \text{ or } \log \chi(T) = \log A - \gamma \log T. \tag{16}$$

The exponent γ has been found to be usually between 0·72 and 0·89. A plot of $\log \chi(T)$ *vs* $\log T$ yielded in the case of TMPD$^+$ Ni(mnt)$_2^-$ the value of γ as 0·84. The concentration of breaks in the otherwise infinite regular chain was estimated to be 0·20. Below 100 K a decomposition procedure (Tomkiewicz *et al* 1980) was used to separate out the χ contributions from the individual stacks of TMPD$^+$ and Ni(mnt)$_2^-$. At 4·2 K, 90 % of the susceptibility is from Ni(mnt)$_2^-$ and this contribution decreases as the temperature is increased and becomes 83 % at 100 K.

On the other hand very strong antiferromagnetic exchange has been observed in NMP$^+$ Ni(mnt)$_2^-$ (Kuppusamy *et al* 1984a) which has dimeric Ni(mnt)$_2^-$ anions stacked along the crystallographic a-axis. A $2J$ value of -241 cm^{-1} could be obtained by fitting the measured χ values down to 90 K into the expression

$$\chi_M = \frac{N\bar{g}^2\beta^2}{3kT}\left[1 + \tfrac{1}{3}\exp(J/kT)\right]^{-1} + N\alpha, \tag{17}$$

with $N\alpha = 206$ cgsu/mol. The fitting is shown in figure 8. Below 90 K an increase in susceptibility was observed, obeying the power law expression (equation (16)) with

$\gamma = 0{\cdot}85$. By assuming the exchange coupled model (ECP) of Tippie and Clark (1981) for random exchanges in alternating chains, the entire data below 70 K could be fit very satisfactorily into the expression

$$\chi = \frac{\bar{g}^2\beta^2 N}{J}\,[2J/kT]^{\gamma} f_1(\gamma), \tag{18}$$

and with $f_1(\gamma) = 0{\cdot}445 \exp(-0{\cdot}633\,\gamma)$ for $\gamma = 0{\cdot}85$ and for a concentration of random exchanges, $c = 0{\cdot}05$. Hence it is observed that 95% of the exchanges are normal with $2J = -241\ \text{cm}^{-1}$ while 5% exchanges are randomly distributed with a maximum cut-off at $2J$.

4.3 *EPR studies*

EPR studies, in general, complements and extends the static magnetic susceptibility results as the integrated absorption intensity is proportional to the susceptibility. It also probes the electronic structure of the spin carriers through the principal g-values and relate them structurally to the lattice through the orientation of the axes of the g-tensor. Finally, it contributes to the study of spin dynamics in coupled spin systems of low dimensionality through the behaviour of absorption linewidth and lineshape. In particular, EPR studies could predict very accurately the existence of small interchain couplings which are otherwise masked in the gross susceptibility. We give below a brief summary of the EPR results of a few metal dithiolene systems studied in our laboratory.

An interesting display of interstack (or intersite) electron spin exchange has been observed (Manoharan *et al* 1981) in (Tropilium)$^+$ Ni $(\text{mnt})_2^-$, where though there are two magnetically distinct sites, the single crystal EPR spectrum at 300 K appears to consist of one single line at all orientations, except in the *ab* plane at Q-band frequency (35 GHz). This will happen if the difference in the Zeeman frequencies of the two spins, $(g_1 - g_2)\beta B$ is larger compared to the exchange frequency between the two sites. Using the modified Bloch equations (Carrington and McLachlan 1967) the spectra in the *ab* plane were simulated. Two such simulated spectra are presented in figure 10. The interstack exchange, J' has been estimated to be 450 ± 30 MHz at 300 K.

The two lines in the *ab* plane at Q-band frequency move close together and coalesce into a single line of 350 G width on decreasing the temperature to about 240 K. Further lowering of temperatures results in a narrowing of the line to a width of less than 100 G at ~ 8 K. This could be accounted for in terms of an increase in J' on cooling the system. In the limit of rapid exchange the linewidth of the coalesced line is given by

$$g_{\text{av}}\beta\,\Delta B_{\text{pp}} = [g_1 - g_2]\beta B]^2/8J', \tag{19}$$

where $g_{\text{av}} = (g_1 + g_2)/2$ and ΔB_{pp} is the peak-to-peak derivative linewidth. Using the above expression the interstack exchange was calculated as a function of temperature and it was estimated that J' increases by a factor of 4 over the range 300–8 K (figure 11). At the coalescence temperature J' is given by

$$J' = \frac{1}{2\sqrt{2}}(g_1 - g_2)\,\beta B, \tag{20}$$

from which one gets $J' = 646$ MHz.

In the ac^* plane, where all the sites are magnetically equivalent due to the two-fold symmetry of the monoclinic system, it has been observed that anisotropic exchange and

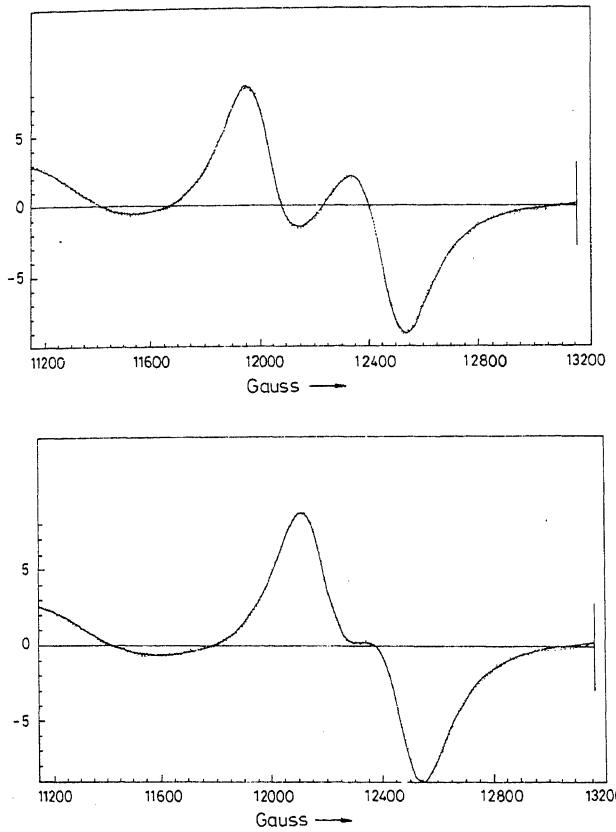

Figure 10. EPR spectra of Trop$^+$Ni(mnt)$_2^-$ single crystal at the orientation of $\theta = 55°$ (top) and $\theta = 65°$ (bottom) in the *ab* plane. Dotted line is the experimental spectrum while the solid line represents the computer simulation.

low dimensionality of the magnetic interactions are responsible for the observed linewidths to a larger extent. Following the approach of McGregor and Soos (1976) an anisotropic exchange contribution of $0{\cdot}26 \pm 0{\cdot}015$ cm^{-1} has been estimated along with a value of $0{\cdot}65 \pm 0{\cdot}15$ for η, a measure of enhanced contribution of secular terms to the total second moment (*cf* equation (14)).

The ion-radical charge-transfer salt TMPD$^+$ Ni (mnt)$_2^-$ is a novel and unique system that has been investigated (Ramakrishna *et al* 1983; Ramakrishna and Manoharan 1983a) in detail to understand the exchange interactions between two $S = 1/2$ spins coming from two chemically different moieties. At 300 K, though the acetone solution of this system gives two resonances corresponding to isolated TMPD$^+$ and Ni (mnt)$_2^-$ at $g = 2{\cdot}0023$ and $g = 2{\cdot}066$ respectively, the larger linewidth (35 G) of the TMPD$^+$ signal compared to other simple TMPD$^+$ salts and the total absence of hyperfine features suggest the formation of weak self-aggregates as a result of CT complex formation. The frozen solution at 77 K yields a three g-pattern corresponding exactly to Ni (mnt)$_2^-$ and no resonance corresponding to TMPD$^+$, quite expected as a result of dimerization of TMPD$^+$ moieties (Thomas *et al* 1963).

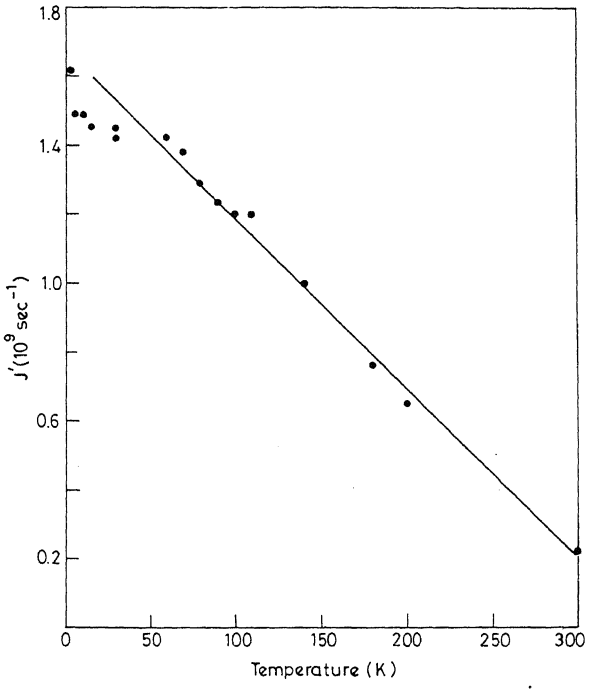

Figure 11. Plot of temperature dependent interstack exchange frequency as calculated by equation (19).

The powder pattern shows a single broad line of $\sim$ 350 G width and X-band and at 300 K centred at $g = 2{\cdot}03$, which is the average of individual g_{av}'s of the two radicals. But it gradually sharpens on cooling and at around 120–130 K it splits into the familiar orthorhomic g-pattern (figure 12) whose principal values are close but do not exactly match with those of isolated $Ni(mnt)_2^-$. The valid reason for the temperature dependence of g is that there is rapid spin exchange between the dissimilar systems. From the frequency and the temperature dependence of the powder line a ratio of $1{\cdot}94 \times 10^{-2}$ was obtained for Γ/J, where Γ is the anisotropic exchange defined in equation (3). Single crystal EPR studies yielded the g-tensor direction cosines that do not coincide with the molecular directions of $Ni(mnt)_2^-$ ion but rather are crystallographic. The g_z (1·992) direction, for example, is tilted by about 40° from the normal to the $Ni(mnt)_2^-$ plane towards the stack direction (a-axis). The line-width analysis in a plane perpendicular to a-axis gives values of J, Γ and η as $8 \pm 2\ cm^{-1}$, $0{\cdot}15 \pm 0{\cdot}05\ cm^{-1}$ and 5 ± 2 respectively. The lineshape analysis at $\vec{B} \parallel a$ (figure 5) shows that the system is quite LD, whereas at $\vec{B} \perp a$, a nearly Lorentian lineshape was observed.

Sometimes, unlike in the normal exchange coupled systems, 'magnetic dilution' achieved through strong anti-ferromagnetic intrachain exchange leads to sharp lines in EPR, which enables the resolution of extremely small fine structural details. NEt_4^+ $Ni(mnt)_2^-$, a strongly exchange coupled system with $2J = -490\ cm^{-1}$ (Weiher *et al* 1964), has been reported to have alternating $Ni(mnt)_2^-$ ions along the stack (Kobayashi and Sasaki 1977). Though the distances are almost close (3·51 Å and 3·53 Å), the various interatomic distances for any reference unit with its neighbouring

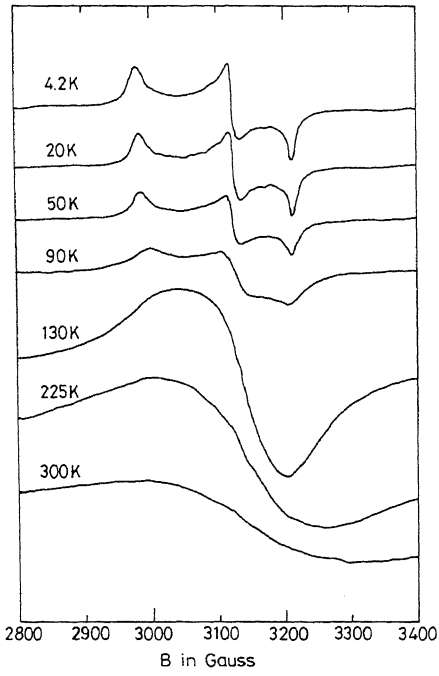

Figure 12. Temperature variation of the powder EPR pattern for TMPD $Ni(mnt)_2$.

units on either side and hence their overlaps are quite different. The exchange interactions which are very sensitive to the relative orientations and overlaps are hence not uniform but alternating. The susceptibility data in the range 100–300 K (Weiher *et al* 1964) could be well accounted by fitting into a Hamiltonian of non-interacting dimers.

The EPR spectrum which is observable only below 100 K is of very weak intensity (Ramakrishna and Manoharan 1983b, 1984). Generally two sets of lines were observed corresponding to the two inequivalent sites of the monoclinic unit cell but with each set having a bunch of lines. The lineshape (figure 5) and linewidth analyses showed clearly the high one-dimensionality of the exchange coupled network. The angular variation of these fine structure lines is shown in figure 13. The fine structure has been simulated on the basis of interchain dipolar interactions with the neighbours on surrounding stacks. The dipolar coupling with the spins on the same stack does not cause splitting as it is averaged out by the strong exchange along the stack and hence has been neglected simulation. The weak interchain exchange is not able to average out the dipolar splittings completely but only reduces it. The method formulated by Anderson (1954) was used to evaluate the effect of weak exchange on splittings in EPR caused by other interactions such as hyperfine, dipolar, etc.

The relatively smaller singlet-triplet separation (241 cm^{-1}) observed in the dimeric stack of (NMP) $Ni(mnt)_2$ compared to other similar dimers provides a convenient means of studying the triplet exciton EPR. At ambient temperatures larger triplet exciton population results in a collision broadening of the triplet signals and hence only one broad signal ($\Delta B_{pp} \simeq 800$ G) is observed. However, the triplet fine structures appear on

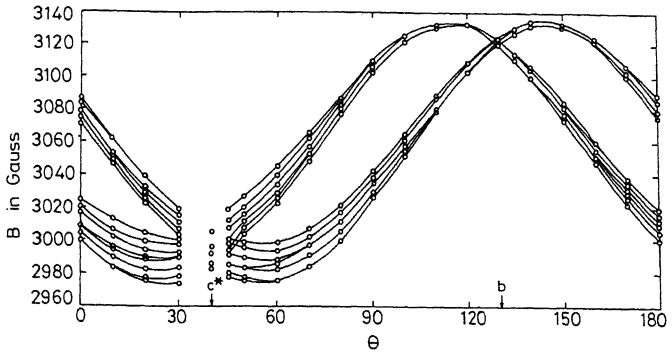

Figure 13. Angular variation of the fine structure lines in the *bc* plane of $NEt_4Ni(mnt)_2$.

cooling the system down to ~ 25 K. A feature similar to what has been observed by Hoffmann *et al* (1983) in Cu (DMP)$_2$ (TCNQ) is seen except that in our system the *g*-tensor anisotropy is large. A detailed investigation is in progress.

Snaathorst *et al* (1981) have reported a non-planar $Cu(mnt)_2^{2-}$ complex with methylene blue counter cation. The x-ray structure shows a dihedral angle of 47·4° between the planes of the two mnt ligands. It shows also that the anions are paired, with a Cu–Cu distance of 7·115 Å. The electrostatic interaction between the two unpaired electrons gives rise to a singlet ground state and a triplet excited state, 5·2 cm^{-1}, above it, as determined from the magnetic susceptibility data. The EPR spectra of the excited triplet state were measured at 4·2 K. The *g*-, copper hyperfine- and zero field splitting tensors were determined and could be reproduced quantitatively with semi-empirical MO calculations.

For systems with $J < 1$ cm^{-1}, the decisive evidence for LD magnetic properties rests on detailed analysis of spin dynamics as manifested in EPR or neutron diffraction studies. Generally Cu(II) dithiolenes are found to be weakly exchange coupled. Plumlee *et al* (1975) have studied $(NBu_4)_2Cu(mnt)_2$ and they report a *J* value of ~ 107 G which is of comparable magnitude with hyperfine interactions. At certain orientations of the crystal *J* is actually less than the hyperfine interaction resulting in a multiline EPR spectrum. Using a degenerate perturbation theory the multiline spectrum has been analysed directly (without having to resort to linewidth analysis) to estimate the exchange parameter. Both the smallness of *J* and the smallness of dipolar interactions are unusual features of $(NBu_4)_2Cu(mnt)_2$.

The situation would be different if *J* exceeds magnetic interactions such as dipolar or hyperfine terms, in which case one would observe only a single exchange narrowed line. Then an indirect calculation of *J* through linewidth analysis would be necessary and this would require a knowledge of the dipolar and hyperfine second moments. The analysis would be further complemented by studying the lineshapes as well as Fourier coefficients of various two-spin and four-spin correlation functions.

An example of such a weak exchange regime has been observed in $(NMP)_2Cu(mnt)_2$, (Kuppusamy and Manoharan 1983; Kuppusamy *et al* 1984b) where the relative Hamiltonians are:

$$\mathcal{H}_Z > \mathcal{H}_{ex} > \mathcal{H}_{hyp} > \mathcal{H}_{dip}$$

$(NMP)_2Cu(mnt)_2$ forms a kind of mixed stack with a donor acceptor sequence DAD–DAD along a-axis of the monoclinic unit cell. Static susceptibility measurements down to 4·2 K showed the exchange to be very small ($J = -0{\cdot}13\ cm^{-1}$). Single crystal EPR in the ac^* plane, where the two sites are magnetically equivalent showed single exchange narrowed Lorentzian lines with hyperfine dominated linewidth. The angular dependence of the linewidth in the ac^* plane along with the computed second moments was used to evaluate the high temperature Fourier components of the autocorrelation functions $C(t)$ and $C^2(t)$. The computed nonsecular components were shown to follow from either the Blume-Hubbard model within $\hat{J} = 2100$ G or from the Anderson-Weiss model with $J = 1175$ G. The calculated linewidth in the ac^* plane is compared with the experimental linewidths in figure 14. The prediction of the correct order of exchange coupling through EPR linewidth, in line with the susceptibility prediction has been found to be fairly successful using the existing theories for weak exchange.

Sometimes an estimate of J'/J can be made by using the frequency dependence of the linewidth. Except along symmetry directions, the two types of chains (*eg.* in a monoclinic system) have different g-factors and therefore two separate EPR lines would be seen in the absence of J'. The coupling J' merges the lines, but the width of the single observed line is proportional to the square of the microwave frequency. A rough determination of J'/J can be made even if the chains are not magnetically inequivalent by using the frequency dependence of the linewidth due to anisotropic dipolar interactions between chains to determine the Fourier components of the spin correlation function (Soos *et al* 1973; Huang and Soos 1974). Theories of exchange narrowing predict that the frequency dependent linewidth due to inequivalent sites (Yokota and Koide 1954; Hughes *et al* 1975) depends on the square of the splitting, ΔB_Q or ΔB_X, which ought to have been but for exchange,

$$\Delta B_{pp}(Q) - \Delta B_{pp}(X) = \frac{\Delta B_Q^2 - \Delta B_X^2}{H_e}, \tag{21}$$

where H_e, the interstack exchange frequency is given by

$$(g\beta/h)H_e = 4t_c^{-1}(\sqrt{3}/2). \tag{22}$$

In equation (22), t_c is the correlation time given by

$$t_c = |J|^{1/3}/|J'|^{4/3}. \tag{23}$$

The weak exchange system $(NMe_4)_2Cu(mnt)_2$ shows a single EPR line both at X- and Q-band frequencies in the bc plane, where there must be two separate resonances due to the magnetic inequivalency of the sites but for J'. The Q-band linewidths are larger for any orientation, except $\vec{B}$ along b- or c^*-axis of this monoclinic system (figure 15). Using equation (21), the value of H_e has been estimated to be 300 ± 50 G. This along with a value of 600 G for J, obtainable using the linewidth data in the ac^* plane, gives 50 G for J'. This observation is consistent with the fact that in the ab plane the two resonances could be resolved at Q-band frequencies. The ratio $J'/J \simeq 10^{-1}$ also shows the close-to-one dimensionality of the interactions.

5. Conclusions

The metal dithiolene systems, thus, provide a convenient basis for studying various cooperative interactions, like intrastack and interstack exchange interactions, aniso-

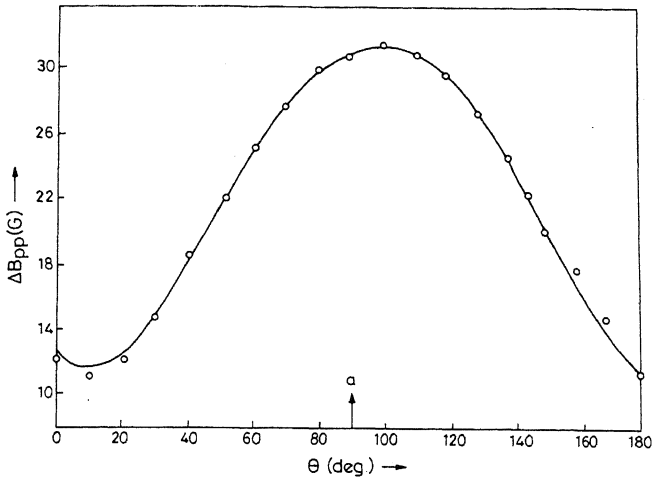

Figure 14. Experimental (solid line) and calculated (o) linewidths for $(NMP)_2Cu(mnt)_2$ in the ac^* plane. The calculated linewidths are based on Blume-Hubbard $C_{BH}(t)$ with $\hat{J} = 2100$ G and with Fourier components $g(0) = 0{\cdot}64 \times 10^{-3}\,G^{-1}$; $g(\omega) = 0{\cdot}06 \times 10^{-3}\,G^{-1}$; $f(0) = 2{\cdot}79 \times 10^{-3}G^{-1}$; $f(\omega) = 0{\cdot}145 \times 10^{-3}\,G^{-1}$ and $f(2\omega) = 0{\cdot}006 \times 10^{-3}G^{-1}$ at $\omega = 9{\cdot}47$ GHz.

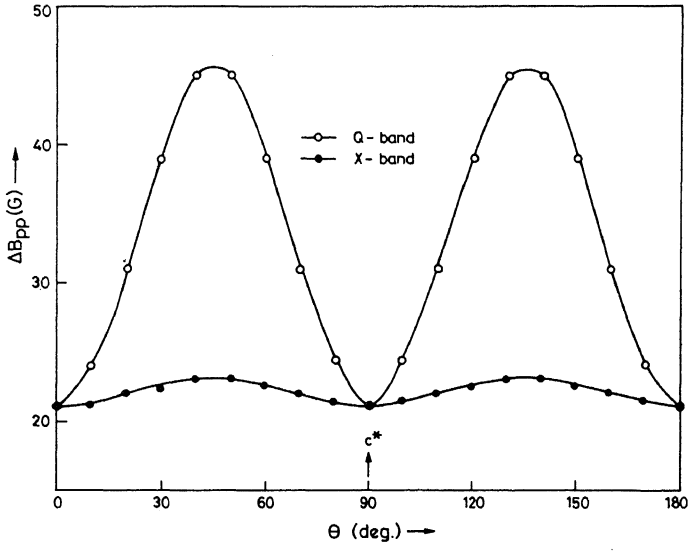

Figure 15. Linewidth *vs* angle of applied field $\vec{B}$ in the *bc* plane of $(NMe_4)_2\,Cu(mnt)_2$ at X- and *Q*-band frequencies.

tropic exchange, etc occurring in magnetically condensed solids. We have studied several *J* regimes with respect to temperature, Zeeman frequency and broadening mechanisms such as dipolar, hyperfine and anisotropic exchange. We could establish successfully the dimensionality of the exchange coupled network by an analysis of the position, width and shape of EPR lines using the existing theories of exchange narrowing aided by susceptibility and structural results.

Acknowledgements

PK is grateful to the UGC, New Delhi for providing a fellowship (FIP) and to the Pachaiyappa's Trust, Madras for allowing him to take up the fellowship. This work was supported by a scheme from the Department of Science and Technology, Government of India, New Delhi, for which we are grateful.

References

Alcacer L, Novais H, Pedroso F, Flandrois S, Coulon C, Chasseau D and Gaultier J 1980 *Solid State Commun.* **35** 945
Anderson P W 1954 *J. Phys. Soc. Jpn* **9** 316
Anderson P W and Weiss P R 1953 *Rev. Mod. Phys.* **25** 269
Bartowski R R and Morosin B 1972 *Phys. Rev.* **B6** 4209
Blume M and Hubbard J 1970 *Phys. Rev.* **B1** 3815
Bonner J C and Fisher M E 1964 *Phys. Rev.* **135** 640
Bulaevskii L N 1962 *Zh. Eksp. Theor. Fiz.* **43** 968 (1963 *Sov. Phys. JETP* **16** 685)
Bulaevskii L N 1969 *Fiz. Tverd. Tela.* **11** 1132 (*Sov. Phys. Solid State* **11** 921)
Carboni F and Richards P M 1969 *Phys. Rev.* **177** 189
Carrington A and McLachlan A D 1967 *Introduction to magnetic resonance* (New York: Harper and Row) p. 204
Cooper J R, Miljak M, Underhill A E and Ahmad M M 1983 *J. de Physique Colloque* **44** 1391
Davidson A, Edelstein N, Holm R H and Maki A H 1963 *J. Am. Chem. Soc.* **85** 2029
de Jongh L J and Miedema A R 1974 *Adv. Phys.* **23** 1
Dietz R E, Merrit F R, Dingle R, Hone D, Silbernagel B G and Richards P M 1971 *Phys. Rev. Lett.* **26** 1186
Duffy Jr W and Barr K P 1968 *Phys. Rev.* **165** 647
Endres H, Keller H J, Moroni W and Nothe D 1979 *Acta. Crystallogr.* **B35** 353
Fritchie Jr C J 1966 *Acta Crystallogr.* **20** 107
Gray H B, Williams R, Bernal I and Billig E 1962 *J. Am. Chem. Soc.* **84** 3596
Hatfield W E 1979 *Molecular Metals* (New York: Plenum) A NATO conference series Vol I series VI
Hennesey M J, McElwee C D and Richards P M 1973 *Phys. Rev.* **B7** 930
Hoffman S K, Corvan P J, Singh P, Sethulakshmi C N, Metzger R M and Hatfield W E 1983 *J. Am. Chem. Soc.* **105** 4608
Hone D W and Richards P M 1974 *Annu. Rev. Mater. Sci.* **4** 337
Hove M J, Hoffman B M and Ibers J A 1972 *J. Chem. Phys.* **56** 3490
Huang T Z and Soos Z G 1974 *Phys. Rev.* **B9** 4981
Hughes R C, Morosin B, Richards P M and Duffy Jr W 1975 *Phys. Rev.* **B11** 1795
Interrante L V 1974 *Extended interactions between transition metal ions in transition metal complexes*, ACS Symposium series No. 5
Interrante L V, Bray J W, Hart H R, Kasper J S, Piacente P A and Watkins G D 1978 *Ann. NY Acad. Sci.* **313** 407
Isett L C, Rosso D M and Bottger G L 1980 *Phys. Rev.* **B22** 4739
Jacobs I S, Bray J W, Hart H R, Interrante L V, Kasper J S, Watkins G D, Prober D E and Bonner J C 1976 *Phys. Rev.* **B14** 3036
Keller H J 1975 *Low dimensional cooperative phenomena* (New York: Plenum)
Keller H J 1977 *Chemistry and physics of LD metals* (New York: Plenum)
Kobayashi A and Sasaki Y 1977 *Bull. Chem. Soc. Jpn* **50** 2650
Krogmann K and Hausen H D 1968 *Z. Anorg. Chem.* **358** 67
Kubo R and Tomita K 1954 *J. Phys. Soc. Jpn* **9** 888
Kuppusamy P, Mahadevan C, Seshasayee M and Manoharan P T 1984a *J. Cryst. Spect. Res.* (in press)
Kuppusamy P and Manoharan P T 1983 *Bull. Mag. Res.* **5** 207
Kuppusamy P and Manoharan P T 1984a (to be published)
Kuppusamy P and Manoharan P T 1984b (to be published)
Kuppusamy P, Ramakrishna B L and Manoharan P T 1984b *Inorg. Chem.* (in press)
Kuppusamy P, Venkatalakshmi N and Manoharan P T 1984c (to be published)

Little W A 1964 *Phys. Rev.* **134** 1416
Mahadevan C, Kuppusamy P, Seshasayee M and Manoharan P T 1984a *J. Cryst. Spect. Res.* (in press)
Mahadevan C, Kuppusamy P, Seshasayee M and Manoharan P T 1984b *J. Cryst. Spect. Res.* **14** 177
Mahadevan C and Seshasayee M 1984 *J. Cryst. Spect. Res.* **14** 213
Mahadevan C, Seshasayee M, Murthy B V R, Kuppusamy P and Manoharan P T 1983 *Acta. Cryst.* **C39** 1335
McCleverty 1968 Progress in *Inorg. Chem.* **10** 49
Manoharan P T, Noordik J H, de Boer E and Keijzers C P 1981 *J. Chem. Phys.* **74** 1980
Mazid M A, Razi M T and Sadler P J 1981 *Inorg. Chem.* **20** 2872
McGregor K T and Soos Z G 1976 *J. Chem. Phys.* **64** 2506
Melby L R, Harder R J, Hertler W R, Mahler W, Benson R E and Mochal W E 1962 *J. Am. Chem. Soc.* **84** 3374
Miller J S and Epstein 1976 *Progress in inorganic chemistry* (ed.) S J Lippard (New York: John Wiley) Vol. 20, p. 1
Miller J S 1982 *Extended linear chain compounds* (New York: Plenum)
Moriya T 1963 *Magnetism* (eds.) G T Rado and H Suhl (New York: Academic Press) Vol. I, Ch. III
Petersen J L, Schramm C S, Stojakovic D R, Hoffman B M and Marks T J 1977 *J. Am. Chem. Soc.* **99** 286
Plumlee K W, Hoffman B M, Ratajack M T and Kannewurf C R 1974 *Solid State Commun.* **15** 1651
Plumlee K W, Hoffman B M, Ibers J A and Soos Z G 1975 *J. Chem. Phys.* **63** 1926
Ramakrishna B L, Kuppusamy P, Manoharan P T and Hunziker M 1983 *J. de Physique Colloque* **44** 1409
Ramakrishna B L and Manoharan P T 1983a *Inorg. Chem.* **22** 2113
Ramakrishna B L and Manoharan P T 1983b *J. de Physique Colloque* **44** 1405
Ramakrishna B L and Manoharan P T 1984 (to be published)
Schmidt R D, Wing R M and Maki A H 1969 *J. Am. Chem. Soc.* **91** 4391
Schrauzer G N and Mayweg 1962 *J. Am. Chem. Soc.* **84** 3221
Shchegolev I F 1972 *Phys. Status Solidi* **A12** 4
Snaathorst D, Doesburg H M, Perenboom J A A J and Keizers C P 1981 *Inorg. Chem.* **20** 2526
Soos Z G and Bondeson S R 1980 *Phys. Rev.* **B22** 1793
Soos Z G, Huang T Z, Valentine J S and Hughes R C 1973 *Phys. Rev.* **B8** 993
Soos Z G and Klein D J 1975 *Molecular association* (ed.) R Forster (New York: Academic Press) Vol. 1
Soos Z G and Klein D J 1976 *Treatise on solid state chemistry* (ed.) N B Hannay (New York: Plenum Press) Vol. III, Ch. IX
Steiner M, Villain J and Windsor C G 1976 *Adv. Phys.* **25** 87
Thomas D D, Keller H J and McConnel H M 1963 *J. Chem. Phys.* **39** 2321
Tippie L C and Clark W G 1981 *Phys. Rev.* **B23** 5846
Tomkiewicz Y, Taranko A R and Terrance J B 1980 *Phys. Rev.* **B22** 3113
Underhill A E and Ahmad M M 1981 *Chem. Commun.* 67
Valade C, Bousseau M and Cassoux P 1983 *J. Chem. Soc. Chem. Commun.* 110
Van Vleck J H 1932 *The theory of magnetic and electric susceptibilities* (London: Oxford) Ch. XII
Venkatalakshmi N, Kuppusamy P and Manoharan P T 1984 (to be published)
Weiher J F, Melby L R and Benson R E 1964 *J. Am. Chem. Soc.* **86** 4329
Windsor C G 1967 *Proc. Phys. Soc. (London)* **91** 353
Wing R M and Schlupp R L 1970 *Inorg. Chem.* **9** 471
Yokota M and Koide S 1954 *J. Phys. Soc. Jpn* **9** 953

Proc. Indian Acad. Sci. (Chem. Sci.), Vol. 93, No. 6, August 1984, pp. 1003–1014.
© Printed in India.

Photoredox processes in coordination compounds

P NATARAJAN

Department of Inorganic Chemistry, University of Madras, Guindy Campus, Madras 600 025, India

Abstract. Transition metal complexes display a number of charge-transfer bands in the absorption spectra. Optical excitation of the metal complexes produces a variety of products depending upon the nature of the excited state. Cobalt(III) ammine complexes on excitation in the CTTM bands produce cobalt(II) and oxidised ligand. Ruthenium(II) complexes on excitation in the CTTL band leads to the oxidation of the metal centre. In certain reactions participation of the solvent in the primary photoredox reactions has also been reported. In recent years extensive investigations have been undertaken to utilize the photoredox systems of coordination compounds to convert solar energy to electricity or hydrogen.

Keywords. Excited state processes; redox reactions; coordination compounds; transition metal complexes.

1. Introduction

One of the most important reactions catalysed by light in natural systems namely photosynthesis involves electron transport *via* the excited chlorophyll molecules. In recent years, chemical reactions induced by light have been understood by directly investigating the nature of electronic excited states (Turro 1978). The primary reactions in photosynthetic systems are known to take place in picosecond time scale (Miller *et al* 1980). In this system and in other natural systems it is now well established that metal ions are involved in electron transfer reactions as mediators of charge transport (Elchhorn 1973). Biological electron transfer reactions are brought about by specific environment of the metal ion coordinated to the macromolecular ligands.

Electron transfer reactions of coordination compounds have been the subject of intense investigations by inorganic chemists both experimentally and theoretically for many years (Sutin 1968). Much of the earlier studies pioneered by Taube and coworkers (see Taube 1959) are concerned with the thermal electron transfer reactions and the theoretical framework was worked out by Marcus (1956), Hush (1967) and others (see Marcus and Sutin 1975). In recent years considerable amount of work has been done on excited state electron transfer processes of coordination compounds (Balzani *et al* 1979). Several attempts have been made to extend these studies to the photoelectrochemistry of liquid junction semiconductors. It looks promising that photoinduced redox reactions should serve to convert solar energy into fuels and electricity.

2. Excited states of coordination compounds

Reasonably good theoretical models (Figgis 1967) exist to understand electronic excited states of coordination compounds where the excitation is localised to metal centered orbitals and to derive the nature of the energy levels of the compounds. The electronic excited states of a typical octahedral coordination compound are schemati-

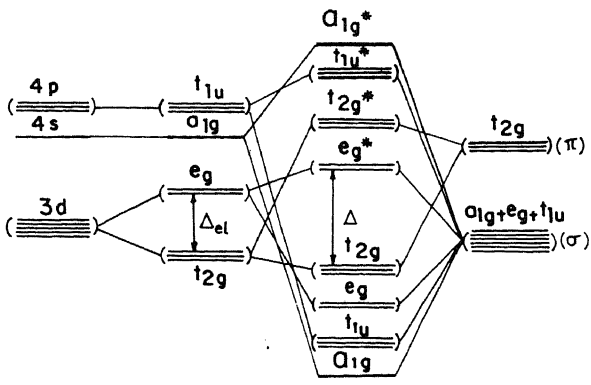

Figure 1. Electronic excited states for a coordination compound with O_h symmetry.

cally depicted in figure 1. The excited states in a transition metal compound are classified (Balzani and Carassiti 1970) into ligand-field bands and charge-transfer or electron transfer bands. In the latter category three types of transitions are assigned: metal-to-ligand charge-transfer transitions (MLCT); ligand-to-metal charge-transfer and charge-transfer-to-solvent transitions (SCT).

The charge transfer bands in the electronic spectra of coordination compounds have been identified and assigned based on experimental data. Jorgensen (1968) attempted to work out theoretical models to explain the electron transfer spectra of Werner type coordination compounds. As far as the ligand field transitions are concerned, the assignment could be done based on the ligand field model more successfully with first row transition metal compounds whereas in higher transition metals the theoretical model does not adequately interpret the absorption spectra. Emission spectral studies in organic systems have provided valuable information on the relaxation processes of excited states (Birks 1970). In fact many important excited state processes involving organic systems such as exciplex or excimer formation have been extensively investigated using emission spectroscopy. Comprehensive models proposed by Rehm and Weller (1969) on excited state electron transfer reactions are based on fluorescence studies. In transition metal complexes, room temperature emission has been observed only in a small number of compounds for these studies to be of much assistance in the understanding of electronic excited states (Fleisauer and Fleisauer 1970). In a few metal-complex systems where emission has been observed considerable information has been derived on the nature of excited states and their deactivation pathways.

In contrast to the organic molecules, coordination compounds which carry charge interact considerably strongly with the solvents or other environments. Interpretation of the excited processes becomes more complicated as the interaction between the solvent and the excited state is not understood well. In non-polar solvent most of the Werner type complexes are insoluble. In fact photochemical studies reveal information on the interaction of the excited states with solvent molecules.

The nature of excited states in organometallic systems (Geoffroy and Wrighton 1979) is not well understood as extensive pi-bonding occurs and most of the transitions seem to involve charge transfer processes. It is a long way before the excited state processes of organometallic complexes are understood based on the nature of the knowledge of the excited states.

3. Photochemical reactions of coordination compounds

In the ground state, coordination compounds give rise to either ligand labilisation reactions or redox reactions (Basolo and Pearson 1967). Ligand labilisation leads to aquation, anation or isomerisation reactions. Redox reactions lead to the oxidation or reduction of the metal centre with corresponding changes in the coordinating ligands. In general, photochemical reactions are different from the thermal reactions since the excited states have different electronic structure and as a consequence different geometry and other chemical properties from the ground state.

Absorption of light by ligand field bands produces excited states restricted to metal centred orbitals. From the emission spectral studies depending upon the nature of the transitions involved (for instance $t_{2g} \rightarrow t_{2g}$ or $t_{2g} \rightarrow e_g$ in the octahedral complexes) extent of distortion of the geometry of the excited states from the ground state could be determined. This is schematically illustrated in figure 2 for chromium(III) systems (Kirk 1981). Excitation of ligand field band produces thermal or antithermal products. Not much information is available on the rate of deactivation processes of ligand field excited states. For coordination compounds it appears that in the cases studied thus far the relaxation pathways and their characteristics differ markedly from those observed for organic systems (Porter 1975). Charge-transfer excitation of complexes leads to either ligand labilisation or redox reactions. (Endicott 1975).

4. Electron transfer reactions of metal complexes

Electron-transfer reactions mediated by metal ions have been recognised long ago. The importance of the electron transport in natural systems led Taube (1970) to investigate these reactions systematically. Depending upon the ligands coordinated, the redox potentials of metal complexes vary dramatically as shown in table 1. This property is found utilised in many biological reactions where the same metal ion brings about different types of redox reactions depending upon the nature of the coordinated ligands. Thus, copper or iron is found to undergo large number of enzymatic reactions involving number of metalloenzymes.

Using very simple systems electron-transfer reactions have been classified as inner-sphere or outer-sphere reactions (Reynolds and Lumry 1966):

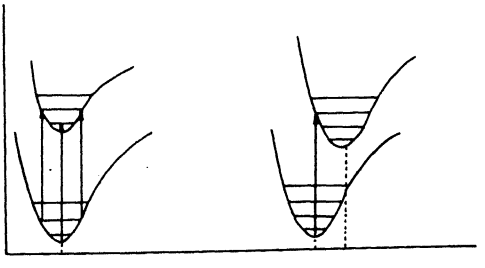

Figure 2. Geometry of the quartet and doublet excited states of chromium(III) complex.

Table 1. Redox potentials of metal complexes depending upon the coordinated ligand.

Couple	Redox potential *V*
$Fe(H_2O)_6^{3+} + e \longrightarrow Fe(H_2O)_6^{2+}$	0.77
$Cr(H_2O)_6^{3+} + e \longrightarrow Cr(H_2O)_6^{2+}$	−0.44
$Fe(bpy)_3^{3+} + e^- \longrightarrow Fe(bpy)_3^{2+}$	1.05
$Ru(bpy)_3^{3+} + e^- \longrightarrow Ru(bpy)_3^{2+}$	1.26

Inner sphere

$$Co(NH_3)_5Cl^{2+} + Cr(H_2O)_6^{2+} \rightarrow [Co(NH_3)_5ClCr(H_2O)_5]^{4+} \rightarrow Co(NH_3)_5^{2+} + Cr(H_2O)_5Cl^{2+},$$

Outer sphere

$$Co(NH_3)_5Cl^{2+} + Cr(bpy)_3^{2+} \rightarrow Co(NH_3)_5Cl^{+} + Cr(bpy)_3^{3+}.$$

For the same metal ions depending upon whether the reactions are innersphere or outersphere the reaction rate is changed. In the innersphere reactions formation of a bridge between the oxidant and reductant makes energetics of the reaction different from the outer sphere reactions where the electron transfer is not mediated through a bridging ligand. Marcus has proposed a theoretical model for explaining the electron transfer reactions and derived a simplified relationship $k_{12} = (k_{11}k_{22}K_2f)^{1/2}$ relating the rate constant for the cross-reaction k_{12}, the equilibrium constant K_{12} and the self exchange rate constant k_{11} for the oxidant and k_{22} for the reductant respectively; f is a factor close to unity. For some ground state reactions the electron transfer rate constants are given in table 2.

Bimolecular electron transfer reactions occur in three steps (Chow *et al* 1977)

$$A + B = (AB),$$

$$(AB) = (A^+B^-),$$

$$(AB) \rightarrow A^+ + B^-.$$

The first equilibrium involves the formation of the precursor complex where no strong interactions occur between the reactants. In the second step the coordination spheres of the reactants are altered to facilitate electron transfer. In the innersphere electron transfer reactions the bridge formation occurs in this step. In the outersphere electron transfer reactions the coordination environment including the solvent sphere around the reactants are altered appropriate to the formation of the activated complex.

5. Reactions from the charge-transfer-to-metal excited states

5.1 *Photochemistry of cobalt(III) complexes*

Cobalt(III) ion with nd^6 configuration forms low spin octahedral complexes which are kinetically inert. Cobalt(III) ammines have well separated charge-transfer and ligand

Table 2. Rate constants for electron transfer reactions in the ground state.

System	Rate constants (M^{-1} sec^{-1})
$Cr^{2+} + Cr(NH_3)_5Br^{2+}$	$5{\cdot}1 \times 10^{-2}$
$Fe^{2+} + Fe(dipy)_3^{3+}$	2.7×10^{4}
$Fe(CN)_6^{4-} + IrCl_6^{2-}$	1.9×10^{6}
$Cr^{2+} + Co(NH_3)_6^{3+}$	$8{\cdot}9 \times 10^{-5}$
$V^{2+} + Co(NH_3)_5Br^{2+}$	25
$Ru(NH_6)_6^{2+} + Co(NH_3)_5Br^{2+}$	1.6×10^{3}
$Eu^{2+} + Co(NH_3)_5OH_2^{3+}$	0·15

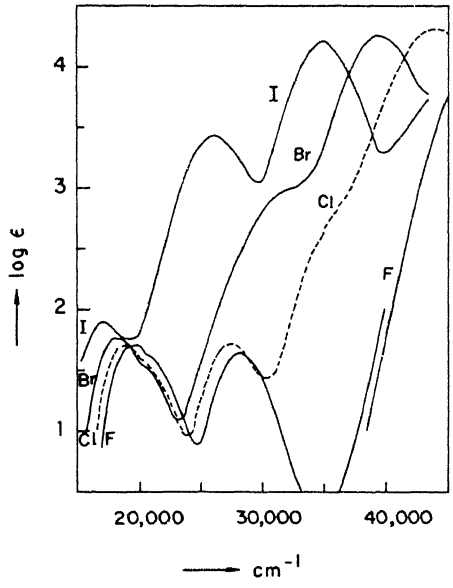

Figure 3. Charge-transfer transitions for $[Co(NH_3)_5X]^{2+}$, X = (Cl, Br, I) complexes.

field bands, these complexes do not show any emission. The photochemistry of the ammines and acidoammines of cobalt(III) ion has been extensively investigated (Ferraudi *et al* 1975). Depending upon the ease of oxidation of the ligand, CTTM transitions shift as shown in figure 3 for a series of acidoammine complexes. An empirical relationship is derived to relate the absorption band maximum and the electronegativity of the ligand (Jorgensen 1962). Irradiation in the CTTM band of the complex in aqueous solution in general results in the charge transfer to the metal centre which leads to the decomposition of the complex to give redox products. Quantum yields for cobalt(II) for the acidoammine complexes on irradiation at different wavelengths are given in table 3.

The redox reaction occurs exclusively on irradiation in the charge-transfer band; irradiations in the ligand field bands do not produce cobalt(II). The proposed

Table 3. Quantum yield for the reduction of cobalt III amine complexes.

Complex	(nm) of excitation	Quantum yield
$Co(NH_3)_6^{3+}$	254	0·16
$Co(en)_3^{3+}$	254	0·13
$Co(dien)_2^{3+}$	254	0·03
$Co(NH_3)_5Cl^{2+}$	254	0·25
Cis $Co(en)_2Cl_2^+$	254	0.06
$Co(NH_3)_5N_3^+$	254	0·20
$Co(EDTA)^-$	254	0.06

mechanism for the photoreduction of cobalt(III) ammines is given by the following scheme (Simic and Lilie 1974):

$$[Co^{III}(NH_3)_5x] \xrightarrow{2+h\nu} {}^*(Co^{III}(NH_3)_5x)^{2+} \text{ (CTTM)}$$

$$\text{CTTM} \longrightarrow (Co^{II}(NH_3)_5 \cdot x),$$

$$(Co^{II}(NH_3)_5 \cdot x) \longrightarrow Co^{II}(NH_3)_5^{2+} + \cdot x,$$

$$Co^{II}(NH_3)_5^{2+} \xrightarrow{H^+} Co(NH_3)_2^{2+} + 3NH_4^+,\ k > 10^6\ \text{sec}^{-1},$$

$$Co(NH_3)_2^{2+} \rightarrow Co(II) + 2NH_4^+.$$

It has also been observed that with polydentate ligands the redox quantum yield decreases compared to the monodentate complexes (Natarajan and Endicott 1973).

One of the important reactions occurring from the charge transfer excited states of cobalt(III) complex is the linkage isomerization reaction. For instance $(Co(NH_3)_5NO_2)^{2+}$ ion on irradiation in the CTTM band produces cobalt(II) and the linkage isomer, (Balzani *et al* 1968).

$$(Co(NH_3)_5\,NO_2)^{2+} \longrightarrow Co(II) + (Co(NH_3)_5ONO)^{2+}.$$

Considerable interest was shown to understand the process by which the nitrite isomer was formed. Scandola *et al* (1973) carried out the irradiation of the complex in water-glycerol mixtures and suggested that the increased formation of the linkage isomer with the concomitant decrease in cobalt(II) yield as the viscosity of the irradiated solution is due to the geminate radical recombination.

$$((NH_3)_5Co^{II} \cdot NO_2),$$
$$\downarrow$$
$$(NH_3)_5Co^{III} - NO_2).$$

However investigations on the photochemical behaviour of $Co(NH_3)_5N_3^{2+}$ ion and *cis* $Co(en)_2(NO_2)_2^+$ ion in highly viscous solutions containing synthetic high polymers or other alcohols did not show evidence for radical recombinations. It was suggested (Natarajan 1977; Arunachalam and Natarajan 1983) that the excited state relaxation process itself is affected by the nature of the medium which affects the quantum yields for products. More recently Natarajan and Radhakrishnan (1982) have studied the photoreaction of the complex *cis*-$Co(en)_2(NO_2)_2^+$ in neat acetonitrile and compared

the behaviour with that in aqueous solution. It is indicated that more the hydrophylic environment of the excited state of cobalt(III) complex, cobaltous ion formation is facilitated.

Several attempts to photosensitize cobalt(III) complexes have been made (Gafney and Adamson 1972; Natarajan and Endicott 1973; Navon and Sutin 1974; Demas 1973; Berkoff *et al* 1980). Photosensitization of cobalt(III) complexes gives rise to cobalt(II) ions. However, the mechanism of photosensitization is still ambiguous. Although many early results have indicated that the photosensitization occurs by an energy transfer mechanism later it turned out that reexamination of the systems has shown that the quenching is due to a chemical mechanism in some cases and in other cases both physical and chemical mechanisms of sensitization take place (Kalyanasundaram 1982; Balzani *et al* 1978).

It is also of interest to investigate the extent of communication between different types of excited states. On irradiation in the ligand field bands the quantum yield for redox decomposition is negligibly small (10^{-3}) whereas excitation in the charge transfer region does not lead to aquation or photoanation reactions. It thus appears that higher energy charge transfer excited states do not relax passing through the low lying *d–d* excited states. The surfaces of the *d–d* and CTTM states do not seem to cross each other (Ferraudi *et al* 1976).

5.2 *Photoredox reactivity of CTTM states of the complexes of Cu(II) and other metal ions*

Copper(II) forms kinetically labile complexes which on irradiation in aqueous solution produces copper(I) and ligand radical. The secondary reactions and the lability of copper(II) complexes make the systems more difficult to understand. Copper(II) acetate on irradiation in aqueous solution produces copper(I) and methyl radical (Ferraudi 1978). Flash photolysis studies indicate the formation of methyl radicals. Recently the photochemistry of copper(II) aminoacid complexes has been investigated using flash photolysis technique (Namasivayam and Natarajan 1983; Natarajan and Ferraudi 1981). The primary photochemical reaction involves the formation of copper(I) coordinated to the free radical. The copper I radical species are shown to initiate vinyl polymerisation reactions and steps involved in the photochemistry of copper(II)-aminoacid are shown below.

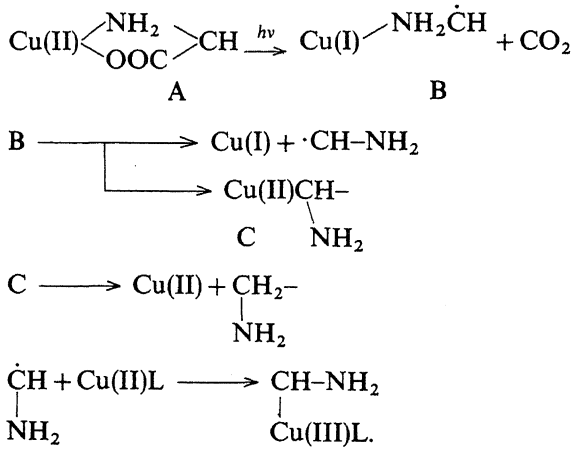

Studies of polymerisation kinetics have led to the calculation of primary quantum yields for the formation of the copper I coordinated free radical which is difficult to measure directly since secondary reactions enhance the extent of formation of copper(I). Copper(II) complexes with polypyridyl ligands undergo photoreactions to produce copper(I) with low quantum yields (Ferraudi and Muralidharan 1981).

6. Photochemistry from CTTL states

In the case of metal complexes in which the metal is present in low oxidation states and the ligand electron-deficient or aromatic systems intense charge-transfer to ligand transitions have been observed in the visible or near UV region. Excitation of CTTL bands of metal complexes produces CTTL excite states and the photochemistry of these systems has been of much interest in recent years.

Ruthenium(II) ammines form complexes with pyridine and substituted pyridines. $Ru(NH_3)_5py^{2+}$ (py = pyridine) has absorption maximum in the visible region at 407 nm with molar absorptivity of 7500. The transition is assigned as MLCT and the peak shifts depending upon the substituents on pyridine (Ford 1978). Corresponding ruthenium(III) complexes do not show this band supporting the MLCT assignment for the ruthenium(II) systems.

On irradiation, the complex ion does not undergo redox reaction. On the other hand aquation of pyridine ligand takes place. Flash photolysis of the complex ion produces (Natarajan and Endicott 1972) a transient and the transient has been proposed to have the structure.

$$(NH_3)_5\,Ru\,N\langle\ominus\rangle$$

The intermediate rearranges to assume a π-bonded pyridine with the metal which eventually is replaced by water.

In the polypyridyl complexes of ruthenium(II), osmium(II) and iron(II) charge-transfer-to-ligand transitions have been observed in the visible region. In recent years the photochemistry of these complexes has been investigated in great detail (Sutin 1979). *Tris*(2,2′-dipyridine) ruthenium(II) complex, $Ru(bpy)_3^{2+}$ is a well-known compound which on excitation in the CTTL band produces an excited state with a lifetime of 0·5 μsec and whose thermodynamic properties are quite different from those of the ground state. The excited state, $Ru(bpy)_3^{2+}$ serves as a good reducing agent.

7. Photochemistry from the charge-transfer to solvent excited states

Excited states of molecules which involve the surrounding medium have been studied in detail. In particular interactions between the solute and solvents are more in polar solvents and depending upon the polarity of the solvent changes in absorption spectra are observed. One of the well-known systems in which photochemistry from the CTTS excited state occurs is potassium hexacyanoferrite(II) (Matheson 1963). The photochemical reaction is given by

$$Fe(CN)_6^{4-} \xrightarrow[H_2O]{h\nu} Fe(CN)_6^{3-} + e^-(H_2O)$$

and hydrated electron has been detected by scavenging experiments and in absorption spectra.

8. Excited states as electron transfer reagents

While the redox reactions have been studied extensively the excited state electron transfer reactions have been discovered only in recent years. Pioneering work on excited state electron transfer reactions has been carried out by Weller (1968) and his coworkers in the case of organic molecules. Electron transfer reactions of excited states of transition metal complexes are of particular interest since they are promising for solar energy conversion to fuels or electricity and also for the production of metal ions in unusual oxidation states. In general, excited state electron transfer reactions with a quencher may be given by the scheme.

$$\begin{array}{ccccc} {}^*A + B & \underset{k_{21}}{\overset{k_{12}}{\rightleftharpoons}} & {}^*A \cdot B & \underset{k_{32}}{\overset{k_{23}}{\rightleftharpoons}} & [A^+ B^-] \\ \Big\uparrow h^\nu \quad \Big\downarrow r_0 & & & & \Big\downarrow \quad \Big\downarrow \\ A + B & \longleftarrow & & A \cdot B & A^+ + B^-. \end{array}$$

The rate constant for the excited state electron transfer reaction is given by

$$kq^{\text{obs}} = \frac{k_{12}}{1 + \dfrac{k_{12}}{\Delta v \cdot k_{30}} \exp\left(G^*_{23}/RT\right) + \exp\left(\Delta G_{23}/RT\right)}.$$

One of the most important bimolecular redox reactions involving an excited state of a coordination compound is (Bock 1974)

$$^*\text{Ru(bpy)}_3^{2+} + \text{Fe(III)} \rightarrow \text{Fe(II)} + \text{Ru(bpy)}_3^{3+}.$$

The rate constant for the reaction is determined to be 10^9 M^{-1} sec^{-1} in aqueous acidic solution at 25°C. The reaction products are of high energy and they recombine to produce the ground states of the starting materials. The energetics of the Ru(bpy)_3^{2+} – Fe(II) system in different oxidation states is given in figure 4. When

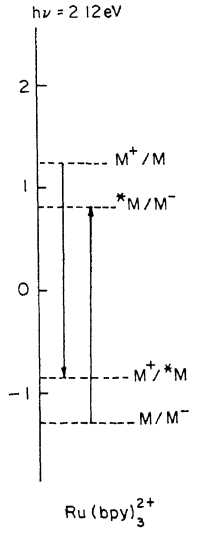

Figure 4. Redox potentials (Volts) of the ground and excited states of Ru(bpy)_3^{2+} ion.

methylviolegen (Whitten 1980) is used as a quencher of $*Ru(bpy)_3^{2+}$ the following reactions take place

$$*Ru(bpy)_3^{2+} + PQ^{2+} \xrightarrow{kq} Ru(bpy)_3^{3+} + PQ^{+},$$

$$PQ^{+} + Ru(bpy)_3^{3+} \rightarrow PQ^{2+} + Ru(bpy)_3^{2+}.$$

A plot of the electron transfer quenching constant versus reduction potential of the quenchers clearly shows the point at which electron transfer quenching becomes endothermic. From the ground state potential in the same medium, ($E_{1/2}$ for $Ru(bpy)_3^{3+}/Ru(bpy)_3^{2+} = 1{\cdot}29$ V) it can be seen that photoexcitation increases the oxidising power by 2·10 V, a value very close to the spectroscopic excited state energy (2·18 V) of $*Ru(bpy)_3^{2+}$.

Europium(II) aquo ions (Creutz and Sutin 1976) can reduce the excited state of $Ru(bpy)_3^{2+}$ to $Ru(bpy)_3^{3+}$ to produce europium(III) ions.

9. Application of photoredox processes in solar energy conversion

Conversion of sunlight to fuel or electricity has received wide attention in recent years (Anon 1981). Much of the activity is related to the photoexcitation of charge-transfer electronic excited states of coordination compounds. Homogeneous photoreactions containing transition metal compounds produce energy-rich compounds. However these products readily recombine in homogeneous solution to give back the starting materials. Research interest in the conversion of solar energy to fuel or electricity centres around the photoredox reactions of the type

$$A + D \rightleftharpoons A^{-} + D^{+},$$

in which $A + D$ are solutes of which one is exited by light. Major problems to overcome before these systems are put to practical use are concerned with the retardation of the back thermal reaction and the production of fuel or electricity using A^{-} and D^{+}. Attempts have been made in recent years (Kiwi *et al* 1982) through judicious choice of molecular systems in particular the use of functional electron relays to effect separation of A^{-} and D^{+}.

A system which is known for a considerable amount of time is the iron-thionine photogalvanic cell (Wildes *et al* 1977). In this cell moderate photopotential is known to be generated in a homogeneous solution containing iron(II) and thionine on absorption of visible photons. However the efficiency of the cell is very low due to competing energy wasting back reactions shown below.

$$Fe(II) + Th \underset{Fe(III)}{\overset{h\nu}{\rightleftharpoons}} S \rightarrow L.$$

In addition, the solubility of the dye was low in water to use a thin cell which to some extent overcomes the thermal recombination reactions. More soluble thiazine dye derivatives have been shown to increase the efficiency of this photogalvanic cell (Albery 1982).

A different approach was made to condense the thionine dye with a macromolecule and use the macromolecular dye in the photogalvanic cell (Tamilarasan and Natarajan

1981). In homogeneous cell the efficiency did not improve. On the other hand when the polymeric dye was coated to an inert electrode a new type of electrode reaction occurred with appreciable current flow even in fairly thick (10 μ) polymer-dye coated electrodes. The following electrode reactions are proposed for the polymer-dye coated electrode (Tamilarasan and Natarajan 1984).

$$P-{}^*TH^+ + Fe(II) \rightarrow [P-TH-Fe]^{3+},$$

$$[P-TH-Fe]^{3+} + e^- \rightarrow [P-TH^{+\cdot}] + Fe(II),$$

$$P-TH + \cdot + Fe(III) \rightarrow P-TH^+ + Fe(II).$$

Photogalvanic cells using $Ru(bpy)_3^{2+}$-iron(III) have also been reported (Lin and Sutin 1976). In homogeneous solution thermal back reactions effectively reduce the efficiency of the cells to very low levels. The knowledge that the excited state of $Ru(bpy)_3^{2+}$ ion can absorb visible light and almost quantitively transfer its excitation energy in a redox reaction has induced enormous activity to use this ion for the development of electrochemical cells to produce electricity or hydrogen splitting water. In recent years Kiwi and Gratzel (1979) have used colloidal catalysts to bring about hydrogen and oxygen formation from water.

$$A^- + H_2O \xrightarrow{Pt} \tfrac{1}{2}H_2 + OH^- + A$$

$$2D^+ + H_2O \xrightarrow{RuO_2} 2H^+ + \tfrac{1}{2}O_2 + D$$

A^- and D^+ were produced in a photochemical reaction.

References

Albery W J 1982 *Acc. Chem. Res.* **15** 142
Ahuja 1981 *Photoelectrochemistry, Disc. Faraday Society*
Arunachalam S, Natarajan P 1983 *J. Chem. Soc., Chem. Comm.* 472
Balzani V, Ballardini R, Sabbatini N and Moggi L 1968 *L. Inorg.* 7 1398
Balzani V, Bolleta M, Gandolfi M T and Maestri M 1978 *Topics Curr. Chem.* **19** 75
Balzani V, Bolleta F, Scandola F and Ballardini R 1979 *Pure Appl. Chem.* **51** 299
Balzani V and Carassiti V 1970 *Photochemistry of coordination compounds* (New York: Academic Press)
Basolo F and Pearson R G 1967 *Mechanisms of inorganic reactions* (New York: Wiley)
Berkoff R, Krist K and Gafney H D 1980 *Inorg. Chem.* **19** 1
Birks J B 1970 *Photophysics of aromatic molecules* (New York: Wiley)
Bock C R, Meyer T J and Whitten D G 1974 *J. Am. Chem. Soc.* **96** 4710
Chow M, Creutz C and Sutin N 1977 *J. Am. Chem. Soc.* **99** 5615
Creutz C and Sutin N 1976 *J. Am. Chem. Soc.* **98** 6384
Demas J N and Adamson A W 1973 *J. Am. Chem. Soc.* **95** 5159
Eichhorn G L 1973 *Bioinorganic chemistry* (New York: Elsevier)
Endicott J F 1975 in *Concepts of inorganic photochemistry* (eds) A W Adamson, P D Fleisauer (New York: Wiley)
Ferraudi G 1978 *Inorg. Chem.* **17** 2506
Ferraudi G and Endicott J F 1976 *J. Phys. Chem.* **80** 949
Ferraudi G J, Endicott J F and Barber J R 1975 *J. Am. Chem. Soc.* **97** 6406
Ferraudi G and Muralidharan S 1981 *Coord. Chem. Rev.* **36** 45
Figgis B 1967 *Introduction to ligand fields* (New York: Wiley)
Fleisauer P D and Fleisauer P 1970 *Chem. Rev.* **70** 199
Ford P C 1978 *Adv. Chem.* **168** 73

Gafney H D and Adamson A W 1972 *J. Am. Chem. Soc.* **94** 8238
Geoffroy and Wrighton M 1979 *Organometallic photochemistry* (New York: Academic Press)
Hush N S 1967 *Prog. Inorg. Chem.* **8** 391
Jorgensen C K 1962 *Orbitals in atoms and molecules* (New York: Academic Press)
Jorgensen C K 1968 *Inorg. Chim. Acta Rev.* 65
Kalyanasundarm K 1982 *Coord. Chem. Rev.* **46** 159
Krik A D 1981 *Coord. Chem. Rev.* **39** 181
Kiwi J and Gratzel M 1979 *Nature (London)* **281** 657
Kiwi J, Kalyanasundaram K and Gratzel M 1982 *Structure Bonding* **49** 37
Lin C T and Sutin N 1976 *J. Phys. Chem.* **80** 97
Marcus R A 1956 *J. Chem. Phys.* **24** 966
Marcus R A and Sutin N 1975 *Inorg. Chem.* **14** 213
Matheson M S, Mulac W A and Rabani J 1963 *J. Phys. Chem.* **67** 2613
Miller D P, Robins R J and Zewail A H 1980 *Proc. Natl. Acad. Sci. USA* 77 5593
Namasivayam C and Natarajan P 1983 *J. Polym. Sci.* **A1** 21
Natarajan P 1977 *J. Chem. Soc. Dalton* 1400
Natarajan P and Endicott J F 1972 *J. Am. Chem. Soc.* **94** 5909
Natarajan P and Endicott J F 1973 *J. Phys. Chem.* 77 1823, 2049
Natarajan P and Ferraudi G 1981 *Inorg. Chem.* **20** 3708
Natarajan P and Radhakrishnan A 1982 *J. Chem. Soc., Dalton* 2403
Navon G and Sutin N 1974 *Inorg. Chem.* **13** 2159
Porter G B 1975 in *Concepts of inorganic photochemistry* (eds) A W Adamson, P D Fleisauer (New York: Wiley)
Rehm D and Weller A 1969 *Ber. Bunsenges. Phys. Chem.* **73** 834
Reynolds W L and Lumry R W 1966 *Mechanisms of electron transfer* (New York: Ronald Press)
Scandola F, Bartocci C and Scandola M A 1973 *J. Am. Chem. Soc.* **95** 7898
Simic M and Lilie J 1974 *J. Am. Chem. Soc.* **96** 291
Sutin N 1968 *Acc. Chem. Res.* **1** 225
Sutin N 1979 *J. Photochem.* **10** 19
Tamilarasan R and Natarajan P 1981 *Nature (London)* **292** 224
Tamilarasan R and Natarajan P 1984 *Photochem. Photobiol.* (submitted)
Taube H 1959 *Adv. Inorg. Chem. Radiochem.* **1** 1
Taube H 1970 *Electron transfer reactions of complex ions in solution* (New York: Academic Press)
Turro N J 1978 *Modern molecular photochemistry* (California: Benjamin)
Weller A 1968 *Pure Appl. Chem.* **16** 115
Whitten D G 1980 *Acc. Chem. Res.* **13** 83
Wildes P D, Hobart D R, Lichtin N N, Hall D E and Eckert J A 1977 *Solar Energy* **19** 657

Proc. Indian Acad. Sci. (Chem. Sci.), Vol. 93, No. 6, August 1984, pp. 1015–1030.
© Printed in India.

Cycloartenol to *Buxus* alkaloids

SUKH DEV
Malti-Chem Research Centre, Nandesari, Vadodara 391 340, India

Abstract. Cycloartenol, a pentacyclic triterpene alcohol, has emerged as an obligatory intermediate in the biosynthesis of sterols in higher plants and algae. Cycloartenol has also been implicated in the biosynthesis of steroidal alkaloids. The *Buxus* alkaloids, which have a pregnane-type framework, are considered to arise from cycloartenol by catabolic processes with nitrogen incorporation at an appropriate stage, although no biosynthetic studies appear to have been carried out. Thus, cycloartenol is an important substrate in nature for elaborating a rather large group of secondary metabolites. In an effort to mimic some of these processes in the laboratory, we have carried out transformations of cycloartenol into *Buxus* alkaloids. New routes for side-chain degradation of cycloartenol and cyclolaudenol have been developed. A novel method for functionalization at C-16 has been worked out and a new strategy for regioselective oxygenation of 4-methyl has been exploited. Synthesis of buxandonine, cycloprotobuxine-F, cycloprotobuxine-A, cyclobuxophyllinine-M and 31-norcyclolaudenone have been achieved.

Keywords. Cycloartenol; *Buxus* alkaloids; cyclolaudenol; side-chain degradation; reductive alkylation; Buxandonine; cycloprotobuxine-F; cycloprotobuxine-A; cyclobuxophyllinine-M; Schenk oxidation; pyridinium chromate-on-silica gel; cycloeucalanone; 31-Norcyclolaudenone.

Cycloartenol (1), a pentacyclic triterpene alcohol, has emerged as an obligatory intermediate in the biosynthesis of sterols in higher plants and algae (see *e.g.* Goodwin 1979). Cycloartenol has also been implicated in the biosynthesis of steroidal alkaloids (see *e.g.* Heftmann 1983; Roddick 1980). The *Buxus* alkaloids, which have a pregnane type framework, are considered to arise from cycloartenol by catabolic processes with nitrogen incorporation at an appropriate stage, although no biosynthetic studies appear to have been carried out. Thus, cycloartenol is an important substrate for nature for elaborating a rather large group of (so-called) secondary metabolites. Chemists often seek to mimic nature's processes in the laboratory (see *e.g.* Scott 1976) and the work to be reviewed in this brief article summarises our efforts aimed at transformations of cycloartenol into *Buxus* alkaloids. Another reason for undertaking this research was the rather easy accessibility to cycloartenol and the related cyclolaudenol (2) from opium marc in which they occur in over 1% (separately) concentration (Narula and Sukh Dev 1971).

Before proceeding with the main theme it appears appropriate to preface this with a brief introduction to *Buxus* alkaloids. These compounds have a rather narrow distribution in nature and are restricted to the family Buxaceae consisting of six genera and some 80 species. Of these, the genus *Buxus* which is composed of over 10 species is responsible for almost all the known alkaloids of this type. So far, more than 70 alkaloids have been isolated and characterised. Of these, not less than 35 have been isolated from only one species—*Buxus sempervirens*. These plants occur in India only in the Himalayan region, that is from Kashmir, North Western Himalayas to North East. No work on these plants has been carried out in India and the entire work on *Buxus*

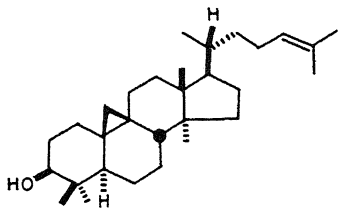

1

Cycloartenol

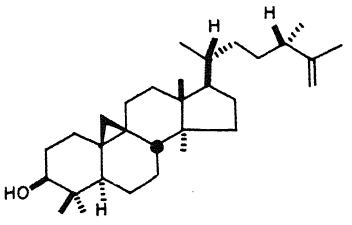

2

Cycloläudenol

alkaloids—isolation and structure determination—has been done abroad. These alkaloids are important because of their broad spectrum of pharmacological activity—against rheumatism, dermatitis, malaria, tuberculosis etc. They also have an important place in biochemical research (Tomko and Voticky 1973).

Chemical investigations were started as early as 1830. However, pure bases could be isolated only a century or so later and thus, all earlier work had been done on mixtures! There was intense structural activity between 1958 and 1962, in no less than nine laboratories. The first structure of the *Buxus* alkaloids—that of cyclobuxine-D—was elucidated in 1962 by Brown & Kupchan (1962). Two years later (Brown and Kupchan 1964), cyclobuxine-D was correlated with cycloeucalenol, a derivative of cycloartenol. As a result of these extensive studies, which were carried out in a number of laboratories, several structural varieties have been characterised. There are three main types (3, 4, 5) and all these are hexanor compounds based on cycloartenol: in structure 4, one more methyl is lost, while in 5, the six-membered ring has been expanded into a seven-membered ring by way of cleavage of the cyclopropane ring. Invariably, there is an amine function at C-3 or C-20; in a majority of cases both C-3 and C-20 carry this functionality. The C-20 functionality is always *S*-configurated, while at C-3, the nitrogen function is invariably β. Whenever, there is no nitrogen function at C-3 or C-20, there is an oxygen function instead, a carbonyl or an hydroxyl. Other usual positions for carbonyl/hydroxyl functions are: C-16, C-11 and C-4 methyls, especially the 4α-methyl. Olefinic linkage is usually found between C-2/C-3, C-6/C-7, C-16/C-17 or C-17/C-20.

With this background, we can now proceed to describe our work. When we started this work in 1970 there was only one report, that from Prof. Arigoni's laboratory (Calame and Arigoni 1964), on the conversion of cycloartenol into the *Buxus* alkaloid,

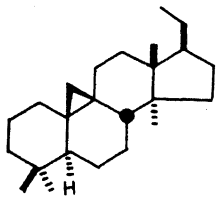

3

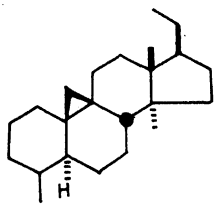

4

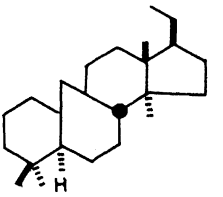

5

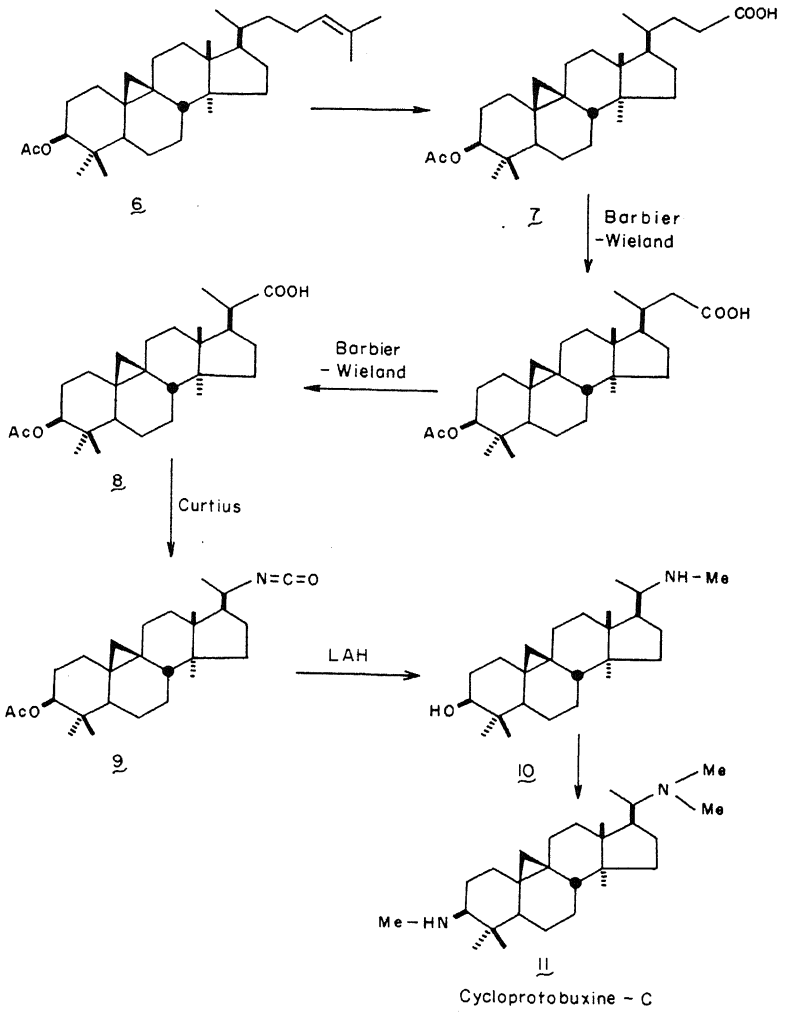

Figure 1. ETH route to cycloprotobuxine-C.

cycloprotobuxine-C. The route developed by these authors is shown in figure 1. Cycloartenyl acetate (6) was degraded by the usual method of ozonolysis to the corresponding acid (7), which by a double Barbier-Wieland degradation was converted to the pentanor acid 8. Curtius degradation led to the isocyanate 9, which on reduction gave the methylamine 10; the latter could be readily elaborated into cycloprotobuxine-C (11). We set before us the following scope:

(i) Side-chain degradation of cycloartenol to the hexanor derivative 12.
(ii) Development of a suitable method for C-16 oxygenation.
(iii) Regioselective oxygenation of 4α-methyl and elaborating it further to a nor-derivative.

Cycloprotobuxine-F (13), cyclobuxophyllinine-M (14) and cyclobuxosuffrine (15)

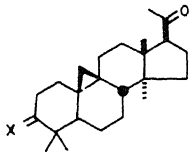

X = O; H, OH

12

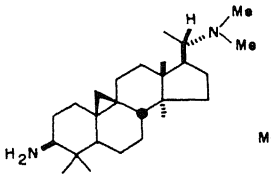

13 (17)

Cycloprotobuxine – F

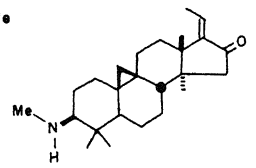

14 (38)

Cyclobuxophyllinine – M

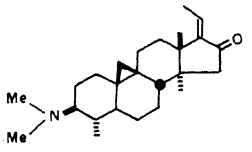

15

Cyclobuxosuffrine

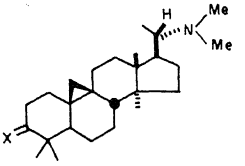

Buxandonine (16) : X = O

Cycloprotobuxine – F (17/13) : X = H(α), NH_2

Cycloprotobuxine – A (18) : X = H(α), NMe_2

were selected as the representative target molecules, requiring one or more of the above transformations.

Buxandonine, cycloprotobuxine-F and cycloprotobuxine-A

The first phase of the work was directed towards synthesis of buxandonine (16) and the related alkaloids cycloprotobuxine-F (17) and cycloprotobuxine-A (18). Towards this end we developed efficient procedures for side-chain degradation, and these enabled us to convert cycloartenol (1) and the related cyclolaudenol (2) into the key hexanor derivative 12. Before we discuss these transformations, it will not be out of place to recount the state-of-art pertaining to side-chain degradation of triterpenes/steroids, in general, at the time we started our investigations. The classical Barbier-Wieland degradation (see *e.g.* Fieser and Fieser 1959) proceeds through Grignard reaction with phenyl magnesium bromide on an ester, followed by dehydration and oxidative cleavage of the resulting diphenylethylene giving the nor derivative (acid or ketone). The only other method available then was an important modification of this sequence first published in 1945, and known as the Meystre-Miescher modification (Meystre *et al* 1944, 1946). In this, an additional double bond is created through NBS bromination followed by dehydrobromination. Oxidative cleavage now results in reducing the chain by three carbons. This modification was investigated by Calame (1965) for side-chain degradation of cycloartenol, but the yields were extremely poor because the NBS reaction resulted in considerable opening of the cyclopropane ring. As matter of fact, only a year before this work we had demonstrated (Gaitonde *et al* 1964) that cyclopropane rings indeed open up on exposure to NBS.

Thus, our first objective became the development of new strategy for the side-chain degradation. Since the thermodynamic stability of an olefin increases with increasing alkyl substitution it should be possible to migrate an ethylenic linkage in a chain upto a point where the terminus is more substituted. Various reagents are available (see *e.g.*

Hubert and Reimlinger 1969, 1970) for such isomerizations: acids, bases or metals like palladium, nickel, rhodium etc. It was obvious that for the purpose on hand the most useful route would be base isomerization, as skeletal rearrangements and cyclopropane ring cleavage must be avoided. A variety of bases have been used including potassium *tert*-butoxide in *tert*-butanol, potassium *tert*-butoxide in dimethyl sulphoxide, high surface sodium, lithioethylene diamine, etc. Thus, for the immediate purpose, it was planned to suitably modify cycloartenol molecule to get a nor-olefin with a terminal olefinic bond suitable for isomerization towards the ring. The sequence finally worked out (Narula and Sukh Dev 1971) is shown in figure 2. The first step was to cleave the side-chain at the olefinic linkage to get the carboxylic acid (20). Surprisingly, ozonolysis of cycloartenyl acetate (19) has been reported (Bentley *et al* 1953) to give none of this acid. To overcome this difficulty we finally succeeded in devising a modified procedure

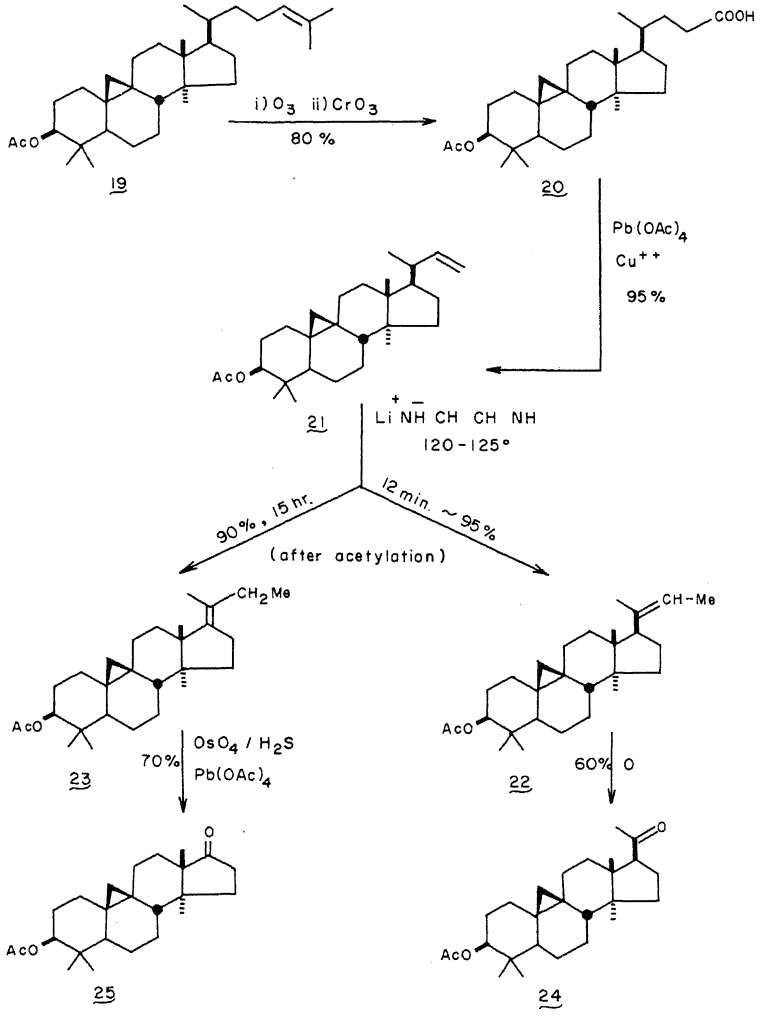

Figure 2. Side-chain degradation of cycloartenol.

(Narula and Sukh Dev 1969) entailing chromic acid oxidation of the ozonide, which gave the trisnor acid in excellent, consistent yields. This sequence has been applied to several other olefins and the results have always been superior to those reported earlier. Oxidative decarboxylation with lead tetraacetate in the presence of Cu^{++}, according to Kochi and coworkers (Bacha and Kochi 1968; Kochi *et al* 1969), furnished an excellent yield of the tetranorolefin (21). This could now be isomerized by a suitable base. Our choice fell on lithioethylenediamine (Reggel *et al* 1958; Tyagi *et al* 1962) which is a rather strong base. Depending on the time of exposure to the reagent, we could get the trisubstituted (22) or the tetrasubstituted olefin (23). Ozonolysis of 22 furnished the required hexanorketone (24). The tetrasubstituted olefin was also oxidatively cleaved, as shown in figure 2 to the octanor-cyclopentanone (25) which was needed for certain other conversions in the steroid area (Narula and Sukh Dev 1971). Later, based on this concept of base-catalysed isomerization of olefins, a very simple route to the target molecules 24 and 25 could be developed (Narula and Sukh Dev 1971; Singh *et al* 1977): cycloartenol itself was subjected to base-isomerization, the product acetylated and the ozonide oxidised by Jones' reagent to get about 25% acids (not investigated further), and a neutral fraction from which 24 and 25 could be isolated in yields of 30% and 15% respectively, based on cycloartenol. Evidently, in terms of the time involved and the cost, this method came very handy and was used for the preparation of the required intermediate (24).

Cyclolaudenol (2) could also be degraded (Narula and Sukh Dev 1971) to the same required hexanorketone 24 by a slight modification of this sequence: the main idea was to get to the trisnoracid (20) from cyclolaudenol, and then proceed to the target molecule, as already discussed. Cyclolaudenol was isomerised to the thermodynamically more stable double bond isomer, which after acetylation was subjected, sequentially, to ozonolysis and hypobromite oxidation and acetylation to furnish the same trisnoracid (20). Another alternative method (Singh *et al* 1977) for the degradation of cyclolaudenol for the same purpose was also worked out and is summarised in figure 3. Ozonolysis of cyclolaudenyl acetate, followed by $NaBH_4$ reduction yielded the nor-alcohol (26), which on exposure to hypoiodite, fragmented to the iodide (27; X = I). The corresponding chloride (27; X = Cl) was readily reached by the sequence shown (figure 3): isomerization followed by ozonolysis to get ketone 28, reduction to the alcohol 29, followed by reaction with $POCl_3$ to give the chloride 27. Both of these halides, iodide or the chloride, could be converted by treatment with lithio ethylenediamine into olefin (30), suitable for degradation by ozone to the required hexanor ketone (24). It may be noted that lithio ethylene-diamine caused dehydrohalogenation and isomerization of the resulting olefin in one experimental step.

Thus, we could develop several methods for the preparation of the key intermediate 24, required for further elaboration into *Buxus* alkaloids. At this stage, it may be pointed out that while we were engaged on these investigations two publications describing preparation of the hexanorketone (24) appeared. Adam *et al* (1970) described a 15-step degradation of cycloartenol to 24, a series of Hofmann acidamide degradations being employed. Another group (Nakano *et al* 1970) reported its elaboration from lanosterol (31), through the intermediate 32, already described by Ruzicka many years earlier (Voser *et al* 1952).

It is gratifying to note that the side-chain degradation sequence, as developed by us, has been exploited by other workers, later, for side-chain degradation of lanosterol (Kreiser and Ulrich 1976).

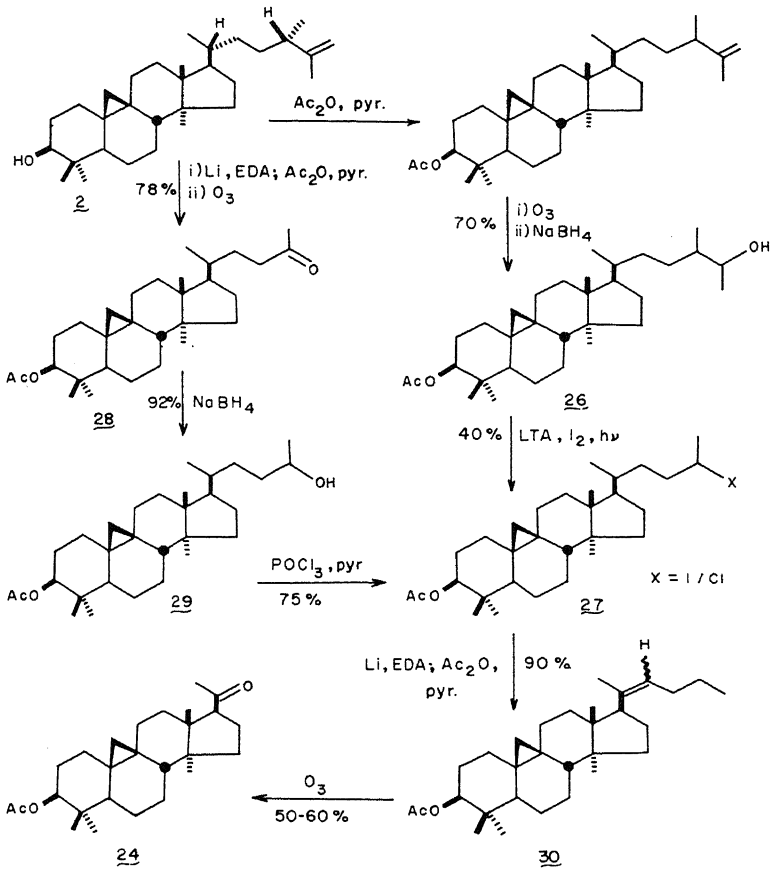

Figure 3. Side-chain degradation of cyclolaudenol.

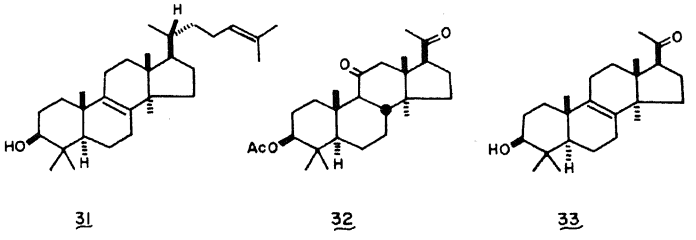

After having developed viable methods for the conversion of cycloartenol or cyclolaudenol into the hexanorketone 24, stage was set for its elaboration into simple *Buxus* alkaloids of type 3. Towards this end, one must convert C-20 carbonyl into an amino function with the required *S*-chirality, and C-3 oxygen function into a β-amino derivative. The latter conversion is straightforward, as hydrogenation or reduction of carbon nitrogen or carbon oxygen or carbon carbon double bond in the steroid nucleus takes place, preponderatingly, from the α-face to furnish stereoselectively the β-product. However, conversion of C-20 carbonyl into an amine function with the

required configuration is less simple. Since, the reduction of 20-oxo-pregnanes with complex hydrides is known (Kirk and Hartshorn 1968a) to furnish predominantly *R*-configurated alcohols and since, the immediate environment at C-20 in 24 is similar to that in 20-oxo-pregnanes, it was argued that a similar hydride reduction of 24 would furnish as the chief product a 20*R*-alcohol. Furthermore, since the reduction of oximes or imines is mechanistically akin (Kirk and Hartshorn 1968b) to the reduction of ketones, routes to the C-20 amine using such intermediates, would result predominantly in the unwanted *R*-chirality. Hence, the most promising approach appeared to be one involving a single S_{N^2} displacement of a suitable C-20 derivative. The sequence successfully worked out (Singh and Sukh Dev 1977) involved reduction of the hexanorketone acetate (24) by $NaBH_4$ to give the R-alcohol (34) as the major product, which *via* tosylation and displacement by sodium azide could be converted into the azide 35. This latter reaction proved quite unsatisfactory and it was after a lot of experimentation that satisfactory conditions could be established and these required hexamethylphosphoric triamide as a solvent and $\sim 25°$ as the reaction temperature. Yields of $\sim 65\%$ could thus be secured. This compound was then reduced by LAH to the corresponding amine (36), which now has the right stereochemistry.

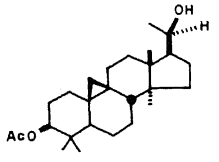

34

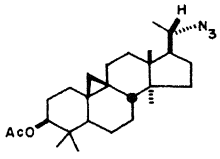

35

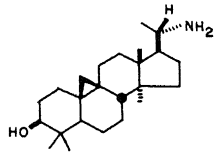

36

With these methods on hand it was rather simple to convert 36 into the targeted *Buxus* alkaloids. This is shown in figure 4 (Singh and Sukh Dev 1977). It may be noted that the key amine (36) is available in eight steps from cycloartenol. Reductive alkylation (Leuckart reaction) of 36 gave the dimethyl derivative 37, which on Jones' oxidation furnished buxandonine (16), a minor alkaloid of *Buxus sempervirens* (Dopke and Muller 1967). Transformation of its carbonyl function *via* oximation and LAH reduction to amine results in cycloprotobuxine-F (17), which, by reductive alkylation was converted into cycloprotobuxine-A (18). These alkaloids occur in *Buxus madagascarica* and *Buxus balearica* respectively (Tomko and Voticky 1973).

Cyclobuxophyllinine-M

In the next phase, attention was directed to the conversion of cycloartenol *via* the hexanorketone into C-16 oxygenated *Buxus* alkaloids. Specifically, our aim was to synthesise cyclobuxophyllinine-M (Buxenone-M) (38), an alkaloid isolated from *Buxus microphylla* var. *Suffruticosa* and *B. sempervirens* (Nakano *et al* 1966; Dopke *et al* 1966). This compound has been earlier converted into the related *Buxus* alkaloids cyclobuxophylline-K (39) and buxanine-M (40) (Nakano *et al* 1966; Dopke and Muller 1966).

Elaboration of the hexanorketone (24) to the targeted cyclobuxophyllinine-M (38) would involve: (i) generation of *E*-configurated $\Delta^{17(20)}$-16-keto system, and

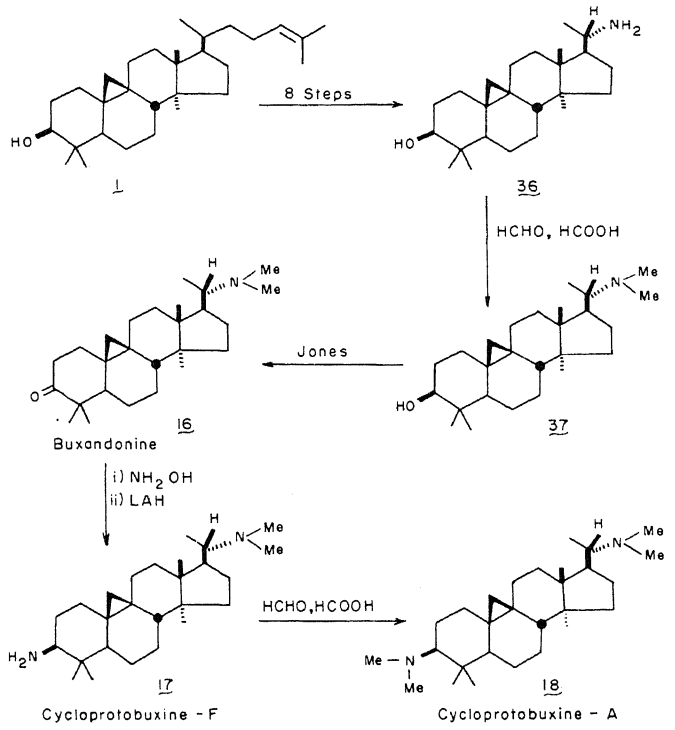

Figure 4. Synthesis of buxandonine, cycloprotobuxine-F and cycloprotobuxine-A.

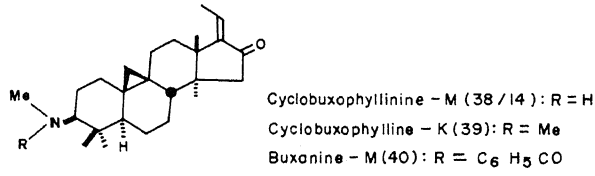

(ii) conversion of 3β-acetoxy group into 3β-methylamino function. For the introduction of the $\Delta^{17(20)}$-16-keto function, advantage was sought to be taken of the known (Benn and Dodson 1964) acid-catalysed isomerization of pregn-16-en-20-ols to preg-17(20)-en-16-ols, while the introduction of the 3β-methylamino group appeared reasonably feasible by the standard (Emerson 1948; Borch *et al* 1971) reductive amination of the 3-keto function. However, sequence of reactions had to be so chosen that the oxygenated functions at C-3 and C-16/C-20 are properly differentiated.

It has been well-established (Benn and Dodson 1964) that acid-catalysed equilibration of steroidal allylic alcohols of type 41 generates an isomeric mixture in which the isomer 42 predominates. It has also been established that configuration at C-20 has no effect on the equilibrium. Also, the olefin which is formed is always *Z*-configurated and the stereochemistry at C-16 is preponderatingly β. Since in a cycloartane analogue such as 43, the D-ring structure is essentially similar to that in the steroid case, just discussed,

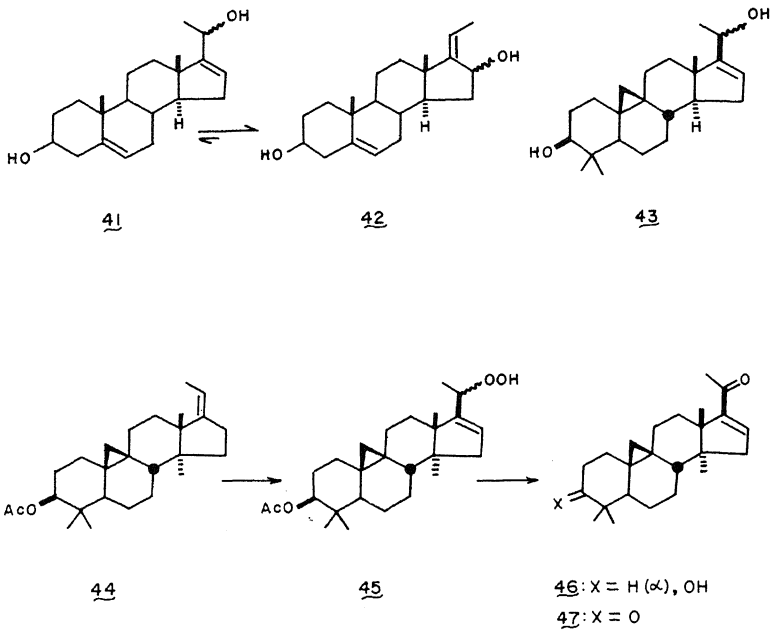

it should be possible to isomerise such an alcohol to the more stable 17(20)-ene-16-ol. Thus the immediate requirement became the synthesis of such a compound from the hexanorketone. This was achieved in two ways (Desai *et al* 1981). In one approach the hexanorketone was converted into olefin 44 *via* reduction, tosylation and dehydrotosylation with collidine in ~ 70% yield. This on Schenk oxidation, in the presence of methylene blue, gave the required hydroperoxide 45, which on treatment with acetic anhydride furnished the required unsaturated ketone 46. The same olefinic ketone could be more directly prepared by bromination of 24 followed by dehydrobromination. Hydrolysis, followed by chromic acid oxidation yielded the diketone 47, which had been obtained earlier by Ruchig degradation of the *Buxus* alkaloid cyclovirobuxine-D (Brown and Kupchan 1964).

The series of reactions, which permitted the successful transformation of the unsaturated ketone 46 into cyclobuxophyllinine-M (38) is shown in figure 5 (Desai *et al* 1981). LAH reduction of 46 gave the diol 43 in which the two hydroxyls should now be distinguished. It was found that one could conveniently acetylate the allylic hydroxyl function by acetic acid in the presence of a trace of toluene sulphonic acid and we thus obtained acetate 47 in about 80% yield. This was next oxidised by chromic acid to 48; for this we utilized pyridinium chromate-on-silica gel—a convenient off-the-shelf Sarett-type reagent, introduced by us sometime back (Singh *et al* 1979). This, on isomerization in the presence of acetic acid, acetic anhydride and toluene sulfonic acid, furnished as the major product 49 with *Z*-configuration. This was then converted into the methylamino derivative by reductive amination, using methylamine, sodium cyanoborohydride in MeOH in the presence of type A_4 molecular sieves. The product 50 was saponified and the resulting hydroxy compound oxidised by active MnO_2 to furnish 51, which differs from the target compound in being its *Z*-geometrical isomer.

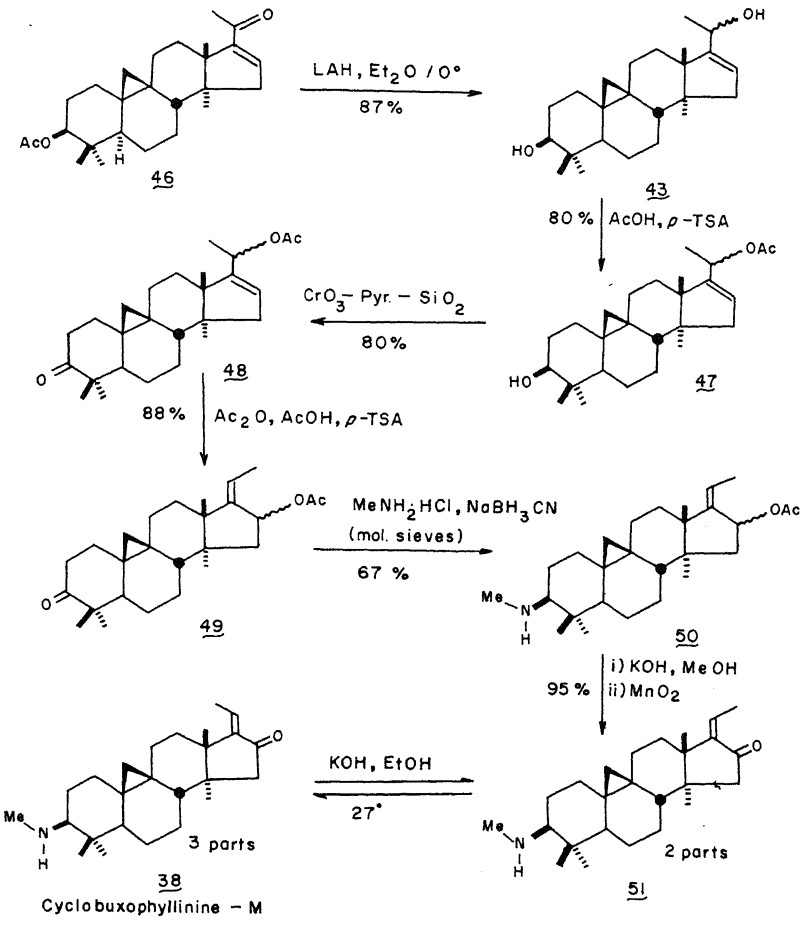

Figure 5. Synthesis of cyclobuxophyllinine-M.

On equilibration with ethanolic KOH, a 3 : 2 ratio of the *E* and *Z* isomers resulted, from which the required cyclobuxophyllinine-M (38) could be isolated by fractional crystallisation.

Cycloeucalanone and 31-*norcyclolaudenone*

The third phase of our investigations was aimed at development of a method for the regiospecific/regioselective functionalization of C-4α-methyl. Such a method was necessary for the synthesis of *Buxus* alkaloids lacking a C-4 methyl or oxygenated at one of these (invariably the α-methyl). An example of such an alkaloid is cyclobuxosufferine (15). As an immediate objective, we set before us the conversion of cyclolaudenol into 31-norcyclolaudenone (52) a component of *Musa sapientum*. It may be pertinent to point out at this stage that at the time we started this work several methods were available for desmethylation of C-4, especially because there has been a lot of interest in mimicking this transformation, which is an obligatory step in the conversion of

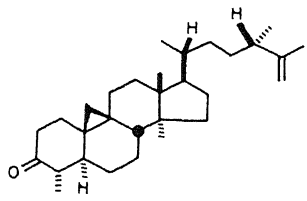

52

triterpenes (lanosterol) into steroids. In the biological system, specific 4-α-methyl hydroxylation occurs (Rees and Goodwin 1972; Nelson *et al* 1975a). Two approaches have been described. In the first approach, ring A′ is cleaved to get a 3,4-seco derivative, which is further manipulated towards the desired end (see *e.g.* Cohen *et al* 1973). In the second approach direct functionalization of a C-4 methyl is aimed at. In a method, reported in 1975 (Nelson *et al* 1975b), an N-oxyl derivative is prepared and photolysed resulting in oxygenation of the axial methyl (*i.e.* 4β-methyl). A second method utilises thermal cleavage of an azidoformate, leading to functionalization of the 4α-methyl as well as of C-2, almost to the same extent (Jones *et al* 1976). Another method, reported in 1977 (Midgley *et al* 1977), is not very versatile as it requires a C-6/C-7 double bond: through hydroboration, C-6 alcohol is obtained, the nitrite of which is photolysed to effect selective 4α-functionalization.

As can be seen, all the above methods are either rather involved or have poor regioselectivity. For our purpose on hand, we thought it worthwhile to develop a more selective method. Figure 6 depicts our approach to the problem. The well-known photolysis of suitably constituted hypoiodites, leading to an ether/iodoether, readily convertible into the corresponding lactone, appeared appropriate. The structural and stereochemical requirements of this reaction have been well-delineated (see *e.g.* Heusler and Kalvoda 1964, 1972). The reaction proceeds well in the desired direction only if the internuclear distance between the oxygen and the concerned carbon falls between 2·5 and 2·7 Å, and a 6-membered chair conformation transition state is possible. In terms of these considerations, a β-hydroxymethyl function at C-3 on a triterpene nucleus (e.g. 53) appeared suitable for functionalization of C-4 methyls, as the distance between O and either of the C-4 methyl C falls in the desired limit and a 6-membered chair conformation transition state is also feasible (54, 55). However, a closer scrutiny reveals that functionalization of 4α-methyl should be preferred for the following two reasons: (a) in conformation 54, the 6-membered transition state simulates a *trans*-fused relationship with ring A and hence should experience less 1,3-diaxial type interactions and should be preferred over 55 which has a similar '*cis*-fused' disposition, (b) in 54 C-OH is flanked by a 'small' (H atom) and a 'large' (C-4) groups in contrast to 55 in which these groups are 'medium' (C-2) and 'large' (C-4). Thus, if these reasonings are correct, one can expect a high degree of regioselectivity for the reaction, resulting in the desired functionalization of 4α-methyl.

To evaluate this strategy conversion of cyclolaudanone (56) to the known cycloeucalanone (64), along the lines shown in figure 7, was investigated (Desai *et al* 1982a). Cyclolaudenone was converted *via* Wittig reaction into the methylene derivative 57 which was hydroborated to give a mixture of the β (major) and α methanols; the major product was recognised as β from its spectral data. It was

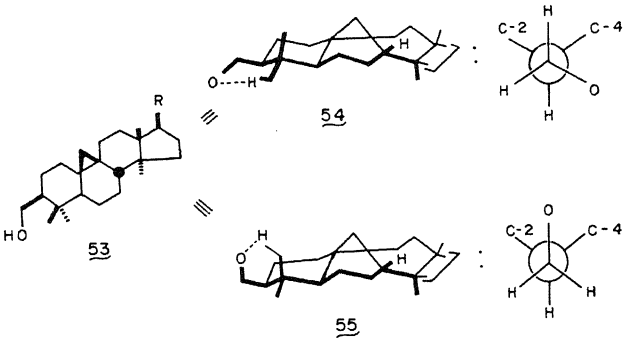

Figure 6. Preferred conformations in the functionalization reaction.

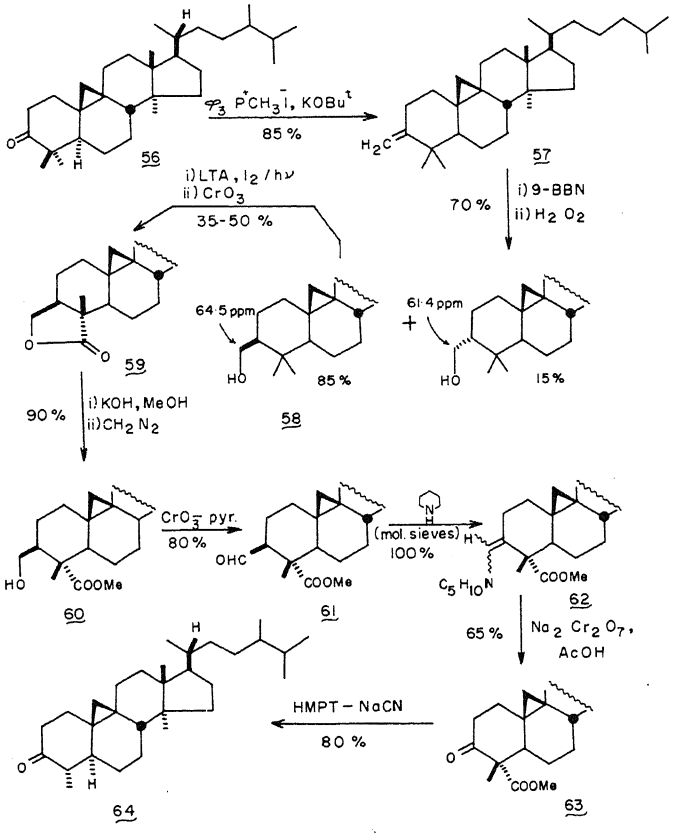

Figure 7. Synthesis of cycloeucalanone.

subjected to the action of LTA/I_2/*hv*, and the crude product from the photolysis reaction oxidized with chromic acid to give lactone 59 in yields of 35–50%. The lactone on base hydrolysis, followed by esterification with diazomethane furnished 60. The methoxycarbonyl group in 60 was readily assigned α-configuration on the basis of its

spectral characteristics, especially its ^{13}C-NMR spectrum. Oxidation of 60 with CrO_3-pyridine smoothly furnished the corresponding formyl ester (61). This was converted into the corresponding enamines (*E*/*Z*), which were directly oxidised ($Na_2Cr_2O_7$-AcOH) to furnish the desired β-keto ester (63) in an overall yield of 50% from the hydroxy ester 60. Exposure of 63 to NaCN in hexamethylphosphoric triamide resulted in hydrolysis with concomitant decarboxylation to furnish the known cycloeucalanone (64) in over 80% yield.

The successful completion of the above transformation vindicated the strategy we had envisaged for regioselective functionalization of 4α-methyl in a triterpene system. We were now all set to apply this method to a more difficult case, namely, the conversion of cyclolaudenol into 31-norcyclolaudenone (52), a triterpene isolated from *Musa sapientum* (Knapp and Nicholas 1970). Figure 8 summarises the sequence of reactions successfully exploited for the purpose (Desai *et al* 1982b). It was clear from the outset that the olefinic bond in the side-chain of cyclolaudenol (2) would have to be protected in a manner that the sequence of reactions for the functionalization of 4α-methyl and final removal of C-29 can be easily carried out and after these operations,

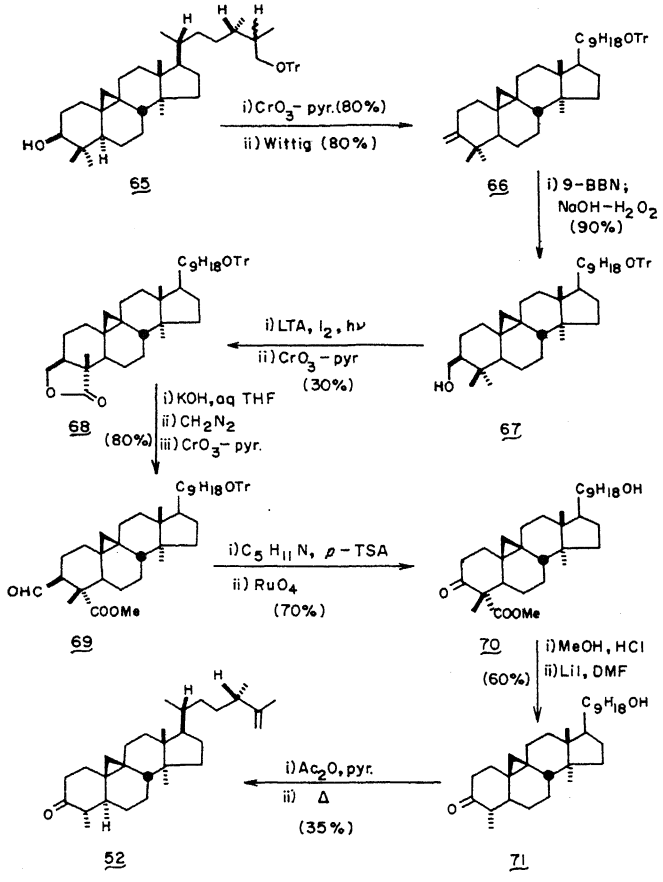

Figure 8. Transformation of cyclolaudenol to 31-norcyclolaudenone.

the double bond can be regenerated. On hydroboration followed by oxidative work-up, cyclolaudenol furnished a mixture of epimeric 26-hydroxycyclolaudan-3β-ols, in which the primary hydroxyl could be smoothly protected by tritylation. The trityl derivative 65 was oxidised with CrO_3-pyridine to the corresponding ketone, which was converted to the methylene derivative 66, as before. This on hydroboration (with 9-BBN)-oxidation gave a product, of which the major component (diastereomeric at C-26) was assigned 3β-configuration (67) based on the expected preferential attack by the hydroborating agent from the less hindered α-face of the olefins (66). Irradiation of alcohols 67 along with the 3α-isomers, in the presence of LTA and iodine, followed by Collin's oxidation, gave a product from which lactones 68 were isolated by inverted-dry-column chromatography (Bhalla *et al* 1967). Spectral data were fully consistent with the assigned structure. Lactones 68 were hydrolysed and esterified to give hydroxyesters, which on oxidation with Collin's reagent gave the formyl esters (69). The latter were converted to their enamines, and conveniently cleaved with RuO_4 to the keto esters 70. Incidentally, this is the first report of the use of RuO_4 for the cleavage of C=C bond in enamines. Exposure of 70 to methanolic HCl resulted in detritylation to the alcohols which were subjected to saponification-decarboxylation, in presence of LiI/DMF to get the nor-derivative 71. This material was acetylated and pyrolysed to furnish the required 31-norcyclolaudenone (52). The product was characterised by the usual spectral methods and the data were identical to those reported for the natural product.

We hope to extend the above methodology to the conversion of cycloartenol/cyclolaudenol into cyclobuxosuffrine (15), a typical *Buxus* alkaloid lacking a C-4 methyl.

Acknowledgement

The work described in this paper has been possible with the dedicated efforts of my students and colleagues, whose names appear in the various references. The author takes this opportunity to express his sincere thanks and appreciation. Special mention must be made of the contributions of Dr H P S Chawla who was actively involved in the third phase of this work. It is a pleasure to specially thank him for his collaboration.

References

Adam G, Voigt B and Schreiber K 1970 *J. Prakt. Chem.* **312** 1027, 1063
Bacha J D and Kochi J K 1968 *Tetrahedron* **24** 2215
Benn W R and Dodson R M 1964 *J. Org. Chem.* **29** 1142
Bentley H R, Henry J A, Irvine D S and Spring F S 1953 *J. Chem. Soc.* 3673
Bhalla V K, Nayak U R and Sukh Dev 1967 *J. Chromatogr.* **26** 54
Borch R F, Bernstein M D, and Durst H D 1971 *J. Am. Chem. Soc.* **93** 2897
Brown K S and Kupchan S M 1962 *J. Am. Chem. Soc.* **84** 4590, 4592
Brown K S and Kupchan S M 1964a *J. Am. Chem. Soc.* **86** 4414, 4424
Brown K S and Kupchan S M 1964b *Tetrahedron Lett.* 2895
Calame J P 1965 E.T.H. Dissertation
Calame J P and Arigoni D 1964 *Chimia* **18** 185
Cohen K F, Kazlauskas R and Pinhey J T 1973 *J. Chem. Soc. Perkin I* 2076
Desai M C, Singh J, Chawla H P S and Sukh Dev 1981 *Tetrahedron* **37** 2935
Desai M C, Chawla H P S and Sukh Dev 1982a *Tetrahedron* **38** 379

Desai M C, Singh C, Chawla H P S and Sukh Dev 1982a *Tetrahedron* **38** 201
Dopke W and Muller B 1966 *Pharmazie* **21** 769
Dopke W and Muller B 1967 *Pharmazie* **22** 666
Dopke W, Muller B and Jeffs P W 1966 *Pharmazie* **21** 643
Emerson W S 1948 *Org. React.* **4** 174
Fieser L F and Fieser M 1959 *Steroids* (New York: Reinhold) pp. 68–69
Gaitonde M, Vatakencherry P A and Sukh Dev 1964 *Tetrahedron Lett.* 2007
Goodwin T W 1979 *Annu. Rev. Plant Physiol.* **30** 374
Heftmann E 1983 *Phytochemistry* **22** 1843
Heusler K and Kalvoda J 1964 *Angew. Chem. Int. Ed.* **3** 525
Heusler K and Kalvoda J 1972 in *Organic reactions in steroid chemistry* (eds) J Fried and J A Edwards (New York: Van Nostrand Reinhold) Vol. II p. 237
Hubert A J and Reimlinger 1969 *Synthesis* 97
Hubert A J and Reimlinger 1970 *Synthesis* 405
Jones A J, Alewood P E, Benn M and Wong J 1976 *Tetrahedron Lett.* 1655
Kirk D N and Hartshorn M P 1968a *Steroid reaction mechanisms* (Amsterdam: Elsevier) p. 139
Kirk D N and Hartshorn M P 1968b *Steroid reaction mechanisms* (Amsterdam: Elsevier) p. 146
Knapp F F and Nicholas H J 1970 *Steroids* **16** 329
Kochi J K, Sheldon R A and Lande S S 1969 *Tetrahedron* **25** 1197
Kreiser W and Ulrich W 1976 *Liebig's Ann.* 1199
Meystre C, Frey H, Wettstein A and Miescher A 1944 *Helv. Chim. Acta* **27** 1815
Meystre C, Frey H, Wettstein A and Miescher A 1946 *Helv. Chim. Acta* **29** 627
Midgley J M, Perkin J E and Whalley W B 1977 *J. Chem. Soc. Perkin I* 834
Nakano T, Alonso M and Martin A 1970 *Tetrahedron Lett.* 4929
Nakano T, Terao S, Saeki Y 1966 *J. Chem. Soc.* (*C*) 1412
Narula A S and Sukh Dev 1969 *Tetrahedron Lett.* 1733
Narula A S and Sukh Dev 1971 *Tetrahedron* **27** 1119
Nelson J A, Chou S and Spencer T A 1975b *J. Am. Chem. Soc.* **97** 648
Nelson J A, Kahn S, Spencer T A Sharpless K B and Clayton R B 1975a *Bioorganic Chem.* **4** 363
Rees H H and Goodwin T W 1972 *Biosynthesis* (Specialist Periodical Reports) (London: The Chemical Society) **1** 76
Reggel L, Friedman S and Wender I 1958 *J. Org. Chem.* **23** 1136
Roddick J G 1980 in *Secondary plant products* (eds) E A Bell and B V Charlwood (Berlin: Springer-Verlag) pp. 173–180
Scott A I 1976 in *Applications of biochemical systems in organic chemistry* (eds) J B Jones, C J Sih and D Perlman (New York: John Wiley) part II, pp. 555–625
Singh C, Singh J and Sukh Dev 1977 *Tetrahedron* **33** 1759
Singh C and Sukh Dev 1977 *Tetrahedron* **33** 1053
Singh R P, Subbarao H N and Sukh Dev 1979 *Tetrahedron* **35** 1789
Tomko J and Voticky Z 1973 in *The alkaloids* (ed) R H F Manske (New York: Academic Press) Vol. XIV, pp. 32–82
Tyagi B S, Ghatge B B and Bhattacharyya S C 1962 *J. Org. Chem.* **27** 1430
Voser W, Jeger O and Ruzicka L 1952 *Helv. Chim. Acta* **35** 503

Proc. Indian Acad. Sci. (Chem. Sci.), Vol. 93, No. 6, August 1984, pp. 1031–1057.
© Printed in India.

Recent advances in the chemistry of lignans

A CHATTERJEE,* A BANERJI, J BANERJI, S C PAL and T GHOSAL
Chemistry Department, University College of Science, Calcutta 700 009, India

Abstract. The recent literature on the chemistry of simple lignans has been comprehensively reviewed.

Keywords. Lignans; aryltetralin; arylnaphthalide; tetrahydrofuranoid; furofuranoid; dibenzocyclooctadiene; absolute configuration.

1. Introduction

Lignans constitute an important class of natural products, which are biogenetically derived from C_6-C_3 units. The chemistry of lignans has been extensively reviewed up to 1976 (Rao 1978). Since then a large number of publications have appeared in the literature, some of which report the discovery of lignans of novel structural patterns. Hence, it seemed necessary to review the literature appearing subsequent to those covered in Prof. Rao's book. The present review, which sums the literature up to 1983, deals with the chemistry of the new lignans reported. The review deals only with the simple lignans, and papers on sesqui-, bi- and neo-lignans have not been included. Synthetic approaches to lignans have also been omitted as these have been reviewed elsewhere (Ward 1982).

2. Dibenzylbutane lignans

Acanthotoxin (1), $C_{20}H_{18}O_6$ (M^+ 356), m.p. 123°, $[\alpha]_D$ −133° and podotoxin (2), $C_{21}H_{22}O_6$ (M^+ 370), m.p. 140–42°, $[\alpha]_D$ −5.3°, are the two germination inhibiting lignans isolated from *Zanthoxylum acananthopodium* D.C. (Chakravorty *et al* 1977, 1979). In the ^{1}H-NMR spectra of these compounds the ethylenic (1H) and aromatic protons (7H) appeared in the region δ6·65–6·80 (m), the exchangeable lactol proton at 4·75, the oxy-methylene protons (2H) at δ4·02–4·38 (m) and the benzylic protons at 2·65–3·91 (m).

On oxidation by Collin's reagent both of these furnished γ-lactones, acanthotoxin (3) and podotoxin (4). The authors have reported that (1) and (2) on heating were cyclised to dihydronaphthalenes (5) and (6) which were aromatised by 10% Pd-C to justicidin-E (7) and the compound (8) respectively. The mass peak at m/z 203 defined the position of the methylenedioxy moiety in ring A of podotoxin.

(+)-Nortrachelogenin (9), $C_{20}H_{22}O_7$, $[\alpha]_D$ +15·4° isolated from *Wikstroemia indica*, (Kato and Hashimoto 1979) appears to be the enantiomer of (−)nortrachelogenin (10), $[\alpha]_D$ −16·8° from the identity of their UV, IR, ^{1}H- and ^{13}C-NMR spectra. The

* To whom all correspondence should be addressed.

enantiomeric relationship was confirmed by CD measurements showing positive and negative Cotton effects respectively for (9) and (10) with maxima at 236 nm. (9) was the 2*R*, 3*R* compound as the previously reported (10) was shown to possess 2*S*, 3*S* configuration. (+)Nortrachelogenin seems to be identical with wikstromol (Tandon and Rastogi 1976) isolated from the same plant by comparison of their given structures, though the specific rotation value of the latter was reported as +72°. (+)-Arctigenin (11) (Suzuki *et al* 1982), $C_{21}H_{24}O_6$, $[\alpha]_D$ +28·05° (EtOH), was isolated from the same plant. The identical physical and spectral properties of (11) with (−)-arctigenin (12), but opposite sign of both specific rotation and Cotton effects in CD spectra ($[\theta]$ +24180 for (11) and $[\theta]$ −23250 for (12) at 230 nm) indicated (11) to be (+)-arctigenin.

The structure of (−)*trans*-2-(3′,4′-dimethoxybenzyl)-3-(3″,4″,5″-trimethoxybenzyl) butyrolactone (13), $C_{23}H_{28}O_7$, reported from *Cinnamomum camphora* Sieb (Takaoka *et al* 1977), was established from spectral analyses. The *trans*-substituted γ-lactone system was indicated by the signals of the aliphatic protons (δ 2·55 (4H, m), 2·90 (2H, m) and 3·8–4·25 (2H, m)) in the ^{1}H-NMR spectrum; this was also supported by the presence

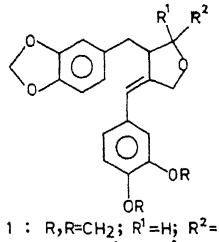

1 : R,R=CH_2; R^1=H; R^2=OH
2 : R=Me; R^1=H; R^2=OH
3 : R, R=CH_2; R^1, R^2=O
4 : R=Me; R^1, R^2 = O

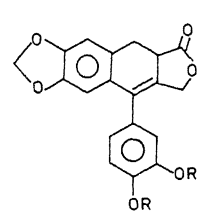

5 : R,R = CH_2
6 : R = Me

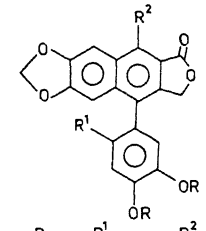

	R	R^1	R^2
7 :	CH_2	H	H
8 :	Me	H	H
81 :	CH_2	OMe	OMe
82 :	CH_2	OH	H

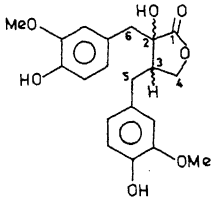

9 : α-OH; β-H
10 : β-OH; α-H

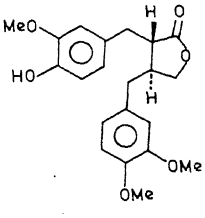

11

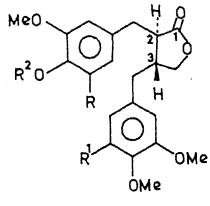

12 : R=R^1=R^2=H
13 : R=H; R^1=OMe; R^2 = Me
14 : R = OMe; R^1=H; R^2=Me

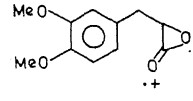

m/e 208
15

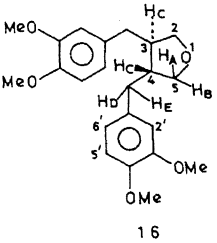

16

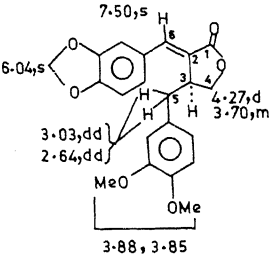

3·88, 3·85
17

of an absorption band at 1760 cm^{-1} in the IR spectrum. The aromatic region of the ^{1}H-NMR spectrum suggested the presence of a symmetrically substituted trimethoxyphenyl (δ6·18, 2H, s) and a disubstituted phenyl group having two *ortho*-protons (δ6·61, 1H, d, J = 8 Hz; δ6·75, 1H, d, J = 8 Hz and δ6·68, 1H, broad s). This led to two possibilities (13) and (14) for the new lignan. The occurrence of a mass fragment at *m/z* 208 (15) in the MS favoured structure (13). The absolute configuration was settled as 2*R*, 3*R* from CD studies.

The first report of the natural occurrence of brassilignan (16) was claimed by Taylor and co-workers (Nimgirawath *et al* 1977) from *Flindersia brasii* although it, along with several stereoisomers, was reported earlier as a synthetic compound. Brassilignan, $C_{22}H_{28}O_5$, m.p. 120°, $[\alpha]_D$ −56°, was shown to be symmetrical from the doubling of peaks in ^{1}H-NMR spectrum. The ion peaks at *m/e* 152 ($C_9H_{12}O_2^+$) and *m/e* 151 ($C_9H_{11}O_2^+$) suggested it to contain the 3,4-dimethoxyphenyl group(s). ^{1}H-NMR signals at *ca* δ6·60 (m) were assigned to H-2′, H-5′ and H-6′; the pattern was matched by iterative computation (LACON 3) yielding the following parameters: $\delta_{2'}$ 6·59; $\delta_{5'}$ 6·75; $\delta_{6'}$ 6·63; $J_{2',5'}$ 1·97; $J_{2',6'}$ 0·60; $J_{5',6'}$ 7·95 Hz. Each of the geminal protons, H_A, H_B, H_D and H_E appeared as *d* of *d* and the proton H_C as a broadened sextet. The ^{13}C-NMR spectrum supported the structure (16). The absolute configuration (3*R*, 4*R*) was determined from the work of Row *et al* (1966).

Two new lignans, *viz.* jatrophan (17) (Chatterjee *et al* 1981) and gadain (20) (Chatterjee *et al* 1984) were isolated from *Jatropha gossypifolia.* These are the first lignans obtained from the genus *Jatropha.* Jatrophan, $C_{21}H_{20}O_6$, m.p. 129°, $[\alpha]_D$ +87° ($CHCl_3$) showed IR absorptions at 1725 (α,β-unsaturated γ-lactone), 1630 (olefinic double bond), 1595, 1480 (aromatic) and 910 cm^{-1} (methylenedioxy group) (Chatterjee *et al* 1981). A comparison of its UV absorption spectrum with that of (−)-hibalactone (18) (Schrecker and Hartwell 1954), showed jatrophan to be a lignan of dibenzylbutyrolactone skeleton with a 2,6-double bond. The ^{1}H-NMR data (given on the structure) as well as the MS fragments at *m/z* 368, 217, 152, 151 and 135 were in accordance with the formulation of jatrophan as 2-piperonylidene-3-veratryl-3R-γ-butyrolactone (17). The structure and stereochemistry were finally confirmed from x-ray diffraction studies (Chatterjee *et al* 1981). Jatrophan (17) was converted into two naturally occurring arylnaphthalide lignans, retrochinensin (8) and justicidin-B, (19) by treatment with DDQ and N-bromosuccinimide respectively. Jatrophan showed strong insecticidal activity against the storage grain pest, *Tribolium castaneum.*

Gadain (20), $C_{20}H_{16}O_6$, m.p. 145°, $[\alpha]_D$ +86° ($CHCl_3$) exhibited UV absorption (λ_{max} 337, 293, 235 nm; log ε4·20, 3·95, 4·18) characteristic of dibenzylbutyrolactone lignans having a double bond in the 2,6-position (Chatterjee *et al* 1984). The IR spectrum showed characteristic absorptions for an α,β-unsaturated γ-lactone (1725 cm^{-1}), olefinic double bond (1620 cm^{-1}) and a methylenedioxy group (915 cm^{-1}). Structure (20) for gadain was proposed from its MS fragmentation pattern and from 300 MHz ^{1}H-NMR studies and 2D HOMCOR (COSY) experiments. It was observed that gadain was isomerised to its isomer (21) even in the presence of traces of HCl. The structure and stereochemistry of gadain was confirmed by its synthesis from jatrophan (17). The latter was demethylated with BBr_3 to (22), which on treatment with bromochloromethane and potassium carbonate afforded (21). UV-irradiation of the latter caused a double -bond isomerisation to give gadain (20). DDQ treatment of gadain gave justicidin E (7), through the intermediate formation of (21).

The total synthesis of (±)-gadain has been carried out as outlined in chart I. Stobbe

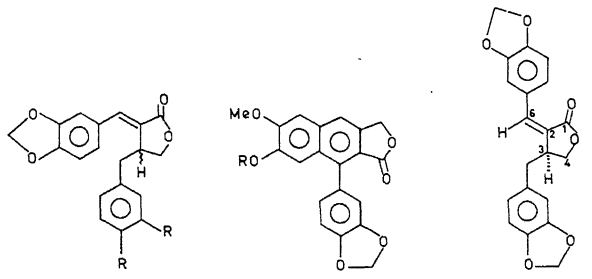

17 : R = OMe; α-H
18 : R,R = OCH_2O ; β-H
21 : R,R = OCH_2O
22 : R = OH

19 : R = Me
63 : R = H

20

Chart I

Synthesis of (±)-Gadain

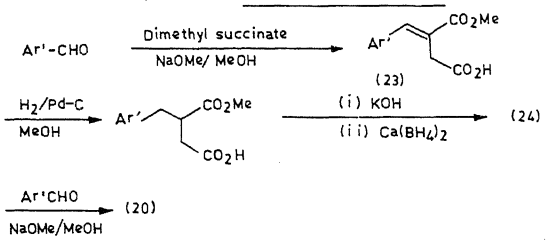

Ar' = 3,4-methylenedioxyphenyl

condensation of piperonal with dimethyl succinate furnished (23) which on catalytic hydrogenation followed by hydrolysis and selective hydride reduction gave the lactone (24). Condensation of (24) with piperonal furnished gadain (Chatterjee *et al* 1984).

Pregomisin (25), $C_{22}H_{30}O_6$, mp 130–31°, $[\alpha]_D$ 0°, isolated by Ikeya *et al* (1978a, 1979a) from *Schizandra chinensis* Baill, showed UV maxima (λ_{max} 208, 225 and 270; log ε 4·81, 4·30 and 3·15 nm) similar to those of meso-dihydroguaiaretic acid and seco-isolariciresinol. The ^{1}H-NMR data (on structure) accounted for just half the protons indicating it to be a symmetrical molecule- a 1,4-bisphenyl-2,3-dimethylbutane derivative. MS data also supported this structure. The CD curve, with no absorption between 200–400 nm suggested it to have the *meso*-configuration (2*S*, 3*R*). From the appearance of a pair of *meta*-coupled aromatic protons in the ^{1}H-NMR spectrum and biogenetic considerations the structure of the aryl groups were derived as shown. Finally the structure (25) was confirmed by its synthesis from guaiaretic acid (26). Hydrogenation of (26) to the dihydroanalogue (27), followed by nitration yielded a dinitro derivative (28). Reduction by tin/HCl of its dimethyl derivative (29) gave the corresponding diamino compound (30). Diazotisation and subsequent treatment with 5% H_2SO_4 afforded pregomisin (25).

Bohlmann *et al* (1978) have isolated three diester lignans, bisdihydro-coniferyl-alcohol-diisovalerate (from *Flavaria chloriefolia*), heliobuphthalmin and dehydro-heliobuphthalmin (from *Heliopsis buphthalmoides*). From spectral data, ^{1}H-NMR in particular, the structures were established as (31), (32) and (33) respectively. All the compounds showed an ester absorption band at 1740 cm^{-1} (the last compound showed another at 1710 cm^{-1} for its conjugated ester function). They were reduced by

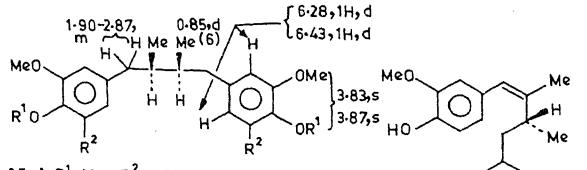

25 : R^1=Me; R^2 = OH
27 : R^1=R^2=H
28 : R^1=H; R^2=NO_2
29 : R^1=Me; R^2=NO_2
30 : R^1=Me; R^2=NH_2

26

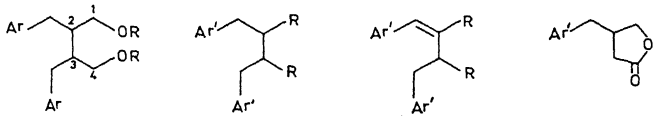

31 : R=$COCH_2CHMe_2$
34 : R=H
43 : R=H; 2S, 3R

32 : R = CO_2Me
35 : R = CH_2OH

33 : R = CO_2Me
36 : R = CH_2OH

24

(Ar = 4-Hydroxy-3-methoxyphenyl ; Ar' = 3,4-methylenedioxyphenyl)

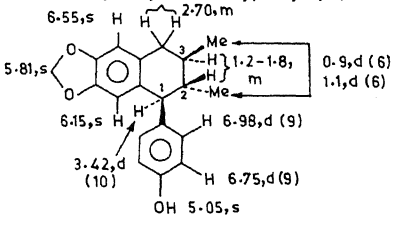

37

38 : 2-epimer of 37

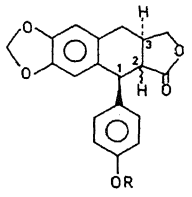

39 : R = CH_2Ph; 1,2-dehydro
40 : R = H; 2 β-H
41 : R = CH_2Ph; 2β-H
42 : R = CH_2Ph; 2α-H

lithium aluminium hydride to the corresponding diols (34), (35) and (36) respectively. The stereochemistry of the chiral centres was not defined for any of these compounds.

Agrawal and Rastogi (1982) reported the first natural occurrence of *meso*-secoisolariciresinol (structure 43; 2*S*, 3*R*), $C_{20}H_{26}O_6$, from *Cedrus deodara* as a liquid. Its structure was confirmed by ^{1}H-NMR comparisons with related compounds and the previously reported synthetic *meso*- seco- isolariciresinol.

3. Aryltetralin and arylnaphthalide lignans

Attenuol, $C_{19}H_{20}O_3$, m.p. 160–61°, $[\alpha]_D$ −20·5°, was obtained from *Knema attenuata* (Joshi *et al* 1978). The structure was suggested to be (37) from a detailed study of its ^{1}H-NMR spectrum. ORD studies led to the assignment of absolute stereochemistry at the chiral centres as 1*S*, 2*S*, 3*R*.

The structure and the relative stereochemistry were confirmed by the synthesis of (±)-attenuol (37) and its all -*cis* isomer, (±)-2-epiattenuol (38) (Joshi *et al* 1979). A Diels-Alder reaction between methyl-*p*-benzyloxyphenyl acetylene carboxylate and 6,7-methylenedioxy cinnamyl alcohol with simultaneous lactonisation produced a 1,2-dialin (39). Its catalytic hydrogenation furnished the tetralin (40) which was used as the precessor by Joshi *et al* (1979). Benzylation of (40) in presence of K_2CO_3 in acetone gave (41), but in the presence of sodium acetate in ethanol (42) was obtained. Reduction

of the lactone ring and debenzylation of these afforded (±)-attenuol (37) and its 2-epimer (38) respectively.

Brown *et al* (1979) have also reported the synthesis of (±)-attenuol. Condensation of racemic (24) with *p*-benzyloxybenzaldehyde in presence of $(Me_3Si)_2N^-Li^+$ followed by hydrolysis gave a diastereoisomeric mixture of alcohols. The latter were cyclised to (41) by TFA. Reduction of the lactone ring by successive treatment with $LiAlH_4$, $MeSO_2Cl$/pyridine, $LiAlH_4$ and finally hydrogenolysis of the benzyloxy group over Pd/C gave (±)-attenuol (37).

The structure and stereochemistry of morelensin (44), $C_{21}H_{20}O_6$ (M^+ 368), mp 181°, $[\alpha]_D$ −125°, isolated from *Bursera morelensis* (Jolad *et al* 1977) was established by a comparative study of its spectral properties, particularly the ^{1}H-NMR and mass spectra, with those of deoxypodophyllotoxin (45) and 5-methoxy-deoxypodophyllotoxin (46). The ^{1}H-NMR signals of its γ-lactone moiety (ν_{max} 1775 cm^{-1}) and rings A, B were identical with those of (45), whereas the signals for the protons in ring C were similar to those of the corresponding signals of (46).

Podophyllotoxone (47), $C_{22}H_{20}O_8$, m.p. 189–92°, $[\alpha]_D$ −128° ($CHCl_3$) was isolated as a natural product from *Podophyllum hexandrum* and *Podophyllum peltatum* by Dewick and Jackson (1981), although it was known previously as a synthetic compound (Gensler *et al* 1960) of established 1*R*, 2*R*, 3*R* stereochemistry.

Hernandin (48), $C_{23}H_{24}O_8$, m.p. 210–13°, $[\alpha]_D$ −70° ($CHCl_3$) was isolated from the seeds of *Hernandia ovigera* L. (Yamaguchi *et al* 1982). Its IR and ^{1}H-NMR spectra indicated the presence of a lactone methylene, a methylenedioxy group, three aromatic protons and four methoxyl groups. A comparison of the ^{1}H-NMR data of (48) with those of the isomeric β-peltatin A methyl ether (49) (Hartwell and Detty 1950) showed differences in the chemical shifts of an aromatic proton of the tetralin ring (δ6·24 in 49, δ6·40 in 48) and those belonging to a methoxyl group (δ3·60 in 48, δ4·04 in 49). The MS fragmentation patterns of the two compounds were similar. On DDQ oxidation, (48) and (49) aromatised to give two different compounds (50) and (51) respectively thereby indicating that the original compounds were not stereoisomers. A comparison of the ^{1}H-NMR spectra of (50) and (51) indicated the location of the methoxyl group at C–5 in the former as it appeared at a higher field (δ3·47) due to the anisotropic effect of the 4-phenyl group, than the C-8 methoxyl in (51) (δ4·20). It was further reported that in type-A lignans (52), the lactone methylene and the C-1 proton should appear at δ5·32–5·52 and δ7·6–7·7 respectively whereas for type-B lignan (53) the corresponding values are δ5·08–5·23 and δ8·25. In the ^{1}H-NMR spectrum of hernandin the appearance of those signals at δ5·30 and δ7·64 respectively indicated the relative position of the lactone carbonyl group as that in type-A (52). The CD spectrum of hernandin showed a positive first Cotton effect at 286 nm [(θ) + 2083] thereby showing it to be a 4α-aryl-tetralin lignan (Klyne *et al* 1966; Swan *et al* 1967). The *trans*-configuration of the lactone ring was indicated by its base-catalysed epimerisation to picrohernandin (54), mp 90–92°, $[\alpha]_D$ +100°. Thus hernandin was 5-methoxypodophyllotoxin (48). This was further confirmed by x-ray crystallographic analysis.

The isolation of a arylnaphthalene lignan, 1,2,3,4-dehydrodesoxypodophyllotoxin (55), $C_{22}H_{18}O_7$, mp 276–78°, was reported in the same paper as hernandin (Yamaguchi *et al* 1982). (55) could be obtained by the DDQ oxidation of desoxypodophyllotoxin.

Five new lignans, one of the furofuranoid and four of arylnaphthalene skeleton (56–59) were obtained from *Cleistanthus collinus* (Anjaneyulu *et al* 1981). This was the first Euphorbiaceae plant from which both these classes of lignans have been obtained.

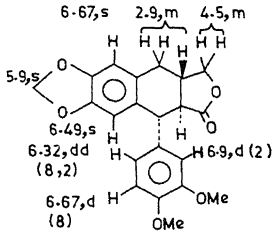

44

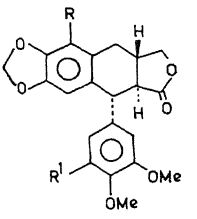

45 : R=H; R¹=OMe
46 : R=OMe; R¹=H

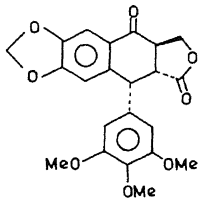

47

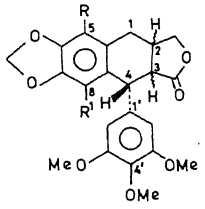

	R	R¹	
48 :	H	OMe	2α-H; 3β-H
49 :	MeO	H	2α-H; 3β-H
54 :	H	OMe	2α-H; 3α-H

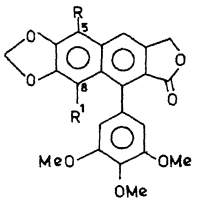

	R	R¹
50 :	H	OMe
51 :	MeO	H
55 :	H	H

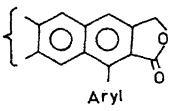

Type A
52

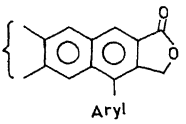

Type B
53

One of the new compounds was 3,4-dihydrotaiwanin C (56), $C_{20}H_{14}O_6$, mp 199–200°, whose structure was established by comparing its ^{1}-NMR spectral data with those of the known collinusin (60). The ^{1}H-NMR showed that the two methoxyls in (60) had been replaced by a methylenedioxy group in (56).

All the other three new compounds were glycosides. Cleistanthin D (57), $C_{29}H_{30}O_{11}$, mp 199–200°, $[\alpha]_D$ +25°, showed an IR absorption at 1755 cm^{-1} for a lactonic carbonyl. On acid hydrolysis it yielded diphyllin (61) and 2,3,5-tri-O-methyl-D-xylose. Thus cleistanthin D had the structure (57). Cleistanthin E (58), $C_{42}H_{52}O_{20}$, mp 177–80°, $[\alpha]_D$ −40°, on hydrolysis with methanolic HCl gave diphyllin, D-glucose, 2,3-di-O-methyl-D-xylose and 2,3,5-tri-O-methyl-D-xylose. Permethylated cleistanthin E on hydrolysis gave 2,3,6-tri-O-methyl-D-glycose, 2,3-di-O-methyl-D-xylose and 2,3,5-tri-O-methyl methyl-D-xylose, showing that 2,3,5-tri-O-methyl-D-xylose was the terminal sugar. On mild hydrolysis with 0·05 N H_2SO_4 in methanol at 60° (12 hr), only 2,3-di-O-methyl-D-xylose and 2,3,5-tri-O-methyl-D-xylose were obtained, thereby proving that D-glycose was the monosaccharide unit directly attached to the diphyllin nucleus. All these observations established structure (58) for this new glycoside. The third new glycoside, $C_{27}H_{24}O_{11}$, mp 210–12°, $[\alpha]_D$ + 11°, gave on hydrolysis taiwanin E (62) and 3,4-di-O-methyl-D-xylose. Hence it was taiwanin E 3,4-di-O-methyl-D-xylopyranoside (59).

The isolation of a new aryl naphthalide lignan, designated daurinol (63), from *Haphlophyllum dauricum* has been reported (Batsuren *et al* 1981).

Justicinol (64), $C_{20}H_{12}O_7$, mp 250–52°, was isolated from *Justicia flava* (Olaniyi and Powell 1980). Its UV spectrum was very similar to that of helioxanthin (65), while its IR

spectrum showed the presence of a γ-lactone moiety, a methylenedioxy and a hydroxyl group. The existence of a phenolic group in justicinol was confirmed by its conversion to a monoacetate (66) and a mono-methyl derivative (67). The position of the oxygen substituents, particularly the presence of the additional phenolic hydroxyl, were settled from ^{1}H-NMR comparisons of justicinol with its mono-acetate and helioxanthin.

The first natural occurrence of a cyclolignan hemiacetal, africanal (68), $C_{20}H_{22}O_7$, was reported from *Olea africana* by Viviers *et al* (1979). Subsequently the diacetylated derivatives of three cyclolignan acetals, namely 3a-methoxy-3a-deoxy-α-conidendrin (75), 3a-methoxy-3a-deoxy-β-conidendrin (76) and 3a-ethoxy-3a-deoxy-β-conidendrin (77) were obtained from the acetylated extract of the plant *Dacrydium intermedium* (Cambie *et al* 1979a, b).

The structure of africanal was elucidated from spectral studies of the compound and its various derivatives (69)–(72) and by its chemical conversion to cyclo-olivil or isoolivil (73) and the corresponding pentaacetate (74). A comparison of ^{13}C-NMR spectra of (68) and (73) revealed their close resemblance. The ^{13}C-chemical shifts of C_1, C_2, C_{2a}, C_3, C_{3a} and C_4 for (+)-africanal were δ48·5, 45·1, 70·3, 79, 103·3 and 37·3 respectively, whereas for (73) the corresponding values were δ44.8, 47.6, 60·5, 73·4, 69·4 and 40·1. This similarity taken in conjunction with superimposable CD curves of (68) and (73) defined the stereochemistry at all the chiral centres (1*R*, 2*R*, 3*R*) except at C_{3a}. The large deshielding (1·14 ppm) of the C_{3a}-proton of the tetraacetyl derivative (72) compared with that of the triacetyl derivative (71) strongly indicated a β-axial orientation of the C_{3a}-OH and therefore *S*-configuration at C_{3a}.

The structure and stereochemistry of (75), (76) and (77) were deduced from their correlation with the diacetates of α- and β-conidendrin, (78) and (79). Similarities in ^{1}H-NMR spectral data of (75) and (78) allowed their assignment to the same stereochemical series (all *trans*), while the results of (76), (77) and (79) indicated the B/C ring juncture to be *cis*. The appearance of H_{3a} as singlet in the ^{1}H-NMR spectra of (76) and (77) was consistent with a dihedral angle H-C_3-C_{3a}-H of ~ 90° as observed in models. In the MS of these compounds strong peaks corresponding to the loss of ROH and RO from M^+ ions were evident. In addition, the structures were consistent with decomposition of phenyltetralin skeleton giving peaks at *m/e* 341, 340, 216, 175 and 137. Structure and stereochemistry of (75) and (76) were confirmed by conversion into optically active compounds (78) and (79) respectively by treatment with BF_3-etherate and *m*-chloroperbenzoic acid.

Ghosal *et al* (1979a) reported four aryl naphthalide lignans prostalidin-A (80), prostalidin-B (81), prostalidin-C (82) and retrochinensin (8) from *Justicia prostata*. The mass [*m/e* 394 (M^+), 379, 365, 364, 351 and 197 (M^{++})] and UV [λ_{max} 230, 255, 300–305, 310, 315 and 345 nm] spectra of prostalidine A, mp 303–305°, were characteristic of 4-aryl-2,3-naphthalide skeleton. It was methylated with diazomethane to the monomethyl derivative (81), mp 245–47° (M^+ 408), which on oxidation by $KMnO_4$ afforded 6-methoxypiperoxylic acid, thus setting the C-ring oxygenation pattern as shown. Prostalidin-B (81) was identical to the monomethyl derivative of prostalidin-A. Prostalidin-C, mp 263–265°, resembled prostalidin-A in spectral properties with the exception of having an additional aromatic proton (~ δ6·80) in place of the –OMe signal (δ4·25) in the latter. Retrochinensin (8) was identical with the DDQ-oxidation product of suchilactone (4).

Ward *et al* (1979) predicted the chemical shifts of compounds with oxygenation patterns (83–86) on the basis of ^{13}C-NMR spectral data of some aryl-tetralin lignans and

known substituent parameters. Comparison of these values with those reported for hypophyllanthin led to the revision of its structure as (87) instead of (88) as suggested earlier by Row *et al* (1970). However, Ganeshpure *et al* (1981) carried out a total synthesis of hypophyllanthin and showed (89) to be the correct formulation. Stobbe condensation of aldehyde (90) with dimethyl succinate followed by catalytic hydrogenation and calcium borohydride treatment furnished the lactone (91). This was brominated to (92) to protect this position from cyclisation in a subsequent step. The corresponding lithium enolate was condensed with veratraldehyde and the resulting product cyclised with TFA to (93). Removal of bromine and reduction of the lactone ring to (94) was achieved by the use of lithium aluminium hydride. Methylation of (94) furnished ± (89), which was identical with the naturally occurring hypophyllanthin (Ganeshpure *et al* 1981).

4. Tetrahydrofuranoid lignans

Machilus japonica afforded machilusin (Takaoka *et al* 1979), $C_{21}H_{24}O_5$, mp 121–22°, $[\alpha]_D$ −130·6°, the ^{1}H-NMR spectrum of which suggested its 2,5-diaryl-3,4-dimethyl

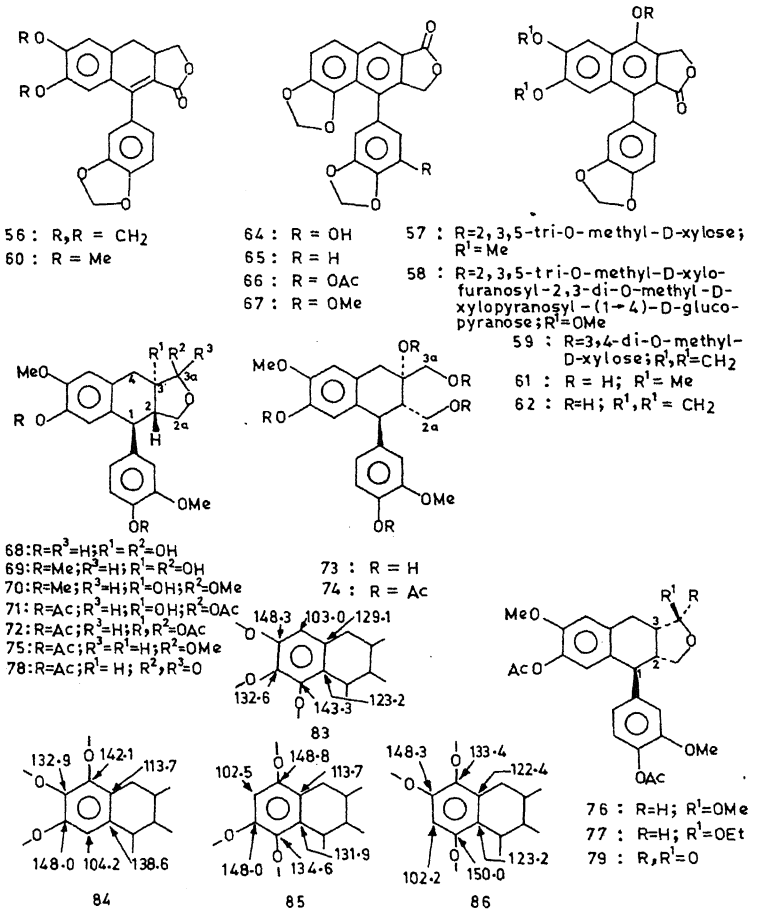

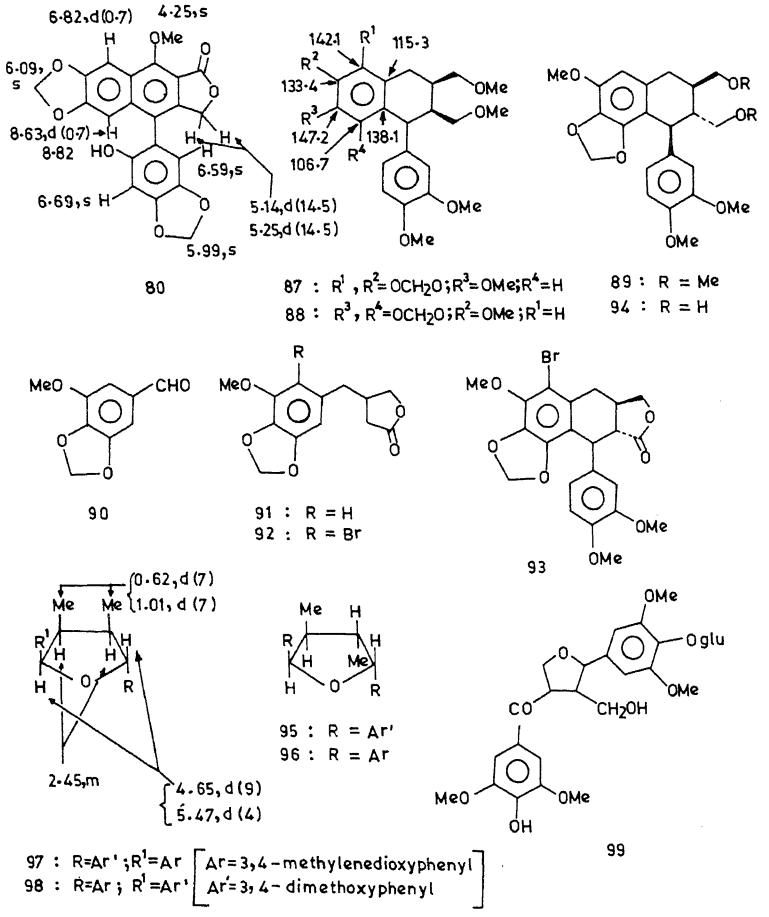

furanoid skeleton. The MS fragmentation pattern, similar to those for galbelgin (95) and galbacin (96) supported this, and in addition gave information regarding the substituents in the two aryl groups. The stereochemistry of the methyl groups at C_3 and C_4 was assigned to be *cis* as the signals for its H-3 and H-4 were different from those having *trans* relationship ($\sim \delta 2{\cdot}25$, 1H, m and $\delta 1{\cdot}80$, 1H, m *e.g.* in verangensin). However, the stereochemistry at C_2 and C_5 remained undecided and accordingly the structure was given as either (97) or (98).

Mangnolenin-C (99), a glucoside with a novel ketolignan skeleton was isolated from *Magnolia grandiflora* (Rao and Wu 1978). A syringoyl unit in it was indicated by its UV spectrum (λ_{max} 310 nm, shifted to 360 nm on addition of alkali), its oxidation by Fremy's salt to a 2,6-dimethoxybenzoquinone and a 2H singlet at $\delta 7{\cdot}20$ in its ^{1}H-NMR spectrum. Another 2H singlet at $\delta 6{\cdot}72$ suggested a syringeresinol unit. A comparison of the ^{1}H-NMR spectra of acetylated derivatives of the glucoside and its aglycone led to the speculation of the glycosidic linkage through one of the phenolic hydroxyl groups.

Another novel lignan, designated sylvone, has been isolated from *Piper sylvaticum* (Banerji *et al*, communicated). This compound has been shown to be (100) (relative configuration) on the basis of chemical and spectroscopical studies. The relative

configuration has been established on the basis of extensive NMR studies including NOE measurements.

Nectandrin A (101), $C_{21}H_{26}O_5$, $[\alpha]_D$ + 10° and nectandrin B (102), $C_{20}H_{24}O_5$, $[\alpha]_D$ 0°, were isolated as oily products from *Nectandra rigida* (LeQuesne *et al* 1980). Their ^{1}H-NMR and MS fragmentation data were in accordance with their formulation as tetrahydrofuranoid derivatives. On methylation, both compounds yield galgravin (103). Structure (101) was assigned to nectandrin A on the basis of the above facts and its likely biogenesis from isoeugenol. The MS of the *bis*-trimethylsilyl derivative of nectandrin B (102) indicated a symmetrical structure for it.

Neo-olivil, $C_{20}H_{24}O_7$, a component of *Thymus longiflorus*, was not obtained in the pure state (Hernandez *et al* 1981), though its MS indicated it to be a tetrahydrofuranoid lignan. Its structure was settled as (104) from spectroscopy studies carried out with its tetra-acetate (105). The IR spectrum of (105) showed bands for both aromatic and aliphatic acetate carbonyls (1735 and 1765 cm^{-1}). The ^{1}H- and ^{13}C-NMR spectra indicated a symmetrical structure. Hence the four substituents were either all *trans*- or in the *cis-trans-cis* configuration. Previous work on the ^{1}H-NMR spectra of similar compounds showed that when the adjacent methyl (corresponding to the $-CH_2OH$ in neo-olivil) and aryl groups were *trans*, the benzylic proton appeared at δ4·48–4·6. Whereas, if these substituents were *cis* this signal appeared at around δ5·1. The benzylic methine appeared at δ5 in neo-olivil tetra-acetate. This was consistent only with the stereochemical formulation (relative configuration) shown in (104).

Chicanine (106), $C_{20}H_{22}O_5$, mp 122–24°, $[\alpha]_D^{31}$ +118·8° ($CHCl_3$), occurs in the fruits of *Schisandra sphenanthera* Rehd et Wils and *S. henryi* Clarke (Liu *et al* 1981). Its spectral properties as well as those of its acetate and monomethyl ether indicated it to be a diastereoisomer of austrobailignan-7 (107). The relative stereochemistry of chicanine was elucidated by ^{1}H-NMR studies (including decoupling and NOE) of dinitrochicanine ethyl ether (108). The absolute configuration of chicanine (106) was established as 2*S*, 3*R*, 4*S*, 5*S* from the transformations outlined in Chart 2 to the known compounds (109) and (110).

Isolivil (111), $C_{20}H_{24}O_7$ (M^+ 376), mp 170–172°, $[\alpha]_D$ −47·9°, is a constituent of *Taxus wallichiana* Zucc (Miller *et al* 1982). Its structure was settled as (111) from detailed ^{1}H and ^{13}C-NMR studies of its tetra-acetate (112).

5. Furofuranoid lignans

Ghosal *et al* (1979b, 1980) have isolated three new lignans belonging to this class from *Justicia simplex*. The first compound was a 2,6-aryloxy furofuranoid lignan, simplexolin (113) (Ghosal *et al* 1979b), $C_{20}H_{18}O_8$, mp 160–62°, whose ^{1}H-NMR spectrum indicated it to be a symmetrical molecule. The UV spectrum (λ_{max} 235, 292 nm) was characteristic of a 1,3,4-trialkoxybenzene. Its structure elucidation rested mainly on correlation of MS data [*m/e* 249 (M-OAr), 219 (2-(3′,4′-methylenedioxyphenyloxy)-2-pyran), 138 $(ArOH)^{\cdot+}$, 137 (ArO) and 81 (pyrylium cation)] with those of sesamolin (114). The ions resulting from aryloxy cleavage (*m/e* 249, 81) (with or without proton transfer) are of diagnostic importance.

Justisolin (115) (Ghosal *et al* 1980), $C_{20}H_{18}O_7$, mp 146–48°, $[\alpha]_D$ +42·7° (chloroform) exhibited a bathochromic shift of its UV maxima from 228 and 282 nm to 245 (sh) and 295–300 nm in presence of base. Its MS showed fragments characteristic of

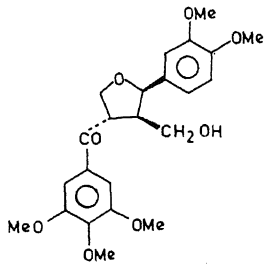

100

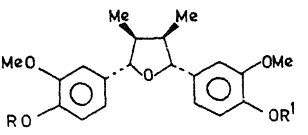

101 : R = H, R^1 = Me
102 : R = R^1 = H
103 : R = R^1 = Me

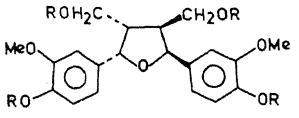

104 : R = H
105 : R = Ac

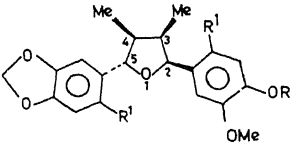

106 : R = R^1 = H
108 : R = Et; R^1 = NO_2

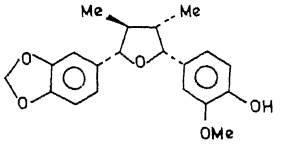

107

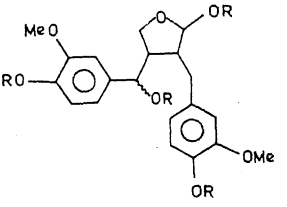

111 : R = H
112 : R = Ac

a furofuranoid lignan bearing a piperonyl and a hydroxymethylenedioxyphenyl moieties. Methylation with diazomethane and permanganate oxidation furnished piperonylic acid and 6-methoxypiperonylic acid. Structure (115) was proposed on the basis of the above facts and a detailed ^{1}H-NMR analysis. Simplexoside (116) (Ghosal *et al* 1980), $C_{26}H_{30}O_{11} \cdot H_2O$, mp 205–10°, $[\alpha]_D$ −12·5° (methanol), was a glycoside which on emulsion hydrolysis afforded the aglycone (117) and glucose. The physical properties of the methyl ether of the aglucone were very similar to those of methylpiperitol (118). The position of the glucosyloxy moiety and the diequatorial configuration of the aryl rings followed from ^{1}H-NMR investigations.

From a comparative study of the ^{13}C-NMR values of several related 2,6-biaryl furofuranoid lignans, Pelter and Ward (1977) revised the structures of epiaschantin and epimagnelin as (119) and (120) in place of (121) and (122) as suggested by Nishino and Mitshui (1973). The C-1″ (belonging to piperonyl and veratryl groups) of these compounds appeared at δ135·2 and δ135·5 respectively indicating their equatorial rather than axial (expected chemical shift in the region δ130–132) orientation. Also the C-1′ (belonging to the 3,4,5-trimethoxyphenyl group) resonated at δ134·1 and δ134·2 respectively to show that these were axial as otherwise these should appear at ~ 136·6 ppm as in aschantin and yangambin.

CHART 2

TRANSFORMATION REACTIONS OF CHICANINE

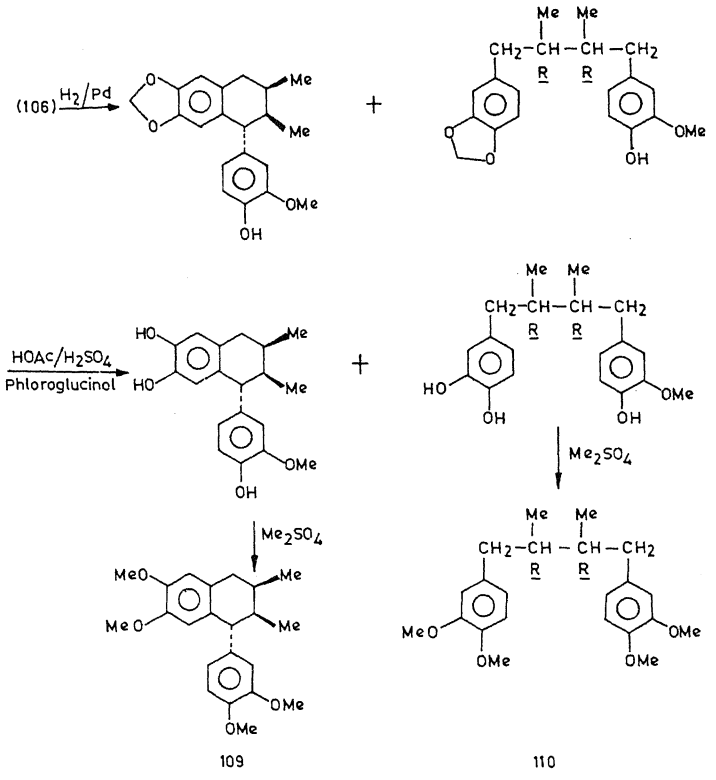

Sylvatesmin (123), $C_{21}H_{24}O_6$ (M^+ 372), mp 122–23°, $[\alpha]_D$ + 158°, is a furofuranoid lignan isolated from *Piper sylvaticum* (Banerji and Pal 1982). Its unsymmetrical ^{1}H- and ^{13}C-NMR spectra and specific rotation value indicated that it belonged to the unsymmetrical epieudesmin series. It was converted by methyl iodide-sodium hydride in THF to a monomethyl derivative, which was identical with (+)-epieudesmin (125). Thus sylvatesmin was a desmethyl-(+)-epieudesmin. The comparatively low-field signal of the two unoxygenated quaternary carbons δ130·7 and δ132·6, assignable to C-1′ and C-1″, suffered a downfield shift by 6·3 ppm in the monoacetyl derivative (126) confirming the position of the phenolic hydroxyl group at C-4′ of the equatorially substituted aryl ring. Sylvatesmin is thus a monomethyl ether of (+)-epipinoresinol (127). (+)-Phyllygenol (forsythigenol), also a monomethyl ether of (+)-epipinoresinol, has been reported earlier to occur as the β-D-glucoside, phyllyrin (forsythin) in various Phyllyrea and Forsythea (Gripenburg 1949) species. The earlier papers on this compound had not confirmed the substitution patterns of the two aryl groups at C-2 and C-6, and therefore two alternative structures (123) and (124) were proposed. Chiba *et al* (1980) confirmed the structure (123) for phylligenol. Thus sylvatasmin and phylligenol are identical to each other. Direct comparison with a sample of phylligenol, obtained in 1983 from Prof. Gripenburg of Helsinki University after the publication of our paper (Banerji and Pal 1982), confirmed their identity.

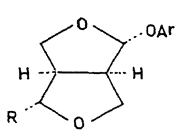

113 : R = OAr
114 : R = Ar

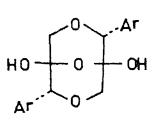

134

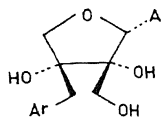

135

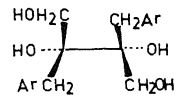

135a

Ar = 3,4-methylenedioxyphenyl

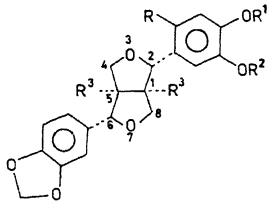

115 : R=OH; R^1, R^2= CH_2 ; R^3=H
116 : R=R^3=H; R^2=Me; R^1=Glu
117 : R=R^1=R^3=H; R^2=Me
118 : R=R^3=H; R^1=R^2=Me
133 : R=H; R^1, R^2=CH_2; R^3=OH

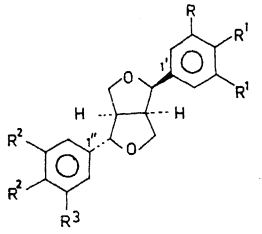

119 : R=R^1=OMe; R^3=H; R^2,R^2=OCH_2O
120 : R=R^1=OMe; R^3=H; R^2 = OMe
121 : R^2=R^3=OMe; R=H; R^1, R^1=OCH_2O
122 : R^2=R^3=OMe; R=H; R^1 = OMe
139 : R^1, R^1=OCH_2O; R=R^2=R^3=OMe

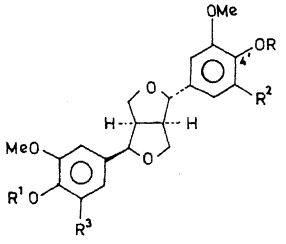

123 : R=R^2=R^3=H; R^1=Me
124 : R^1=R^2=R^3=H; R=Me
125 : R=R^1=Me; R^2=R^3=H
126 : R=Ac; R^1=Me; R^2=R^3=H
127 : R=R^1=R^2=R^3=H
140 : R, R^2=-CH_2O-; R^1=Me; R^3=OMe

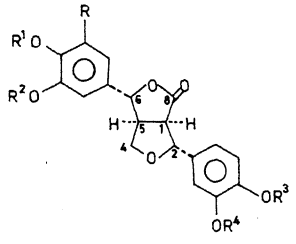

128 : R = R^3 = H; R^4 = Me; R^1,R^2 = CH_2
129 : R^1=R^4=H; R^2=R^3=Me; R = OMe
132 : R=R^1=R^4=H; R^2=R^3=Me
131 : R=H; R^1, R^2=R^3, R^4=CH_2

Ulubelen *et al* (1978) have reported an epoxylignanolide (128), styroxin, $C_{20}H_{18}O_7$ (M^+ 370·1027), mp 146–147°, from *Styrox officinalis*. The furofuranoid skeleton and the structure of the aryl groups were deduced mainly from ^{1}H-NMR and mass spectral data. The stereochemistry at C-2 and C-6 and the position of the lactone carbonyl at C-8 were ascertained by x-ray analyses. The structure of another epoxylignanolide (129), $C_{21}H_{22}O_8$, isolated from *Aegilops ovata* (Cooper *et al* 1977), was established by ^{1}H-NMR and MS studies. The third methoxyl group was placed in the aryl ring attached to C-6 because irradiation at δ6·96 caused narrowing of the signal for H-2, whereas irradiation at δ6·48 showed a similar effect on the 6-H signal.

The 2,4-diaryl furofuranoid structure (130) given earlier to a germination inhibiting epoxylignanolide from *Aegilops ovata* was questioned by Anjaneyulu *et al* (1977) on the basis of its similarity in spectral properties with an epoxylactone having 2,6-diaryl structure (131) obtained by oxidation of 4-hydroxysesamin with CrO_3/pyridine. The

structure was finally revised to (132) as a consequence of its synthesis involving oxidative phenolic coupling of ferulic acid and coniferyl alcohol.

Wodeshiol (133), $C_{20}H_{18}O_8$, mp 153–54°, $[\alpha]_D$ − 12°, was isolated from *Cleistanthus collinus* by Anjaneyulu *et al* (1981). Inoue *et al* (1981) isolated the same compound from *Kigelia pinnata* and designated it kigeliol, mp 150–51°, $[\alpha]_D^{24}$ − 34·6° ($CHCl_3$). Its MS fragmentation was characteristic of a furofuranoid lignan. Its ^{1}H- and ^{13}C-NMR spectra indicated a symmetrical structure. These spectra further indicated the equatorial disposition of the two aryl groups, and showed that positions C-1 and C-5 had hydroxyl substituents. Periodic acid oxidation of wodeshiol afforded the cyclic hemiketal (134). Hydrogenolysis over 10% Pd-C in methanol afforded dihydrokigeliol (135) and tetrahydrokigeliol (135a). The relative stereochemistry was further confirmed by the comparison of the ^{1}H-NMR of (135) with those of similar compounds of established configuration.

Princepiol, $C_{20}H_{22}O_8$ (M^+ 390), mp 190–92°, $[\alpha]_D$ − 18·4° (EtOAc) is a constituent of the oil of *Prinsepia utilis* (Kilidhar *et al* 1982). The symmetrical structure (136) was established from spectroscopical studies of princepiol and its tetraacetate (137). The ^{1}H-NMR spectrum of the latter showed signals for two alcoholic acetoxyls (δ1·80), two phenolic acetoxyls (δ2·32) and two methoxyls (δ3·88). The characteristic high-field signals for the C-1 and C-5 protons were, however, lacking which indicated that these positions were substituted by hydroxyl groups in princepiol. The slight upfield shift ($\sim \delta$0·2) of the aliphatic acetoxyl signals from the normal value suggested shielding by the aryl rings, which is only possible if these groups bear a *cis*-relationship to the acetoxyls. Princepiol and wodeshiol are the only two furofuranoid lignans known so far having a ditertiary glycol system.

A group of four stereoisomeric lignans were isolated by Greger and Hofer (1980) from *Artemisia absinthium*. These were sesartemin (138), mp 112–13°, $[\alpha]_D$ + 52°, episesartemin A (139), mp 112–14°, $[\alpha]_D$ + 115°, episesartemin B (140), mp 115–16°, $[\alpha]_D$ + 127° and diasesartemin (141), mp 102–4°, $[\alpha]_D$ + 315°. These had almost identical UV absorption characteristics. IR and NMR data indicated the presence of a 3,4,5-trimethoxyphenyl and a 3,4-methylenedioxy-5-methoxyphenyl substituents in all the compounds. While the stereochemistry of (138) and (141) could be established fairly easily from their characteristic spectroscopical properties, the distinction between (139) and (140) was more difficult due to the close similarity of their spectral characteristics. However, this was achieved by the use of lanthanide-shift reagents. Comparison of the LIS-shifts between the four compounds allowed unequivocal assignment of the stereochemistry of (139) and (140).

Liriodendrin (142), a di-β-D-glucoside furofuranoid lignan was previously isolated and characterised by Dicky (1958) from *Liriodendrin tulipifera*, who, however, failed to elucidate the stereochemistry of the lignan portion. Jolad *et al* (1980) reported the isolation of liriodendrin from *Penstemon denstus* Dougl ex Lindl and established the diequatorial orientation of the aryl substituents from spectroscopic investigations particularly ^{1}H-NMR studies.

6. Dibenzocyclooctadiene lignans

The first representative member of this type *viz* schizandrin, and a few other compounds were first reported by Kochetkov *et al* (1961, 1962). However, it is the

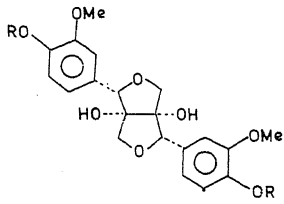

136 : R = H
137 : R = Ac

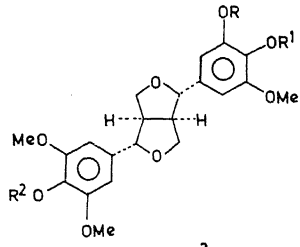

138 : R, R^1 = CH_2; R^2 = Me
142 : R=Me; R^1 = R^2 = Glu

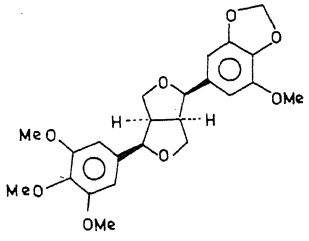

141

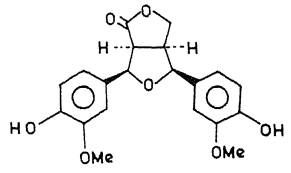

130

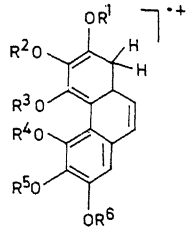

143

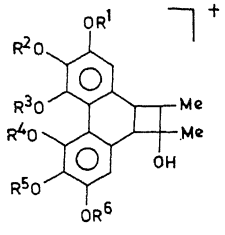

144

recent work of Ikeya, Taguchi and their co-workers which clarified the chemistry of these compounds. Most of these have been isolated from *Schizandra chinensis* Baill, the fruits of which are used as an antitussive and a tonic under the names 'Hoku (or kita) gomishi' in Japan and 'Wu-Wei-Zi' in China. All these lignans have been given the general name of gomisin. Three more lignans of the same skeleton were obtained by the same group from *Kadsura japonica* Dunal (Ookawa *et al* 1981), the dry fruits of which were used as a substitute for those of the former plant under the name 'Nan-gomishi'. These compounds were designated binankadsurins. All the natural compounds are unsubstituted in two, *viz* C-4 and 11 of their aromatic positions, while the other six positions (C-1, 2, 3, 12, 13 and 14) are attached to an oxygen substituent each. The latter are usually –OMe, –OH, $-OCH_2O-$ or occasionally an acyloxy group as at C-14 in derivatives of gomisin H. One of the two benzylic positions is free in all the lignans while the other may or may not carry a substituent—a free hydroxyl or an acyloxy group. Both non-benzylic positions of the cyclooctadiene ring carry a methyl substituent each. While C-8 is always a secondary carbon, C-7 may be either secondary or tertiary. The acyloxy group at C-6 and/or C-14 is usually angeloyloxy, tigloyloxy, acetoxy, caproyloxy or benzoyloxy. However, in gomisin D and E the acyloxy group at

C-6 is part of the cyclic system that is linked to C-14. The structure-elucidation of the compounds were achieved both from spectroscopical and chemical investigations. The UV spectra of these lignans are very characteristic of the basic skeleton and exhibited maxima in the regions 214–225 (log $\varepsilon > 4$), 248–257 (log $\varepsilon > 4$) and 275–294 nm (log $\varepsilon > 3$–4); for certain compounds two maxima rather than one were observed in the latter region. The specific rotations of the lignans could be correlated with their absolute configurations. Those having the *R*-biphenyl configuration showed dextro-rotation while those possessing the *S*-biphenyl configuration showed laevo-rotation. The only exception was gomisin E. Mass spectral studies have also proved useful in the structure-elucidation of the gomisins. In those compounds where acyl groups were present, fragments arising from the acyl groups were most abundant. Besides the molecular-ion peak, fragments (143) and (144) were important for those lignans which have oxygen functions both at C-6 and C-7.

The structure of schizandrin (145) was established from spectral analyses, particularly ^{1}H-NMR and by its conversion into dimethyl-4,4′,5,5′,6,6′-hexamethoxydiphenate on permanganate oxidation followed by methylation (Ikeya *et al* 1978a, 1979a).

Gomisin A (146), mp 88–89°, $[\alpha]_D$ + 67·9°, was characterised by its close resemblance to schizandrin in spectral properties (Taguchi and Ikeya 1977). Treatment of gomisin A with Br_2/CCl_4 saturated with water afforded a dibromo derivative, the ^{1}H-NMR spectrum of which lacked the two aromatic protons and showed a downfield shift of the

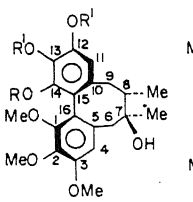

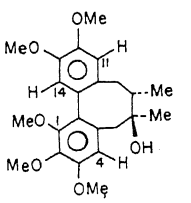

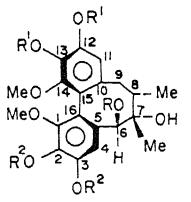

145 : R = R^1 = Me
146 : R = Me; R^1,R^1=CH$_2$
147 : R^1 = Me; R = H
148 : R^1 = Me; R = angeloyl
149 : R^1 = Me; R = tigloyl
150 : R^1 = Me; R = benzoyl
151 : R^1 = Me; R = 2,4-dinitrophenyl
211 : R^1 = Me; R = CH$_2$Ph

152

154 : R^1,R^1 = CH$_2$; R^2 = Me; R = H
155 : R^1,R^1 = CH$_2$; R^2 = Me; R = angeloyl
156 : R^1,R^1 = CH$_2$; R^2 = Me; R = benzoyl
158 : R^1 = Me; R^2,R^2 = CH$_2$; R = H
159 : R^1 = Me; R^2,R^2 = CH$_2$; R = angeloyl
160 : R^1 = Me; R^2, R^2 = CH$_2$; R = benzoyl
162 : R^1 = R^2 = Me; R = H
163 : R^1 = R^2 = Me; R = angeloyl
164 : R^1 = R^2 = Me; R = acetyl

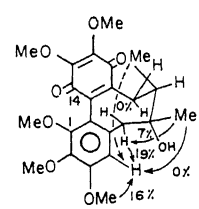

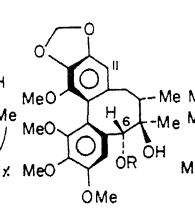

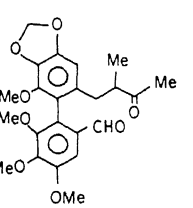

153

166 : R = H
167 : R = tigloyl
168 : R = angeloyl

165

Fig.1

benzylic methylene signals as observed for 4,11-dibromoschizandrin. This suggested proximity of the two aromatic protons (C-4, 11) and the benzylic methylenes. The appearance of H-4 at a higher field in comparison to H-4 of schizandrin (*vide* NOE in figure 2, table 2) established the position of the methylenedioxy moiety at C-12,13.

Gomisin H (147), mp 144–45°, $[\alpha]_D$ +41·2°, gave a monomethyl derivative identical with schizandrin (Ikeya *et al* 1979a). When treated with 2,4-dinitrofluorobenzene ether/NaH gomisin-H yielded the 2,4-dinitrophenyl ether (151). The latter on catalytic hydrogenation over PtO_2 followed by Na/liquid NH_3 treatment afforded (152), whose ^{1}H-NMR showed three singlets for the three aromatic protons. This indicated that the phenolic hydroxyl in gomisin H was *para* to either H-4 or H-11. The oxidation of gomisin H with Fremy's salt produced a *p*-quinonoid compound (153), NOE measurements on which confirmed the location of the phenolic hydroxyl at C-14 (figure 1). The following acylated derivatives of gomisin H were also isolated as amorphous solids (Ikeya *et al* 1978a, 1979a)—angeloylgomisin H (148), $[\alpha]_D$ +19·4°, tigloylgomisin H (149), $[\alpha]_D$ +67·7° and benzoylgomisin H (150), $[\alpha]_D$ +96·8°. These on hydrolysis with methanolic KOH provided gomisin H. All the deacylated derivatives of gomisin B (155) (Ikeya *et al* 1979a; Taguchi and Ikeya 1977), mp 95–97°, $[\alpha]_D$ −26·6°; gomisin C (156) (Ikeya *et al* 1979a; Taguchi and Ikeya 1977), mp 119·5–120·5°, $[\alpha]_D$ −186°; gomisin F (159) (Ikeya *et al* 1979a; Taguchi and Ikeya 1977), mp 119·5–120·5°, $[\alpha]_D$ 0°; gomisin G (160) (Ikeya *et al* 1979a; Taguchi and Ikeya 1977), mp 97–98°, $[\alpha]_D$ −126° and angeloyl gomisin Q (163) (Ikeya *et al* 1979b), mp 82·5–83·5°, $[\alpha]_D$ −26·4°, showed a deshielded methine proton (δ 4·55 ± 0·50) and a non-phenolic hydroxylic proton each. The ^{1}H-NMR spectra of these lignans were otherwise similar and all showed a benzylic methylene signal associated with an ABX octet indicating the presence of Ar–CH_2–$\underset{|}{C}$H–CH_3 moiety in them.

The deacylgomisin B (154), mp 209–10°, $[\alpha]_D$ −91·8°, which was identical with deacylgomisin C, was oxidised by CrO_3/AcOH to the ketoaldehyde (165) and by CrO_3/pyridine to the ketone (157). The spectral characteristics of the compound itself and the oxidised products established its structure as (154). The positions of the functional groups on aromatic rings were ascertained by NOE studies (figure 3) in C_6D_6 (Ikeya *et al* 1979a; Taguchi and Ikeya 1977).

Both gomisin F and G were hydrolysed to a common diol (158), mp 224°, $[\alpha]_D$ −73·1° that yielded a ketone (161) on oxidation with CrO_3/pyridine. The spectral data of gomisin F, G, the diol (158) and the ketone (161) closely resembled those of the corresponding series of gomisin B, C, the diol (154) and the ketone (157) respectively suggesting that the former had the same overall structure as the latter, the only difference being in the arrangement of the substituents on aromatic rings. The actual structures were confirmed by NOE experiments (figure 3) (Ikeya *et al* 1979a; Taguchi and Ikeya 1977).

The structure of gomisin Q (162), mp 191–193°, $[\alpha]_D$ −106°, the hydrolysed product of naturally occurring angeloylgomisin Q (163) (Ikeya *et al* 1979b) was firmly established by its correlation with deangeloyl gomisin B (154). The acetate of the latter was treated with $Pb(OAc)_4$ in dry benzene to cleave the methylenedioxy moiety to an *ortho*-diphenol. Methylation of the latter with Me_2SO_4–K_2CO_3 in dry acetone afforded acetylgomisin Q (164).

Gomisin P (166), $[\alpha]_D$ −94·3°, the hydrolysis product of the naturally occurring lignans tigloylgomisin P (167) (Ikeya *et al* 1978b, 1980b), $[\alpha]_D$ −64·2°, and angeloylgomisin P (168) (Ikeya *et al* 1980b), $[\alpha]_D$ −98·5°, was indicated to be a

diastereoisomer of deacylgomisin B (154) at C-6 and C-7 by ^{1}H-NMR spectroscopy. This was confirmed by the observations that oxidation of gomisin P with CrO_3/pyridine or MnO_2/acetone yielded the same ketoaldehyde (165) derived from (154). Treatment with $CuSO_4$ and 0·25 % H_2SO_4 in dry acetone afforded an acetonide which showed the cis-disposition of the C-6 and C-7 hydroxyls.

The dimethylether of gomisin J was identified as-(−)-deoxyschizandrin (169), *viz* the enantiomer of naturally occurring (+)-deoxyschizandrin (170) (Ikeya *et al* 1978a, 1979a). The positions of the two phenolic hydroxyls were established by NOE measurements (figure 5) in the compound itself (171), mp 149–50°, $[\alpha]_D$ −43·9°, and its dibenzylether (172).

Seven new deoxyschizandrin-type lignans have been reported recently (Ikeya *et al* 1980a, 1982a). These are gomisin L_1 (173) (Ikeya *et al* 1982a), mp 194–96°, $[\alpha]_D$ −53·5° ($CHCl_3$); gomisin L_2 (174), $[\alpha]_D$ −91° ($CHCl_3$); gomisin M_1 (175) (Ikeya *et al* 1982a), mp 116–119°, $[\alpha]_D$ 0° ($CHCl_3$); gomisin M_2 (176) (Ikeya *et al* 1982a), mp 159–60°, $[\alpha]_D$ +54·2° ($CHCl_3$); gomisin K_1 (177) (Ikeya *et al* 1980a), mp 99–101°, $[\alpha]_D$ −96·7° ($CHCl_3$); gomisin K_2 (178) (Ikeya *et al* 1980a), $[\alpha]_D$ +81·7° ($CHCl_3$) and gomisin K_3 (179) (Ikeya *et al* 1980a), mp 100–101°, $[\alpha]_D$ +60·8° ($CHCl_3$). Methylation of gomisin L_1 and L_2 gave the same mono-methylated derivative (180) (Ikeya *et al* 1982a). The appearance of an upfield methoxyl signal at δ 55·7 and two downfield methoxy signals

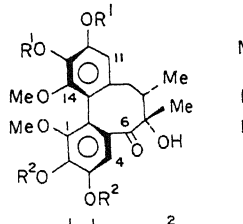

157 : R^1,R^1=CH_2; R^2=Me
161 : R^2,R^2=CH_2; R^1=Me
191 : R^1=R^2=Me
192 : R^1,R^1=CH_2; R^2=Me

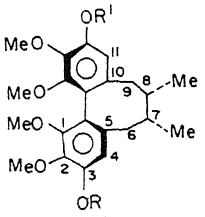

169 : R=R^1=Me
171 : R=R^1=H
172 : R=R^1=CH_2Ph
177 : R=Me; R^1=H

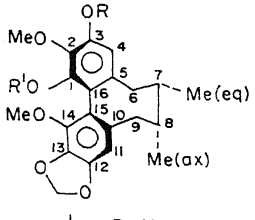

173 : R^1=H; R=Me
174 : R^1=Me; R=H
180 : R=R^1=Me
181 : R^1=Ac; R=Me
182 : R^1=Me; R=Ac
193 : R^1=Me; R=p-bromobenzoyl

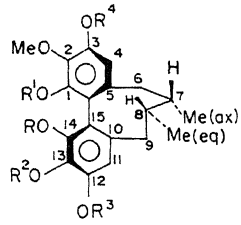

170 : R=R^1=R^2=R^3=R^4=Me
175 : R^1=H; R=R^4=Me; R^2,R^3=CH_2
176 : R^1=R^4=Me; R=H; R^2,R^3=CH_2
178 : R=R^1=R^2=R^3=Me; R^4=H
179 : R=R^2=R^3=R^4=Me; R^1=H
183 : R=R^1=R^2=R^3=Me; R^4=Ac
184 : R=R^2=R^3=R^4=Me; R^1=2,4-dinitrophenyl

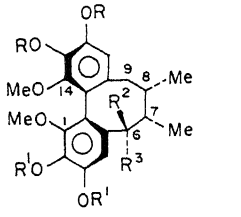

185–190 : R, R=CH_2; R_1=Me

185 : R^2=R^3=H
186 : R^2=OH; R^3=H
187 : R^2=D; R^3=H
188 : R^2=O-Angeloyl; R^3=H
189 : R^2=H; R^3=OH
190 : R^2,R^3=O

194–198 : R=Me; R^1, R^1=CH_2

194 : R^2=O-Angeloyl; R^3=H
195 : R^2=$PhCO_2$; R^3=H
196 : R^1=OH; R^3=H
197 : R^2=R^3=H
198 : R^2, R^3=O

199 : R, R=R^1, R^1=CH_2; R^2=OH; R^3=H
200 : R, R=R^1, R^1=CH_2; R^2, R^3=O
201 : R, R=R^1, R^1=CH_2; R^2=R^3=H

at δ59·7 and δ61 in the ^{13}C-NMR of (173) indicated the presence of a methoxyl at C- adjacent to an aromatic proton, and an hydroxyl either at C-1, C-2 or C-14 Comparison of chemical shifts with (180) and the acetate (181) showed that C- underwent a shift of +3·6 ppm on methylation and +6·2 ppm on acetylation of (173) Thus the hydroxyl must be at C-1 in gomisin L_1. For gomisin L_2 (174), the occurrenc of three downfield methoxyl signals at δ59·6, δ60·1 and δ61 indicated the location o the hydroxyl at C-3. This was confirmed by comparing ^{13}C-chemical shifts with (180 and its acetate (182). Similar comparisons of the ^{13}C-NMR data of gomisins M_1 (175 and M_2 (176) with their corresponding derivatives indicated the positions of th hydroxyls to be C-1 and C-14 respectively. The lack of extrema in the CD curve o gomisin M_1 indicated that it was racemic. The three isomeric compounds, gomisins K_1 K_2 and K_3, all had five methoxyl and one hydroxyl aromatic substituents. Gomisin K underwent mono-methylation to give (169). Its structure was settled as (177) from NO measurements (figure 5) which located the hydroxyl at C-12. Methylation of gomisi K_2 (178) and K_3 (179) gave (+)-deoxyschizandrin (170). ^{13}C-NMR comparisons of (178) (170) and the corresponding acetate (183) fixed the position of the hydroxyl at C-3 i gomisin K_2. Here the ortho-C-4 carbon experienced downfield shifts of 2·5 ppm an 9·8 ppm on methylation and acetylation respectively. Treatment of gomisin K_3 wit 2,4-dinitrofluorobenzene/NaH gave the 2,4-dinitrophenyl ether (184) which o reduction afforded deoxygomisin K_3 where the hydroxyl had been replaced by hydrogen. The ^{1}H-NMR spectrum of the latter showed three singlets for the thre aromatic protons thereby indicating that in the original lignan (179), the hydroxy group was located at the *para*-position (C-1 or C-14) to an aromatic proton. Finally, th ^{13}C-NMR spectrum of (179) showed that the hydroxyl group was present at C-1.

The structure of gomisin N (185) (Ikeya *et al* 1978b, 1979a), mp 105–107°, $[\alpha]_D$ −84·7 was firmly established by subjecting it to cleavage of its methylenedioxy moiety wit lead tetra-acetate in benzene and then converting the resulting biphenol into dimethy gomisin J (169) by reacting with Me_2SO_4/K_2CO_3.

Gomisin O (186), mp 145–146·5°, $[\alpha]_D$ −33·9° is 6β-hydroxygomisin N and this wa confirmed by (i) identification of its hydrogenolysis (over PtO_2 in AcOH) product a gomisin N, (ii) characterisation of the hydrogenolysis (over PtO_2 in AcOH-d_4) product $C_{23}H_{27}DO_7$ (M^+ 401) as 6β-deuterogomisin N (187) (6α−H at δ2·56, d J = 8 Hz) and (iii) its preparation from gomisin N on oxidation with $Pb(OAc)_4$ i AcOH followed by hydrolysis with 0·5 M KOH in methanol (Ikeya *et al* 1979a). It structure was confirmed by NOE experiments (figure 6). Angeloyl gomisin O (188), $[\alpha]_D$ 47·1° ($CHCl_3$), has been obtained recently (Ikeya *et al* 1982b).

The fact that epigomisin O (189) (Ikeya *et al* 1979a), $[\alpha]_D$ −66·7°, is epimeric wit gomisin O at C-6 was proved by transforming this chiral centre into a carbonyl grou on oxidation with CrO_3/py yielding the same ketone (190). Also the reduction of th latter with $NaBH_4$ in MeOH furnished the two epimers in almost equal amounts i support of the above view.

A notable observation is the oxidation of (±) deoxyschizandrin {(169) and (170)} with $KMnO_4$/2% NaOH in pyridine to a ketoalcohol (191) (Ikeya *et al* 1979a). In th process the C-6 benzylic methylene was converted to a keto group and C-7 methine int a carbinol accompanied by the inversion of the configuration at this centre. Followin the same procedure gomisin N was transformed into a mixture of ketoalcohol (192) an the ketone (190)—the latter being oxidisable further by alkaline $KMnO_4$ in dioxane t the former. The compound (192) is reduced by $NaBH_4$ in methanol to deacyl gomisin (154) as the only product (*cf.* reduction of (191) into two epimers).

Angeloyl isogomisin O (194), mp 122–23°, $[\alpha]_D$ +52·2° ($CHCl_3$) and benzoyl isogomisin O (195), $[\alpha]_D$ −14·7° ($CHCl_3$), on hydrolysis yielded isogomisin O (196) (Ikeya *et al* 1982b). Comparison of the ^{13}C-NMR data of (196) with those of the isomeric gomisin O (186) showed close similarity between the chemical shifts except for C-4 and C-11. This indicated that isogomisin O possessed a methylenedioxy group at the C-2, 3 positions instead of at C-12, 13, a *cis*-dimethyl configuration, a $C_6\beta$-hydroxyl group and a similar conformation to (186). The structure was finally confirmed by correlating it with (±)-γ-schizandrin (197). The latter on $KMnO_4$-pyridine-NaOH oxidation yielded (±) (198), whose optically active form was obtained by CrO_3 oxidation of isogomisin O (196).

The ^{13}C-NMR chemical shifts of gomisin R (199) (Ikeya *et al* 1982a), $[\alpha]_D$ −21·1° ($CHCl_3$), were similar to those of gomisin O regarding the alicylic portion, thereby indicating the similarity in stereochemistry and conformation. The ^{13}C-NMR data exhibited two downfield methoxyls at δ59·5 and δ59·6, which must therefore occupy positions C-1 and C-14. The structure of gomisin R(199) was finally confirmed by establishing the identity of its CrO_3 oxidation product (200), with the alkaline permanganate oxidation product of wuweizisu C (201). The structure of the latter, which occurs in the same plant, was established by its correlation with dimethylgomisin J (169).

The structural pattern of gomisin D (202) (Ikeya *et al* 1976), mp 194°, $[\alpha]_D$ −58·8°, and gomisin E (203) (Ikeya *et al* 1979a), $[\alpha]_D$ +28·1° was elucidated by comparison of their ^{1}H-NMR spectra with that of gomisin B. The presence of the partial structure, Ar–CH(COOR)–CH–CH_3 was confirmed by double irradiation experiments in gomisin E. The cyclic ester system in both the lignans was confirmed by their hydrolysis with 3% KOH in MeOH followed by methylation with CH_2N_2 leading to products (204) and (205) respectively. The ion peaks at *m/e* 145·0820 [$\overset{+}{C}H_2CHMeCMe$ (OH) CO_2Me], 127·08, 113·06, 103·04 and 85·07 in the MS of (204) and (205), taken in conjunction with ^{1}H-NMR data confirmed the structure of the side-chain.

Three lignans with an oxygen substituent at C-9, *viz* acetylbinankadsurin A (214), mp 188–92° $[\alpha]_D$ ~ 0°, angeloylbinankadsurin A (206), mp 121–22°, $[\alpha]_D$ +61·5°, and caproylbinankadsurin-A (207), mp 83–87°, $[\alpha]_D$ +14·7°, were isolated from *Kadsura japonica* Dunal (Ookawa *et al* 1981).

Binankadsurin-A (208) was obtained by the ethanolic KOH hydrolysis of these compounds. The CD spectrum of acetylbinankadsurin-A (214) indicated that the compound possessed the S-biphenyl configuration. This compound on methylation afforded kadsurin (209) and on oxidation with Fremy's salt gave the quinone (210). ^{13}C-NMR comparisons of (214) with (209) and (210) settled the substitution pattern in the aromatic rings.

Certain general features of the dibenzocyclooctadiene lignans are discussed below. These lignans can have either the R– or the S-biphenyl configurations. Further the 8-membered ring can take up either a boat (figure 6) or a twist chair-boat (figure 5) conformation—this depends on the substitution pattern in these rings.

a. ^{13}C-NMR spectra

A detailed and systematic ^{13}C-NMR of the gomisin-type compounds has been reported earlier (Ikeya *et al* 1980c).

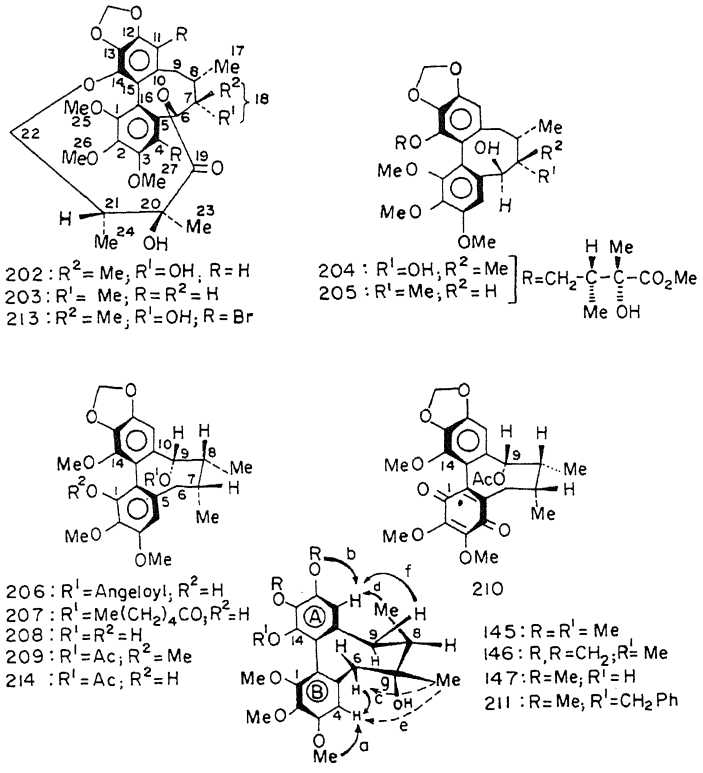
202 : R² = Me; R¹ = OH; R = H
203 : R¹ = Me; R = R² = H
213 : R² = Me; R¹ = OH; R = Br
204 : R¹ = OH; R² = Me
205 : R¹ = Me; R² = H
R = CH₂-C(H Me)-C(H Me)-CO₂Me
Me OH
206 : R¹ = Angeloyl; R² = H
207 : R¹ = Me(CH₂)₄CO; R² = H
208 : R¹ = R² = H
209 : R¹ = Ac; R² = Me
214 : R¹ = Ac; R² = H
210
145 : R = R¹ = Me
146 : R, R = CH₂; R¹ = Me
147 : R = Me; R¹ = H
211 : R = Me; R¹ = CH₂Ph

Fig. 2

b. ^{1}H-NMR spectra

All the lignans exhibited two singlets in the region δ6·4–7·0 for the two aromatic protons, H-4 and H-11. In compounds having a planar structure with a mirror plane of symmetry the two protons resonate at the same position, *e.g.* in deoxyschizandrin (169) at δ6·55 and in gomisin J (171) at δ6·63.

The C-6 methylene in a lignan having R-biphenyl configuration is in an exactly similar environment as the C-9 methylene of its enantiomer. An analogous situation arises for H–C^7–Me and H–C^8–Me between the two enantiomers provided the C-7 and C-8 methyls are in the *cis* configuration. In the twist boat-chair conformation of the cyclooctadiene ring the H-6α and H-9β are in the diamagnetic shielding cone of ring B and A respectively and therefore resonate upfield of H-6β and H-9α in both the R- and S-biphenyl compounds. The C-8 methyl (axial) in R-biphenyl compounds having a twist boat-chair conformation experiences shielding by ring A and therefore appears upfield in comparison to the C-7 methyl (equatorial). In some compounds of the S-biphenyl series (figure 5) the opposite observation is noted for good reasons since only the C-7 methyl (axial) experiences shielding by ring B. But in gomisin B, C, F, G, Q the C-7 methyl is equatorial and hence does not suffer any upfield shift, and appear at δ1·33, 1·36, 1·25, 1·33 and 1·40 respectively.

However, in gomisin O the two secondary methyls at C-7,8 appears together at δ0·92,

while in gomisin E the C-8 methyl (δ0·70) appears upfield of the C-7 methyl (δ0·92), though these two lignans possess S-biphenyl configurations. This is due to the boat conformation of their cyclooctadiene ring (figure 6).

c. NOE measurements (figures 2–6, table 1)

Nuclear overhauser effect measurement technique is extensively utilised to find out the proximity of various protons. This helps in elucidation of the structure, assignment of the signals to the appropriate protons as well as in the determination of conformation and relative stereochemistry.

The position of methylenedioxy moiety adjacent to H-4 or H-11 in various lignans was unequivocally decided by irradiation at each methoxyl signal in which case the protons H-4 or H-11 adjacent to the methylenedioxy remained unaffected. In gomisin J (171) irradiation at each methoxyl caused no enhancement in the integrated intensity of the aromatic protons while irradiation at the oxymethylene protons in its dibenzyl ether (172) intensified both of these (figure 5) showing the positions of the two phenolic hydroxyls at C-3 and C-12. In benzyl gomisin H (211) each of H-4 and H-11 suffered NOE by irradiation of methoxyls eliminating the possibility of the only phenolic hydroxyl being at either the C-3 or C-12 positions in gomisin H (147, figure 2).

NOE was observed at H-4 and H-11 upon irradiation of H-6α and H-9β respectively since these are in close proximity with each other. This would help to determine the α- or β-configuration of the substituent, if there be any, at these benzylic positions. Thus NOE was felt at H-4 of angeloyl gomisin B (155), F (159), D (202) (figure 3) and E (203) (figure 4) upon irradiation of H-6, but the effect was absent in epigomisin O (189) and tigloylgomisin P (167, figure 5).

The axial group at C-8 is close to H-11; hence irradiation of the secondary methyl at C-8 would determine its axial or equatorial orientation depending upon whether or not NOE is observed at H-11. As the experiments reveal in *R*-biphenyl lignans this methyl is axial, whereas in S-biphenyl compounds it is equatorial. From similar analyses of NOE between the C-7 methyl and H-4 it becomes apparent that in all of the reported *R*-biphenyl lignans this is equatorial (figure 2) but in some (figure 4) of the S-biphenyls it is equatorial while in others (figure 3) it is axial. This criterion is of use for the lignans having the twist boat-chair conformation of the cyclooctadiene ring, whereas it fails for those having the 8-membered ring in the boat conformation (186 and 212 in figure 6).

NOE measurement data also provided clear distinction between the geometrically isomeric acyl groups-angeloyl and tigloyl. In the angeloyl group the olefinic proton suffered NOE upon irradiation of both allylic methyls, whereas in the tigloyl group it showed NOE upon irradiation of one methyl only. This is important since the tigloyl group is isomerised yielding angelic acid during hydrolysis of the acylated lignans, and since the ^{1}H-NMR data on their own are inadequate to solve the problem satisfactorily.

d. Absolute configuration

The absolute configuration of gomisin D (202 shown in figure 3) has been established from the x-ray study of its 4,11-dibromoderivative (213) as 6S, 7S, 8S, 20R, 21R and S-biphenyl. The absolute stereochemistry of gomisin E (203, figure 4) at C-8, -20, -21

Table 1. Results of NOE measurements.

Compounds	Measurements							Compounds	Measurements						
	a	*b***	*c*	*d*	*e*	*f*	*g*		*a*	*b***	*c*	*d*	*e*	*f*	*g*
177	12	0†	—	0	12	13	0	203	12	0	12	—	0	9	15
145	14	13	15	11	0	10	—	172	14	12	15	0	10	16	—
146	14	0	12	10	0	12	—	185	14	0†	—	0	14	13	—
211	17	13	—	10	0	—	—	186	10	0†	14	0	—	12	15
155	12	0†	21	0	—	29	11	189	15	0†	0(*c'*)	0	14	13	0
159	0†	10	22	0	—	13	20	167*	14	0	0(*c'*)	0	0	10	0
202+	13	0	28	0	—	15	14								

Results given as percentage enhancements of signal intensities.
* C_8-H 13% C_6-H. ** Irradiations were done at C_{12}-OMe (where enhancements are observed or at each –OMe (where the result is zero). † Irradiation at each –OMe.
+ –C_8-H 8% C_{11}-H.

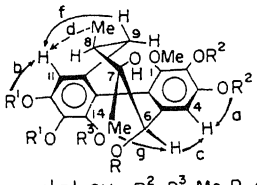

155 : R¹,R¹=CH₂; R²=R³=Me; R=angeloyl
159 : R²,R²=CH₂; R¹=R³=Me; R=angeloyl
202 : R¹,R¹=CH₂; R²=Me
R+R³=-CH₂-CHMe-CMe(OH)-CO-

Fig. 3

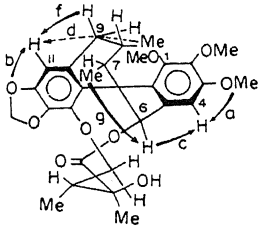

203

Fig. 4

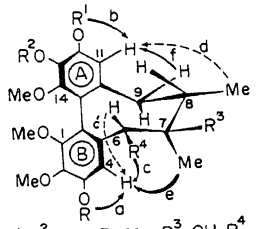

167 : R¹,R²=CH₂; R=Me; R³=OH; R⁴=MeCH=CMeCOO
171 : R=R¹=R³=R⁴=H; R²=Me
172 : R=R¹=CH₂Ph; R²=Me; R³=R⁴=H
185 : R¹,R²=CH₂; R=Me; R³=R⁴=H
189 : R¹,R²=CH₂; R=Me; R³=H; R⁴=OH

Fig. 5

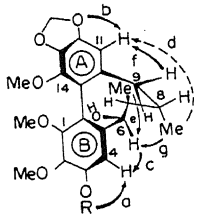

186

212 : C_8-epimer of 186

Fig. 6

Table 2. CD data of lignans.

Compound		Configuration of biphenyl part	[θ] (nm)
	(204)	S	−72400 (249); −78500 (240); +54000 (216)
Schizandrin	(145)	R	+95000 (250); +75000 (235); −100000 (214)
Gomisin B	(155)	S	−52000 (252); +46000 (223)
Gomisin A	(146)	R	+120000 (253); +88000 (242); −110000 (222)
Gomisin J	(170)	S	+9800 (278); −83000 (248); −62000 (236); +62000 (214)
Gomisin G	(160)	S	−12000 (285); −44000 (255); −77000 (239); +38000 (222)
Gomisin D	(202)	S	−3900 (248); +116000 (230)
Gomisin E	(203)	S	−19000 (288); −31000 (243); +47000 (228)
Epigomisin D	(189)	S	−10000 (290); −54000 (251); +40000 (227)
Tigloylgomisin P	(167)	S	−76000 (253); −66000 (242); +62000 (221)
Gomisin L_1	(173)	S	−3700 (298); −1400 (287); −96000 (252); −16000 (230); 17000 (228)
Gomisin L_2 *p*-bromobenzoate	(193)	S	−61000 (254); −17000 (239); −25000 (231); 0 (224); 24500 (218)
Gomisin M_2	(176)	R	+87000 (249); 0 (232); −80000 (217)

and the biphenyl part has been confirmed by correlation with gomisin D. The configuration in the biphenyl part of all other lignans has been decided by comparison of their CD spectra with that of (204) derived from gomisin D. The configurations are S or R according as their CD curves are similar or almost mirror images of the latter (204) (table 2).

The conformations of the alicyclic ring including configurations at various chiral centres have been determined by NOE measurements (figures 2–6). The conformations have been verified by Dreiding model construction and by comparison of the dihedral angles between adjacent protons in models with the values calculated from the observed J values. Thus in most of the lignans the values $J_{8,9\alpha} = 8\text{-}9$ Hz and $J_{8,9\beta} = 1\text{-}2$ Hz are in conformity with the dihedral angles, $H\text{–}C_8\text{–}C_9\text{–}H_\alpha \approx 150°$ or 30° and $H\text{–}C_8\text{–}C_9\text{–}H_\beta \approx 90°$ respectively.

However, the NOE results of gomisin O are consistent with three forms which are (186), its C_8-epimer (212) (figure 6) and (189: 6β-OH) (figure 5). The latter has been excluded by a study of Dreiding models showing $H\text{–}C_6\text{–}C_7\text{–}H \approx 90°$, which would have the J zero contrary to observed value of 8 Hz. Thus gomisin O should correspond to (186) or its C_8-epimer (212) ($H\text{–}C_6\text{–}C_7\text{–}H \approx 150\text{–}180°$). The boat conformation (figure 6) has been accepted in preference to the twist boat-chair (figure 5) in which the steric interaction between ring A and the C_6-axial hydroxyl group and also that between ring B and the C_7-axial methyl would be extremely severe.

References

Agrawal P K and Rastogi R P 1982 *Phytochemistry* **21** 1459

Anjaneyulu A S R, Rao A M, Rao V K, Row L R, Pelter A and Ward R S 1977 *Tetrahedron* **33** 133

Anjaneyulu A S R, Ramaiah P R, Row L R, Venkateswarlu R, Pelter A and Ward R S 1981 *Tetrahedron* **37** 3641

Banerji A and Pal S 1982 *Lloydia J. Nat. Pdts.* **45** 672

Banerji A, Pal S C, Sarkar M and Ghosal T *Tetrahedron* (communicated)

Batsuren D, Batirov E K, Malikov V M, Zemlyanskii V N and Yagudaev M R 1981 *Khim. Prir. Soedin* 295

Bohlmann F, Lonitz M and Knoll K H 1978 *Phytochemistry* **17** 330

Brown E, Loriol M and Robin J P 1979 *Tetrahedron Lett.* 1389

Cambie R C, Parnell J C and Rodrigo R 1979a *Tetrahedron Lett.* 1085

Cambie R C, Pang G T M, Parnell J C, Rodrigo R and Weston R J 1979b *Aust. J. Chem.* **32** 2741

Chakravorty D P, Roy R and Guha R 1977 *Chem. Ind.* 231

Chakravorty D P, Roy S, Sinha Roy S P and Mazumdar S 1979 *Chem. Ind.* 667

Chatterjee A, Banerji J, Das B and Shoolery J N 1984 *Phytochemistry* (accepted for publication)

Chatterjee A, Das B, Pascard C and Prangé T 1981 *Phytochemistry* **20** 2047

Chiba M, Misada S, Nishibe S and Thieme H 1980 *Phytochemistry* **19** 335

Cooper R, Levy E C and Lavie D 1977 *J. Chem. Soc. Chem. Commun.* 794

Dewick P M and Jackson D E 1981 *Phytochemistry* **20** 2277

Dicky E E 1958 *J. Org. Chem.* **23** 179

Ganeshpure P A, Schneiders G E and Stevenson R 1981 *Tetrahedron Lett.* 393

Gensler W J, Johnson F and Sloan A D B 1960 *J. Am. Chem. Soc.* **82** 6074

Ghosal S, Banerjee S and Frahm A W 1979a *Chem. Ind.* **23** 854

Ghosal S, Banerjee S and Jaiswal D K 1980 *Phytochemistry* **18** 332

Ghosal S, Banerjee S and Srivastava R S 1979b *Phytochemistry* **18** 503

Greger H and Hofer O 1980 *Tetrahedron* **36** 3551

Gripenburg J 1949 *Acta Chem. Scand.* **3** 898

Hartwell J L and Detty W E 1950 *J. Am. Chem. Soc.* **72** 246

Hernandez A, Pascual C and Valverde S 1981 *Phytochemistry* **20** 181

Ikeya Y, Taguchi H and Iitaka Y 1976 *Tetrahedron Lett.* 1359

Ikeya Y, Taguchi H and Yosioka I 1978a *Chem. Pharmacol. Bull.* **26** 378, 682
Ikeya Y, Taguchi H and Yosioka I 1979b *Chem. Pharmacol. Bull.* **27** 2536
Ikeya Y, Taguchi H and Yosioka I 1980a *Chem. Pharmacol. Bull.* **28** 2422
Ikeya Y, Taguchi H, Yosioka I and Kobayashi H 1980b *Chem. Pharmacol. Bull.* **28** 3357
Ikeya Y, Taguchi H, Sasaki H, Nakagima K and Yosioka I 1980c *Chem. Pharmacol. Bull.* **28** 2414
Ikeya Y, Taguchi H and Yosioka I 1982a *Chem. Pharmacol. Bull* **30** 132, 3209
Ikeya Y, Ookawa N, Taguchi H and Yosioka I 1982b *Chem. Pharmacol. Bull.* **30** 3202
Ikeya Y, Taguchi H, Yosioka I and Kobayashi H 1978b *Chem. Pharmacol. Bull.* **26** 3257
Ikeya Y, Taguchi H, Yosioka I and Kobayashi H 1979a *Chem. Pharmacol. Bull.* **27** 1383, 1576, 1583, 2695
Inoue K, Inouye H and Chan C C 1981 *Phytochemistry* **20** 2271
Jolad S D, Hoffmann J J, Cole J R, Tempesta M S and Bates R B 1980 *J. Org. Chem.* **45** 1327
Jolad S D, Wiedhopf R M and Cole J R 1977 *J. Pharmacol. Sci.* **66** 892
Joshi B S, Ravindranath K R and Viswanathan N 1978 *Experientia* **34** 422
Joshi B S, Viswanathan N, Balakrishnan V, Gawal D H and Rabindranath K R 1979 *Tetrahedron* **35** 1655
Kato A and Hashimoto Y 1979 *Lloydia* **42** 159
Kilidhar S B, Parthasarathy M R and Sharma P 1982 *Phytochemistry* **21** 796
Klyne W, Stevenson R and Swan R J 1966 *J. Chem. Soc.* (*C*) 893
Kochetkov N K, Korlin A, Chizhov O S 1962 *Tetrahedron Lett.* 361
Kochetkov N K, Korlin A, Chizhov O S and Scheichenko V I 1961 *Tetrahedron Lett.* 730
LeQuesne P W, Larrahondo J E and Raffauf R F 1980 *Lloydia-J. Nat. Pdts.* **43** 353
Liu J S, Huang M F, Gao Y L and Findlay J A 1981 *Can. J. Chem.* **59** 1680
Miller R W, McLaughlin J L, Powell R G, Plattner R D, Weisleder D, and Smith C R 1982 *Lloydia–J. Nat. Pdts.* **45** 78
Nishino C and Mitshui T 1973 *Tetrahedron Lett.* 335
Nimgirawath S, Ritchie E and Taylor W C 1977 *Aust. J. Chem.* **30** 451
Olaniyi A A and Powell J W 1980 *Lloydia–J. Nat. Pdt.* **43** 482
Ookawa N, Ikeya Y, Taguchi H and Yosioka I 1981 *Chem. Pharmacol. Bull.* **29** 123
Pelter A and Ward R S 1977 *Tetrahedron Lett.* 4137
Rao C B S 1978 *Chemistry of lignans* (Andhra Pradesh: Andhra University Press and Publications)
Rao V K and Wu W 1978 *Lloydia–J. Nat. Pdts.* **41** 56
Row L R, Srinivasulu C, Smith M and Subba Rao G S R 1966 *Tetrahedron* **22** 2899
Row L R, Satyanarayan P and Srinivasulu C 1970 *Tetrahedron* **26** 3051
Schrecker A W and Hartwell J L 1954 *J. Am. Chem. Soc.* **76** 4896
Suzuki H, Lee K H, Hawna M, Iida T, Ito K and Huang H C 1982 *Phytochemistry* **21** 1824
Swan R J, Klyne W and MacLean H 1967 *Can. J. Chem.* **45** 319
Taguchi H and Ikeya Y 1977 *Chem. Pharmacol. Bull.* **25** 364
Takaoka D, Imooka M and Hiroi M 1977 *Bull. Chem. Soc. Jpn.* **50** 2821
Takaoka D, Watanabe K and Hiroi M 1979 *Bull. Chem. Soc. Jpn.* 3554
Tandon S and Rastogi R P 1976 *Phytochemistry* **15** 1789
Ulubelen A, Saiki Y, Lotter H, Chari V M and Wagner H 1978 *Planta Medica* **34** 403
Viviers P M, Ferreira D and Roux D G 1979 *Tetrahedron Lett.* 3773
Ward R S 1982 *Chem. Soc. Rev.* 75
Ward R S, Satyanarayan P, Row L R and Gopala Rao B V 1979 *Tetrahedron Lett.* 3043
Yamaguchi H, Arimoto M, Tanoguchi M, Ishide T and Inoue M 1982 *Chem. Pharmacol. Bull.* **30** 3212

Proc. Indian Acad. Sci. (Chem. Sci.), Vol. 93, No. 6, August 1984, pp. 1059–1078.
© Printed in India.

Studies directed towards the total synthesis of anthracycline antibiotics

A V RAMA RAO
National Chemical Laboratory, Pune 411 008, India

Abstract. At present anthracycline antibiotics have proven to be the most exciting agents in cancer chemotherapy. Both adriamycin and daunomycin are proven to be effective against a variety of human tumour cells, despite their cardiotoxicity. However, some synthetic analogues, such as 4-demethoxydaunomycin, are shown to be better therapeutic ratios compared to adriamycin or daunomycin. Various approaches have been successfully made for the total synthesis of (±) 4-demethoxydaunomycinone, the aglycone of (±) 4-demethoxydaunomycin, starting from benzoquinone, napthalene or anthraquinone precursors. Finally an elegant approach for the stereoconvergent synthesis of (+) 4-demethoxydaunomycinone has been worked out.

New methods involving both Diels-Alder and Friedal-Crafts acylation, have been developed for the total synthesis of daunomycinone and 11-deoxydaunomycinone. The synthesis of L-daunosamine, the amino sugar unit present in the antitumor anthracyclines has been successfully elaborated starting either from D-glucose or D-glucosamine.

Keywords. Anthracyclines; antitumor antibiotics; adriamycin; daunomycin; daunomycinone; 4-demethoxydaunomycinone; 11-deoxydaunomycinone; L-daunosamine; 2-acetyl-2-hydroxy-5,8-dimethoxy 1,2,3,4-tetrahydronaphthalene.

1. Introduction

About 20% of the deaths in Western countries are currently ascribed to neoplastic diseases, *i.e.* those associated with growth of new abnormal body tissues commonly referred as 'cancer'. This disease has engaged the worldwide attention of a variety of research workers.

Radiation and surgery have certainly a curative effect as long as it is detected at an early stage and localized. But unfortunately by the time it is detected, the disease often spreads to other organs of the body and then the answer lies in chemotherapy either exclusively or in combination with surgery and radiation.

A large number of anti-cancer drugs are now being used in medical practice which have been approved by the National Cancer Institute (USA). Further, many are undergoing clinical trials. All these drugs can be broadly classified into (a) alkylating agents, (b) antimetabolites, (c) antibiotics, and (d) miscellaneous compounds.

Among the various compounds which are promising as antitumor agents, natural products, either of plant or microbial origin, are showing much more specificity in their anti-cancer properties. Many of them possess structures and clinical properties which suggest that they may act by selective alkylation of growth regulatory macromolecules.

The usefulness of certain anthracycline antibiotics as anti-neoplastic agents are now widely accepted. Both daunomycin (Arcamone *et al* 1964) (daunorubicin; 1a) and adriamycin (Arcamone *et al* 1969) (doxorubicin; 1b) produced by *Streptomyces peucetius* (Family: *Streptomycetacea*) and a mutant strain respectively, have shown pronounced anti-cancer activity in some types of human cancer (Arcamone 1977; Di Marco *et al* 1969). However, their use is restricted by a dose-limiting cardiotoxicity

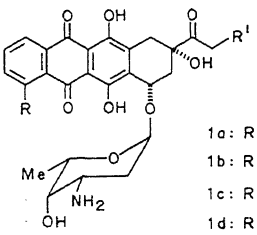

1a: R = OMe; R^1 = H
1b: R = OMe; R^1 = OH
1c: R = OH; R^1 = H
1d: R = R^1 = H

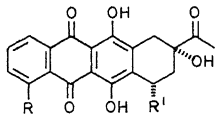

2a: R = OMe; R^1 = OH
2b: R = H; R^1 = OH
2c: R = R^1 = H

(congestive heart failure). Recently, carminomycin (1c), (Wani *et al* 1975; Pettit *et al* 1975) isolated from *Actinomadura carminata* sp. nov. and *Streptosporangium* sp has shown to be more effective than other two antibiotics (1a and 1b) in inhibiting DNA synthesis (Henry 1974). Further, carminomycin is found to suppress the growth of a murine brochogenic lung carcinoma to indicate that it has less severe cardiotoxicity and is better absorbed from gastro-intestinal tract than daunomycin.

The biological activity of the antitumor anthracyclines is related to their ability to bind with DNA. Adriamycin displayed a more favourable therapeutic index than daunomycin in different experimental tumors in laboratory animals and particularly an impressive broad spectrum of activity. Adriamycin however is not devoid of serious side effects such as dose-limiting myclosuppression and cardiomyopathy etc. All toxic effects, with the exception of cardiotoxicity which in its fatal form, congestive heart failure, affects approximately 1 % of patients, are dose-related and reversible (Lenz and Page 1976).

Much effort has been directed to obtain either new derivatives or develop new dose regimes that show decrease in undesirable side effects and/or increased anticancer activity and selectivity. Such goals are common to many areas of cancer chemotherapy; however, in the case of daunomycin and adriamycin, it is now possible to consider the recent knowledge concerning their mode of action.

A detailed examination of the daunomycin-DNA model reveals that intercalation of the chromophore is only partial and one might speculate the removal of bulky methoxy group which would result in a molecule that could intercalate more effectively. In fact demethoxydaunomycin binds to DNA somewhat better than its parent compound. Significantly, *in vivo* testing demethoxy derivative in mouse cancer shows that it is as effective as daunomycin itself, but at dose levels four to eight times lower (Neidle 1977 and references therein).

The best possible way of elaborating the synthesis of anthracyclines is illustrated by Smith *et al* (1977), in which the degradation of daunomycin (1a) to tetracyclic ketone and its refunctionalization of the A ring to daunomycin (1a) and adriamycin (1b) were carried out as depicted in scheme 1.

As several suitable syntheses of L-daunosamine (Marsh *et al* 1967; Horton and Weckerle 1975; Yamaguchi and Rojima 1977; Medgyes and Kuszmann 1981) including our two approaches starting either from D-glucose (Ingle *et al* 1983; Gurjar *et al* 1984a) or from D-glucosamine (Gurjar *et al* 1984b) and its coupling to daunomycinone (2a) have been accomplished, most of the efforts were directed by many to the synthesis of the aglycone moieties (anthracyclinones). For a comprehensive review of synthetic studies, see Kelly (1980) and Arcamone (1981).

Our interest in antitumor agents in general and the synthesis of anthracyclines in

SCHEME–1

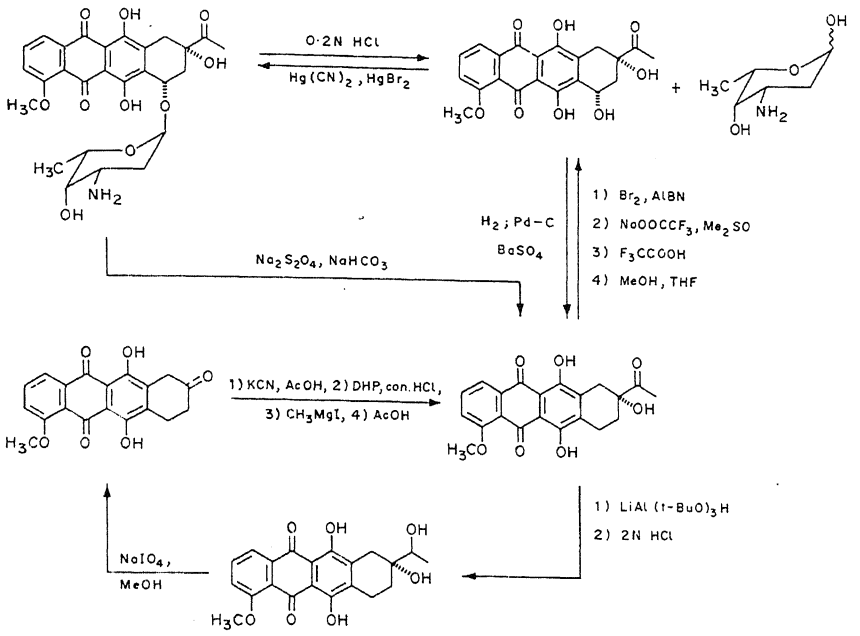

particular was initiated in late 1979 with partial financial support from the Government of Maharashtra. Our main aim was first directed towards the total synthesis of 4-demethoxydaunomycin (1d) as it was shown to be 8 times more effective compared to daunomycin and adriamycin (Kelly 1979; Arcamone 1981). An interesting feature of 1d is its activity by the oral route. Daunomycin showed a more than 10-fold lower potency when administered orally. Further its initial clinical trials are reported to be very promising. As there is no possibility of obtaining (1d) by fermentation, many schools have undertaken its synthesis (Kelly *et al* 1980; Rama Rao *et al* 1980; Farina *et al* 1980; Kerdesky *et al* 1981; Swenton *et al* 1981; Rao and Bhatt 1981; Kraus and Pezzanite 1981; Broadhurst *et al* 1982a, b, c; Andrecky *et al* 1982; Tamura *et al* 1982; Farina and Uega 1982; Tanno and Terashima 1983; Penco *et al* 1983; Cambie *et al* 1983). This involves the synthesis of the aglycone, (+)-4-demethoxydaunomycinone (2b), the amino sugar, L-daunosamine separately and finally building (+)-4-demethoxydaunomycin (1d).

Our efforts are first directed for the synthesis of 4-demethoxy-7-deoxydaunomycinone (2c) as this key product can be elaborated to 4-demethoxydaunomycin (1d) by following the sequence of reaction depicted in scheme 1.

2. Synthesis of 4-demethoxydaunomycinone

The high intrinsic bioactivity of 4-demethoxydaunomycin (1d) has attracted the attention of many experienced investigators with expertise in the chemistry of natural products, to undertake the total synthesis of 4-demethoxydaunomycinone (2b). In fact

the synthesis of (2b) has represented a simplified model of (2a) owing to the absence of the regioselectivity problems connected with the latter. As a result, innumerable approaches have already appeared in literature displaying original features in the choice of reactants and in the solution of important details related with functionalization and stereochemistry which can be broadly divided into two basic types. One type involves preparation of a tetraline derivative representing final AB rings and its condensation with phthalic acid and finally leading to the tetracyclic product. A second approach is based on building of A ring on the tricyclic BCD intermediate. This article summarizes different approaches made by the present author's group during the past 4 years.

2.1 *Diels-Alder reactions on* 1,4-*anthraquinone*

Our first attempt was to look into the feasibility of utilizing quinizarine (1,4-dihydroxyanthraquinone) and building the A ring of the anthracyclinone moiety by the Diels-Alder reaction (Rama Rao *et al* 1983). Many have investigated this approach by first converting quinizarine to quinizarine quinone, which served as the dienophile, but the main limitation was that most of the dienes add preferentially to the 'internal' double bond (Kelly *et al* 1980). Although several methods to resolve this difficulty have been devised, including the preparation of a few dienes with substituents that are likely to promote the addition at the 'terminal' double bond (Chandler and Stoodley 1980), the most attractive one is to make use of 1,4-anthraquinone (3) in the Diels-Alder (DA) reaction by which any diene can be added to build the tetracyclic system. Further, it is easy to oxidize the 9,10-positions of the anthracene system to the corresponding anthraquinone derivative. Accordingly, we have shown that DA reaction between 3 (prepared from quinizarine by $NaBH_4$ reduction in AcOH, Grinev *et al* 1972) and 2-methoxy-1,3-butadiene gave the adduct 4, which was converted to the tetracyclic ketone, 5 in 95 % yield. The side-chain elaboration on the ketone of 5 by a two-carbon homologation either by reacting with 2-lithio-2-methyl-1,3-dithiane (Corey and Erickson 1971) or with ethynylmagnesium bromide met with failure, probably due to base-catalyzed enolization of the starting ketone (5).

Our next attempt was to prepare a suitably protected (as ketal or thioketal) 2-acetyl-1,3-butadiene, which on DA reaction with (3) was expected to give the desired product (6). The diene (7) was made by starting from ethyl acetoacetate as shown in scheme 2. DA reaction between (3) and (7) resulted in the formation of (6) which was converted

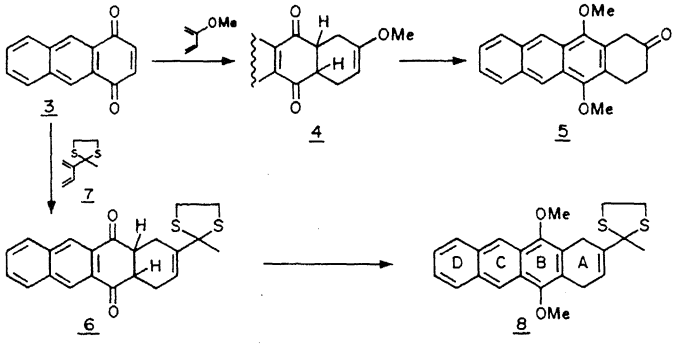

to (8) in 90% yield. However, all our attempts at dethioketalization (HgO, $HgCl_2$, aqueous CH_3CN or NCS, $AgNO_3$, aqueous CH_3CN) resulted in the aromatization of the A ring.

While the preparation of the diene (7) is straightforward and can be carried out by starting from readily available intermediates, it has a few drawbacks. Its synthesis involves several steps, and the overall yield is not satisfactory for it to be considered an efficient synthesis. We have therefore considered an alternative route (scheme 3) for obtaining a 2-acetyl-1,3-butadiene in which the ketone group is protected by thioketalization with 1,3-propanedithiol. Addition of methyl vinyl ketone to 2-lithio-2-methyl-1,3-dithiane in THF at $-30°C$ and usual work-up gave the alcohol (9), which was dehydrated ($MeSO_2Cl$, Et_3N, 0°C) to give the diene (10) (65% overall yield). The DA reaction between (3) and (10) however did not proceed even in refluxing toluene, and the quinone (3) was recovered. Our attempts to add the diene (10) even with reactive dienophiles such as 1,4-benzoquinone and 1,4-naphthoquinone did not proceed. This led us to suspect the structure, (10) assigned to this diene. Careful ^1H NMR analysis cannot rule out an alternate structure for this diene as (11) and its formation can be rationalized from (9) as shown in scheme 3. To remove this ambiguity we have now undertaken the synthesis of (10) by adopting a similar approach followed for the preparation of (7).

The observation that the A ring of (8) is prone to easy aromatization during deketalization can be attributed to the extended conjugation of the tetracyclic system. This unexpected trouble can be avoided if the A ring is built first on a dienophile such as (13) and bridged ultimately to form B ring of the anthracyclinone moiety. Compound

SCHEME-2

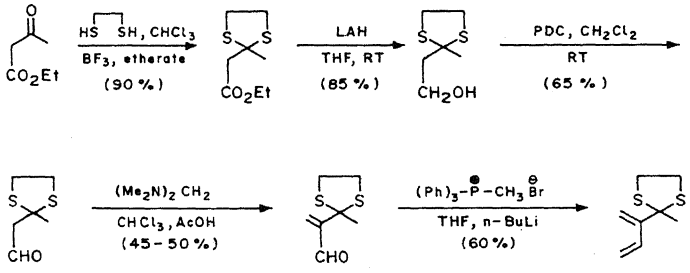

SCHEME-3

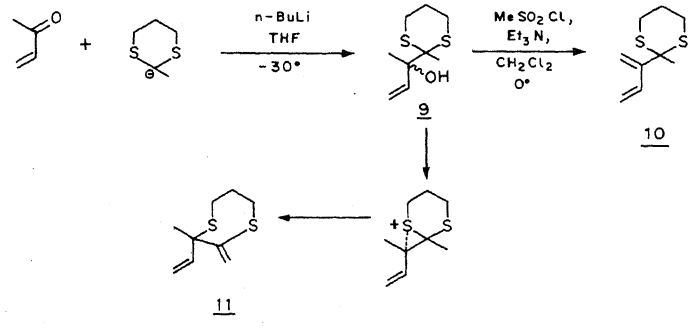

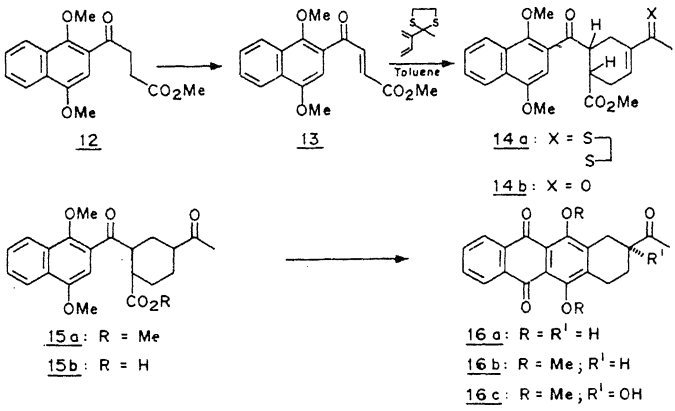

(13) has been made by bromination of methyl 3-(1,4-dimethoxy-2-naphthoyl)pro pionate (12) followed by dehydrobromination (Et_3N, CCl_4, room temperature). D reaction between (13) and (7) (toulene, reflux, N_2, 60 hr) resulted in the formation o (14a). Dethioketalization of (14a) (N-chlorosuccinimide, $AgNO_3$, aqueous CH_3CN 0·5 hr) gave (14b), which was subjected to hydrogenation (Pd/C 10%, EtOH, 20 psi 2 hr) to give (15a). Alkaline hydrolysis of (15a) and ring closure of the resultant aci (15b) with concentrated H_2SO_4 gave 4-demethoxy-7,9-dideoxydaunomycinone (16a in 71% yield. Methylation of (16a) gave (16b) which was converted to (16c) (accordin to the method adopted by Suzuki *et al* (1978) for daunomycinone synthesis) in 55% overall yield from 16a. As the conversion of (16c) to 4-demethoxydaunomycinone (2b has already been described, we consider that our new synthesis of (16c) in effec constitutes a total synthesis of (2b).

2.2 *Synthesis of 2-acetyl-5,8-dimethoxy-1,2,3,4-tetrahydro-2-naphthol—A key intermediate for the synthesis of anthracyclinones (Diels-Alder approach)*

One of our earlier approach for the synthesis of (±)-4-demethoxydaunomycinone (2b is by first preparing 2-acetyl-5,8-dimethoxy-1,2,3,4-tetrahydro-2-naphthol (17) startin from 1,4-dimethoxy-6-tetralone by a two-carbon homologation, using an acyl anio equivalent such as 2-lithio-2-methyl-1,3-dithiane and transforming finally to th desired product (Rama Rao *et al* 1980).

1,4-Dimethoxy-6-tetralone (19) was prepared by a slightly modified procedure. Th Diels-Alder adduct (18), obtained from benzoquinone and 2-methoxybutadiene wa methylated in boiling acetone followed by acid work-up (HCl) of the acetone filtrate t give the tetralone (19) (75% overall yield from benzoquinone). Reaction of 2-lithio-2 methyl-1,3-dithiane in THF (prepared from 2-methyl-1,3-dithiane with 1·1 eq. of *n*-BuL −15°, 3 hr) with 1,4-dimethoxy-6-tetralone (−15°, 3 hr, then 0°, 18 hr) and usual work up gave a mixture which can be easily separated on silica gel column (benzene-aceton mixture as eluent) to the desired thioketal derivative (20) and the rest as startin material. Hydrolysis of the thioacetal (20) in aqueous acetonitrile with mercuri chloride and mercuric oxide for 2·5 hr afforded 2-acetyl-5,8-dimethoxy-1,2,3,4 tetrahydro-2-naphthol (17).

The dimethoxytetralin (17) was condensed with excess of methyl hydrogen phthalat

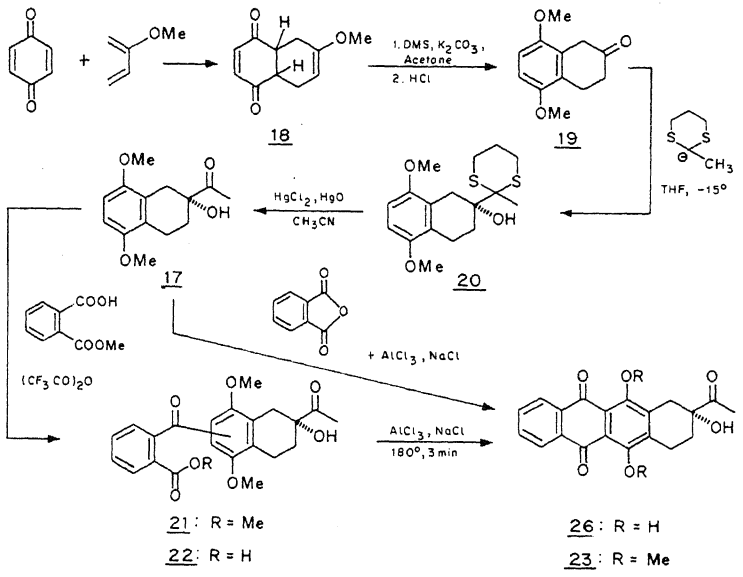

in refluxing trifluoroacetic anhydride (40 hr) to give a mixture of isomeric keto-esters (21) in almost equal ratio (NMR) and was directly saponified (8 % KOH, MeOH, RT) to yield the corresponding isomeric keto-acids (22) in 63 % yield from (17). Earlier, the ring closure to give anthracyclinone derivatives was accomplished using either H_2SO_4 or commonly with anhydrous HF in poor yield. The cyclisation of (22) now best achieved by intimately mixing it with a ten-fold mixture of $AlCl_3$–NaCl (5 : 1) heating at 180° for 3 min and treating the resultant reddish mass with a saturated solution of oxalic acid to give 4-demethoxy-7-deoxydaunomycinone (2c). Methylation of (2c) with Me_2SO_4 in the presence of K_2CO_3 in refluxing acetone gave the dimethyl ether (23) in almost quantitative yield.

The dimethoxytetralin (17) can be best converted directly to 4-demethoxy-7-deoxydaunomycinone (2c) by fusing with an intimate mixture of phthalic anhydride 2 eq., $AlCl_3$-NaCl, (5 : 1), ten-fold excess at 180° for 3 min and treating the resultant reddish mass with a saturated solution of oxalic acid. Extraction with chloroform and chromatography over silica gel column and usual work-up gave the desired product (2c). The conversion of (2c) to 4-demethoxydaunomycinone (2b) has already been described.

2.3 *Friedel-Crafts acylation approach*

Both the earlier methods, although novel, suffer from various disadvantages and are not suited for preparation of anthracyclinones in multigram quantities. However, it was clear that the assemblage of the tetracyclic system of AB + CD coupling making use of the key intermediate, 2-acetyl-5,8-dimethoxy-1,2,3,4-tetrahydro-2-naphthol (17) as the starting material is the most versatile method for the synthesis of different unnatural anthracyclinones including 4-demethoxydaunomycinone (2b) (Wong *et al* 1971). Hence our attention was directed for the synthesis of (17) by different approaches. One

simpler approach is by starting from 2-methylhydroquinone, employing easil accessible organic intermediates and reagents.

2-Methylhydroquinone dimethyl ether (24) was converted to 2,5-dimethoxy benzylbromide (25) by treatment with N-bromosuccinimide in boiling carbo tetrachloride in 80% yield. Condensation of (25) with 2,4-pentanedione in acetone i the presence of anhydrous pot. carbonate at room temperature gave 3-acetyl-4-(2'-5 dimethoxyphenyl)-2-butanone (26) in 70% yield. Alkylation of (26) with ethy bromoacetate under very mild condition using anhydrous pot. carbonate in acetone a room temperature gave the keto ester (27). Earlier Wong *et al* (1971) did the sam alkylation using sodium hydride in refluxing THF under strictly anhydrous conditions t give (27). In fact both the alkylations can be carried out as one pot. reaction employin anhydrous potassium carbonate in acetone at room temperature without affecting th overall yield of (27) from (25) (scheme 4). Hydrolysis of (27) with aqueous sodiur hydroxide underwent a reversed Claisen followed by the hydrolysis of the ester an gave the keto acid (28). Operationally the conversion of methyl hydroquinone to th keto acid (28) can be smoothly carried out in an overall yield of 36%. Attempts wer made to convert the keto acid (28) to 2-acetyl-5,8-dimethoxy-1,2,3,4-tetrahydro naphthalen-4-one (29) by a variety of reagents (see scheme 5). Our first attempt of thi conversion with conc. sulphuric acid at room temperature met with failure and (28) wa recovered unchanged. Employing an equal quantity of trifluoroacetic acid an trifluoroacetic anhydride at room temperature for 8 hr and usual work-up resulted i

SCHEME-4

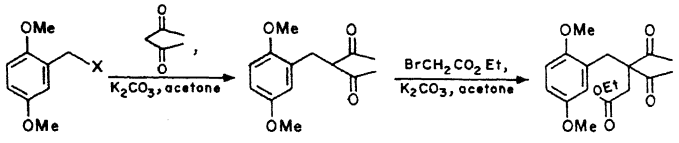

24: X = H
25: X = Br

26

27

SCHEME-5

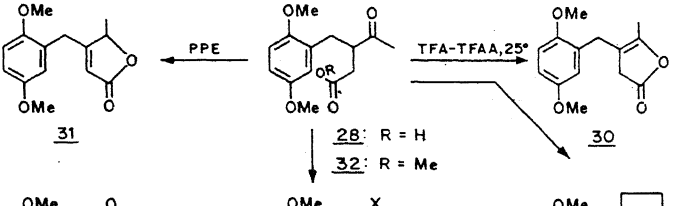

the formation of a product whose IR and PMR spectra clearly indicated that it is a lactone (30). Treatment of (28) with polyphosphate ester (P_2O_5, Et_2O, $CHCl_3$) at reflux temperature resulted in the formation of an isomeric lactone (31) in more than 80% yield.

To surmount this obstacle, it appeared necessary to protect the acetyl carbonyl group so that the lactone formation can be avoided totally. Although, ketalisation is the obvious choice of protecting the ketone, we preferred thio-ketalisation for reasons of its stability during cyclisation under acid conditions. Thus the keto-acid (28) was first converted to its ester by diazomethane and the resultant ester (32) was then treated with ethane dithiol in the presence of a small amount of BF_3 etherate to give the thioketal derivative (33). Alkaline hydrolysis of (33) gave the corresponding acid (34) which was then subjected to cyclisation with polyphosphate ester to obtain (35). Dethioketalisation of (35) by treatment with mercuric oxide and mercuric chloride in boiling acetonitrile resulted in the formation of the desired tetralone (29). However, (29) can be obtained from the keto-acid (28) by subjecting it to hydrofluoric acid cyclisation in 60–65% yield. Catalytic hydrogenation of the tetralone (29) using 10% Pd/C gave the desired synthon, 2-acetyl-5,8-dimethoxy-1,2,3,4-tetrahydronaphthalene (36) in 95% yield. Having obtained (36), which constitutes the AB synthon, our next step was to introduce the tertiary hydroxyl group either at this stage or to build the anthracyclinone skeleton and subsequently introduce the *tert.* hydroxyl at 9-position. We preferred the latter course as in our experience introduction of *tert.* hydroxyl employing the method described by Wong *et al* (1971) by oxidation in *t*-butanol with potassium *t*-butoxide and oxygen followed by reduction with zinc gave the hydroxy-ketone (17) together with substantial quantities of 2-acetyl-5,8-dimethoxynaphthalene due to the aromatisation of the A-ring. Fusion of an intimate mixture of (36) with phthalic anhydride in $AlCl_3$-NaCl (5:1) melt maintained at 180–190° for 3 to 5 min gave 4-demethoxy-7,9-dideoxydaunomycinone (16a) in 76% yield. Methylation of (16a) with dimethyl sulphate in the presence of anhydrous pot. carbonate in boiling acetone gave the dimethyl ether (16b). Hydroxylation of C-9 in (16b) was achieved *via* a four-step reaction sequence which was commonly employed for the introduction of C-17 hydroxyl group in steroids and the same was adopted by Suguki *et al* (1978) for the synthesis of 7-deoxydaunomycinone. This involved the preparation of enol acetate (PTS acid, Ac_2O), followed by epoxidation and the resultant epoxy acetate was then treated successively by base and acid to ensure complete hydrolysis and rearrangement to give 7-deoxy-4-demethoxydaunomycinone dimethyl ether (16c), which after chromatographic purification resulted in 55% overall yield from (16b).

2.4 *Metal-ammonia reduction on naphthalene precursors*

Another alternate approach for the synthesis of (17) was starting from an aromatic precursor such as 1,4-dimethoxynaphthalene and building the AB synthon in a three-step synthesis (Rama Rao *et al* 1982).

Acylation of 1,4-dimethoxynaphthalene with acetic anhydride (1:2 eq) using anhydrous aluminium chloride (2.2 eq.) in ethylene dichloride at 60° (3 hr) gave on usual work-up and chromatographic separation (silica gel, pet. ether-acetone mixture) 1-hydroxy-4-methoxy-2-acetylnaphthalene (50%) and 2-acetyl-5,8-dimethoxy-naphthalene (37) (30% yield).

Metal ammonia reduction on (37) with potassium (8 g atom eq.) in liquid ammonia

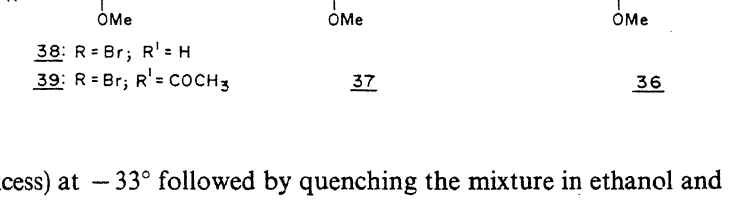

38: R = Br; R' = H
39: R = Br; R' = $COCH_3$

37 36

(50-fold excess) at $-33°$ followed by quenching the mixture in ethanol and the usua work-up gave 2-acetyl-5,8-dimethoxy-1,2,3,4-tetrahydronaphthalene (36) in 75% yield. Oxidation of (36) in *t*-butanol with potassium-*t*-butoxide and oxygen followe by reduction (Zn-AcOH) gave 2-acetyl-5,8-dimethoxy-1,2,3,4-tetrahydro-2-naphth (17) in 60% yield.

The only disadvantage by this above approach is the preparation of 2-acetyl-5,8 dimethoxynaphthalene (37) which happened to be a byproduct in the acylation of 1,4 dimethoxynaphthalene. This has now been achieved in a better manner starting fro 1,4-dimethoxynaphthalene by first bromination to give 1,4-dimethoxy-2-bromo naphthalene (38) which was then acylated with acetic anhydride ($AlCl_3$-EDC) to giv 1,4-dimethoxy-2-bromo-6-acetylnaphthalene (39). This on dehalogenation (H_2, Rane Nickel) gave exclusively (37).

2.5 *Practical approach for the total synthesis of* (+)-4-*demethoxydaunomycinone*

All our methods were directed to obtain the recemic 4-demethoxydaunomycinone (2b *via* the key intermediate (17) by different approaches. Earlier, it was shown that (17 can be resolved to obtain optically pure R(−) 17 and the same can be made use of t obtain (+)-4-demethoxydaunomycinone (2b) (Tanno and Terashima 1983). We hav achieved this goal of making R(−) 17 *via* Sharpless asymmetric epoxidation (kineti resolution method) (Martin *et al* 1981) on the recemic allylic alcohol (44) prepare from benzoquinone. The undesired antipode (44b) is then epimerized and recycle Our present method is exceptionally simple and easy to operate for the synthesis of variety of aglycones in optically active form (Rama Rao *et al*, unpublished).

The Diels-Alder reaction of benzoquinone with butadiene in acetic acid at roo temperature afforded the adduct (40) in 90% yield. *O*-Methylation (Me_2SO_4, K_2CO boiling acetone, 4 hr) gave 5,8-dimethoxy-1,4-dihydronaphthalene (41). Base-catalyse isomerization (41) (*t*BuOK, Me_2SO_4, r.t., N_2) resulted in the formation of 5,8 dimethoxy-3,4-dihydronaphthalene (42) in 100% yield. Vilsmeir formylation of (42 ($POCl_3$, DMF, 80°, 4 hr) gave the aldehyde (43) (Reddy and Krishna Rao 1981 Grignard reaction on (43) (MeMgI, Et_2O, r.t., 1 hr, N_2) afforded the (±)-2-(hydroxyethyl)-5,8-dimethoxy-3,4-dihydronaphthalene (44).

Kinetic resolution of (±)-44 was carried out at $-50°$ by subjecting (44) in CH_2C and adding sequentially titanium tetraisopropoxide (TIP), (+)-diisopropyltartra L(+) DIPT and *t*-butylhydroperoxide (TBHP) in 1 : 1 : 1 : 0·6 molar ratio. The progress the reaction was monitored by titrating the concentration of TBHP. After the completio of the reaction (10 hr), the reaction was worked up in the usual manner, to give mixture of two products (45 and 44b) which was directly subjected (without separatio to reduction (LAH, THF, r.t.) followed by chromatographic separation to give *R*-(+ (44 b) (38% yield m.p. 88–89°) $[\alpha]_D^{20}$ +20·3 (*c* 0·5, EtOH) and *R*-(−)-2-(*S*-1-hydrox

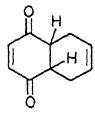

40

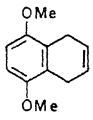

41

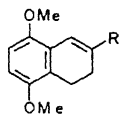

42: R = H
43: R = CHO

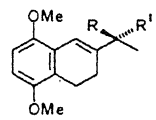

44a: R = OH, R' = H
44b: R = H, R' = OH

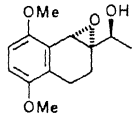

45

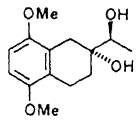

46

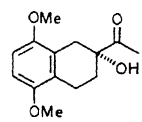

17

ethyl)-2-hydroxy-5,8-dimethoxy-1,2,3,4-tetrahydronaphthalene (46), 40% yield, m.p. 154–55° $[\alpha]_D^{20}$ −49·4° (*c* 0·5, EtOH). The undesired antipode (+)-(44b) was inverted by reacting with triphenylphosphine, diethyl diazodicarboxylate and benzoic acid in THF to give the benzoate (−)-(44a). Hydrolysis (NaOMe, MeOH) followed by purification afforded (−) (44a), 70% yield, m.p. 86–88°; $[\alpha]_D^{20}$ −18·6 (*c* 0·5, EtOH). Epoxidation of (−) (44a) (CH_2Cl_2, −55° to −50° TIP, L(+)-DIPT, TBHP, N_2) followed by reduction with LAH gave (−) (46), 83% yield, m.p. 152–4°, $[\alpha]_D^{20}$ −47·6 (*c* 0·5, EtOH).

Oxidation of (−) (46) with Fetizone reagent (Ag_2CO_3, celite) gave *R*-(−) (17), m.p. 128–29°, $[\alpha]_D^{20}$ −48·8° (*c* 1, $CHCl_3$). Fusion of *R* (−) (17) with an intimate mixture of $AlCl_3$-NaCl (5:1) at 180° (2 min) and usual work-up gave (−)-4-demethoxy-7-deoxydaunomycinone, m.p. 227–8°, $[\alpha]_D^{20}$ −84°. This was converted to (+)-4-demethoxy daunomycinone (2b) by established methods.

3. Synthesis of 11-deoxyanthracyclinones

Although daunomycin and adriamycin continue to enjoy the clinical effectiveness in the treatment of human cancers, their main disadvantage of having irreversible cardiomyopathy have prompted the search for new compounds that show decreased side effects and/or increased antitumour activity. This has resulted in the isolation of new anthracycline antibiotics lacking a hydroxyl group at C-11 position, 11-deoxydaunomycin (47a) and 11-deoxyadriamycin (47b) etc., (Arcamone *et al* 1980) related to aclacinomycin A, (48) which showed a low incidence of cumulative dose-dependent cardiotoxicity. In contrast to adriamycin, aclacinomycin A selectively inhibits whole cellular RNA synthesis at concentration six to eight times lower than those required to inhibit DNA synthesis. Although many elegant approaches for the total synthesis of the aglycones of daunomycin (Kelly *et al* 1980; Parker and Kallmerten 1980; Barlon *et al* 1980; Braun 1980; Hauser and Prasanna 1981; Dsolson *et al* 1981; Alexander *et al* 1980; Kimball *et al* 1982; Broadhurst and Hassall 1982; Honek *et al* 1983; Davies *et al* 1983; Gesson *et al* 1983; Tamariz *et al* 1983; Keay and Rodrigo 1983) and its analogues have been developed, only a few recent reports have appeared on the synthesis of 7,11-dideoxydaunomycinone (49a) and 11-deoxydaunomycinone (49b) respectively (Yadav *et al* 1981; Kimball *et al* 1981) before our first communication appeared (Rama Rao *et al*

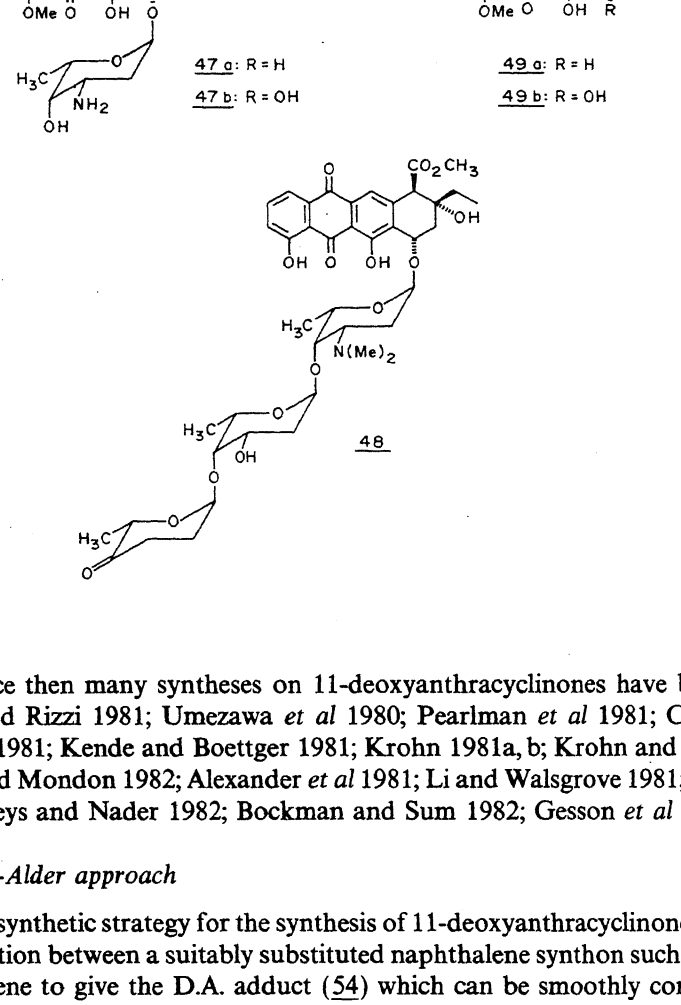

1982). Since then many syntheses on 11-deoxyanthracyclinones have been reported (Kende and Rizzi 1981; Umezawa *et al* 1980; Pearlman *et al* 1981; Confalone and Pizzolato 1981; Kende and Boettger 1981; Krohn 1981a, b; Krohn and Behnke 1981; Gesson and Mondon 1982; Alexander *et al* 1981; Li and Walsgrove 1981; Sekizaki *et al* 1982; Vedeys and Nader 1982; Bockman and Sum 1982; Gesson *et al* 1983).

3.1 *Diels-Alder approach*

Our main synthetic strategy for the synthesis of 11-deoxyanthracyclinones is the Diels-Alder reaction between a suitably substituted naphthalene synthon such as (53) with a desired diene to give the D.A. adduct (54) which can be smoothly converted to the tetracyclic dione (56) and transforming the latter product to an appropriate 11-deoxyanthracyclinone.

Our regiospecific synthesis of 11-deoxyanthracyclinones involve the preparation of the dienophile (53) and an appropriate diene as precursors. The obvious intermediate for the synthesis of (53) is 1,4,5-trimethoxynaphthalene-2-acetaldehyde (52) which was prepared starting from 2-allyl-5-methoxynaphthoquinone (50). Reduction of the quinone (50) to the corresponding hydroquinone with sodium hydrosulphite followed by methylation (DMS, K_2CO_3, acetone) afforded the trimethyl ether (51). Oxidation of the olefin (51) using an osmium tetroxide-potassium chlorate system gave the corresponding diol which is converted directly to the aldehyde (52) with sodium periodate or by lead tetraacetate in benzene.

Wittig condensation of the aldehyde (52) with triphenylcarboethoxymethylene phosphorane in THF at room temperature afforded (53). Treatment of (53) with

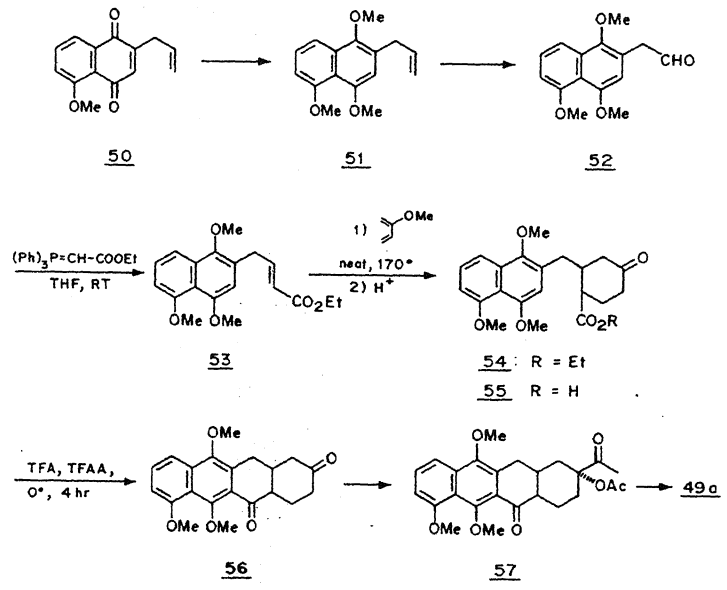

2-methoxybutadiene at 170° (sealed tube) for 48 hr gave exclusively the desired adduct which on acid work-up (aq. HCl) and silica gel chromatographic purification gave (54). Alkaline hydrolysis (2N, NaOH in MeOH, r.t.) gave (55) which was subjected to cyclisation by treating with a mixture of $(CF_3CO)_2O$ and CF_3COOH (2:1) at 0° for 4 hr to give the tetracyclic dione (56).

Yadav *et al* (1981) have converted the dione (56) to (57) by treatment with $HC{\equiv}CMgBr$ followed by $Hg(OAc)_2$-H_2S. The latter product converted to (49a) by ceric ammonium nitrate oxidation followed by bromination and dehydrobromination and finally deacetylation with NaOMe in MeOH. The conversion of (49a) to (49b) has been carried out by the well-known procedure (Kimball *et al* 1981).

This approach to 11-deoxyanthracyclinones is more elegant and regiospecific. The possibility of extending this approach to other anthracyclinones, in particular, the synthesis of aklavinone, utilizing a more highly functionalised A ring synthon is under investigation.

3.2 *Synthesis of* 11-*deoxyanthracyclinones by Friedel-Crafts acylation approach*

Having dealt with the synthesis of 11-deoxydaunomycinone by Diels-Alder approach, our attention was directed to synthesize the same by a non-D.A. reaction (Rama Rao *et al* 1982).

The main synthetic strategy in our new approach centred upon the concept of constructing AB ring, utilizing inexpensive intermediates and reagents and condensing a D-ring unit to form the anthracyclinones system (66), which can be transformed to (±)-11-deoxydaunomycinone (49b).

The requisite AB synthon (64) is made from *m*-cresol in eight-steps as shown in scheme 6. 4-Bromo-*m*-cresol is acetylated (Ac_2O, pyridine, RT) to give (58), which is then brominated (NBS, CCl_4, 6 hr, reflux) to afford 3-acetoxy-6-bromobenzyl bromide (59) in 80% yield. Condensation of (59) with acetyl acetone in the presence of

SCHEME-6

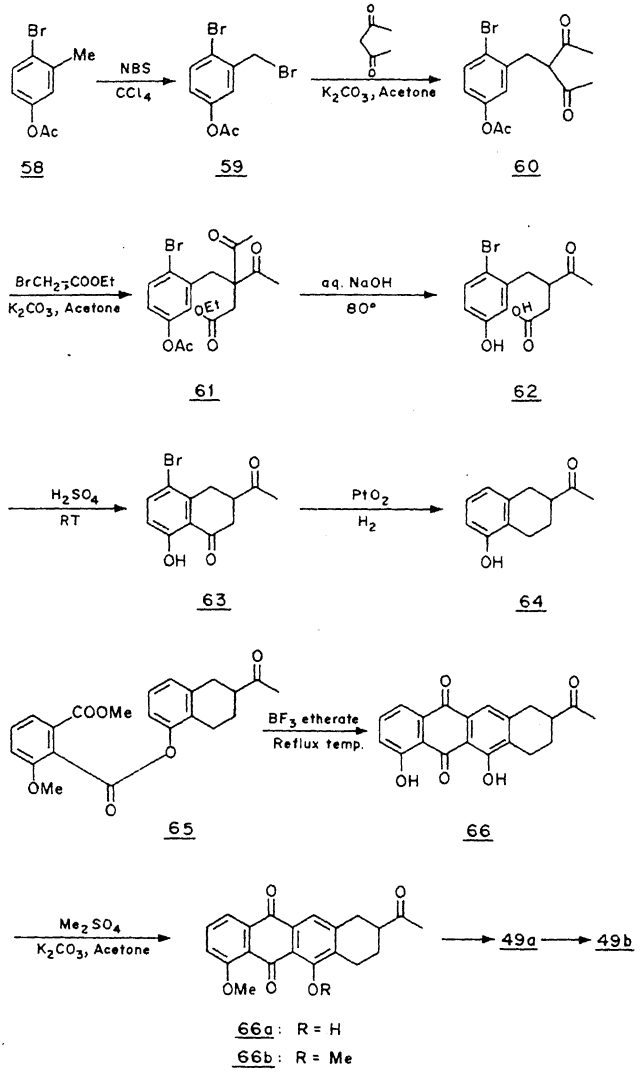

potassium carbonate in acetone at room temp. gave (60). Alkylation of (60) with ethyl bromoacetate (K_2CO_3, acetone, RT) gave (61). Saponification (10% NaOH 80°, 6 hr) of (61) followed by acidification afforded the desired acid (62), which on treatment with conc. H_2SO_4 at room temperature is smoothly converted to 2-acetyl-8-bromo-5-hydroxy-1,2,3,4-tetrahydro-4-naphthalenone (63). Hydrogenation of (63) (PtO_2, EtOH, 6 hr, RT) afforded 2-acetyl-5-hydroxy-1,2,3,4-tetrahydronaphthalene (64) together with a small quantity of the corresponding α-hydroxyethyl tetralin.

Condensation of 2-carbomethoxy-6-methoxy-benzoyl chloride (prepared from 3-methoxyphthalic acid-1-methyl ester with $SOCl_2$ and catalyst DMF) with (64) (pyridine, benzene, 6 hr, RT) gave the benzoyl ester (65). Fries rearrangement of the ester (65) by subjecting it in BF_3-etherate at reflux temp for 20 min afforded directly

7,9,11-trideoxycarminomycinone (66) in 40% yield after purification over silica gel column. Methylation of (66) (DMS 1·5 eq., K_2CO_3, acetone) gave a mixture (1 : 1) of mono and dimethyl ethers (66a and 66b) together with trace quantities of the starting material.

4. Regiospecific and flexible approach for the synthesis of (±) daunomycinone and (±) 11-deoxydaunomycinone

Having successfully carried out the syntheses of 4-demethoxydaunomycinone and 11-deoxydaunomycinone by different approaches, our attention was directed towards the total synthesis of daunomycinone. In view of the fact that the key synthon (63) which was used for the total synthesis of 11-deoxydaunomycinone was considered to serve as an intermediate for achieving the regiospecific synthesis of both daunomycinone and 11-deoxydaunomycinone (Rama Rao *et al* 1983).

The requisite AB synthon (63) was converted into the keto compound (67) by protecting the acetyl carbonyl group (ethylene glycol, toluene-*p*-sulphonic acid, C_6H_6, reflux 6 hr), followed by Wolff-Kishner reduction ($H_2NNH_2 \cdot H_2O$, KOH, 160–165°C, 4 hr; acid work-up). Condensation of (67) with 3-bromo-4-methoxyphthalide (68) (Kim *et al* 1979) ($SnCl_4$, CH_2Cl_2, room temp., 4 hr) resulted in the formation of (69). The ethylene acetal (70) prepared from (69) was reduced with zinc dust in ethanolic KOH (20%, 80°C, 4·5 hr; acid work-up) to the bromo-acid (71). Alternatively, heating (71) with zinc dust in aqueous KOH (20%, 100°C, 6 hr; acid work-up) gave (72) (70% m.p. 156–157°C). Compound (71) was used in the synthesis of (±)-daunomycinone (2b) while (72) was utilized for (±)-11-deoxydaunomycinone (49b) (scheme 7). The bromo-acid (71) was premethylated (Me_2SO_4, K_2CO_3, acetone) to give (73), which was hydrolysed to give (74) (83%, m.p. 220–201°C). Compound (74) was cyclised by treatment with $(CF_3CO)_2O$ in CH_2Cl_2 at room temp. for 12 hr to give the anthrone (75). Oxidation of (75) (Jones reagent, acetone, room temp., 2 hr) gave (76). The acetyl carbonyl group in (76) was protected ($HSCH_2CH_2SH$, $BF_3 \cdot OEt_2$, $CHCl_3$, room temp., 1 hr) to afford (77), which was converted into (78) by displacing the bromine by a methoxy group (NaOMe-pyridine-Cu_2Cl_2, room temp., 6 hr). Dithioacetalization of (78) [$HgCl_2$-HgO, aq. MeCN (80%), reflux 1 hr] and chromatographic purification of the products resulted in the isolation of orange crystals of 7,9-dideoxydaunomycinone dimethyl ether (79a), which was identical with the product prepared by a different procedure (Kim *et al* 1979). Conversion of (79a) into 7-deoxydaunomycinone dimethyl ether (79b) and subsequently into (±)-daunomycinone (2a) has already been known.

The acid (72) was converted into (±)-11-deoxydaunomycinone (49b) by the following sequence of reactions. Cyclisation of (72) (HF, 5–10°C, 4 hr) afforded the anthrone (80). Oxidation of (80) (Jones reagent, acetone, room temp., 0·5 hr) led to the tetrahydronaphthecene quinone (81). Hydroxylation of the tertiary carbon (C-9) to give (49a) was accomplished by the standard procedure adopted by Suzuki *et al* (1978). The conversion of (49a) into (±)-11-deoxydaunomycinone (49b) has been reported earlier (Kimball *et al* 1981).

The above approach is flexible and sufficiently versatile for the synthesis of other analogues. Based on similar strategy, the synthesis of 4-demethoxydaunomycinone and 4-demethoxy-11-deoxydaunomycinone was achieved (Rama Rao *et al* 1983) starting from the intermediate, 63.

SCHEME 7

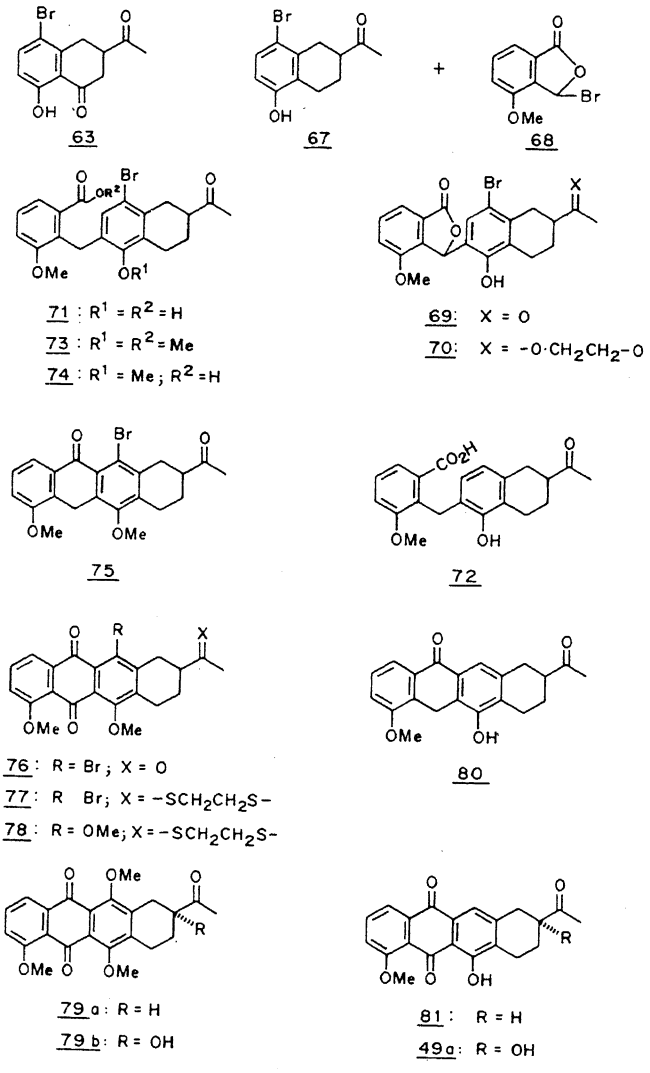
63
67
68
71 : R¹ = R² = H
73 : R¹ = R² = Me
74 : R¹ = Me; R² = H
69: X = O
70: X = -O·CH2CH2-O
75
72
76: R = Br; X = O
77: R Br; X = -SCH2CH2S-
78: R = OMe; X = -SCH2CH2S-
80
79 a: R = H
79 b: R = OH
81: R = H
49a: R = OH

5. Syntheses of L-daunosamine

While our efforts to synthesize anthracyclinones (both natural and unnatural) are being perceived vigorously, we have simultaneously embarked on the total synthesis of L-daunosamine (84) from easily accessible carbohydrates such as D-glucose or D-glucosamine. Among the reported methods for the synthesis of 84, the most attractive route is that of Horton and Weckerle (1975) utilizing the intermediate, methyl 4,6,*O*-benzylidine-2-deoxy-α-D-erythropyranosid-hexo-3-ulose (83) and converting the same by a convenient approach to 84. However, their method of synthesising 83 from methyl 2,3,4,6-di-*O*-benzylidine-α-D-mannopyranoside (82) employing *n*-butyl

lithium is more tedious and not suitable for large scale preparation. We have therefore worked out two alternate approaches for the synthesis of 82 from D-glucose or D-glucosamine. Both these methods offer various advantages compared to the earlier reports.

5.1 *From D-glucose*

Our first approach is to make 83 starting from methyl 2,3-anhydro-4,6-*O*-benzylidine-α-D-allopyrenoside (85) which in turn was obtained from D-glucose in two steps. LAH reduction of 85 gave the alcohol 86 which was oxidised with pyridinium dichromate (PDC) in CH_2Cl_2 to give 83 in excellent yield. The conversion of 83 to 84 has been well optimised by Crugnola *et al* (1981).

An alternate approach for the synthesis of 83 has also been worked out starting from 85. 85 was converted to methyl 4,6-*O*-benzylidine-2-iodo-2-deoxy-α-D-altropyranoside (87) by treating with magnesium iodide-etherate. We have now demonstrated that 87 can be smoothly dehalogenated to give 86 under reductive conditions using tri-*n*-butyltin chloride together with excess of sodium borohydride (Corey and Suggs 1975). Oxidation of 86 with PDC gave 83 in good yield.

5.2 *Synthesis of L-daunosamine starting from D-glucosamine hydrochloride*

Our strategy in converting D-glucosamine 88 into 84 involved (a) the migration of the amino function of glucosamine at C-2 to C-3 *via* epimine, and (b) the introduction of the C-methyl function at C-5 with change of chirality at C-5 *via* 5,6-ene (scheme 8).

Methyl 2-*N*-benzoyl-α-*D*-glucopyranoside (89) obtained from glucosamine hydrochloride (88), was converted to methyl 4,6-*O*-benzylidene-2-*N*-benzoyl-α-*D*-glucopyranoside (90) by treating with α,α-dimethoxytoluene in acetonitrile in the presence of toluene-*p*-sulphonic acid in excellent yield. Conventional tosylation followed by treatment with 1 molar equivalent of sodium hydride in dry THF at room temperature afforded directly the *N*-benzoyl epimine (92) without any concommitant debenzoylation. The ring opening of 92 with ammonium chloride gave the 2-chloride, 93.

Dehalogenation of 93 was effected with tri-*n*-butyl chloride-sodium borohydride in

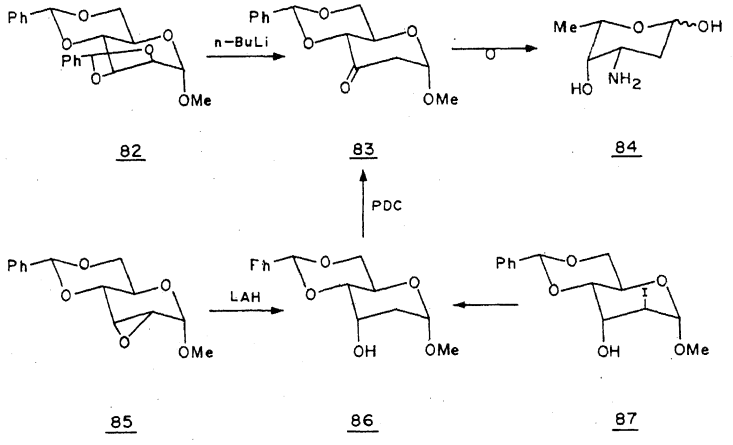

SCHEME-8

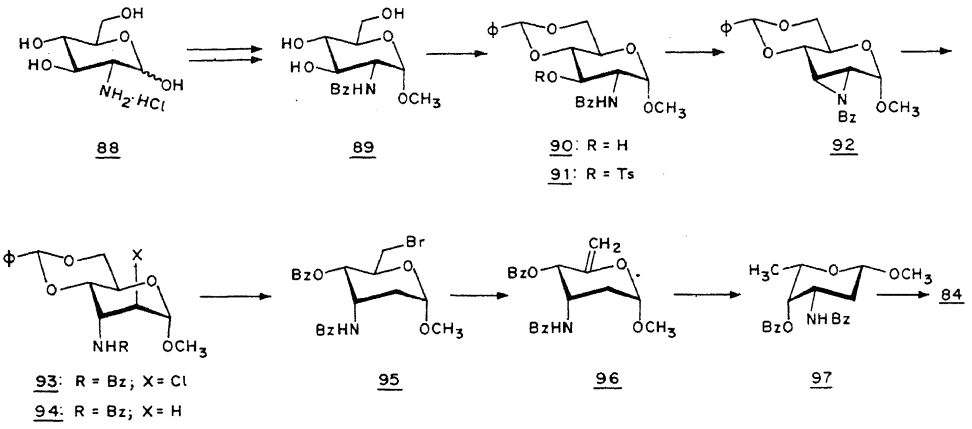

ethanol to give the deoxy compound 94. Treatment of 94 with *N*-bromosuccinimide in CCl_4 opened the 1,3-dioxane ring and yielded methyl-6-bromo-3-*N*-benzoyl-2,3,6-trideoxy-α-*D*-ribohexopyranoside (95). Dehydrobromination was accomplished by treating 95 with DBU in HMPT affording the 5-hexenopyranoside (96). Hydrogenation of 96 with 10% Pd/C at 40 psi in ethyl acetate resulted in the formation of methyl 4-*O*-benzoyl-3-*N*-benzoyl-β-*L*-daunosaminide (97). Debenzoylation by acid hydrolysis gave the desired *L*-daunosamine (84).

6. Conclusion

The development of daunomycin and adriamycin has greatly contributed to the present-day re-evaluation of cancer chemotherapy. The trend during the last one decade is mostly on the development of anthracycline analogues with reduced toxicity and enlarged spectrum of activity which would eventually result in the availability of new anti-cancer compounds with enhanced clinical usefulness. A programme directed to this objective has finally led to the manipulation of the molecules with total synthetic approaches in the anthracycline class, previously unexplored by many organic chemists. Although the author's group at the National Chemical Laboratory initiated the total synthesis of anthracyclinones much later compared to other well-known schools in U.S. and Europe, the progress made during the last four years appears to be exceedingly good. It is our desire to explore the possibility of synthesising one or two anthracycline analogues with proven biological activity in the near future.

Acknowledgements

The author is indebted to many of his colleagues whose devotion and hard work have finally resulted in shaping this project. He is especially thankful to V H Deshpande, J S Yadav, A R Mehendale, Bhanu Chanda, K Bal Reddy, N Laxma Reddy, M Jaweed and Borate for the synthesis of various anthracyclinones and T R Ingle, M K Gurjar and V J Patil for the synthesis of *L*-daunosamine.

References

Alexander J, Bhatia A V, Clark G W, Leutzow A, Mitscher L A, Omoto S and Suzuki T 1980 *J. Org. Chem.* **45** 24

Alexander J, Flynn D L, Mitscher L A and Veysoglu T 1981 *Tetrahedron Lett.* **22** 3711

Andrecky R J, Dominguez D and Cava M P 1982 *J. Org. Chem.* **47** 409

Arcamone F 1981 *Medicinal chemistry* (New York: Academic Press) 17

Arcamone F, Cassinelli G, Dimatts F, Forenza S, Ripamonti M C, Rivola G, Vigevani A, Clardy J and MeCabe T 1980 *J. Am. Chem. Soc.* **102** 1462

Arcamone F, Franceschi G, Orezzi P, Cassinelli G, Barbier W and Mondelli R 1964 *J. Am. Chem. Soc.* **86** 534

Arcamone F, Franceschi G, Penco S and Selva S 1969 *Tetrahedron Lett.* 1007

Arcamone F, Lloydia 1977 *Cancer Chemother. Rep.* **40** 45

Barton D H R, Dawes C C, Franceschi G, Foglio M, Ley S V 1980 *J. Chem. Soc. Perkin Trans I* 643

Braun M 1980 *Tetrahedron Lett.* **21** 3871

Broadhurst M J and Hassall C H 1982 *J. Chem. Soc. Perkin Trans I* 2227

Broadhurst M J, Hassall C H and Thomas G J 1982a *J. Chem. Soc. Chem. Commun.* 158

Broadhurst M J, Hassall C H and Thomas G J 1982b *J. Chem. Soc. Perkin Trans I* 2239

Broadhurst M J, Hassall C H and Thomas G J 1982c *J. Chem. Soc. Perkin Trans I* 2249

Bockman Jr R K and Sum F W 1982 *J. Am. Chem. Soc.* **104** 4604

Cambie R C, Larsen D S, Mcdonald H, Rutledge P S and Woodgate P D 1983 *Tetrahedron Lett.* **24** 2319

Chandler M and Stoodley R J 1980 *J. Chem. Soc. Perkin Trans I* 1007

Confalone P N and Pizzolato G 1981 *J. Am. Chem. Soc.* **103** 4251

Corey E J and Erickson B W 1971 *J. Org. Chem.*

Corey E J and Suggs J W 1975 *J. Org. Chem.* **40** 2554

Crugnola A, Lombardi P, Gandolfi C and Arcamone F 1981 *Gazz. Chim. Ital.* 111

Davies D T, Jones D S and Sutherland J K 1983 *Tetrahedron Lett.* **24** 519

Di Marco A, Gaetani M and Scarpinato B 1969 *Cancer Chemother. Rep.* **53** 33

Dsolson M G, Chenard B L and Swenton J S 1981 *J. Am. Chem. Soc.* **103** 5263

Farina F, Primo J and Torres T 1980 *Chem. Lett.* 77

Farina F, Vega J C and Prados P 1982 *An. Quim.* **C78** 354

Gesson J P, Jacquesy J C and Mondon M 1983 *Nouvo. J. Chim.* 7 205

Gesson J P, Jacquesy J C and Renoux B 1983 *Tetrahedron Lett.* **24** 2757

Gesson J P and Mondon M 1982 *J. Chem. Soc. Chem. Commun.* 421

Grinev A N, Protopov I S and Cherkasova A 1972 *J. Org. Chem. USSR* (Engl. Transl.) **8** 220

Gurjar M K, Yadav J S and Rama Rao A V 1984a *Indian J. Chem.* (in press)

Gurjar M K, Patil V J, Yadav J S and Rama Rao A V 1984b *Carbohydr. Res.* (in press)

Hauser F M and Prasanna S 1981 *J. Am. Chem. Soc.* **103** 6378

Henry D W 1974 *Cancer Chemother. Rep.* Parts 2, 3, 4

Honek J F, Mancini M L and Belleau B 1983 *Tetrahedron Lett.* **24** 257

Horton D and Weckerle W 1975 *Carbohydr. Res.* **44** 227

Ingle T R, Kulkarni V R, Dhekne V V and Rama Rao A V 1983 *Indian J. Chem.* **B22** 69

Keay B A and Rodrigo R 1983 *Can. J. Chem.* **61** 638

Kelly T R 1979 *Ann. Rep. Med. Chem.* **14** 288

Kelly T R, Vaya J and Ananthasubramanian L 1980 *J. Am. Chem. Soc.* **102** 5983

Kende A S and Boettger S D 1981 *J. Org. Chem.* **46** 2799

Kende A S and Rizzi J P 1981 *J. Am. Chem. Soc.* **103** 4247

Kerdesky F A J, Ardecky R J, Lakshmikantham M V and Cava M P 1981 *J. Am. Chem. Soc.* **103** 1992

Kim K S, Vanotti E, Suarato A and Johnson F 1979 *J. Am. Chem. Soc.* **101** 2483

Kimball S D, Kim K S, Mohanty O K, Vanotti E and Johnson F 1982 *Tetrahedron Lett.* **23** 3871

Kimball S D, Walt D R and Johnson F 1981 *J. Am. Chem. Soc.* **103** 1561

Kraus G A and Pezzanite O 1981 *J. Org. Chem.* **47** 4337

Krohn K 1981 *Angew Chem.* (Int. Eng. Ed.) **20** 576

Krohn K 1981 *Tetrahedron Lett.* **22** 3219

Krohn K and Behnke B 1981 *Tetrahedron Lett.* **23** 395

Lenz L and Page J A 1976 *Can Treat. Rep.* **3** 111

Li Tsung-tee and Walsgrove T C 1981 *Tetrahedron Lett.* **22** 3741

Marsh J P Jr, Mosher C W, Acton E M and Goodman L 1967 *J. Chem. Soc. Chem. Commun.* 973

Martin V S, Woodard S S, Katsuki T, Yamada Y, Ikeda M and Sharpless K R 1981 *J. Am. Chem. Soc.* **103** 6237
Medgyes G and Kuszmann J 1981 *Carbohydr. Res.* **92** 225
Neidel S 1977 *Nature (London)* **268** 195
Parker K A and Kallmerten J 1980 *J. Am. Chem. Soc.* **102** 5881
Pearlman B A, McNamara J M, Hasan I, Hatakeyama S, Sekizaki H and Kishi Y 1981 *J. Am. Chem. Soc.* **103** 4248
Penco S, Angelucci F, Arcamone F, Ballabio M, Barchielli G, Franceschi G, Franchi G, Saurato A and Vanotti E 1983 *J. Org. Chem.* **48** 406
Pettit G R, Einek J J, Herald C L, Ode R H, Von Dreele R, Brown P, Brazhnikov M G and Gouse G F 1975 *J. Am. Chem. Soc.* **97** 1387
Rama Rao A V, Bal Reddy K and Mehendale A R 1983 *J. Chem. Soc. Chem. Commun.* 564
Rama Rao A V, Deshpande V H and Laxma Reddy N 1980 *Tetrahedron Lett.* **21** 2661
Rama Rao A V, Deshpande V H and Laxma Reddy N 1982 *Tetrahedron Lett.* **23** 4373
Rama Rao A V, Deshpande V H and Laxma Reddy N 1982 *Tetrahedron Lett.* **23** 775
Rama Rao A V, Deshpande V H and Reddy N L 1980 *Tetrahedron Lett.* **21** 2661
Rama Rao A V, Mehendale A R and Bal Reddy K 1982 *Tetrahedron Lett.* **23** 2415
Rama Rao A V, Mehendale A R and Bal Reddy K 1983 *Tetrahedron Lett.* **24** 1093
Rama Rao A V, Venkatswamy G, Javeed S M, Deshpande V H and Ramamohan Rao B R 1983 *J. Org. Chem.* **48** 1552
Rama Rao A V, Yadav J S, Bal Reddy K and A R Mehendale (Unpublished results)
Rao M V and Bhatt M V 1981 *Indian J. Chem.* **B20** 487
Reddy M P and Krishna Rao G S 1981 *Tetrahedron Lett.* **22** 3549
Sekizaki H, Jung M, McNamara J M and Kishi Y 1982 *J. Am. Chem. Soc.* **104** 7372
Smith T H, Fujiwara A N, Lee W W, Wu H Y and Henry D W 1977 *J. Org. Chem.* **42** 3663
Suzuki F, Trenbeath S, Gleim R D and Sih C J 1978 *J. Org. Chem.* **43** 4159
Swenton J S, Anderson D K, Jackson D K and Narasimhan L 1981 *J. Org. Chem.* **46** 4825
Tamariz J, Schwager L, Stibbard J H A and Vogel P 1983 *Tetrahedron Lett.* **24** 1497
Tamura Y, Wada A, Sasho M, Fukunaga K, Maeda H and Kita Y 1982 *J. Org. Chem.* **47** 4376
Tanno N and Terashima S 1983 *Chem. Pharm. Bull.* **31** 821
Umezawa H, Takahashi Y, Kinoshita M, Naganawa N, Tatsuta K and Takeuchi T 1980 *J. Antibiot.* **33** 1581
Vedeys E and Nader B 1982 *J. Org. Chem.* **47** 3195
Wani M, Taylor H L, Wall M E, McPhail A T and Onan K D 1975 *J. Am. Chem. Soc.* **97** 5955
Wong C M, Popien D, Schwenk R and Te Raa J 1971 *Can. J. Chem.* **49** 2712
Yadav J, Corey P, Hsu C T, Perlman K and Sih C J 1981 *Tetrahedron Lett.* **22** 811
Yamaguchi T and Rojima M 1977 *Carbohydr. Res.* **59** 343

Proc. Indian Acad. Sci. (Chem. Sci.), Vol. 93, No. 6, August 1984, pp. 1079–1097.
© Printed in India.

Recent developments in the chemistry of perhydroindoles and perhydrocinnolines†

K NAGARAJAN
Hindustan CIBA-GEIGY Limited, Research Centre Goregaon East, Bombay 400 063, India

Abstract. Recent synthetic routes to the tetrahydro, hexahydro and octahydro derivatives of indoles are reviewed. An interesting one is the formation of 3-amino-4-oxo-4,5,6,7-tetrahydroindoles in the reaction of 2-phenacyl cyclohexane-1,3-diones with 1,1-disubstituted hydrazines. Antifertility, CNS depressant and antiinflammatory activities have been encountered for perhydroindoles besides other biological activities. Hexahydrocinnolines are obtained from the reaction of 2-phenacyl (acetonyl) cyclohexanones and cyclohexane-1,3-diones with hydrazines, while octahydrocinnolines are formed from cyclohexanone-2-acetic acids and hydrazines in two steps. 5-oxo-5,6,7,8-hexahydrocinnolines and their oximes undergo anomalous and interesting aromatisation reactions. Some hexahydrocinnolines are CNS depressants while octahydrocinnolines are analgesics. More importantly, they are precursors for interesting azamorphinans.

Keywords. Perhydroindoles; perhydrocinnolines; antifertility; CNS depressants; analgesics; azamorphinans; aromatization; antiinflammatory activities.

1. Introduction

There is a growing volume of literature pertaining to heterocycles fused to a cyclohexane ring, much of this from the point of view of biological activity. An outstanding example is perhaps molindone, a 4-keto-4,5,6,7-tetrahydroindole (1) which is a neuroleptic and, in low doses, an anxiolytic (Rubin *et al* 1967). A variety of other biological activities have been also obtained for perhydroindoles (Nagarajan 1981; Nagarajan and Arya 1982). The isolation of mesembrine (2) from *Sceletium namaquense* (Jeffs 1981) and the incorporation of the octahydroindole ring system in the erythrina alkaloids (Dyke and Quessy 1981), hasubanan alkaloids (Inubushi and Ibuka 1977) and in the amaryllidaceae alkaloids (Fuganti 1975) have generated voluminous chemistry. Perhydroindazoles (3) have antiviral properties (Blatter and Lucas 1972), while reduced benzimidazoles (4) are reported to be antiinflammatory (Halpern 1969) (chart 1). Much interesting synthetic chemistry has emanated from the area of perhydroindoles as evidenced by the work of Weiss *et al* (1969) and of perhydrocinnolines (Kametani 1980). For several years, we had been engaged in exploring the potential of perhydroindoles and perhydrocinnolines as candidate drugs for diverse indications and were rewarded both in terms of biological activities as well as novel chemistry. In this article, we propose to summarise our work briefly, while simultaneously noting highlights of other contemporary contributions in this field.

2. Perhydroindoles

2.1 *Synthesis of* 4,5,6,7-*tetrahydroindoles*

2.1a *Knorr synthesis of pyrroles*: Extension of the Knorr synthesis of pyrroles from 1,4-diketones to the diones (6) affords easy access to compounds of type (8). Alkylation

†Contribution No. 736 from Research centre.

of enamine (5) with α-haloketones provides the starting materials, which are condensed with primary amines. An interesting extension is to N,N-disubstituted hydrazines, *e.g.* N-aminopiperidine which is condensed with (7) to lead to the formation of the novel tetrahydroindole (9). The synthesis is applicable for 2,3-trimethylene (10) and 2,3-pentamethylene pyrroles (11) as well (Nagarajan *et al* 1984; Bell *et al* 1970) (chart 2).

2.1b *From cyclohexanone enamines and α-bromoacetaldehyde*: (Zav'yalov and Skoblik 1976) (chart 3).

2.1c *From cyclohexanone enamine and oximes of α-haloketones*: (Nakanishi *et al* 1981) (chart 4).

2.1d *From cyclohexanone oxime and vinyl chloride*: (Trofimov *et al* 1981). A variation of this procedure uses ethylene (Trofimov *et al* 1978) (chart 5).

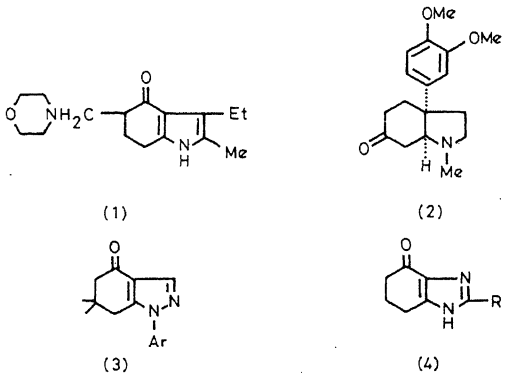

(Chart 1)

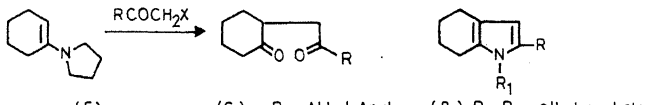

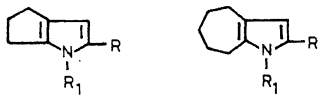

(Chart 2)

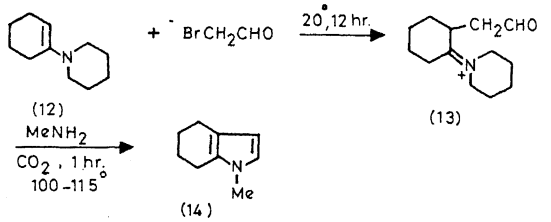

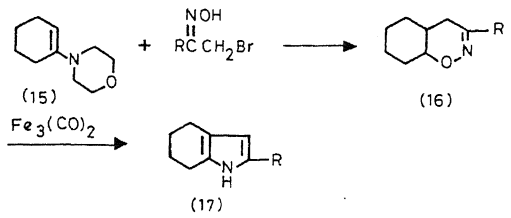

(Chart 4)

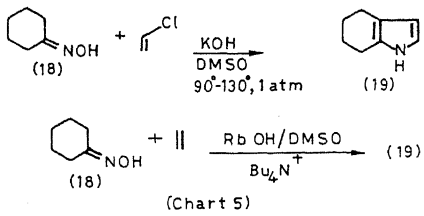

(Chart 5)

2.1e *From cyclohexanoneimines and α-chloroacrylonitrile*: (Olessen *et al* 1978) (chart 6).

2.1f *From 2-formylcyclohexanone and ethyl α-aminoacetoacetate*: (Zav'yalov and Skoblik 1977). Regioselectivity in this condensation reaction has been discussed (chart 7).

2.1g *From cyclohexane-1,2-dione*: (Trost and Keinen 1980) (chart 8).

2.1h *From 4-oxo-4,5,6,7-tetrahydroindoles*: (Remers and Weiss 1972; Takagi *et al*

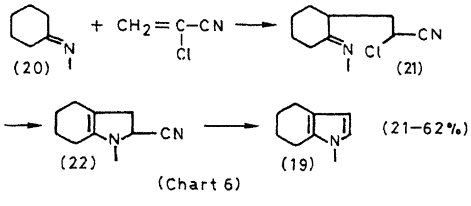

(Chart 6)

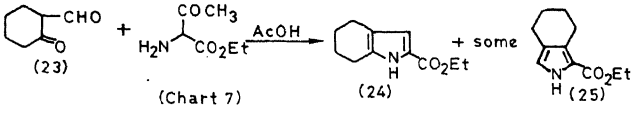

(Chart 7)

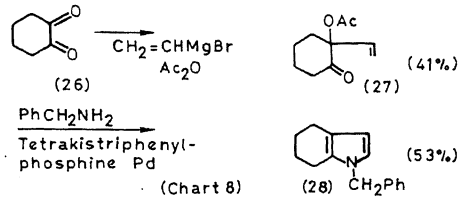

(Chart 8)

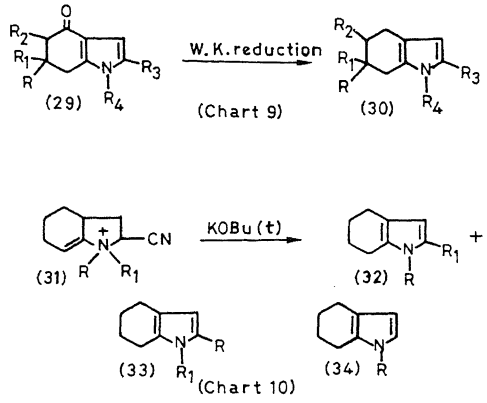

1973; Nagarajan *et al* 1984; Kost *et al* 1966) (chart 9). 4-oxo-4,5,6,7-tetrahydroindoles can be deoxygenated using Wolff-Kischner reaction or catalytic hydrogenation.

2.1i *From a hexahydroindole by Stevens rearrangement*: (Madsen and Lawesson 1976) (chart 10).

From a preparative point of view, route 2.1a may be considered to be most convenient and suitable and expected to provide a wide variety of 4,5,6,7-tetrahydroindoles.

2.2 *4-oxo-4,5,6,7-tetrahydroindoles*

2.2a *'Knorr synthesis'*: This procedure (Stetter and Siehnhold 1955; Stetter and Lanterbach 1962) is versatile and has been used by several groups of workers including our group (Nagarajan *et al* 1984; Remers and Weiss 1965; Ramadas *et al* 1978; Schoen and Finizio 1971) (chart 11). Yields are generally high.

The route has been extended to provide oxotetrahydroindoles (40) and (42) carrying acetic acid side chain at position 3 or 2 (Nagarajan 1981) and to 4-oxo-4,5,6,7-tetrahydrooxindoles (43) (Nagarajan and Shenoy unpublished) (chart 11). Along with (40), occasionally tricyclic products (40a) were isolated. The synthesis of acid (3a) from dimedone and maleic acid is reported (Schaeffer and Vince 1962).

2.2b *An unusual reaction of 2-phenacyl-dimedone formation of 2-aryl-3-amino-4-oxo-4,5,6,7-tetrahydroindoles*: In contrast to the reaction of 2-phenacyl cyclohexanone with 2-aminopiperidine to form 1-piperidino derivative (a), 2-phenacyl dimedone (44) behaves anomalously towards this reagent to form the 3-piperidinoindole (45) in good yield. The reaction is general for other 1,1-substituted hydrazines and 2-phenacyl dimedones carrying substituents on the 2-phenyl group, products analogous to (45) being formed in moderate to good yields (Nagarajan and Shah 1972). 2-Acetonyl dimedone however does not undergo this reaction. 2-Phenacylcyclohexane-1,3-dione and N-aminopiperidine form both types of products. The anomalous reaction is visualised to proceed as shown in chart 12.

In consonance with the proposed mechanism, 2-phenacyldimedone and N,N-dimethyl hydrazine undergo reaction in the presence of excess morpholine to afford the 3-morpholino derivative (51) as the major and the 3-dimethylamino compound (52) as

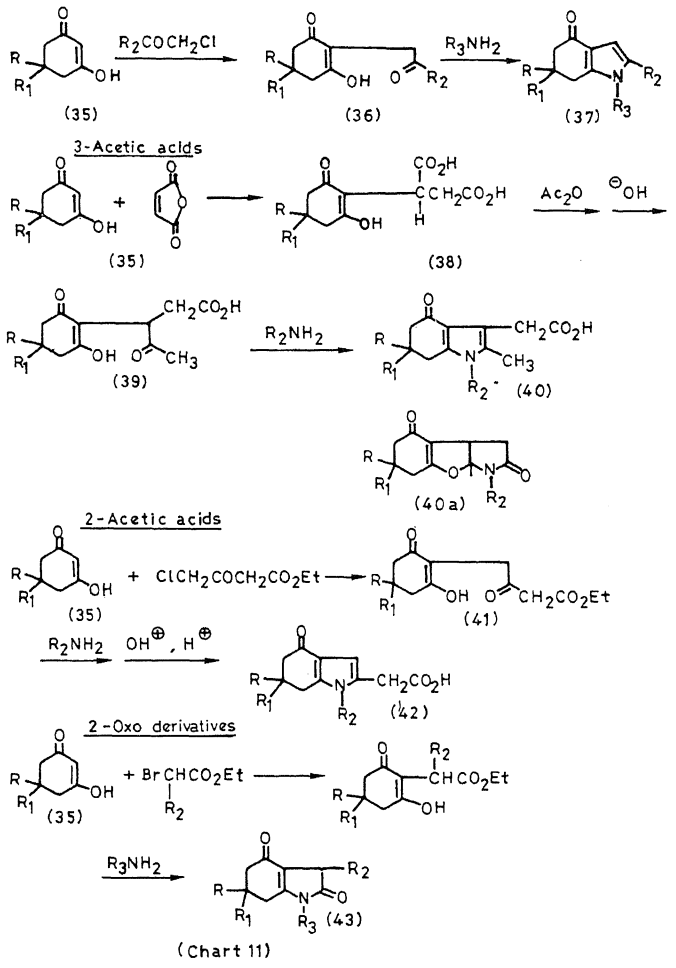

(Chart 11)

the minor products (chart 12). Further, use of excess *n*-propylamine or aniline instead of morpholine in this reaction gave products (53) and (54) respectively incorporating these amines (chart 12).

Blocking of position 3 for aromatisation could be expected to afford further interesting variation. The reaction of propiophenone derivative (55) with N-aminopiperidine did in fact take a slightly different turn, forming (56) and (57) by a sequence of rational reactions (Nagarajan and Shah unpublished) (chart 13).

The proof of the structure of the anomalous products rested both upon a degradation sequence as well as on synthesis (chart 14).

2.2c *From 2-propargylcyclohexane-1,3-diones*: (Schulte *et al* 1963; Schoen and Pachter 1968) (chart 15).

2.2d *From cyclohexane-1,3-diones and isonitrosoketones*: (Hauptmann *et al* 1966) (chart 16). R_2 and R_3 can be varied quite extensively in this route.

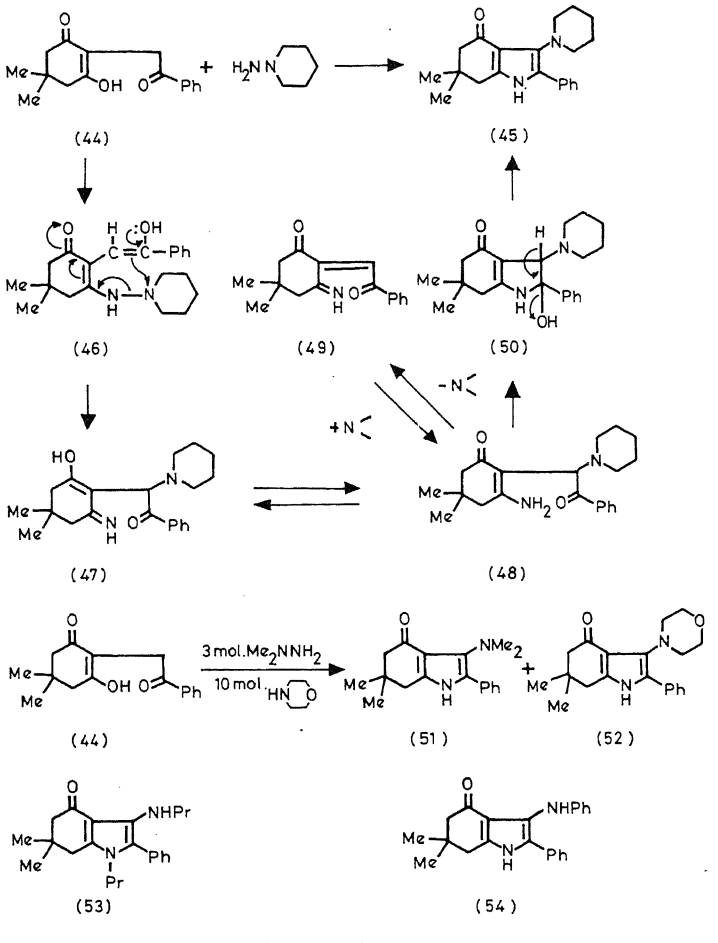

(Chart 12)

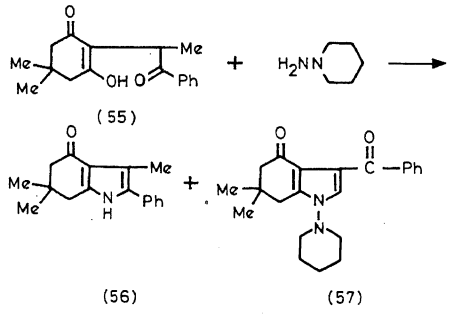

(Chart 13)

2.2e *From cyclohexane-1,3-diones and aminoacetals*: (Bobbit *et al* 1978) (chart 17). Compounds (65) have been converted to β-carbolines.

2.2f *From cyclohexane-1,3-dione enamine and ethyl α-bromoacetate*: (Murata *et al* 1973) (chart 18).

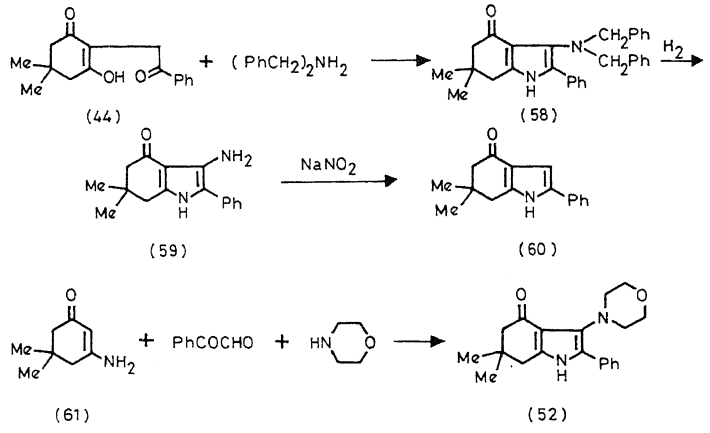

(Chart 14)

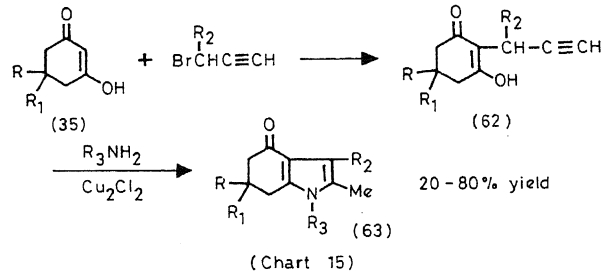

(Chart 15)

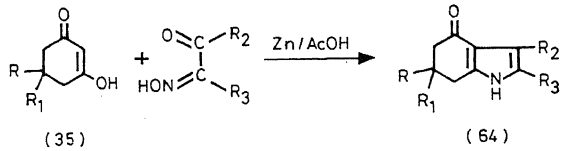

(Chart 16)

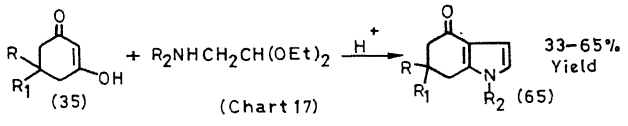

(Chart 17)

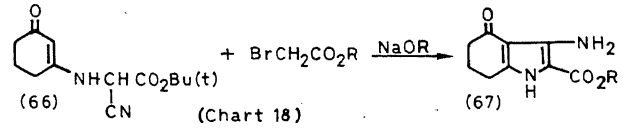

(Chart 18)

2.2g *From 4-oxo-4,5,6,7-tetrahydrobenzofuran carboxylic acid derivatives*: (Stetter and Lauterbach 1962; Nagarajan and Shenoy unpublished) (chart 19).

2.3 *5-Oxo-4,5,6,7-tetrahydroindoles*

Birch reduction of 5-methoxyindole serves as a route for this group of compounds (Teuber and Schmitt 1969; Remers *et al* 1967) (chart 20). In the presence of ruthenium catalyst, (72) is reduced to an octahydroindole (chart 20).

2.4 *Some reactions of 4,5,6,7-tetrahydroindoles*

2.4a *Dehydrogenation*: 4,5,6,7-Tetrahydroindoles are dehydrogenated catalytically into aromatic indoles (Bell *et al* 1970) while the oxo-derivatives are transformed to 4-hydroxyindoles (Remers and Weiss 1965).

2.4b *Mannich reaction*: 4,5,6,7-Tetrahydroindole (75), formaldehyde and morpholine afford readily under acid catalysis, the base (76), while the 4-oxo derivative (77) undergoes aminomethylation reluctantly at both positions 3 and 5 (Nagarajan *et al* 1984) (chart 21). When position 3 is blocked and especially with no alkyl groups at position 6, aminomethylation occurs with great facility at position 5 (Schoen and Pachter 1968).

2.4c *Ring expansion of 4-oxo-4,5,6,7-tetrahydroindoles* 13: Beckmann rearrangement of oxime (80) takes place regiospecifically to afford pyrroloazepine (81) (Nagarajan *et al*

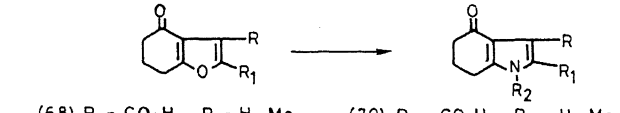

(68) R = CO_2H; R_1 = H, Me (70) R = CO_2H; R_1 = H, Me
(69) R = Me; R_1 = CO_2H (71) R = Me; R_1 = CO_2H

(Chart 19)

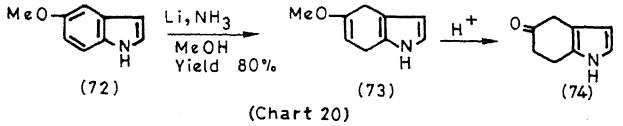

(72) (73) (74)

(Chart 20)

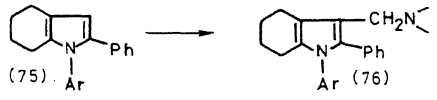

(75) (76)

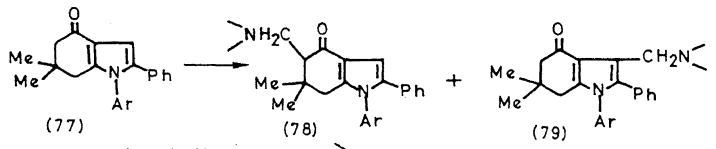

(77) (78) (79)

Ar = 4-fluorophenyl; N = morpholino

(Chart 21)

1984) (chart 22). The formation of both isomeric pyrroloazepines from analogous oximes has been reported earlier (Stoll and Troxler 1968).

2.4d *Villsmeier-Haack and Wittig reactions*: Products of these reactions of 4-oxo-4,5,6,7-tetrahydroindoles and subsequent utilization for the construction of heterocycles have been extensively reviewed (Weiss *et al* 1969).

2.4e *Ring annelation of 4-oxo-4,5,6,7-tetrahydroindoles*: Reaction of the ketocarboxylate (82) with hydrazines gives rise to the tricyclic system (83) (Nagarajan and Shah unpublished; Remers *et al* 1971) (chart 23). With *o*-aminobenzophenones and (84) a tetracyclic system (85) results (Takagi *et al* 1973) (chart 23).

2.5 *Hexahydroindoles*

2.5a 2,3,4,5,6,7-*Hexahydro-4-Oxoindoles*: 2-Allyldimedone (86) heated with *p*-fluoraniline affords (87) in modest yield (Nagarajan *et al* 1984) (chart 24).

2.5b 3*a*,4,5,6,7,7*a*-*Hexahydro-3H-indoles*: Reduction of the unsaturated oxime (88) with zinc and acetic acid leads interestingly to the formation of hexahydroindoles (89) and (90) (Wagner-Jauregg and Roth 1960) (chart 25). Dry distillation of trans-2-

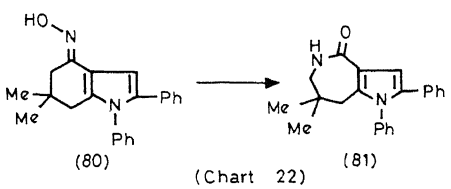

(Chart 22)

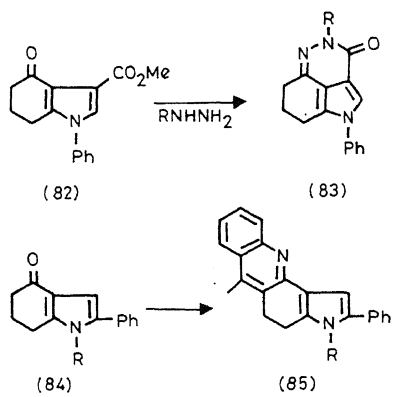

(Chart 23)

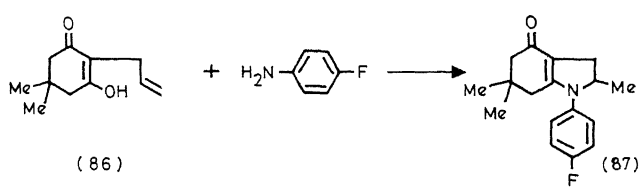

(Chart 24)

acetamido-1-cyclohexane acetic acid (91) gives rise to the trans-derivative (92) which was further reduced to the octahydroindole (93) (Murakoshi *et al* 1964) (chart 25).

2.5c 3*a*,4,5,6,7,7*a*-*Hexahydro*-1*H*-*indoles*: Palladium-catalyzed intramolecular amination of the olefin (94) provides the hexahydroindole (95) in 48% yield (Hegedus and Mckearin 1982) (chart 26).

2.5d 2,3,4,5,6,7-*Hexahydroindoles*: These seem to exist in the enamine form rather than as the imine with the double bond at 1,7a position. However, the imine form is encountered in the nitrone (100) and the 7,7-disubstituted derivative (104).

2.5d(i) *From cyclohexanone and ethanolamine*: (Yusupov *et al* 1979) (chart 27).

2.5d(ii) *From* 2-(*nitroethyl*)*cyclohexanones*: (Moorjani *et al* 1979; Feuer *et al* 1968) (chart 28). The use of zinc and ammonium chloride for the reduction provides a nitrone which undergoes addition of Grignard reagents to give octahydroindoles (Lunt 1963).

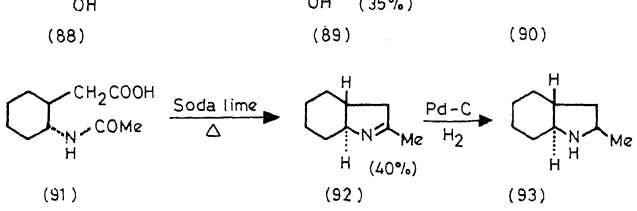

(Chart 25)

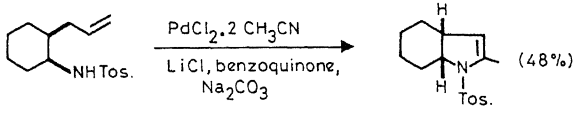

(Chart 26)

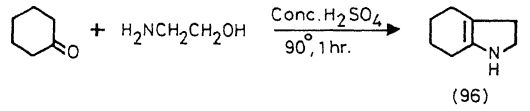

(Chart 27)

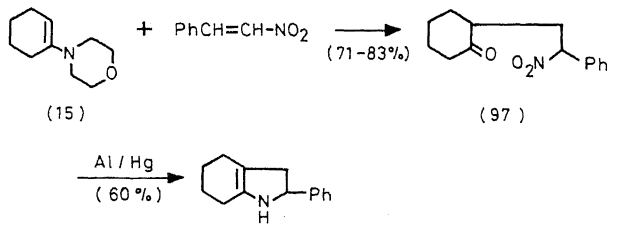

2.5d(iii) *From cyclohexanone-2-propionic acid*: (Kost *et al* 1964) (chart 29).

2.5e 2,3,3*a*,4,5,6-*Hexahydroindoles*: Under certain conditions the intramolecular condensation of an amino group with cyclohexanone leads to products with the double bond at 3a, 7 position.

2.5e(i) *From 7-substituted cyclohexanone-2-acetic acid*: (Bertho and Schmidt 1964; Kost and Rudakova 1965) (chart 30). In the Russian work (106) R = Ph upon hydrogenation with platinum in acetic acid gives the *trans* oxindole. Compounds (106) where R is a β-phenylethyl group have been cyclised to the erythrina skeleton (Mondon *et al* 1959). Fujisawa *et al* (1965a) (chart 31).

2.5e(ii) *From 2-arylcyclohexanone-2-acetic acids*: (Langlois *et al* 1971) (chart 31). (111) has been reduced further and cyclised to give the crinane ring system.

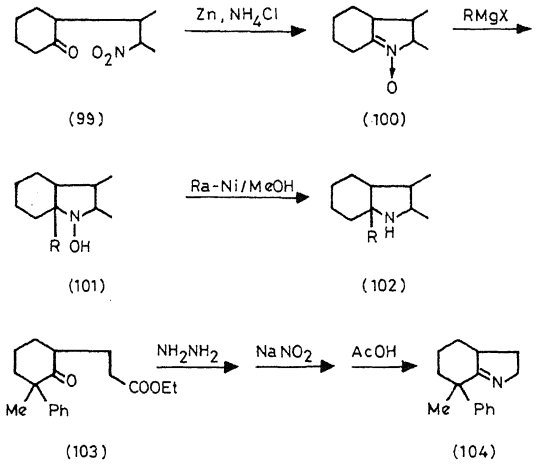

(99) (100) (101) (102) (103) (104)

(Chart 29)

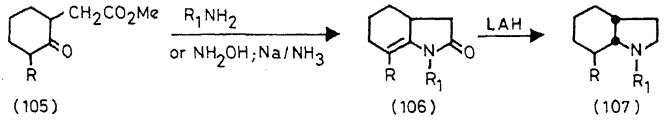

(105) (106) (107)

(Chart 30)

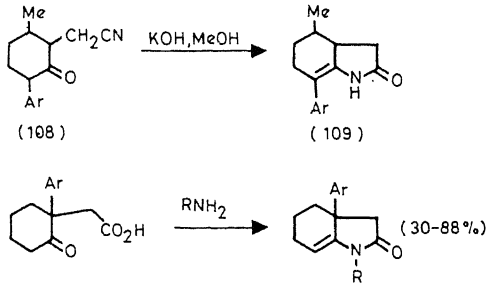

(108) (109) (110) (111)

(Chart 31)

2.5f *From hydrogenation of indoline*: (Butula and Kuhn 1968) (chart 32).

2.6 2,3,3*a*,4,5,6,7,7*a*-1*H*-*Octahydroindoles*

Voluminous chemistry relating to this system as a component of alkaloids has been adequately reviewed (Jeffs 1981; Dyke and Quessy 1981; Fuganti 1975). Hence only very few routes will be mentioned briefly.

2.6a *Catalytic hydrogenation of indoles, and dihydro, tetrahydro and hexahydroindoles*: Reaction of 2-methylindole with *n*-propanol in toluene in the presence of Raney nickel and aluminium *n*-propoxide leads to the *n*-propyl compound as well as the octahydro derivative as a minor basic product (Botta *et al* 1979). 1-Methyl-7-methoxyindole upon reduction using platinum catalyst in acetic acid leads to *cis*-octahydro-1-methylindole along with the 7(e) methoxy derivative (Mokotoff 1973). For other reductions, see Toth (1967), Toth and Gerces (1971), Cohen and Heath-Brown (1965) and Trofimov *et al* (1978a).

2.6b *Addition of aryllithiums to hexahydroindole*: (Godefroi 1962) (chart 33).

2.6c *From cyclohexanone-2-acetic acid*: (Valodine *et al* 1965) (chart 34). With N-methylformamide, both *cis* and *trans* 1-methyloctahydroindoles were obtained.

2.6d *From N-chloramines*: The intramolecular cyclisation of suitable N-chloramines under acidic solvolytic conditions is regioselective for enol ether and dioxalanes and affords octahydroindole (Furstoss *et al* 1976).

2.6e *From aziridine and diethyl malonate*: (Kojima and Tomioka 1976) (chart 35).

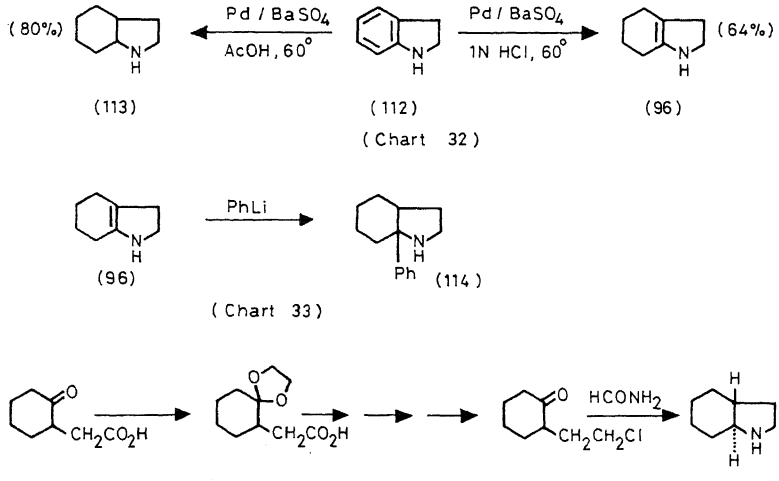

2.6f *From an annealed cyclohexanone*: (Jeffs and Molina 1973) (chart 36). The paper is especially interesting for its discussion of conformational features.

2.6g *Synthesis of mesembrine-like compounds*: (Taguchi *et al* 1970; see also Jeffs 1981) (chart 37). (127) was further reduced to the alcohols and subjected to the Pictet-Spengler reaction to form dihydrocrinine models.

2.7 *Biological activity of perhydroindoles*

2.7a *Antifertility activity*: The following derivatives showed marked antiimplantation activity in the rat (Nagarajan *et al* 1984), (130) being the most potent (chart 38).

2.7b *Hypoglycemic activity*: Oxotetrahydroindole-3-acetic acids (131) and (132) exhibited activity in both the normal and streptozotocin diabetic rat (Nagarajan 1981· Talwalker 1981) which was not mediated by inhibition of gluconeogenesis. Related 2-acetic acids or 2- or 3-carboxylic acids were inactive.

2.7c *Antiinflammatory-analgesic activity*: 4-Oxo-4,5,6,7-tetrahydroindoles (133) and (134) had antiinflammatory activity in the carragenin rat paw oedema test and were also analgesic. They had no prostaglandin synthetase inhibitory activity *in vitro*, and were inactive in the chronic adjuvant arthritis model in the rabbit (Nagarajan and Shenoy unpublished results).

2.7d *Other activities*: The neuroleptic activity of molindone has been mentioned already (Rubin et al 1967). Derivatives of octahydroindoles have been reported to be

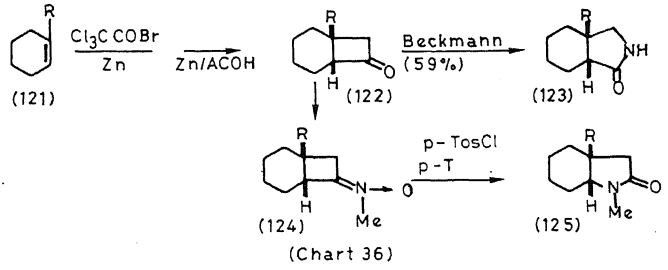

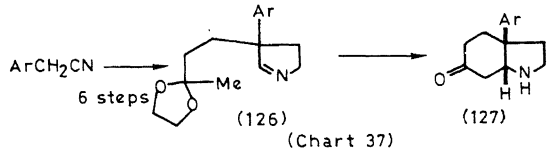

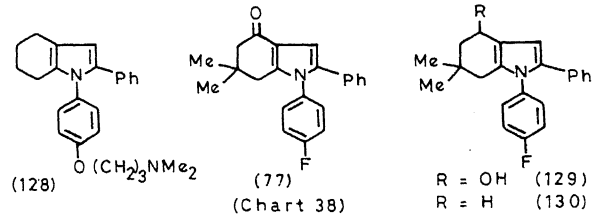

curare-like (Luellmann *et al* 1967), ganglion-blockers (Nerurkar 1968), ataractics (Boehringer and Soehne 1962), spasmolytics (Enenkel *et al* 1963) and useful as intermediates for antitussives (Fujisawa *et al* 1965) and as fungicides and herbicides (Himmele and Pommer 1980; Foerester *et al* 1979; Sturm and Vogel 1974).

3. Perhydrocinnolines

3.1 *Hexahydrocinnolines*

Condensation of 2-phenacylcyclohexanone (7) with hydrazine affords (135), which has been aromatised to (136) (Baumgarten 1958) (chart 39).

3.2 5-*Oxo*-1,4,5,6,7,8-*hexahydrocinnolines*

These became available by the interaction of 2-acetonyl or 2-phenacyl cyclohexane-1,3-diones with hydrazines or monosubstituted hydrazines (chart 40). The reaction is versatile and has been extensively studied (Nagarajan *et al* 1976; Nagarajan *et al* unpublished). Condensation of 2-acetonyl dimedone with *p*-nitrophenylhydrazine

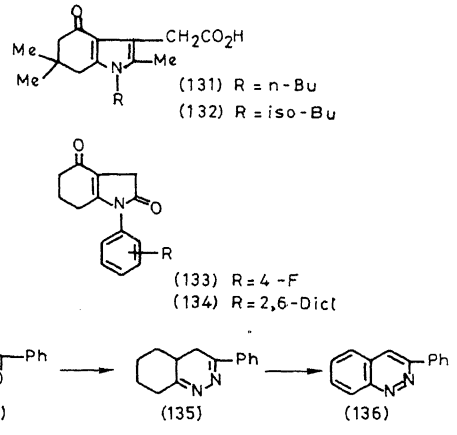

(Chart 39)

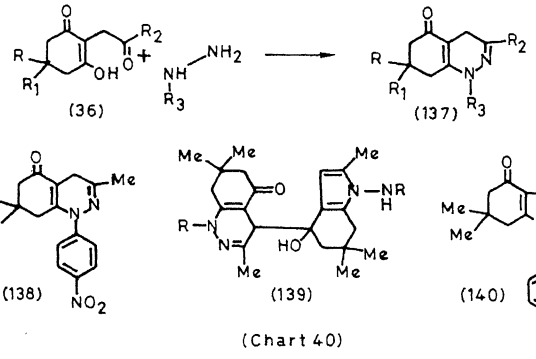

(Chart 40)

afforded (138) and (139) while with 2,4-dinitrophenylhydrazine, indole (140) results presumably because of the low nucleophilicity of the aniline nitrogen.

3.3 *Octahydrocinnolines*

LAH reduction of the condensed pyridazinone leads to a complex mixture of products (Daunis *et al* 1972) (chart 41).

3.4 *Decahydrocinnolines*

A series of publications have appeared from Japan on the synthesis of this class of compounds as analgesics and as intermediates for 9-azamorphinans (Kametani 1980 and references cited therein). These compounds have been covered by patents also (Grelan 1981) (chart 42).

3.5 *An unusual sequence of reactions of 5-oxo-1,4,5,6,7,8-hexahydrocinnolines*

3.5a *Oximination*: We shall describe in this section, published (Nagarajan and Shah 1973) and unpublished (Nagarajan *et al*, unpublished) work on interesting transformations of (149). Prolonged exposure of a hot solution of (149) in pyridine to air, or better to *p*-toluenesulphonyl chloride, led to the formation of the aromatic product (150), while with acid, an internal oxidation-reduction took place to form (151). The oxime (153) (R = Me; R_1 = Ph) of (150) was obtained directly in near quantitative yield by reaction of (149) with excess hydroxylamine in pyridine. 1-Substituted derivatives (152) also afforded the aromatised oximes (153) in low yield. The reaction presumably occurs by hydroxylamine functioning as an oxidising agent, since quaternary salts of the type (154) could be isolated from (152) (R = Me; R_1 = R_2 = Ph). The reaction may be mediated by radicals as evidenced by the isolation of products such as (155) and (156) from the same reaction (chart 43).

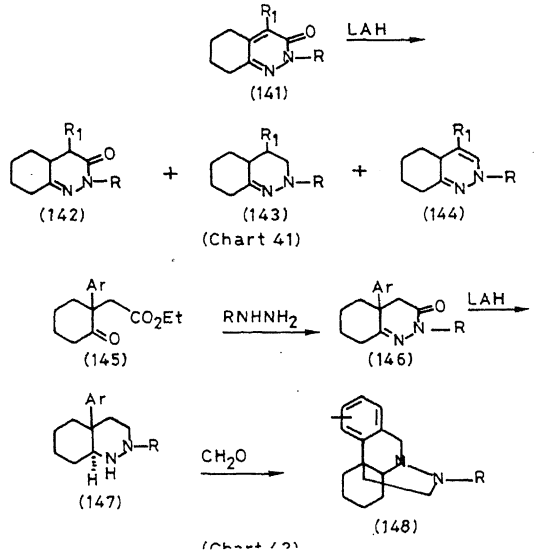

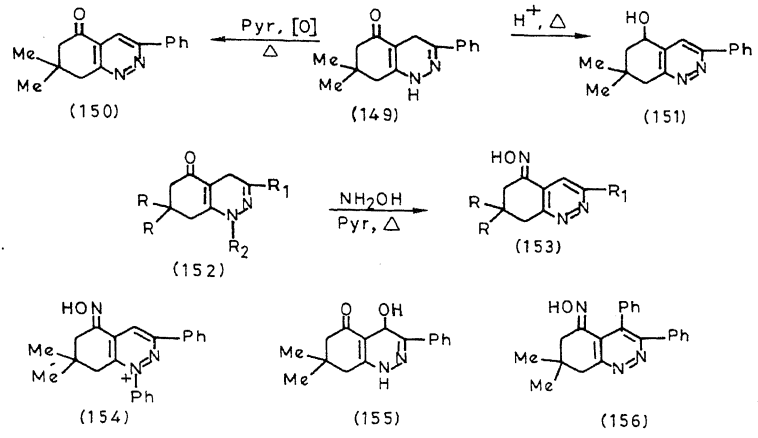

(Chart 43)

3.5b *Attempted Beckmann transformation of oximes* (153) *and Schmidt reaction on ketone* (150): Treatment of the ketone (150) with sodium azide and sulphuric acid gave in high yield 5-aminocinnoline (157) which also resulted from oxime (153) (R = Me; R_1 = Ph) by rearrangement in the presence of PPA, sulphuric acid or $POCl_3$-pyridine. The aromatisation reaction, involving the Semmler-Wolff rearrangement, was general for similar oximes. The position of the methyl group was easily ascertained by the fortuitous formation of the pyrazole (158) during an attempted deamination of (157) after diazotisation. The configuration of oxime (153) as shown and the reluctance of the bond *a* attached to the electron deficient pyridazine ring are considered to be the factors favouring Semmler-Wolff rearrangement (chart 44). Semmler-Wolff rearrangement was observed in the following special case as well (chart 45) (Nagarajan unpublished). While many acidic conditions transformed oximes (153) to 5-aminocinnolines, only PCl_5 brought about the desired Beckmann transformation to (162) but in 10% yield and conc. HCl gave rise to a mixture of products from which the α-chloroketone (163) was isolated (chart 46) (Nagarajan and Shah unpublished). The formation of 2-

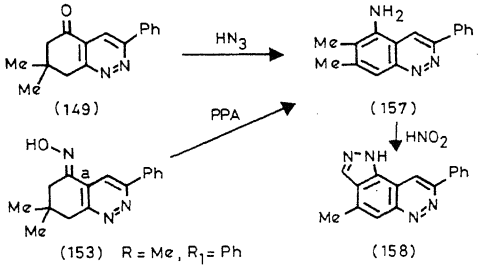

(Chart 44)

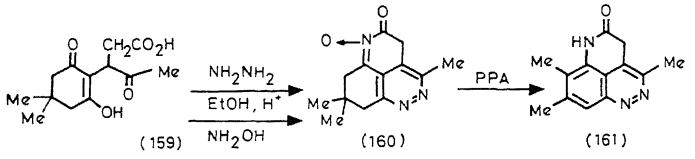

(Chart 45)

(162) (163)

(Chart 46)

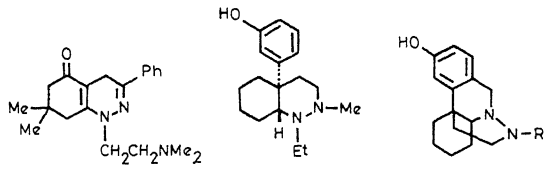

(164) (165) (166)

(Chart 47)

chlorotetralone by the action of Beckmann's mixture on α-tetralone oxime is known (Conley and Ghosh 1971). Reaction of the oxime with formic acid led to hydrolysis, reductive formylation and reductive deoximation.

3.6 *Biological activities of perhydrocinnolines*

A number of 1-aminoalkyl-5-oxo-1,4,5,6,7,8-hexahydrocinnolines, *e.g.* (164) are potent, but toxic CNS depressants (Nagarajan *et al* 1976). Decahydrocinnolines, *e.g.* (165) have analgesic activity (Kametani *et al* 1973) while the derived 9-azamorphinans (166) are even more potent (Kametani *et al* 1970) (chart 47).

Acknowledgement

The author is deeply grateful to Mr B G Advani and Mrs S J Shenoy for help in the preparation of the manuscript.

References

Baumgarten H E, Creger P L and Villars C E 1958 *J. Am. Chem. Soc.* **80** 6609
Bell M R, Zalay A W, Oesterlin R, Schane P and Potts G O 1970 *J. Med. Chem.* **13** 664
Bertho A and Schmidt J F 1964 *Chem. Ber.* **97** 3284
Blatter H M and Lucas R A 1972 US patent 3691180 to CIBA Corporation, September 12; (*Chem. Abstr.* 1972 **77** 152178s)
Bobbit J M, Kulkarni C L, Dutta C P, Kofod H and Chiong K N 1978 *J. Org. Chem.* **43** 3541
Boeringer C F and Soehne 1962 *Br. Patent* 898590, June 14; (*Chem. Abstr.* 1963 **58** 6805a)
Botta M, De Angelis F and Nicoletti R 1979 *J. Het. Chem.* **16** 501
Butula I and Kuhn R 1968 *Angew. Chem. (Int. edn)* **7** 208
Cohen A and Heath-Brown B 1965 *J. Chem. Soc.* 7179
Conley R T and Ghosh S 1971 in *Mechanism of molecular migrations* (ed) B S Thyagarajan (New York: Wiley Interscience) Vol 4 p. 281
Daunis J, Guerret-Rigail M and Jacquier R 1972 *Bull. Soc. Chim. Fr.* 1994
Dyke S F and Quessy S N 1981 *The alkaloids* (ed) R G A Rodrigo (New York: Academic Press) Vol 18 p. 1
Enenkel H J, Mueller H and Schulte K 1963 US Patent 3104241 to E Merck A G September 17 (*Chem. Abstr.* 1964 **61** 6993b)

Feuer H, Hirschfeld A and Bergman E D 1968 *Tetrahedron* **24** 1187
Foerester H, Hofer W, Mues V, Eue L and Schmidt R R 1979; Ger. Offen. 2822155 to Bayer A G; Nov. 22 (*Chem. Abstr.* 1980 **92** 146745t)
Fuganti C 1975 *The alkaloids* (ed) R H F Manske (New York: Academic Press) Vol 15 p. 83
Fujisawa T, Okada M and Saito Y 1965 Japan Patent 9035 (1965) to Fujisawa Pharmaceutical Co. Ltd; May 11 (*Chem. Abstr.* 1965 **63** 5612g)
Fujisawa T, Okada K and Saito Y 1965a Japan Patent 16783 (1965) to Fujisawa Pharmaceutical Co. Ltd; July 31 1968 (*Chem. Abstr.* 1965 **63** 16309e)
Furstoss R, Tadayoni R, Esposito G, Lacrampe J, Heumann A and Waegoll B 1976 *Can. J. Chem.* **54** 3569 (*Chem. Abstr.* 1977 **86** 106443)
Godefroi E F 1962 US Patent 3035059 to Parke, Davis and Co. May 15 (*Chem. Abstr.* 1962 **57** 11174a)
Grelan Pharmaceutical Co. Ltd. 1981 Japan, Kokai Tokyo Koho 817076 June 13 (*Chem. Abstr.* 1981 **95** 169203r)
Halpern B 1968 Fr. patent 1510213 to Syntex Corporation. January 19 (*Chem. Abstr.* 1969 **70** 77972w)
Hauptmann S, Blume H, Hartmann G, Haendel D and Franke P 1966 *Z. Chem.* **6** 107 (*Chem. Abstr.* 1966 **64** 17521f)
Hegedus L S and McKearin J M 1982 *J. Am. Chem. Soc.* **104** 2444
Himmele W and Pommer E H 1980 Ger. Offen. 2825961 to BASF AG; January 3 (*Chem. Abstr.* 1980 **92** 198279p)
Inubushi Y and Ibuka T 1977 *The alkaloids* (ed) R H F Manske (New York: Academic Press) Vol 16 p. 393
Jeffs P W and Molina G 1973 *J. Chem. Soc. Chem. Commun.* 3
Jeffs 1981 *The alkaloids* (ed) R G A Rodrigo (New York: Academic Press) Vol 19 p. 1
Kametani T, Kigasawa K, Hiiragi M, Wagatsuma N, Wakisaka K, Satoh F and Saito S 1970 *J. Med. Chem.* **13** 1064
Kametani T, Kazuo K, Hiiragi M, Wagatsuma N, Uryu T and Araki K 1973 *J. Med. Chem.* **16** 301
Kametani T 1980 *Heterocycles* **14** 449
Kojima M and Tomioka Y 1976 *Chem. Pharm. Bull.* **24** 1613
Kost A N, Sugrobova I P, Krasnova V A and Portnova S L 1964 *Zh. Obshch. Khim.* **34** 2416 (*Chem. Abstr* 1964 **61** 10618)
Kost A N and Rudakova I P 1965 *Zh. Obshch. Khim.* **35** 145
Kost A N, Ovseneva L J and Shuvaeva T G 1966 *Khim Geterotsikl. Soedin* 717 (*Chem. Abstr.* 1967 **66** 115537)
Langlois M, Guillonneau C, Meingan J and Maillard J 1971 *Tetrahedron* **27** 5641
Luellmann H, Mondon A and Seidel P R 1967 *Naunyn-Schmiedebergs. Arch. Pharmacol. Exp. Pathol.* **258** 9 (*Chem. Abstr.* 1967 **67** 89352v)
Lunt E 1963 Nitro compounds, *Proc. Int. Symp.* Warsaw 291 (*Chem. Abstr.* 1966 **64** 676a)
Madsen J O and Lawesson S O 1976 *Bull. Soc. Chem. Belg.* **85** 819
Mokotoff M 1973 *J. Het. Chem.* **10** 1063
Mondon A, Haselmeyer M G and Zander J 1959 *Chem. Ber.* **92** 2543
Moorjani M C, Sheth P J and Trivedi J K 1979 *Indian J. Chem.* **B17** 67
Murakoshi I, Shikakura Y and Haginiwa J 1964 *Yakugaku zasshi* **84** 671
Murata T, Sugawara T and Ukawa K 1973 *Chem. Pharm. Bull. (Jpn)* **21** 2571
Nagarajan K and Shah R K 1972 *Tetrahedron Lett.* 1467
Nagarajan K and Shah R K 1973 *J. Chem. Soc. Chem. Commun.* 926
Nagarajan K, David J and Shah R K 1976 *J. Med. Chem.* **19** 508
Nagarajan K 1981 Abstracts of 32nd *Indian Pharmaceutical Congress*, Nagpur, January 23–25
Nagarajan K and Arya V P 1982 *J. Sci. Ind. Res.* **41** 232
Nagarajan K, Talwalker P K, Shah R K, Mehta S R and Nayak G V 1984 *Indian J. Chem.*
Nakanishi S, Shirai Y, Takahashi K and Stsuji Y 1981 *Chem. Lett.* 869
Nerurkar S A 1968 *Diss. Abstr.* **B28** 3237 (*Chem. Abstr.* 1968 **69** 27165u)
Olessen S O, Madsen J O and Lawesson S O 1978 *Bull. Soc. Chim. Belg.* **87** 535
Ramadas S R, Ramana D V and Padmanabhan S 1978 *Indian J. Chem.* **B16** 1119
Remers W A and Weiss M J 1965 *J. Am. Chem. Soc.* **87** 5262
Remers W A, Gibs G J, Pidacks C and Weiss M J 1967 *J. Am. Chem. Soc.* **89** 5513
Remers W A, Roth R H and Weiss M J 1971 *J. Med. Chem.* **14** 860
Remers W A and Weiss M J 1972 US patent 3652585 to American cyanamide Co. March 28, 1972 (*Chem. Abstr.* 1972 **77** 5330)
Rubin A A, Yen H C and Pfeffer M 1967 *Nature (London)* **216** 578

Schaeffer H J and Vince R 1962 *J. Org. Chem.* **27** 4502
Schoen K and Pachter I J 1968 Br. patent 1108578 to Endo Laboratories Inc. April 3 (*Chem. Abstr.* 1968 **69** 51999)
Schoen K and Finizio M 1971 US patent 3621027 to Endo Laboratories Inc. November 16 1971 (*Chem. Abstr.* 1972 **76** 72403)
Schulte K E, Reisch J and Land H 1963 *Chem. Ber.* **96** 1470
Stetter H and Siehnhold 1955 *Chem. Ber.* **88** 271
Stetter H and Lauterbach R 1962 *Ann* **655** 20
Stoll A P and Troxler F 1968 *Helv. Chim. Acta.* **51** 1864
Sturm E and Vogel C 1974 Swiss Patent 550170 to Agripat S A June 14 (*Chem. Abstr.* 1975 **82** 43188c)
Taguchi H, Ohishi T and Kugita H 1970 *Chem. Pharm. Bull.* **18** 1008
Takagi K, Kobayashi N and Ueda T 1973 *Bull. Soc. Chem. Fr* 2807
Talwalker P K 1981 Abstracts of 32nd *Indian Pharmaceutical Congress*, Nagpur, January 23–25
Teuber H and Schmitt G 1969 *Chem. Ber.* **102** 713
Toth T 1967 *Magy. Kem. Foly.* **73** 114 (*Chem. Abstr.* 1967 **67** 21767)
Toth T and Gerces A 1971 *Acta Chim.* (Budapest) **67** 229 (*Chem. Abstr.* 1971 **74** 125322)
Trofimov B A, Korostova S E, Mikhaleva A I, Balabanova L N, Vasilev A N and Sigalov M V 1978 USSR patent 620486; August 25, 1978 (*Chem. Abstr.* 1978 **89** 163399)
Trofimov B A, Korostova S E, Balabanova L N, Mikhaleva A I and Vasilev A N 1978a *Khim. Geterotsikl. Soedin* 347 (*Chem. Abstr.* 1978 **89** 42978t)
Trofimov B A, Mikaleva A I and Vasilev A N 1981 USSR patent 840038; June 23 (*Chem. Abstr.* 1981 **95** 150444
Trost B A and Keinen E 1980 *J. Org. Chem.* **45** 2741
Valodina M A, Kiryushkina G V and Terentev A P 1965 *Dokl. Akad. Nauk. USSR* **162** 90 (*Chem. Abstr.* 1965 **63** 5583d)
Wagner-Jauregg J and Roth M 1960 *Chem. Ber.* **93** 3036
Weiss M J, Allen C R, Gibs G J, Pidacks C, Poletto J F and Remers W A 1969 Topics in Heterocyclic Chemistry (ed) R N Castle (New York: Wiley Interscience) p. 178
Zavyalov S I and Skoblik T I 1976 *Izv. Akad. Nauk SSSR, Ser. Khim.* 227 (*Chem. Abstr.* 1976 **84** 135405)
Zavyalov S I and Skoblik T I 1977 *Izv. Akad. Nauk SSSR, Ser. Khim.* 2768 (*Chem. Abstr.* 1978 **88** 120915r)
Yusupov D, Akmerov K M, Kuchkarov A B and Tapilov Z 1979 *Khim. Geterotsikl. Soedin* 265 (*Chem. Abstr.* 1979 **91** 39241)

Proc. Indian Acad. Sci. (Chem. Sci.), Vol. 93, No. 6, August 1984, pp. 1099–1107.
© Printed in India.

Towards biochemical fuel cells

H M SONAWAT, RATNA S PHADKE and GIRJESH GOVIL*

Biochemical Fuel Cell Project, Tata Institute of Fundamental Research, Homi Bhabha Road, Bombay 400 005, India

Abstract. A biochemical fuel cell is a device which converts chemical energy into electrical power. The catalysts used in this process can be either inorganic or organic type giving rise to 'inorganic fuel cells' or 'biochemical fuel cells', respectively. Biochemical fuel cells use either micro-organism or enzymes as active components to carry out electrochemical reactions. The efficiency of such a device theoretically can be as high as 90%. The difficulty in attaining these values arises due to sluggishness of electron transfer from active site to conducting electrode. This can be overcome by using mediators or by immobilizing active components on conducting electrode. We have immobilized FAD-glucose oxidase on a graphite electrode using a semiconducting chain as a bridge. At the present stage of development, such a device lacks high current densities, which is essential for commercial power generation but can be used in applications such as pacemakers and glucose sensors.

Keywords. Biochemical fuel cell; enzyme-coenzyme system; immobilization; modified electrode; cyclic voltametry.

1. Introduction

Human body can be considered as the oldest, yet the most refined fuel cell where food (fuel) is catalytically burned (oxidized) in an electrolyte (blood) to produce energy required for cellular functions. In this process, the chemical energy residing in the chemical bonds of fuel molecules is converted directly into other forms of energy without employing an intermediate thermal cycle. The process of conversion of chemical into electrical energy has received increasing attention during the last two decades, following the high demands for fossil fuels and the consequent depletion of the existing stocks of fossil fuels at an alarming rapid rate.

For several years, fuel cell devices which accomplish a direct conversion of chemical to electrical energy, remained a mere laboratory curiosity on account of problems of electrode development, short operational life and high costs. However, the space exploration programme gave an impetus for development and respectability to fuel cell as a practical device for energy transfer and energy storage.

In this article, we wish to review attempts at developing biochemical fuel cells, with some emphasis on our own work in this direction.

2. What is a fuel cell?

A fuel cell consists of two electrodes—an anode and a cathode separated by an electrolyte which transmits ions but not electrons. A fuel (generally hydrogen) is supplied to the anode and oxygen (from air) is supplied to the cathode. A catalyst

* To whom all correspondence should be addressed.

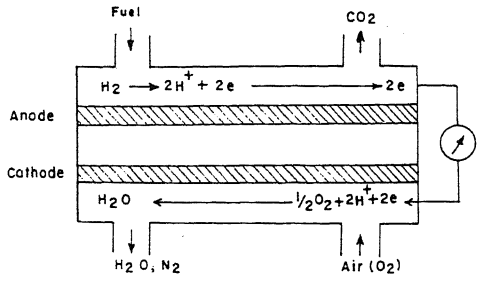

Figure 1. Prototype fuel cell.

situated on the anode causes hydrogen molecules to dissociate into hydrogen ions (H^+) and electrons. If the electrolyte is acidic as in the case of phosphoric acid fuel cells, the hydrogen ions migrate through it to the cathode, where they react with electrons (supplied through the external-circuit load) and oxygen to form water. The nature of migrating ions depends upon the type of electrolyte used. As shown in figure 1, an electric current can flow if the electrodes are connected by means of a conductor.

The maximum direct current developed by a fuel cell is a thermodynamic function of the fuel and the oxidant (Wingard *et al* 1982). Considering that the operation is isothermal and takes place at constant pressure without transference, the efficiency can be calculated. The theoretical amount of work that can be obtained, depends on the net release of Gibb's free energy ΔG during the course of the reaction.

$$\Delta G = nFE,$$

where n is the number of electrons transferred per mole, F is the Faraday constant and E is the net reversible potential. At constant temperature (T) and pressure (P) the free energy is related to the change in enthalpy ΔH and entropy ΔS

$$\Delta G = \Delta H - T\Delta S.$$

The efficiency of fuel cell is defined as

$$\eta = \Delta G/\Delta H = 1 - (T\Delta S/\Delta H).$$

For most systems $T\Delta S$ is 10% of ΔH. Therefore the theoretical efficiency can be as high as 90%. This is considerably higher than that for the systems which are governed by Carnot's cycle $\sim 40\%$. Experimentally efficiencies of the order of 50% have been achieved in fuel cells.

2.1 *Characteristics and disadvantages*

Ideally a fuel cell should possess the following characteristics: (i) the cell should have high conductivity *i.e.* low internal resistance; (ii) the electrodes and electrolyte should be stable *i.e.* there should not be any change due to corrosion or due to accumulation of products leading to a change in the cell reactivity with time; (iii) the cell should exhibit high reactivity; the fuel and oxidant should react rapidly, completely and electrochemically; (iv) It is desirable to have inexpensive materials and the operation should take place under conditions of moderate temperature and pressure.

The majority of inorganic fuel cells in use today, utilize hydrogen as fuel. The electrodes used in these cells are made from expensive materials like platinum, nickel

etc. Moreover, the electrolytes used (*e.g.* phosphoric acid, KOH, molten carbonate) are highly corrosive and the operating temperatures are high, 150–200°C in case of phosphoric acid fuel cell and 600–700°C for molten carbonate device). Some of these problems can be overcome by developing a biochemical fuel cell system.

3. Biochemical fuel cells

In a biochemical fuel cell (BFC), the oxidation of bio-organic materials is catalysed by specific bio-matter either in the form of bacteria (Austin 1967) or purified enzymes (Wingard 1978). There are certain advantages in using biochemical catalysts. Biocatalysts are known to be extremely efficient and selective. They normally operate at neutral pH, at or slightly above room temperature. The concentrations of reactants can be low.

The biochemical fuel cells can be either 'direct' type (figure 2a) or 'indirect' type (figure 2b) (Shaw 1963). In the direct biochemical fuel cell biological oxidation of a raw material (starch, carbohydrate or protein) is achieved with the help of bacteria which facilitate stepwise transfer of protons involving several classes of enzymes and coenzymes provided by the bacteria. The combustion rate in such cells is low since the reactions have to be carried out within narrow temperature and pH ranges. Further the electrodes may get contaminated by bacteria. Moreover, there is very little freedom of

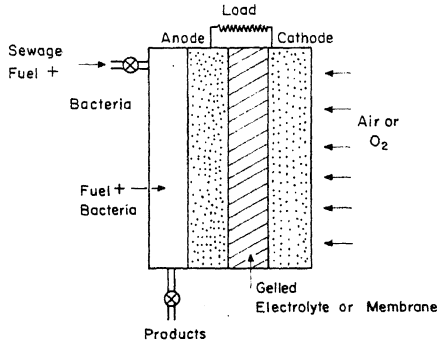

A. DIRECT CELL

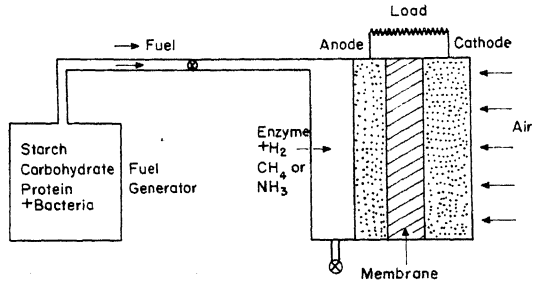

B. INDIRECT CELL

Figure 2. Biochemical fuel cell. (**a**) direct (**b**) indirect.

control or optimisation, as the conditions have to be those which are favourable for bacterial growth.

In indirect biochemical fuel cell, the processes of oxidation and power generation are separated out (figure 2b). The raw fuel is first converted into simpler biochemical end products like H_2, CH_4, CH_3OH, NH_3 etc (secondary fuel) with the help of suitable bacteria in fuel generator (figure 2b). The secondary fuel thus generated is transferred to a second compartment where the electrical power is generated. Such systems are more convenient and easier to optimise but bring in an additional engineering problem, namely, the transfer of secondary fuel.

Efforts have been directed to develop both the direct and indirect fuel cells (Videta and Arvia 1975; Karube *et al* 1977; Ahn *et al* 1976). Almost any waste or organic material can serve as a fuel. The electrical current produced is proportional to the rate of bacterial metabolism. Fifty percent of the bio-fuel gets consumed by the micro-organisms as their nutrient. To date the electrical power produced in such devices is in the milliwatt range (50–60 % efficiency). The inability to attain higher power outputs is probably due to a lack of knowledge about conditions or micro-organisms which can yield higher metabolic rates and/or due to lack of knowledge about the electrode kinetics. Moreover in actual cells when current flows, the potential is not available to produce work as a result of polarization (overpotentials) effects. The main contributions to polarization, arise from activation, concentration and ohmic factors. Activation over-potentials result from the slowness of one of the intermediate steps in the chemical or electron transfer processes. The polarization is due to slow migration of substrate, charge transfer agents or products towards or away from the electrodes. The ohmic over-potentials are on account of slow transport of the ionic species, through the electrolyte medium.

The major difficulty in using micro-organisms is apparently due to the difficulty involved in mild conditions and the process of transferring the electrons across cell membranes. This can be overcome by making fuel matter to undergo electrochemical oxidation with the help of purified enzymes. If the reduced form of an enzyme can be oxidized electrochemically and its oxidized form is allowed to react with a substrate, the enzyme can cycle back and forth, getting oxidized at the electrode surface and reduced by chemical reaction in solution. The net result would be the apparent oxidation of substrate at the electrode.

$$E + R \rightleftharpoons ER$$

$$ER + M \rightleftharpoons M[ER]$$

$$M[ER] \rightleftharpoons M + E + P + H^+ + e^-$$

where E is the enzyme, R is the reactant, M is the electrode surface and P is the product. Several enzyme systems have been examined for their electrochemical activity.

If the enzyme works in conjuction with a coenzyme the whole system can be incorporated into anode or cathode compartment which can act as catalyst for the redox reactions. In the case of enzymes which catalyse redox reactions, the associated cofactors serve as the actual electron and proton transfer agents.

The major problem in such fuel cells is the inefficient transfer of electrons from substrate to electrodes. This can be catalysed by (i) diffusion of cofactor from enzyme active site to the electrode surface; (ii) using electroactive mediators; (iii) immobilization

of enzyme-cofactor system on the electrode using a conducting matrix and; (iv) making the cofactor as an integral part of electrode surface.

Of the schemes described above, immobilization techniques hold great promise and are described below in some detail.

3.2 *FAD based bioanodes*

Though the flavins (flavin mononucleotide FMN and flavin adinine dinucleotide FAD) and nicotinamide (NAD^+, $NADP^+$) coenzymes are primary acceptors of electrons from various substrates and cellular metabolites, the tricyclic flavins are more versatile catalysts as they can undergo facile two-electron as well as one-electron chemistry (Walch 1980). Reduced flavin can readily undertake reductive oxygen metabolism. The isoalloxazine ring system offers several positions at which the coenzyme can be immobilized on the electrodes. Wingard (1980) utilized the 8 methyl position to covalently link riboflavin to carbon electrodes through a conjugated double bond system and report that the immobilized species retains its electroactivity. Other workers (Bourdillon *et al* 1980; Ianniello *et al* 1982) have reported immobilization of glucose oxidase, L-amino acid oxidase and xanthine oxidase on modified carbon electrodes. The attachments in these reports are through ε–NH_2 groups of amino acid residues of the protein part, which may or may not be on the active site of the enzyme.

In our approach to the FAD-glucose oxidase system we have first studied the electron fluxes produced at different sites of the flavin ring system of FAD during its redox reaction. A site for modification has been identified, and used for immobilization of the coenzyme on the electrode. The details are given below.

The oxidation-reduction cycle of FAD involves two protons and two electrons. Schematically the complete cycle is represented in figure 3. When a substrate SH_2 is oxidised in the presence of a suitable enzyme (E) it liberates two protons and two electrons. These can be taken up by the oxidised form of FAD (I) to give $FADH_2$ (III), sequentially giving rise to an intermediate species—protonated form II. Similarly, formation of oxidized form of FAD may involve sequential release of two protons (IV)

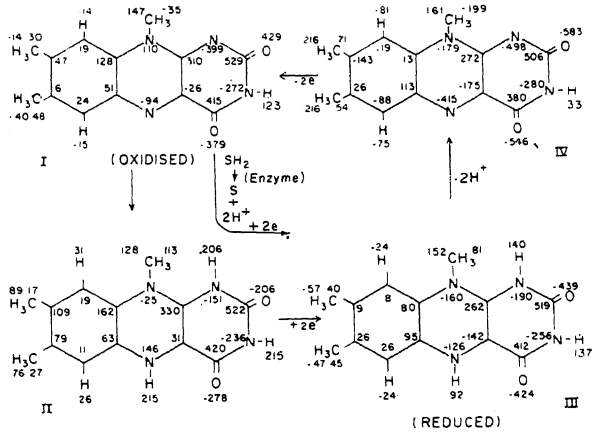

Figure 3. Charge densities obtained from INDO calculations of various redox states of flavin ring of FAD. Charge densities are in units of 10^{-3} atomic units.

and two protons and two electrons from the substrate (I → II → III) and releases them (III → IV → I) on oxidation. The two protons released can be taken up easily by the aqueous medium and the two electrons can be made to pass through an external circuit thereby giving rise to a current in external circuit. The major difficulty arises in affecting efficient electron transfer. One possible way to overcome this difficulty is by immobilising the coenzyme-enzyme system onto an electrode at a site which undergoes large change in electron density during the step IV → I. The charge distribution in FAD molecule was calculated making use of semiempirical quantum chemical technique of INDO. One can notice from figure 3 that in accordance with general expectations, the two carbonyl groups in the isoalloxazine ring and four nitrogens in the two heterocyclic rings possess such characteristics. Of these one of the four nitrogens is substituted by ribose and two are involved in proton transfer reactions, while the fourth nitrogen is known to be involved in coenzyme-enzyme linkage. The two carbonyl sites therefore appear to be potential sites for hooking up the semiconducting side chains.

FAD has been immobilized on carbon electrode employing a series of chemical steps which are schematically shown in figure 4. The steps involve creating suitable active centres on the electrode surface which are then made to react with the carbonyl groups of FAD to form conjugated double bond linkages between FAD molecules and graphite. The linkage is quite stable and FAD is not leached out from the electrode on repeated washing or use in electrochemical cells. This step had been carried out in dark to prevent the photoreaction of FAD.

Glucose oxidase is immobilized by incubating the FAD modified electrode with its apoenzyme. The electrodes were washed till the washings showed no absorbance at 280 nm and stored refrigerated in dark when not in use. Immobilized enzyme activity was assayed by using the modified method of Bergmeyer (1974). The immobilized glucose oxidase is found to be enzymatically active.

The electrochemical activity of modified electrodes has been assessed using cyclic voltametry. A conventional three-electrode system has been used in a cell where platinum mesh is used as counter electrode and saturated calomel electrode as reference. Supporting electrolyte in all cases was 1 M KCl pH 7. The potential was

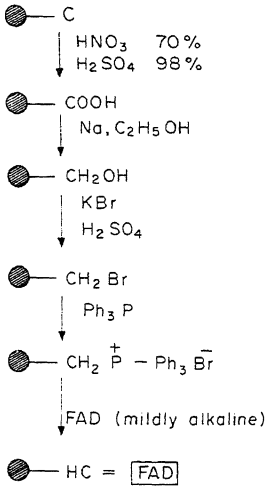

Figure 4. Reaction scheme for immobilization of FAD on graphite electrode.

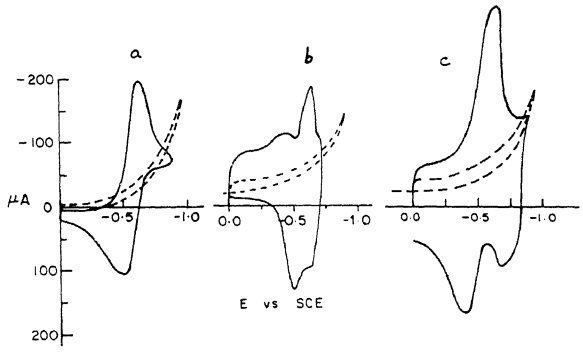

Figure 5. Cyclic voltamograms (**a**) FAD (1 mg/ml) in 1 M KCl pH 7; (**b**) FAD immobilized on carbon black; and (c) glucose oxidase immobilized on FAD modified carbon black; Broken lines—unmodified carbon black in 1 M KCl pH 7.

swept at the rate of 150 mV/sec. Analar grade nitrogen was bubbled through the electrolyte for 30–60 min prior to the experiments which were performed in nitrogen atmosphere.

Cyclic voltametric behaviour of FAD in solution is shown in figure 5a. A well-defined peak centred at −0·62 V is observed corresponding to the reduction of FAD. In the return sweep, a peak is seen at −0·50 V corresponding to its oxidation. Cyclic voltammogram of FAD immobilized on CB (carbon black) in supporting electrolyte is shown in figure 5b. Predominant peaks at 0·62 V and −0·50 V due to reduction and oxidation are observed indicating definite coupling of FAD to the electrode surface. Absorption of FAD on heterogenous electrode surface renders it a bit more difficult to reduction, which occurs at a potential higher than that of the coenzyme in solution (Gorton and Johansson 1980; Ianniello *et al* 1982). As this is not so in the modified electrodes in our case, it is reasonable to overrule the possibility of adsorption being the mode of attachment. Moreover these peaks have been found to be much sharper than those observed when carbon black electrodes dipped in FAD solution (*i.e.* adsorbed FAD) are used. Figure 5c depicts the results when glucose oxidase has been immobilised on FAD modified electrodes. It may be observed that while the reduction potential remained unaltered, the peak potential for oxidation has been shifted by 0·11 V more anodic. The redox peaks are sharper than those when free enzyme was used. In short covalent attachment of FAD on carbon electrode through carbonyl group of the flavin ring structure seems to favour the exchange of electrons between the FAD molecule and the electrode. Immobilization of glucose oxidase on electrode so modified, apparently orients the enzyme molecule with respect to the electrode and leads to direct electron swapping between enzyme active site and electrode.

3.3 *Biocathodes*

The biocathode system in wide use is an oxygen cathode where simultaneous uptake of electrons and reduction of oxygen to water takes place. This reaction is sluggish and mostly results in lower overall efficiency of the fuel cell. The equilibrium potential of the oxidation reduction pair O_2/H_2 of 1·23 V is obtainable only on specially treated platinum (Watanabe and Devartrathan 1964; Bogdanovskaya *et al* 1972). Exchange

currents on platinum are as low as 10^{-11} A/cm^2. This can be overcome by supplying oxygen, to the electrode through photosynthesis of algae (Lewis 1964). In this way the source of oxygen can be put directly on the electrode. But the disadvantage arises due to dependence of the cell on light energy. Alternatively, enzymes which can actively reduce oxygen to water can be immobilized on cathode. Cytochrome C oxidase, ceruloplasmin, ascorbatoxidase and laccase are known to reduce oxygen to water *via* a four-electron mechanism without hydrogen peroxide as an intermediate. Yaropolov *et al* (1976) and Berezin *et al* (1977) have described systems where peroxidase and cytochrome C oxidase have been used as catalysts for oxygen reduction. The electrons get transferred from the electrode to active centres by mediators. The electrode potentials of 0·6–0·8 V have been obtained which is dependent on the ratio of the reduced and oxidized forms of mediators. Berezin *et al* (1977) have described another system where *Poluporos versicolor* laccase has been used as catalyst, laccase had been directly absorbed on the electrode. The maximal potential value of 1·207 V near equilibrium has been obtained on carbon black electrodes that had been kept in 10^{-5} M laccase solution for 24 hr.

4. Scope and future projections

Efficient bridging between the redox proteins and electrodes of the type discussed above can eventually give rise to three types of devices (i) biochemical fuel cells working at low temperatures (ii) sensors based on direct electrode interactions rather than conventional ones which detect products or substrates of biological reactions (iii) bioelectrodes for electrochemical synthesis.

Inspite of the many advantages projected for biochemical fuel cells, work on the preparation of bioelectrodes is still in its infancy. The major constraint, of course, is the poor electron transfer from enzyme active site to electrode. Although, at present, biochemical fuel cells are far from being used as commercial power generators, their use in sensors provides excellent potential. A couple of examples in this regard are the alcohol sensors, the glucose and urea sensors. The glucose sensor for instance can find wide applications in estimating an monitoring glucose in food and fermentation industries and clinical laboratories. One other use of biochemical fuel cells is in running devices which require low power outputs. For example, a micro glucose-electrode conveniently implanted in the body, can serve as an excellent power source for pacemaker, generating low-power pulses from the plasma glucose. However, one can foresee the most potential application of indirect type of biofuel cell as power generators in conjunction with sewage, biomass and agricultural waste fermentation.

Acknowledgement

We are grateful to Prof. K S V Santhanam for his help in cv experiments. Funding of the project by the Department of Science and Technology is gratefully acknowledged.

References

Ahn B K, Wolfson Jr S K, Yao S J, Liu C C, Todd R C and Weiner S B 1976 *J. Biomed. Mater. Res.* **10** 283
Austin L G 1967 Fuel Cells NASA SP-120 US Govt.

Berezin I V, Pobochin A S, Kupriyanov V V and Luzikov V V 1977 *Biorg. Khim.* **3** 989
Bergmeyer H U (ed.) 1974 *Methods in enzymatic analysis* (New York: Academic Press) Vol. 1, p. 457
Bogdanovskaya V A, Burshtein R Kh and Tarasevich M R 1972 *Electrokhimiya* **7** 1011
Bourdillon C, Bourgeois J P and Thomas D 1980 *J. Am. Chem. Soc.* **102** 4231
Gorton L and Johansson G 1980 *J. Electroanal. Chem.* **113** 151
Ianniello R M, Lindsay T J and Yacynych A M 1982 *Anal. Chem.* **54** 1098
Karube I, Matsunaga T, Tsurus S and Suzuki S 1977 *Biotechnol. Bioeng.* **19** 1727
Lewis 1964 *J. Appl. Bacteriol.* **27** 174
Shaw M 1963 *Proc. 17th Annual Power Sources Conference* p. 53
Videta H A and Arvia A J 1975 *Biotechnol. Bioeng.* **17** 1529
Walch C 1980 *Acc. Chem. Res.* **13** 148
Watanabe N and Devartrathan N A V 1964 *J. Electrochem. Soc.* **3** 615
Wingard Jr L B 1978 *Hindustan Antibiot. Bull.* **20** 117
Wingard L B Jr 1980 *Enzyme Eng.* **5** 101
Wingard L B Jr, Ching Hao Shaw and Castner J F 1982 *Enzyme Microb. Technol.* **4** 137
Yaropolov A I, Vartolomeev S D, Berezin I V, Bogdanovskaya V A and Tarasevich N R 1976 *FEBS Lett.* **71** 306

Energy Sources

Towards biochemical fuel cells ..... *H M Sonawat, Ratna S Phadke and Girjesh Govil* 1099

Indexed in CURRENT CONTENTS

Edited and published by C N R Rao for the Indian Academy of Sciences, Bangalore 560 080. Typeset by Macmillan India Ltd., Bangalore 560 025 and printed at the Macmillan India Press, Madras 600 041.

Regd. No. KRN-A 41

Vol. 93 (Chem. Sci.), No. 6, August 1984

Proceedings of the Indian Academy of Sciences

Chemical Sciences

CONTENTS

Solid State Chemistry

Nonstoichiometric compounds: A critique of current structural views ..... *J S Anderson* 861

Physical and Theoretical Chemistry

Radiationless transitions in trivalent lanthanide ions embedded in solids .... *Deb Shankar Ray and Mihir Chowdhury* 905

Use of semiempirical molecular orbital calculations for the evaluation of force fields ..... *A Annamalai, M Kanakavel and Surjit Singh* 917

Correlations between topological features and physicochemical properties of molecules ..... *D V S Jain, Sukhbir Singh and Vijay Gombar* 927

Use of cluster expansion techniques in quantum chemistry. A linear response model for calculating energy differences ..... *Somnath Ghosh and Debashis Mukherjee* 947

Search for a density-based alternative quantum mechanics of many-electron systems ..... *B M Deb* 965

Inorganic Chemistry

Exchange interactions in some low-dimensional metal dithiolene complexes.. ..... *P Kuppusamy, B L Ramakrishna and P T Manoharan* 977

Photoredox processes in coordination compounds ..... *P Natarajan* 1003

Organic Chemistry

Cycloartenol to *Buxus* alkaloids ..... *Sukh Dev* 1015

Recent advances in the chemistry of lignans ..... *A Chatterjee, A Banerji, J Banerji, S C Pal and T Ghosal* 1031

Studies directed towards the total synthesis of anthracycline antibiotics ..... *A V Rama Rao* 1059

Recent developments in the chemistry of perhydroindoles and perhydrocinnolines ..... *K Nagarajan* 1079

(Continued on inside back cover)